Heat pipe

Sidenko Artem

Lyceum of Belarusian National Technical University

In my work I've made the thermosyphon, done the research about it's working principle, and conducted experiments on it. Through experiments the coefficient of thermal conductivity (1250 W / (m · K) was found. I've also made two heat sinks and defined thermal resistance of termoifn with radiators and without them (0.2K / W). In the future, I'm going to find the optimal volume dependence of thermosiphon on the amount of liquid poured into it in which the thermal conductivity is the highest.

Production of thermal siphon:

I've made thermosyphon from copper tube sealed at one end, the opposite end of the tap I welded that we could change the fluid. Then I poured water into the tube and when the water has boiled, the tube expanded and water began to rise in the tube. When the water rose to the faucet, I closed it thus remained in thermosiphon only water and water vapor at low pressure. With a sharp shaking, you can hear the sound of a knock on the bottom of the water resembling the sound of hitting a metal ball. It means that what we've got to make a working thermosyphon.

The first experiment:

To measure the thermal conductivity coefficient I placed in the lower end of thermosiphon vessel continuously with boiling water using a thermometer and every 30 seconds measured dynamic temperature change at the top end of the tube. Next, using the ABAQUS program I built a graph of temperature versus time. With the help of selection method I determined the thermal conductivity thermosiphon constructed and it is equal to 1250 W / (m · K).

Production of radiators:

To measure the thermal resistance I invented and designed two radiators. The first one I made the radiator from the old transistor. The second I made from a sheet of aluminum printing, cut it, and gathered into a single structure.

Second experiment:

To measure a thermal resistance made up with two thermosyphon radiators and without them constant temperature has been measured at the top and at the bottom of the thermosyphon, which was heated using fihralya wound around the lower end of the tube. On fihral fed a constant current of 2.6 Ampere. Next, the temperature measurements from the first and second radiator, using this formula I calculated the thermal resistance thermosiphon. In the second thermosiphon radiator it is higher, then it is more efficient heat dissipation. Thermal resistance thermosiphon is 0.2 K / W

Bottom line:

As a result, I was able to produce and identify thermosyphon heat transfer coefficient, which has the thermal conductivity three times more than copper and approximately equal to the thermal conductivity of a diamond. So I was able to construct two working radiators and measure the thermal resistance of the heat sinks. In the future, I'm going to find the dependence of the amount of fluid that is in the thermosiphon of the volume of thermosiphon.

Eddy currents

Filip Bacinger, Juraj Barlek
Supervisor: Melita Sambolek, prof.
Gymnasium Josip Slavenski Čakovec, Čakovec/Croatia; filipbacinger@gmail.com, jurajbarlek@gmail.com

1. The purpose of the investigation

The goal of this experiment was to investigate the appearance of eddy currents and construct a cheap device which can be used to easily check the dependence of the induction of eddy currents on different parameters and describe them using the phenomenon of damped oscillation.

Our hypothesis was that inducted eddy currents will depend on geometrical properties of the conductor so we tested the dependence on the number of slots on the conductor, width of the slots, size of the magnetic field, conductive material, position in relation to the Earth's magnetic field, shape and direction of slots and filling of the slots with different insulators.

2. Method of the investigation

In this experiment we used a model of Foucault's pendulum for eddy currents in which the conductor is oscillating in a magnetic field and the induced currents are damping its oscillation (Figure 1).

We recorded the movement of the conductors (non-magnetic metal plates) through a variable magnetic field. At the bottom of the pendulum we attached neodymium magnets and swung various metal plates through the magnetic field.

Figure 1 *The pendulum and some of the plates (conductors) used in the experiment*

We calculated the logarithmic decrement λ:

$$\lambda = ln \frac{A_n}{An+1}$$

where A_n is the nth amplitude and A_{n+1} is the following amplitude. Then we used the measured period T to calculate the damping ratio δ:

$$\delta = \frac{\lambda}{T}$$

where λ is the logarithmic decrement and T is the period of oscillation. Finally, we calculated the *Q-factor* using the following formula:

$$Q \approx \frac{\omega_0}{2\delta}$$

where ω_0 is the angular frequency and δ is the damping ratio.

In comparison with other methods, this one is very simple and is similar to the one used by Leon Foucault (the scientist who first described the phenomenon of eddy currents). The whole device was made of widely available and cheap materials. We already had most of the parts since they are used in all physics classrooms (magnets, pulleys, metal stand, and clothespins). Other known devices for testing eddy currents are expensive and unavailable to us.

3. Results of the experiment

As the result of investigating the dependence of induced currents on the position relative to the Earth's magnetic field, we got identical results for the case when the conductor was oscillating parallel to the Earth's magnetic field lines and the case when the conductor was oscillating perpendicular to the Earth's magnetic field lines.

By increasing the number of slots on the conductor, the total time of oscillation was longer – damping ratio was smaller, which meant the Q-factor was greater, matching our expectations (Figure 2)

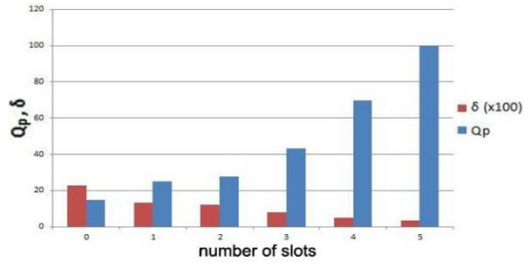

Figure 2 *The relation of the Q-factor and the damping ratio is inversely proportional*

The time of oscillation of the conductor in the magnetic field was longer when the magnetic field was weaker, matching our expectations.

Results showed that the time of oscillation was longer when the width of the slots on the conductor was greater (Figure 3). For greater width of the slots the damping ratio was smaller, i.e. Q-factor was greater.

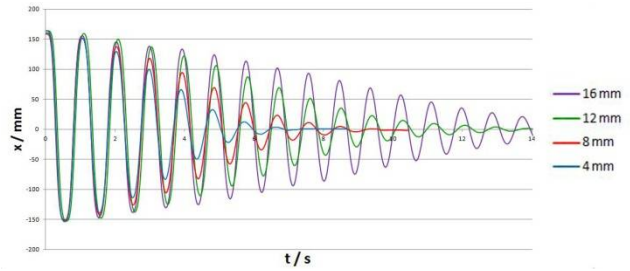

Figure 3 *An example of an x-t graph for conductors with different slot widths*

It is visible from the *lnA-t* graphs that a greater slope of the line shows stronger damping, while a smaller slope shows weaker damping (Figure 4).

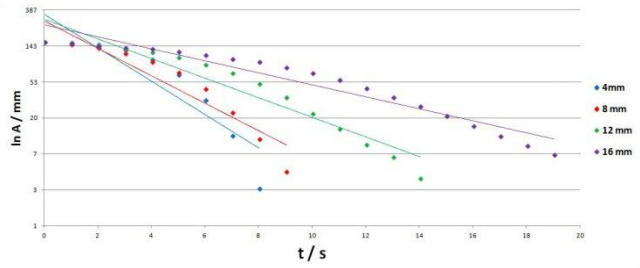

Figure 4 *An example of a lnA-t graph (different slot widths)*

The shortest period of oscillation was measured for aluminium conductors, followed by copper conductors (not matching our expectations), while the longest period was measured for brass conductors. According to theory, we expected greater induced currents in the copper plate instead of the aluminium one. The results for the brass plates were as expected – the damping was weaker than for aluminium and copper.

The results prove that induced currents also depend on the shape and direction of slots. The longest oscillation period was measured when the conductors had slots cut out (including the edge), and the shortest oscillation period was measured when the conductors had holes (not including the edge). The more favourable the shape was for the induction of eddy currents (closed loops), the damping was stronger.

When filling the slots of the conductors with different insulators, we got slight differences between certain insulators. We have proven that oscillation damping depends on the electrical resistance of the material filling the slots, although we were not able to precisely measure or calculate the resistance.

We determined that the damping was weaker, compared to other insulators, if the insulator used was air. The differences between measured data for other insulators were unnoticeable, so we couldn't precisely determine which of them should be used for best results.

4. Conclusions

Geometrical properties of the plates (conductors) had a significant effect on the induction of eddy currents, which confirms this experiment's main hypothesis.

The results show that the Earth's magnetic field either has no effect or has an insignificant effect on our experiment.

Measurements of the dependence on different parameters give a graph of damped oscillation (an x-t graph, where *x* stands for elongation, and *t* stands for time), in which the damping ratio and the *Q-factor* change significantly for different parameters, but the oscillation is quasiperiodic.

When analysing the data it is visible that in order to minimize the effect of eddy currents in a variable magnetic field it would be ideal to pick a conductor as thin as possible, made from a material with electrical resistance as great as possible, with as many slots as wide as possible and in such a shape which doesn't allow the forming of big closed loops of eddy currents. To further minimize the effect of eddy currents, it is possible to fill the slots with a good insulator.

It is also possible for a device such as this one to be used to determine the strength of induced eddy currents in metal bodies of smaller dimensions and in less technically advanced devices by determining the marginal damping ratio for a certain physical procedure.

Chaos: A Thin Barrier Between Order and Disorder

Giorgi Bitchiashvili & Gega Lelashvili

Supervisor: Genadi Kiani

Georgian-American High School, Tbilisi, Georgia, info@gahs.edu.ge

The purpose of the research

Modern science is undergoing the development stage of integration and interdisciplinary research of different fields. The focus of the researches are the systems – particles united by different elements and interconnected ,,networks'' that experience changes, evolution, resonant and catastrophic events.

It is important to determine general regularities of variously organized systems and research on laboratory objects, i. e. analogues, which have system features and it is possible to manage one or several parameters of their state.

Particularly interesting are the systems and relevant laboratory objects, which represent entity of interconnected objects and act chaotically, i.e. each of their consecutive state is hardly predictable or clearly unpredictable. Due to minor external influence or connection changes, such systems sometimes become orderly, but they still return to disorderly, unpredictable state as a result of slight change of any parameter.

The purpose of our research is to investigate the behavior of two laboratory objects having features of self-organized criticality (SOC). SOC is one of the classes of chaos concept, in which relatively simple systems display sufficiently complex behavior. So called relaxators represent this class, which gather energy for some period of time and immediately "discharge". In SOC events relaxators behave chaotically within broad time and energy intervals and display regulation, which can be observed in several natural systems and perceived

The method of the research

Sand cone dynamic is accepted as a model to demonstrate the nature of SOC events: avalanches of different size fall off the sand clock cone. Masses of the avalanches are distributed disproportionally to the frequency. Drop of each grain on sand cone and avalanches are observed in laboratory experiments. Grains are system elements, the unity of unpredictable connections between them determine time and mass of unpredictable avalanche emergence.

We discuss laboratory experiments of such events by using electronic relaxators, multivibrators. Multivibrators are created by two interconnected relaxators. Time of energy accumulation is defined by meaning of R1,C1 and R2,C2 resistors and capacitors couples. If electrical resistance changes its meaning, we get chaotically changing time intervals in each cycle of multivibrator.

Two objects are selected for creating chaotically changing electrical resistance. Graphite grains are used in both of them. In the first object graphite is placed between two electrodes and its state can be changed by piezoelectric actuator, which is supplied by semi-cycle impulse of stable state of multivibrator cycle, i.e. graphite is involved in each cycle with new state.

as identifying sign of its chaotic property - energy of the events are disproportional to the frequency of their appearance.

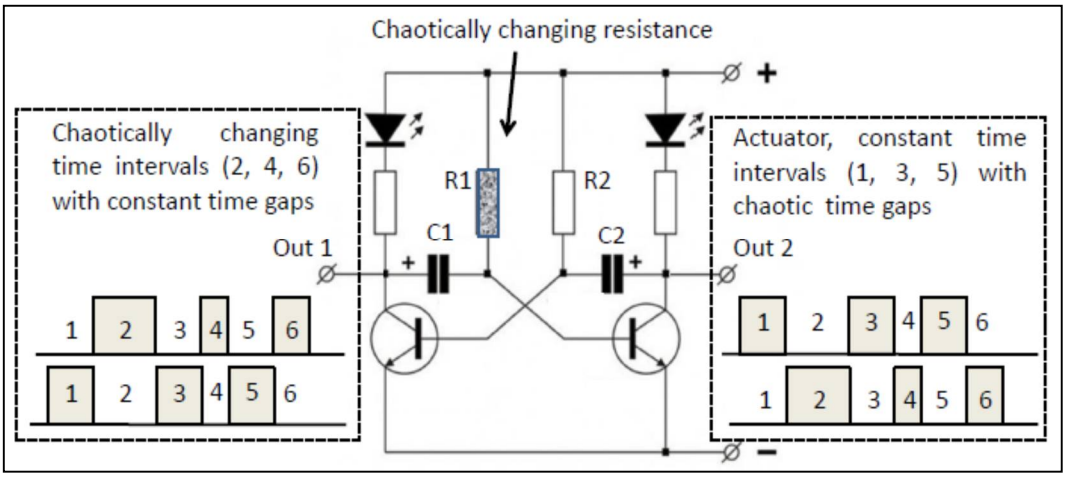

Such object facilitates noise generation in a broad diapason of frequency. Particularly interesting is its behavior in closeness with resonant frequencies of such systems. SOC should be studies in closeness of these frequencies.

The graphite placed between two electrodes in glass cylinder creates resistance in the second object. The avalanches fallen on the free surface of graphite change its electrical state during cylinder rotation. Rotation is carried out by stepper motor. The engine is supplied by stepper impulse during stable semi-cycle of multivibrator cycle.

The results and conclusions of experiments

Digital registration of multivibrator state enables study of chaotic behavior of the presented objects. Self-organized Criticality can be observed in the conducted experiments. Objects facilitate change of several parameters and regime. Due to this, doing experiments on them enables more flexible study of SOC events in comparison with sand piles.

Increasing the Efficiency of Light Bridge Construction

Authors: Mariam Rostomashvili , Mariam Bughadze

Supervisor: Genadi Kiani , Ia Mebonia Georgian-American School, 6 Ramishvili str.

The Purpose of the Investigation

Modern engineering surprises us with its courage and determination to design bridge that using thin, arching cables optimally placed and spread out across the length of the bridge to suspend and hold amazing weights. Structure may give the illusion of being light and flimsy, but its strength is hidden behind the enormous tension that is spread out and supported across the entirety of the bridge. When enjoying the beautiful spectacle of the bridge, of course, the question arises: what should be optimal length and thickness of the material being used, etc. Modern science and engineering can, of course, help to provide answers to these questions.

At this stage, however, these two sciences can't completely explain what type of materials and in what dimensions they should be used to allow bridges to hold the greatest amount of weight. Therefore, it was our goal to discover the optimal shape of a light bridge that could hold the greatest weight (hereafter known as load factor), using materials readily available to us.

Method of Investigation

Experimentation was conducted using a differing amounts of rulers of various materials, secured by an iron bolt, a piece of plastic mesh, and a simple length of ribbon to create a working model of a light-construction bridge, the final design of which is shown in **Figure 1**. The primary aim was to discover the optional shape of the bridge that could hold the greatest load factor.

Figure 1

The plastic mesh was chosen as the most practical and realistic material for its ability to distribute pressure symmetrically from one point to another, as shown in figure 2, the same way real point-construction bridges spread out weight today.

In order to determine how far down the mesh would sink, we needed to consult the textbooks, wherein we discovered the formula, $OO' = \frac{pl}{48EI}$ (a visual explanation of which can be found in figure 2. After crushing the numbers, we determine that $OO' = 3.024 * 10^{-4}$ ∂.

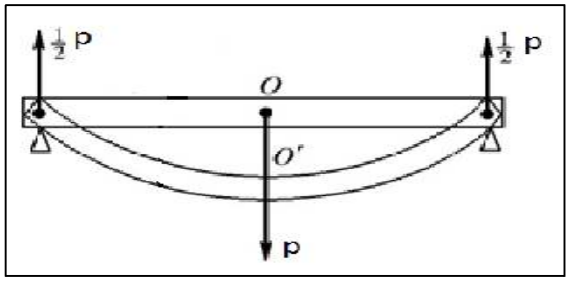

Figure 2

We started with only a single rulers, increasing the number, up to four, in different orientations.

Different amounts of weight were placed upon the center mesh net or hung a ribbon from the apex , up to a maximum of 6.125 kg (the greatest among the great was able to hold), distributed according to figure 3.

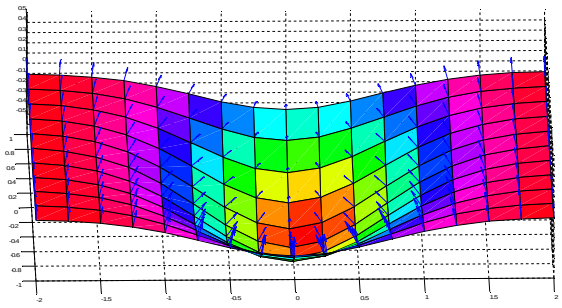

Figure 3, image generated by Matlab 1. (7.12.0 r2011a)

Results of the Experiment

As a result of our experimentation, we discovered that the shape had a profound impact on the model's ability to hold weight. Not the starting shape, before weight was placed upon the mesh surface, but the shape after the load factor had been added.

Furthermore, we needed to discover solutions to tow major problems. First, when the weight was placed upon the mesh surface, the bridge would rotate around the y-axis. In order to combat this challenge, we added a length of rope that connected and stabilized the four legs of the arch.

Secondly, the downward force of the weight caused the four legs of the arch to collapse upon themselves. In order to solve this issue, we placed plastic beams at the same height at the strings between legs A and B and between legs C and D (as seen in **figure 3**), and a string between the top of the construction (at the point where the rules connect) and the center point of the mesh surface where the strings connect.

Conclusions

When supporting a load factor, we found that the best-performing rulers bent along a concave, waveline-like pattern as the legs of the structure subbed against the ground, according to the formula y=Dsin kx, where D represents the rulers' deformation when exposed to the load factor, x, and that the maximum load factor increases exponentially according the to the strength of the materials used.

The maximum load factor (F), which impacts on the top parts of the structure, is represented by the formula, $F = \frac{\pi^2 EI}{l^2} \approx 60$, where K represents division between the length and contortion of the ruler.

Today our, light 90 gram structure is able to hold a load factor of 6. 125 kg. Therefore we can conclude that if a bridge design could take this form and allow for this sort of motion could support a greater amount of weight.

Figure 4

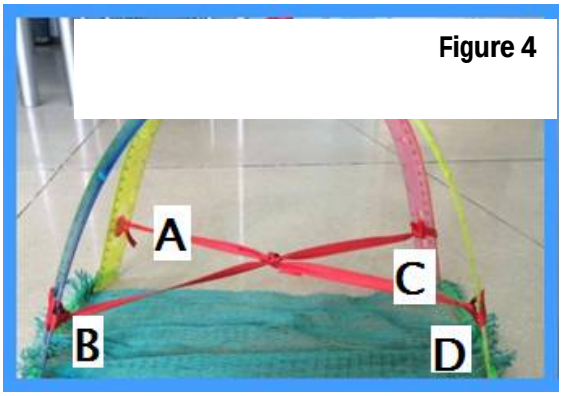

The Project 'Paper-Hercules'

Moritz Petersen, Aaron Hohenfeld, Martin Ramm

Supervisor: Hermann Klein dipl. ph.

1 Introduction

When sheets of two phonebooks are interleaved, a very high effort is needed to pull them apart. We observed this phenomenon in a video of the 'MythBusters'. Even when we tried to separate the books we failed. This observation triggered our interest in the investigation of the parameters influencing the astonishingly large frictional force.

Fig. 1. Even my colleagues and I were not able to pull the interleaved phonebooks apart

2 Experimental Setup

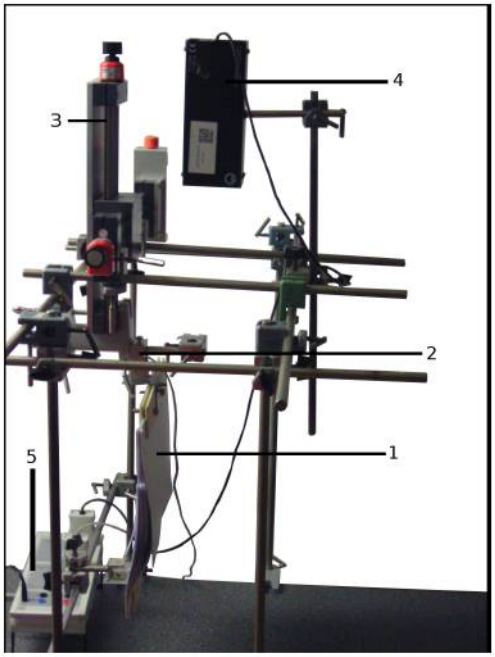

Fig. 2. The device being used to measure the traction

In our experimental setup (Fig. 2) the two books consist of a variable number of fixed sheets (1) in which one spine is fixed to a dynamometer (2). By activating a winch (3) the books are pulled apart. The distance *d* between the overlapping sheets and the spine is measured (4) so that a distance-force diagram can be drawn (5).

3 Measurements

Our measurements showed that the traction increases exponentially with a rising number of sheets, if *d* is kept constant. If *d* decreases, the traction increases exponentially too.

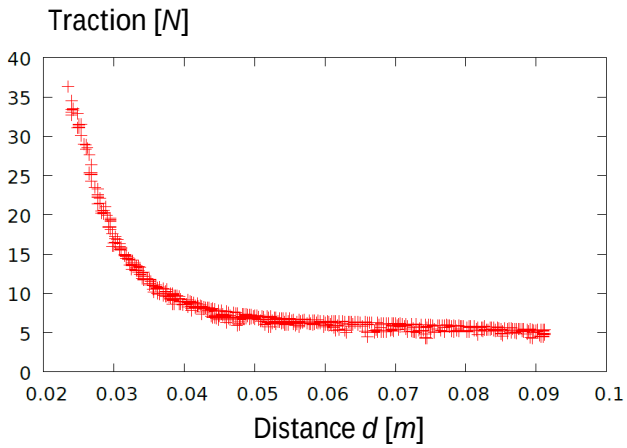

Fig. 3. Correlation of the traction as a function of distance *d*

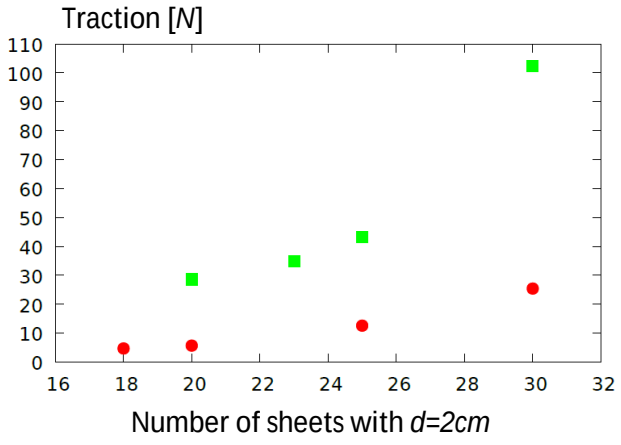

Fig. 4. Correlation of the traction as a function of the number of sheets: squares show the data for a thicker paper and circles the data for a thinner paper

4 Theoretical Contemplation

Taking the article 'The enigma of the two interleaved phonebooks' from 2015 into our considerations we found out that the angle Φ_n (Fig. 5) influences the huge traction necessary to separate the books. This angle, originating from the interleaved book sheets, is

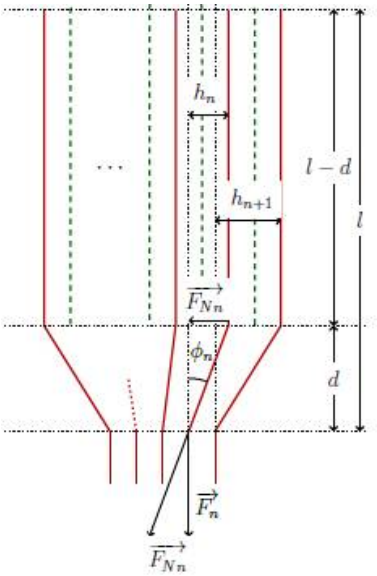

Fig. 5. Illustration of the interleaved books and the angle Φ_n

the most critical parameter determining the traction necessary to pull apart the books. Φ_n results from the number of sheets, the page thickness and the distance *d*. The tangent of it is inversely proportional to *d.* The bigger Φ_n gets the higher the frictional force to be overcome to separate the books.

Finally, the entire traction could be described by a differential equation elaborated with the computer-algebra-system 'Maple'. For this equation certain parameters have been kept constant, as the page thickness or the number of sheets. The equation is as follows:

$$F = M \cdot F^* \cdot \sqrt{\frac{\pi}{2 \cdot \alpha}} \cdot e^{2 \cdot \alpha} \cdot erf(\sqrt{2 \cdot \alpha})$$

in which *F* is the entire traction, *M* half the number of sheets, *F** the traction acting on the outermost sheet, and α a constant resulting from the tangent of Φ_n, the friction coefficient μ, and *M*.

We determined that the frictional force acting on the sheets and hampering the separation of the books increases when the traction rises. This phenomenon is also called 'principle of self-locking' and is, for example, the operation of the so-called 'Chinese finger-trap' (Fig. 6).

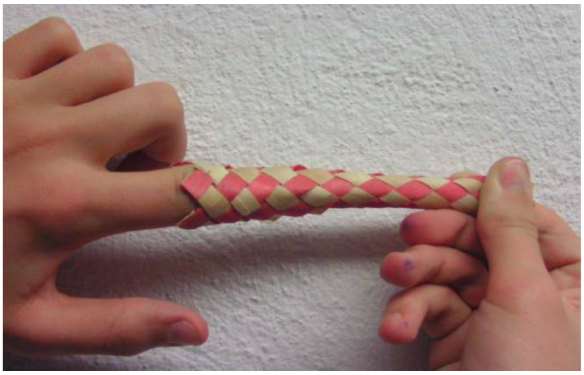

Fig. 6. The 'Chinese finger-trap'

5 Verification

By comparing the theoretical values resulting from the equation with the measure data, we could verify the friction coefficient μ.

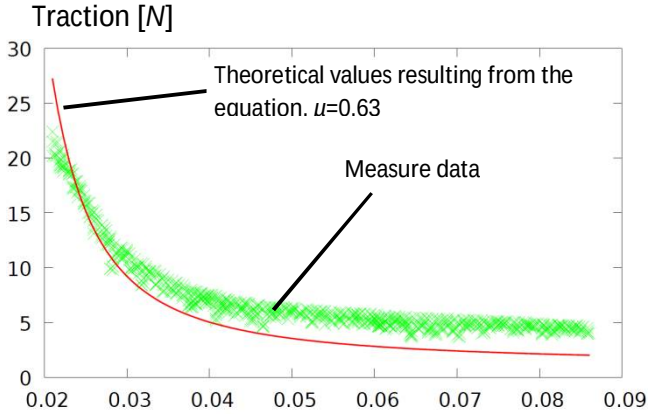

Fig. 7. Comparison between theory and experiment

In subsequent experiments we will try to confirm experimentally that the angle Φ_n is the important parameter causing the high traction.

References:

https://www.youtube.com/watch?v=QMW_uYWwHWQ, Access: 20.10.2015

https://de.wikipedia.org/wiki/Reibung, Access: 08.01.2016

https://www.researchgate.net/publication/280969779_The_enigma_of_the_two_interleaved_phonebooks, Access: 08.01.2016

http://www.weltderphysik.de/gebiet/stoffe/reibung/, Access: 08.01.2016

https://en.wikipedia.org/wiki/Chinese_finger_trap, Access: 10.1.2016

Magnetic Train

Lennart Resch

Supervisor: Hermann Klein, Dipl. Ph.

Hans-Thoma-Gymnasium, 10th grade, Lörrach, Germany, lennart.resch@web.de

1 Introduction

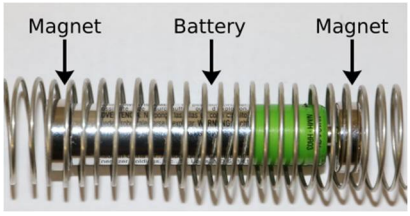

Fig. 1: The "magnetic train"

Two strong neodymium button magnets are attached to both ends of a small cylindrical battery (see Fig. 1). When placed in a copper coil such that the magnets contact the coil, this "train" starts to move and quickly reaches a speed limit. But why does this "train" move as if by magic? Why is there a speed limit? Can this speed limit be increased by varying different parameters such as the number of the magnets on both ends of the train?

To answer these questions we investigated the resulting magnetic fields and their orientation. We designed an experimental setup to measure how relevant parameters affect the train's speed and compared the values to our detailed theory.

2 Theory

Due to the contact of the button magnets and the coil, there is a current. As a consequence the coil turns into an electromagnet with a magnetic field (see Fig. 2, orange field lines).

The button magnet on the left is repelled by this electromagnet. The button magnet on the right is attracted by the electromagnet, so the whole train moves to the right.

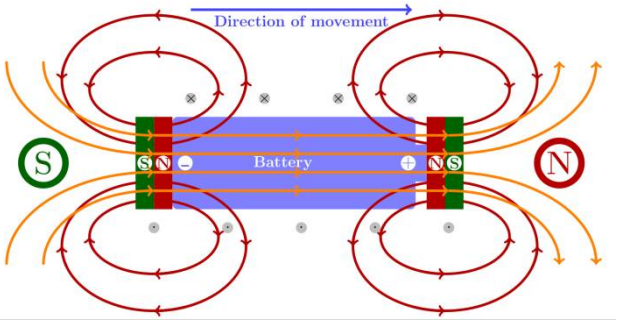

Fig. 2: The different magnetic fields of the train

This movement can also be verified by looking at the lorentz force. On the top of Fig. 2 the electrons move into the layer. The magnetic field points upwards, so the lorentz force points to the left and the counter-force on the train points to the right. The whole train moves to the right again.

A quantitative treatment of the lorentz force [1] shows, that the driving force is proportional to the coil current:

$$F = C \cdot I$$

The speed limit is related to the different magnetic fields and the Faraday's law of induction. If the two magnets move through the coil, there is a induced voltage. This voltage opposes the battery's voltage. The faster the train becomes, the bigger is the induced voltage and the deceleration. The train reaches a speed limit.

By calculating the eddy currents [1] it is possible to determine the total force on the train and the terminal velocity:

$$v = \left(\frac{1}{C}\right) U_B - \left(\frac{mg\mu_k}{C^2}\right) R_T$$

U_B is the voltage of the battery, m is the mass of the train, μ_k is the friction coefficient and R_T is the total resistance.

3 Experiments

As there weren't any silvered copper coils to buy, we decided to wind the coils by ourselves. For the experiments, the thickness of the wire and the number of the button magnets were varied. The magnetic flux density of the different coils as well as the magnetic flux density of the button magnets was measured by hall sensors. The train's driving force was investigated with dynamometers. The explanation for the speed limit of the train was confirmed by a special experimental setup.

To measure the train's speed limit we designed an experimental setup (see Fig. 3). The voltage at a certain section of the circle was logged. If the train passed this section there was a peak in the measurement diagram. We wrote a program in python, which calculates the average lap time.

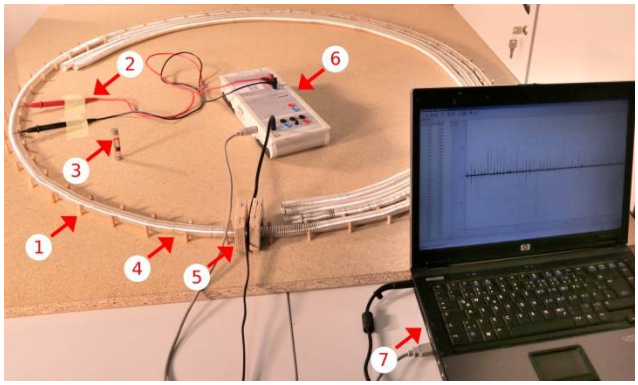

Fig. 3: (1) wooden plate with wooden dowels; (2) current collector; (3) battery with button magnets; (4) silvered copper coil; (5) fixing of the coil; (6) data logging system; (7) laptop

Table 1: The average lap time for different coils and different numbers of magnets per side

		Number of Magnets		
		1	2	3
Diameters of the wire	*8.0 mm*	*4.336 s*	*2.808 s*	*3.132 s*
	1.0 mm	*4.427 s*	*2.290 s*	*2.283 s*
	1.2 mm	*3.279 s*	*2.702 s*	*2.331 s*
	1.5 mm	*7.090 s*	*4.866 s*	*3.984 s*

The more magnets are attached to the battery the higher is the train's speed. If the wire is too thick there is too much friction, so the train is very slow. If the wire is too thin the coil bends out of shape very fast, so it is shaped very irregularly and the train is slow too. A wire with a diameter of *10 mm* is a good compromise. We also measured the speed limit in relation to the voltage.

To verify the connection between the current and the driving force, we measured the force of the train with different currents.

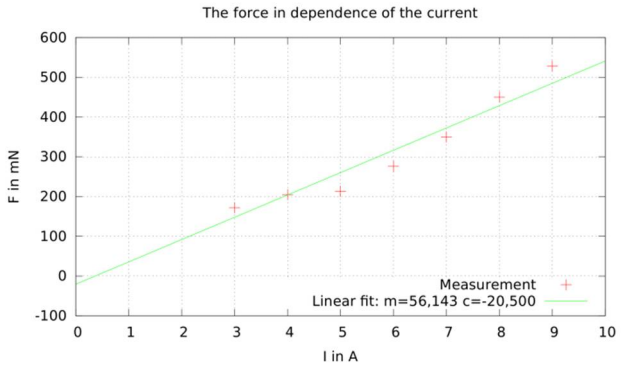

Fig. 4: The train's driving force in relation to the current

To compare our measurement of the speed limit with theoretical values we determined the magnetic moments of the neodymium magnets and the total resistance R_T. This total resistance includes the contact resistance of the magnets with the coil, which revealed to be a very critical parameter for the comparison.

3 Summary and outlook

The “magnetic train” is a surprising and unexpected phenomenon. We found different explanations for the driving force of the train and were able to explain, why there is a speed limit. With the help of diverse experiments we were able to confirm these theoretical considerations. In the future we would like to investigate the dependence of the contact resistance on the velocity of the train.

4 References

[1] C. Criado, N. Alamo: World’s simlplest electric train. American Journal of Physics, January 2016

[2] http://physics.stackexchange.com/questions/150033/how-does-this-simple-electric-train-work

[3] http://skullsinthestars.com/2014/12/12/the-mystery-of-the-magnetic-train/

Hovercraft

Tímea Bánóczki

German Nationality High School, Hungary, banoczki.tina@gmail.com

1) Hovercraft

I have always loved the different means of transport and I have always loved physics. When I was a child I built many times a floating vehicle using a CD a balloon and a valve. Of course I have always tried to maximize the levitation time. So when I grew up I started to investigate the physical background of this vehicle. First of all I made this experiment because this phenomenon is the ground of the floating vehicles and it would be the greatest if I could levitate relative big masses using relative small propellant - in this case air. So I built this simple model - hovercraft - using a weekday CD, a balloon filled with air (I used different types of balloons), which I connected to the disk with a valve. The exiting air can lift the device making it float over a surface with low friction. I investigated the relevant parameters influence the time of the "low-friction" state. During my measurements I investigated different parameters and I could observe some kind of vibration but only in the cases of fast slow. So it was not so important because my first aim was to create such a system which can levitate very long time, so the flow had to be very slow. That is why I tried to approach this problem from this direction and I looked for a theory which describes my problem correctly.

Figure 1. Experimental set up

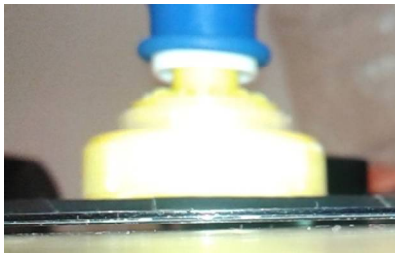

Figure 2. Levitation of the disc

2) Why does this set up levitate?

To understand the problem first I had to understand the cause of the levitation. When we blow up a balloon, there will be an overpressure inside the balloon and when we let it come out during the tube then there will be overpressure under the CD too. I used the well-known Work theorem to describe the phenomenon and the Continuity equation to write down the change of the velocity of the flow. With the help of the cylindrical coordinate system I was able to write down the phenomenon in 3D, so with x-y-z coordinates. Using these theories and after some simplification I can get my main equation for the pressure as the function of the radius.

$$p(r) = -\frac{1}{2}\rho \cdot \frac{Q^2}{(2\pi h)^2} \cdot \frac{1}{r^2} + \frac{6\mu Q}{\pi h^3} \cdot \ln\left(\frac{R_2}{r}\right) + p(R_2)$$

This equation consists 3 different parts. First the velocity part, second the viscosity part and third a constant part which was measured during the experiments at the edge of the CD. So we can say that these parameters can influence the pressure as the function of the radius under the CD.

This formula was also good because later after some rearrangement I could calculate the lifting force of the device.

3) How good does the theory describe the reality?

First of all I measured the overpressure under the CD and compared the measured values with my theoretical line and I could see that it does not fit perfectly but it was better than the literary [1]. To explain the difference I measured the effect of the hysteresis on the balloon and I discovered that the pressure is not the same in the balloon during the phenomenon, so it means that the balloon became tired. But I took it a constant value because it would be very hard to measure the pressure in the balloon

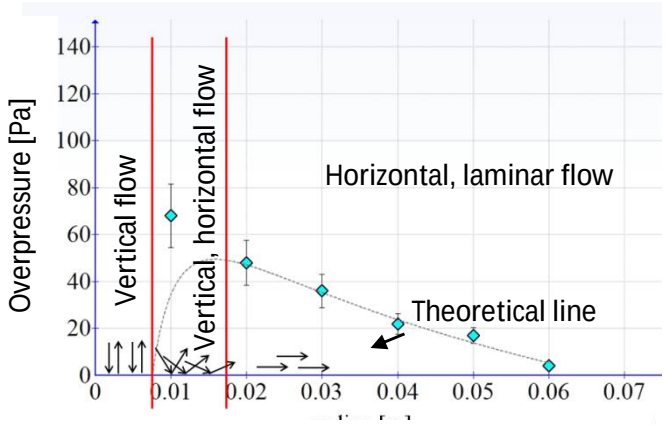

Figure 3. Pressure under the CD

during the measurements and those points where the pressure was higher take only for a short time. So this does not explain the difference between the theory and the measurements. So I measured the pressure under the CD deeper and I discovered that the air flows not in every case horizontal under the disc, but also in vertical direction. Our model describes only the horizontal, laminar flow so this can be the explanation for the difference.

After I understood the theory I measured the different parameters which influence the levitation. First I rearranged my main equation and I wrote down a formula for the lifting force. I compared the calculated lifting force with the measured and I saw that there was only a smaller difference between them, which I could explain with that, that our theory describes only the horizontal flow and under the CD there is not only horizontal flow. From this equation I created a formula as the function of the mass.

$$m = -\frac{V^2 C_1}{t^2 h^2} + \frac{V C_2}{h^3} + \frac{p_{valve} R_1^2 \pi}{g}$$

With this formula I could see in which cases can I lift the biggest masses. So on which parameters does it depends on (different constant values, volume, levitation time, height). So I made measurements with different masses on different surfaces and I saw that there may be a linear connection between the different masses and I also measured such critical masses which the system could not lift.
As I said I made measurements on different surfaces and I discovered that in the case of short levitation the surface has to be rough and in the case of very long levitation the surface has to be smooth and flat.
So I rearranged the mass equation for the levitation time.

$$t = \frac{V \cdot C_2}{m \cdot h^3}$$

Because I could neglect the first and the last part of the mass equation (first part: the flow is very slow, so it can be neglected; last part: the lifting force, which comes from this part is very small compare to the whole lifting force).
So I compared the theoretical and measured levitation times, which is represented at the table 1.

Serial number of measurements	m (kg)	V (m^3)	$h_{average}$ (m)	$t_{theoretical}$ (s)	$t_{measured}$ (s)	Difference (%)
Balloon type 1	0.026	0.017	0.000407	189	265	28.35
Balloon type 2	0.026	0.016	0.000227	1087	960	13.23
Balloon type 3	0.026	0.012	0.000152	2553	2663	4.1

Table 1. Difference between the theoretical and measured levitation times in the case of different balloons

As the table says I get the longest levitation time with the balloon type 3 because it was not so strong and it was already exhausted. In that case was the smallest the difference between the theoretical and the measured time because that describes most the time equation which I have write down for slow flow.
I also measured the connection between the floating time and the volume of the balloon. When the balloon is bigger than the levitation keeps longer. After many measurements I could say that I can lift my set up very long time if the balloon is exhausted, if it has a big volume, if it has a relative small mass, if I lift it on a smooth surface and if I let the air flow out slow. So my maximum levitation time was 44 min 23 sec.

4) Summary

I made actually a toy which is available for everybody, but it also takes us into the world of the physics. I not only investigated the theoretical background of the phenomenon but I also measured the different parameters which can influence the levitation time and I optimized my set up for a maximal load lifting and for a maximal levitation.

Supervisor: Mihály Hömöstrei

5) References

1) Stokesequationin a toy CD hovercraft-Charles de Izarra and Gregoire de Izarra, Eur. J. Phys. 32 (2011) 89–99
2) Viscous Flow in Ducts
available online:
http://www.sfu.ca/~mbahrami/ENSC%20283/Notes/Viscous%20Flow%20in%20Ducts.pdf

Bottles as thick lens

Noel Plaszkó

Supervisors: Ferenc Zámborszky, Mihály Hömöstrei, Mihály Pál

Földes Ferenc Secondary School, Miskolc, Hungary, plaszkonoel@gmail.com

1) The purpose of the investigation

Nowadays, environmental protection is a crucial issue. The bottles left in the nature are highly polluting which is proved by several studies. However, it has not been studied that these may cause fire. Because a fluid-filled bottle can easily work as a thick lens, which focuses the rays of the Sun. In this study it will be examined we can ignite something with the help of a bottle *(Fig. 1.)*.

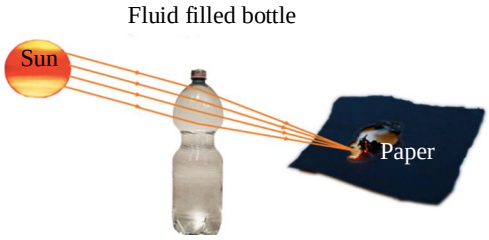

Fig. 5. A bottle focuses the rays of the Sun

2) Methods of the investigations

The problem was investigated theoretically and experimentally [1]. Firstly, the imaging of the thick lens and the conditions for scorching were studied. The differences between a thick lens and a bottle was also investigated. After that theoretical estimation was given for the maximum temperature that we are able to reach by using Stefan's law and simulations (based on Snell's law) were done to determine where the focus area can be found. The estimation is based on the well known solar constant (S_c), and the different weakening effects were also studied, such as atmospheric absorption, reflexion, absorption of the liquid, and that incoming rays are not paraxial rays. For the measurements different bottles and a thermometer with a black body were used *(Fig. 2.)*.

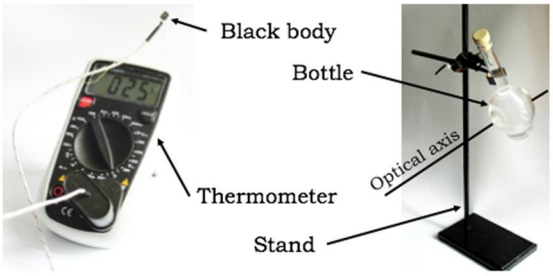

Fig. 6. A bottle focuses the rays of the Sun

Atmospheric absorption was determined by measurement [2]. The temperature was measured in direct sunlight and shade, and the atmospheric absorption coefficient was calculated. It was also investigated how the temperature develops along the optical axis and the plane perpendicular to the optical axis. Finally, different materials were tried to scorch and ignite.

3) Results of the experiment

It was found that the thickness of a bottle is negligible and there is only a small difference between the refractive index of the bottle and the water ($n_{bottle} \approx 1.45$, $n_{water} \approx 1.33$), in this way a bottle can be considered as a thick lens. However, the incoming rays are not paraxial so there is no focal point, only focus area. For scorching approximately 200-250°C is required [3], the aim was to reach this temperature. Based on the simulation we can state that 60% of the total radiation is concentrated in the focus area. 12% of the radiation is reflected and 10% of the radiation is absorbed by the fluid (it was determined by the Beer-Lambert law). The atmospheric absorption coefficient is determined by measurement, using the following equilibrium equation:

$$P_{Sun} + P_{environment} = P_{body} + P_{conduction}$$

where the power of the Sun is given by this formula (α_{atm}: atmospheric absorption coefficient, S_c: solar constant [4]):

$$P_{Sun} = (1 - \alpha_{atm}) \cdot S_c \cdot A_{body}$$

and it was found it is the smallest at noon and 40% of the total radiation is absorbed. On the basis of these and using the equilibrium conditions for power [5]:

$$P_{Sun} + P_{environment} = P_{body} + P_{conduction}$$

the theoretical maximum temperature is approximately 250°C. However, it is only a theoretical estimation. The maximum temperature that I was able to reach with a spherical bottle is 170°C *(Fig. 3.)*.

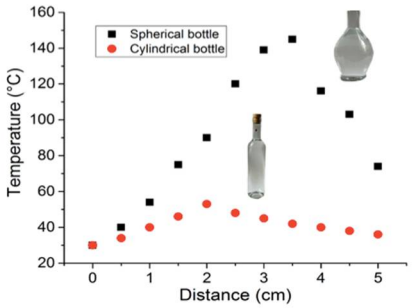

Fig. 3. The temperature along the optical axis in case of a spherical and a cylindrical bottle

Scorching was investigated by this bottle. Here is the table of different material and the success of scorching *(Fig. 4.)*:

Surface	Scorching	Surface	Scorching
Textile	✗	Cardboard	✗
Textile	✓	Cardboard	✗
Textile	✓	Cardboard	✓
Textile	✗	Cardboard	✗
Textile	✓	Cardboard	✗
Uncoated paper	✗	Cardboard	✗
Newspaper	✓	Cardboard	✗
Tobacco	✓	Cardboard	✓

Fig. 4. Darker textiles, cardboards and tobacco can be easily scorched

4) Conclusion

As it can clearly be seen a bottle can easily cause fire. The maximum temperature that we are able to reach is approximately 170°C, which is enough to scorch a surface, but in several case it can ignite something. Dry and rotten leaves can easily catch fire if they are in the focus of this kind of thick lens. This is another reason to never leave a liquid-filled bottle in the nature. They may cause fire.

5) References

[1] Budó-Mátrai: Kísérleti Fizika III. Nemzeti Tankönyvkiadó, Budapest (ISBN 963 18 5969)

[2] APS Laboratory: Measuring the temperature of the sun Researching report
Available online:
http://sbo.colorado.edu/SBO_OLD_SITE/sbo/manuals/apsmanuals/suntemp.pdf

[3] Flammability characteristics of different materials
Available online:
http://tuzvedelem.bloglap.hu/dokumentumok/201401/anyagok_eghetosegi_tulajdonsagai.pdf

[4] Units and symbols in solar energy
Available online:
http://aesl.hanyang.ac.kr/class/are1024/units_and_symbols_in_solar_energy.pdf

[5] Table of total emissivity
Available online:
http://www.monarchserver.com/TableofEmissivity.pdf

ICYS_2016_abstract India (Physics-Design & Static Analysis of Electromagnetic Shock Absorber using electromagnetic induction)

Shikhar Juneja & Vaishali
Ms. Sudha Chand

St. Mark's Senior Secondary Public School, Meera Bagh , New Delhi ,India,
stmarksmb@saintmarksschool.com

The purpose of the investigation

Today, travelling has become a major part of our daily life. Everyone wants to have a comfortable ride, whether in a town or in its outskirts. The repeated jerks experienced by the car results in successive damage to the shockers of the cars further resulting in discomfort. This set us thinking of improving the quality and efficiency of the suspension system by using the principle of Electromagnetism.

Method of the investigation

The first shock absorbers were simply two arms connected by a bolt with a friction disk between them. Its resistance was adjusted by tightening or loosening the bolt. This was followed by the air, fluid and spring shock absorbers. These shock absorbers were not efficient enough for a comfortable ride.

An electromagnetic shocker resembles a telescopic suspension. A permanent strong magnet with same inner diameter of slider is fixed at the base of fork tube. A capacitor plate is fixed just above the permanent magnet connected with positive terminal and an electromagnet (inductor) is fixed at the ends of fork tube and another capacitor plate is attached in front of it connected with negative terminal. The poles of electromagnet and permanent magnet is made same so that they repel each other. The whole system is air tight thus a dielectric medium is created increasing the capacitance. The whole system is connected to a battery eliminator that is being supplied by the vehicle and the capacitors are connected to a rechargeable battery so as to make the circuit economical and ready to use.

Results of the experiment

We believe that this shock absorber will by eradicate the problems caused by the already-in-use shock absorbers due to friction and related factors, this magnetic shock absorber can be used in vehicles carrying variable amount of load.

Conclusion

We conclude that that this type of shock absorber would help the industry to make the ride more efficient and comfortable, also economical and customizable at the same time .Improving on concept we can say that to make these magnetic shock absorbers even better, a chain of more than two permanent magnets can be used to absorb the shocks which will make riding the vehicle more comfortable.

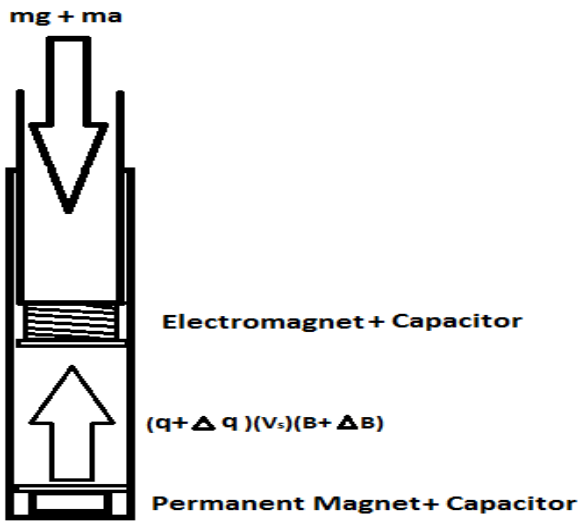

REFERENCES

1. Goldner, R.B., Zerigian, P., and Hull, J.R., "A Preliminary Study of Energy Recovery in Vehicles by Using Regenerative Magnetic Shock Absorbers," SAE Transactions – J.

2. Gupta, A., Various internal communications with Argonne National Laboratory.

3. Graves, K.E., Iovenitti, P.G., and Toneich, D., "Electronic Regenerative Damping in Vehicle Suspension Systems," International Journal of Vehicle Designs, Vol. 24, Nos. 2/3, 2000, pp. 182-197.

3. Suda, Y. and Shiba, T., "A New Hybrid Suspension System with Active Control and Energy Regeneration," Vehicle System Dynamics Supplement, Vol. 25, 1996, pp. 641-654.

4. Karnopp, D. "Permanent Magnet Linear Motors Used as Variable Mechanical Dampers for Vehicle Suspensions," Vehicle System Dynamics, Vol. 18, 1989, pp. 187-200.

Books referred:

1. John C. Dixon, „The Shock Absorber Handbook „, Second Edition , Wiley Professional EngineeringPublishing Series.

2. Tom Denton, "Automobile Electrical and Electronic Systems", Third edition published by Elsevier Butterworth-Heinemann, 2004.

Long Distance Suction Fan Using Tornado Principle

Patricia Tiara Puspitasari
Eko Widiatmoko,S.Si,M.Si.
SMA Santo Aloysius 1, Bandung/Indonesia, patricia_tiara98@yahoo.co.id

1. Introduction

An experiment was conducted to study the suction distance of a fan. An ordinary fan blows air to farther distance than its suction range . For example, a vacuum cleaner should be very close to the floor in order to suck the dust or dirt.

This research focused on creating a new equipment with vents to make circular air motion resembling a tornado that blows the air on the inlet side of the fan. With this apparatus, it is intended to make a suction device which can inhale air from long distance.

2. Problem Statement

The problem to be solved in this research is to find out how the vents affect the air flow to make greater suction distance and how to improve it.

3. Research Methodology

The tornado formation begins with two winds at different direction which meet and form circular air motion. When the radius getting smaller the velocity increases and causes the pressure in the center of the funnels greatly decreases which enable the tornado to suck things.

To imitate this, a construction is made where a fan mounted on a box with the inlet facing upwards encircled by vents at some radius which blew air in a circular motion like a tornado around it (Fig.1). The number of the vents, different vents angle, and box sizes are the variables.

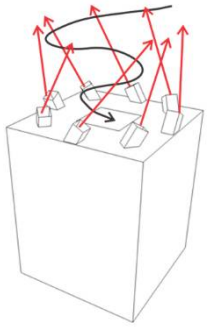

Figure 1. Predicted air flow pattern around suction fan with vents

The suction distance measurement was done by observing smoke stream from a burned tissue paper. It was held on a position above the box (y) to measure the farthest suction distance. Afterwards, the maximum distance of the fan axis to the smoke (x) is measured such that it could be drawn by the fan.

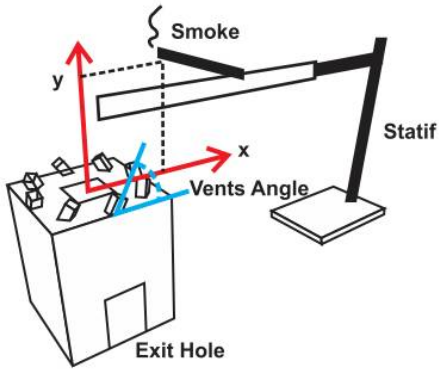

Figure 2. Experiment diagram

4. Result and Analysis

By adding vents to the small suction fan, the maximum distance was increased for the suction fan with 30^o and 45^o vents but not for the 60^o vents. The maximum vertical and horizontal suction distances are 15 cm and 18 cm respectively.

By using the bigger box, the fan could inhale air from 20 cm above the axis and 19 cm radially, while the fan without vents can only inhale air from 10 cm above and 15 cm radially.

Vents at 60^o made the suction area wider while vents at 45^o made the suction area looks like a cone. Vents at 30^o, 20^o, and 10^o made the suction area higher. Another experiment was to place the vents at five and zero degrees, but it did not have higher suction distance. Besides vents angle, the exit hole size also affected the suction distance.

5. Conclusion and Recommendation

Fans with tornadoes were found to have a significantly greater suction distance horizontally and vertically compared to the plain fan system.

The number and the angle of the vents affected the suction distance greatly. The vents at 20^o and 30^o

increased the vertical suction distance by 30-45% for the small suction fan, and 100% for the large suction fan. The improvement also happened in horizontal, although it was not as large as vertical suction distance, which was 27% in the large suction fan with 60^{o} vents.

The result of this experiment can be applied to exhaust fan in large size combined with electrostatic precipitator to relieve smoke problem in forest fire or vacuum cleaner.

References

[1] S. L. Horstmeyer, "Steven Horstmeyer's Tornado Pages," [Online]. Available: http://shorstmeyer.com/tornadoes/scell3.html. [Accessed 9/11/2015].

[2] J. Vasel, "Tornado physics: A terrifying lessons in fluid dynamics," [Online]. Available: http://www.physics.indiana.edu/~dermisek/CM_13/Tornado_Physics_Justin_Vasel.pdf. [Accessed 9/11/2015].

[3] P. A. Tipler, "Mekanika Zat Padat dan Fluida," in Fisika untuk Sains dan Teknik, vol. 1, Jakarta, Indonesia: Erlangga, 1998, pp. 401-404.

[4] H. Thampi, “Interaction of a translating tornado with a low-rise building,” M.S. thesis, Dept. Eng. Math., Iowa State Univ., Ames., Iowa, 2010

A Mechanical Random Number Generator Abstracts of 2016

Meshkat Sadri
Supervisors: Mohammad Mahdi Shariatmadar, Mojgan Issanejad
Farzanegan 2 High School, Tehran/Iran
Accepted and edited by: Araian Young Innovative Minds Institute, AYIMI, www.ayimi.org , info@ayimi.org

1 Introduction

Truly random numbers are a very valuable and rare resource. Design, produce, and test a mechanical device for producing random numbers. Analyse to what extent the randomness produced is safe against tampering. So many ways were in use to generate random numbers until now .There were simple ways like throwing a dice or flipping a coin and some complex ways like lotto machine .Also there are many ways to generate random numbers in computer.

Random numbers are rare, useful and valuable resources and they are used for gambling, statistical sampling, computer simulation, cryptography, completely randomized design, and other areas where producing an unpredictable result is desirable. There are many ways to generate them like mechanical devices as roulette wheels, lotto machine, dice and so on; and the computer methods as defining a function like rand function in quick basic programing language and so on. But how random are they and how can we get sure that no one can cheat?

2 Experiments

To solve this problem two ideas were closer to reality. The first one was to make an icosahedron dice and the second was to prove that a disk gives us numbers randomly. So I have two ways to test the randomness of the numbers; first is the practical way which is to get a large amount of random numbers of the device and calculate the percentage of numbers, and the second is to theoretically prove that they are random. Actually both of them were used to prove that this dice is what the question asked to make.

So I made my icosahedron by magnets and then I put numbers 1 to 20 on its faces. It weights nearly 1kg and its longest diameter is about 8cm and the edges are
4cm. For the first method (to get a large amount of numbers and calculate the percentage of every number), I diced for 640
times.

As we got in the practical way its tolerance of randomness is about 2%. If we use the method of having the highest and the lowest percentage difference as our tolerance, that it should be less than 5%, if we want to assert that it gives us random. The second method is to calculate the average of tolerances of each number. By this way it will become
0.45% and if we want to assert that it's randomly, it
should be less than a limit between 1% and 2% (according to how much random do we expect it to
be); that the dice lives up to this too.

References

1-
http://www.ams.org/samplings/featurecolumn/fcarc-five-polyhedra
2-http://www.cut-the
knot.org/do_you_know/polyhedra

Frisbee vortices

Mohadese Matloub
Supervisors: Mohammad Mahdi Shariatmadar, Mojgan Issanejad
Farzanegan 2 High School, Tehran/Iran
Accepted and edited by: Araian Young Innovative Minds Institute, AYIMI, www.ayimi.org , info@ayimi.org

1 Introduction

When you submerge a large circular disk such as dinner plate vertically and partially into the swimming pool until it covers half of it a pair of interesting vortices is created in the surface of the water. They will persist for long time. They keep going next to each other and the perfect black circle is made on the bottom of pool. If you look from above and dust chalk you can see mushroom spiral pattern is exposed.

2 Experiments

A vortex can be described as a fluid structures that rotating around axis line. When you place a large circular disk, such as dinner plate into a swimming pool the water right next to the plate is moved but the farther water is inert so we have different speeds and when the front water is pulled to the back it is intensified. They can continue going along together, because the vortices want to keep their angular momentum so continue rotating as move to the water but lose some energy because of friction (Fig. 1).

Fig. 1. Experiment shows if the vortices reach the wall they are scattered from each other

Figure 2 shows the velocity contour of the fore going vortices simulated by the software Comsol multiphysics 3.5a.

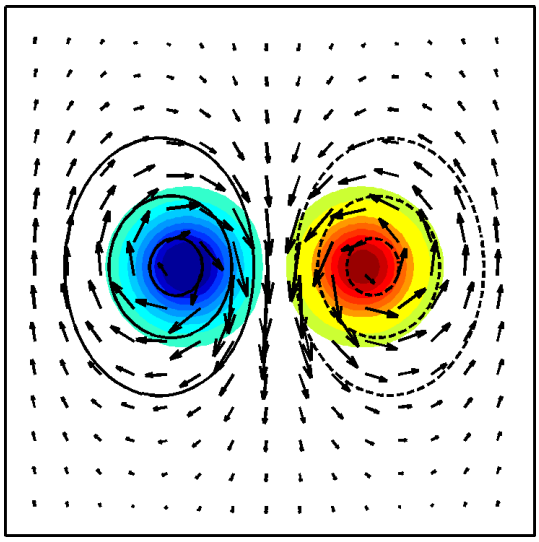

Fig. 2. Velocity contour of vortices

.

Two vortices go along together when the plate is submerging. Figure 3 shows the condition of vortices after formation and reaching a stable condition. The whole pattern is called “mushroom pattern” which is a rotational a linear motion simultaneously.

Fig. 3. The mushroom pattern of vortices motion at stable condition

Some Parameters influence on this phenomenon:

Diameter of the plate,

Viscosity of the fluid,

Temperature,

Shape of the plate

References

1) Experimental evidence for maximal surfaces in a 3 dimensional minkowski space. http//www.cartan.pair.com.
2) Falaco solitons_cosmic strings in a swimming pool. http//www.cartan.pair.com

Hot Water Fountain Phenomenon

Sanaz Nozhati
Farzanegan 1High School , Tehran/Iran
Accepted and edited by: Araian Young Innovative Minds Institute, AYIMI, www.ayimi.org , info@ayimi.org

1 Introduction

If you half fill the pipette with hot water, the water stays at the bottom and the air at room temperature will be in the upper part. Then you block the top end of the pipette with the tip of your finger and turn the pipette upside down, so the hot water starts flowing down to the blocked side. After that you observe the water flowing out from the tip of the pipette. In this paper we investigate the reason and parameters affecting this phenomenon.

2 Experiments

We did our experiments by a pipette (41.4ml volume) filled with different amounts of water and measured the amount of the water which came out from the pipette and calculated the initial and the final volume of the air in the pipette, then the results were compared with what the Ideal Gas Law predicts. But as shown in fig.1 this phenomenon cannot be justified with the Ideal Gas Law.

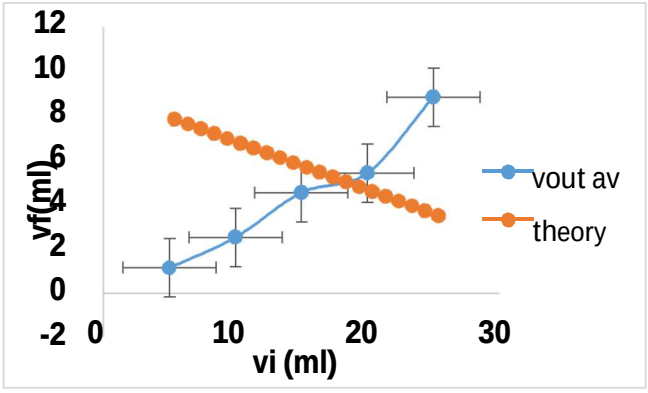

Fig.1.The initial volume of the air versus the final volume

The amount of emerging water from the pipette was investigated by increasing the initial volume of the water and also water temperature in several experiments.

3. Conclusion

Our experiments were compared with a reasonable theory to justify this phenomenon by consideration the effects of the saturated vapour pressure.

The Heinrich Rubens experiment in the 3D model

Dawid Lipski

Supervisor: Urszula Woźnikowska-Bezak
IV Liceum Ogólnokształcące im. Orląt Lwowskich in Gliwice

Creative Group QUARK, The Youth Palace in Katowice, Poland; email: dawidlipsk8@gmail.com

1 Introduction

The Rubens flame tube is a demonstration which is over 100 years old and which allows the observers to visualize acoustic standing wave behavior. Flame gas inside the tube flows through holes drilled on the top, and flames are then lit above. The tube is closed at one end and is driven with a loudspeaker at the other end. When the tube is driven at one of its resonance frequencies, the flames form a visual standing wave pattern as they vary in height according to the pressure amplitude in the tube. I did this experiment but in the box.

2 Theoretical part

The objective of my experiment was to observe the waves Rising a flammable gaseous medium. I calculated and determined through experimentation the frequencies that resonated in a Ruben's Box, causing standing waves to be established. I calculated standing waves from a formula for modes in cubes.

$$f = \frac{V_s}{2}\sqrt{\left(\frac{n}{l_x}\right)^2 + \left(\frac{n}{l_y}\right)^2 + \left(\frac{n}{l_z}\right)^2}$$

3 Experiment

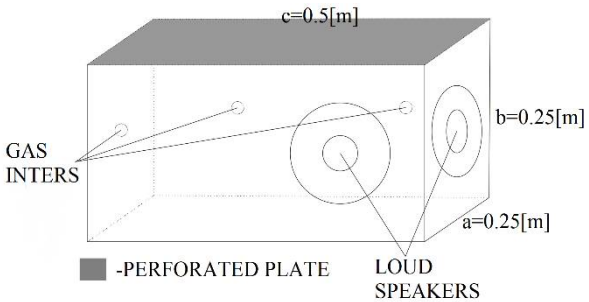

Fig.(1).Scheme of the box.

3.1 Relevant parameters

To create my Rubens box I used 4 metal plates 0,25[m]x0,5[m] and 2 metal plates 0,25[m]x0,25[m], 2 loudspeakers, 3 gas inters and Arduino Uno. Inside I entered thermometer and Pressure sensor connected to Arduino. To do my experiment I had to use my box 1 bottle with propane-butane, tone generator with amplifier and laptop.

3.2 Results

In my experiment I calculated: velocity of sound, resonance, acoustic modes and acoustic impedance of the box. But everything depends on of the temperature in the box because when gas is burning on the top the gas heats up. We can see the temperature in the chart Fig.(2).

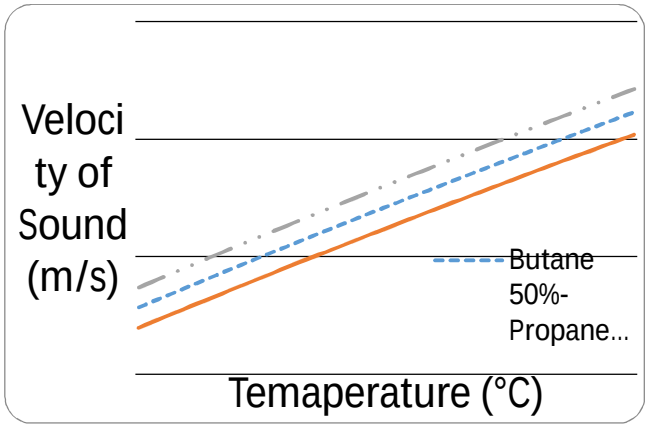

Fig.(2).The chart of velocity of sound vs. temperature.

To calculations in my experiment I used propane-butane in proportions 50%-50%. I conclude that temperature increases very fast and has big impact on all the parameters.

3.3 Dancing flames

It looks impressive when flames are dancing on the top box. However, it is very hard to obtain and keep a standing wave, because the frequency of the mode is dependent on the temperature and the temperature increases very fast.

4 Conclusion

During my research I found out many important dependencies. The temperature is the most important factor and the box works well only for high acoustic modes.

6 References

[1] Z. Żyszkowski: *Podstawy elektroakustyki.* Wydawnictwo naukowo techniczne, Warszawa, 1984r., Wydanie 3

[2] Program WolframAlpha|PRO®© 2016

[3] Morse P.M., Ingard K.U. : Theroretical acoustics. New york, McGraw-Hill 1968.

DEVICE THAT GENERATES ELECTRICITY WITH NOISE BASED ON THE PIEZOELECTRIC EFFECT

Dominik Romanów

Supervisor: mgr Grzegorz Cuber

I Liceum Ogólnokształcące im. I.J. Paderewskiego in Knurów,
Creative Group QUARK, The Youth Palace in Katowice, Poland

1. Introduction

Nowadays the development of our civilization rushes forward. It all happens thanks to the new technologies. My idea is to create a device that generates electric energy from noise with the use of piezoelectric effect.

2. Theoretical part

Principle of operation of my device is based on the piezoelectric effect. Quartz - building blocks of piezoelectric changes its dimension under the influence of electric field and vice versa- it generates electrical charge as a result of mechanical deformation. In my device I used this property.

Sound is an auditory sensation caused by acoustic wave spreading in the solid, liquid or gas. Frequencies of waves audible by human beings are from 16Hz to 20kHz.

3. Experimental part

3.1 Essential parameters

To create the proper source of noise I used the guitar amplifier and the Frequency sound Generator in the form of a phone app. Using this generator I produced the sound in the range of frequency from 20Hz to 70Hz, obtaining characteristic amplitude frequency of the tested setup. I obtained the biggest value at the frequency of 42Hz. In the project I used the piezo converter of 35mm diameter, crystal of 25mm diameter with soldered wires.

3.2 How the device works

When we make the converter vibrate, it generates variable voltage with the frequency that depends on the frequency of vibrations. That's why to power a diode I added the Graetz's bridge. It is a system that consists of four diodes thanks to which variable voltage transforms into constant voltage. The connected capacitor stabilizes the voltage and that makes the diode shine fluently (without pulsing) (see Fig.1). The output voltage under the system and diode loading is 2.64V. Without load it ranges from 3.5V up to 6V. The capacitor charges up to 16V.

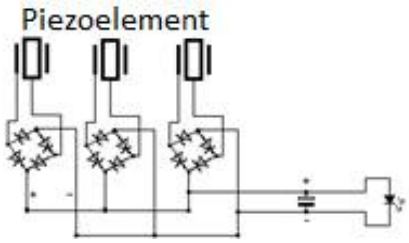

Fig.1 Schematic layout of my device

When building the device I was inspired by the ear construction. As a receiver of vibrations I used silver-gold foil stretched over the ring of a bike's rim. This way I made a membrane (an equivalent to an eardrum). As a repeater of the vibrations I've chosen a steel ball with a diameter of 8mm (an equivalent of a hammer in an ear). A bottle cap played a role of an anvil (see Fig.2). As a strip I used a steel tape 230mm long and 15mm wide. The device was placed in the distance of 30cm from the speaker. The frequency given was 42 Hz. It can be found within the range of frequency of a hammer drill. As the result I succeeded obtaining a light-emitting diode.

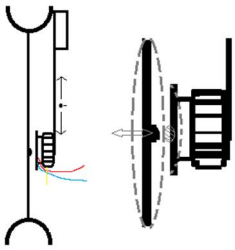

Fig.2 Schematic representation of my device.

4. Summary

The benefit of this device is that it was made of renewable materials and that it creates energy from the renewable source - noise. In the future the device can be upgraded by adding professional electronic setup. This and similar devices could be used to illuminate the airport runways.

Bibliography

https://pl.wikipedia.org/wiki/D%C5%BAwi%C4%99k

http://www.e-spawalnik.pl/?krotka-teoria-piezoelektrycznosci,263

Circularly excited pendulum

Karol Białas

Supervisor: Urszula Woźnikowska-Bezak

II Liceum Ogólnokształcące im. Stefana Żeromskiego in Dąbrowa Górnicza
Creative Group QUARK, The Youth Palace in Katowice, Poland; email: zygzak-1998@o2.pl

5 Purpose of the investigation

A simple pendulum whose support point is moving along horizontal circumference can trace circles whose radius is smaller than the radius of support point trajectory. It only happens when certain conditions are met. Purpose of my investigation was to determine these conditions.

6 Theoretical part

In order to study the motion of said pendulum I wrote its equations of motion using Lagrangian formalism.

θ_1 is a position angle of support point, θ_2 position angle of the bob (horizontal) and θ_3 is an angle between thread and a vertical axis. Those equations can only be solved numerically. I have solved them in Sage environment. After plotting results I found out that motion of the bob is very similar to motion of pendulum with horizontal oscillating support because circular motion can be described as superposition of 2 perpendicular oscillations with equal amplitudes, angular frequencies and with phase difference 0.5π. When angular frequency of support point's oscillation is much bigger than natural frequency of pendulum bob will be almost at rest.

$$\frac{d}{dt}\left(\frac{\partial L}{\partial \dot{q}_j}\right) - \frac{\partial L}{\partial q_j} + \frac{\partial R}{\partial \dot{q}_j} = 0$$

7 Experimental part

I have built my own Circularly excited pendulum, it consists of bob and strong thread attached to engine-powered rotating disc. This experimental setup allowed me to conduct wide range of experiments. I varied not only support point's angular frequency, but also length of thread and radius of support point. After series of experiments I could determine how each parameter affects the motion of bob.

7.1 Motion of bob

After analysis of motion I have concluded that when support point reaches certain value of angular frequency further increasing of it will not affect bob's trajectories. This certain value depends only on pendulum's length and radius support point. When this condition is met bob behaves very similarly to pendulum whose support point is not moving.

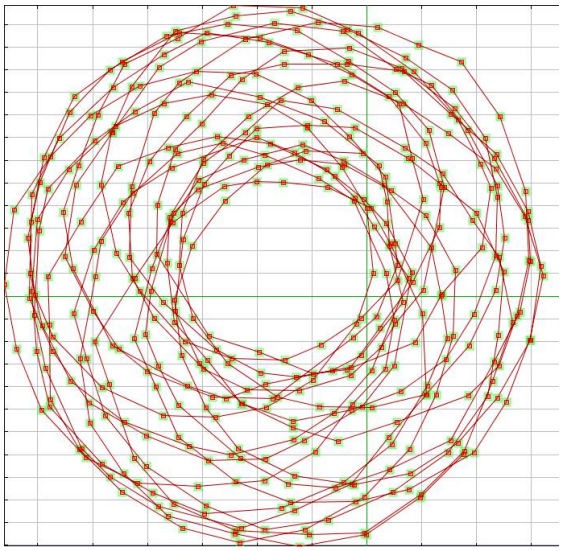

Trajectory example

7.2 Attractors of the system

This system has 2 attractors. First one is an orbit which pendulum would follow due to centrifugal force. Second one is an effect of difference of frequencies. This attractor also is circle shaped and radius of this circle depends on the driving frequency, when this frequency is high enough we can assume that second attractor is a point on rotation axis.

8 Conclusions

"Lagging effect" is caused by frequency difference and

when driving frequency is high enough bob behaves similarly to simple unperturbed pendulum.

9 References

- W. Rubinowicz, W. Królikowski: *Mechanika teoretyczna, wyd.9 Warszawa:* Wydawnictwo Naukowe PWN, 2012

-G. Gonzalez. A pendulum with moving support point (2006), http://www.phys.lsu.edu/faculty/gonzalez/Teaching/Phys7221/PendulumWithMovingSupport.pdf

-Erik Mahieu. Pendulum with Rotating Pivot (demonstrations.wolfram.com), http://demonstrations.wolfram.com/PendulumWithRotatingPivot/

Van der Pauw Method

Przemysław Słota

Supervisor: Urszula Woźnikowska-Bezak

Creative Group QUARK, The Youth Palace in Katowice, Poland

10 Introduction

In 1958 L. J. van der Pauw introduced a new method of measuring electrical properties of a sample. The method uses only four contacts to measure resistivity and hall coefficient of the sample.

11 Theoretical part

The method requires that:

- The sample is simply connected;
- The sample has 4 point contacts on its edge;
- The contacts are points (or at least one order of magnitude smaller than the sample).

The sample does not have to form a particular shape, but for shapes are commonly used (a Greek cross, a disk/cloverleaf, a square/rectangle and a bridge

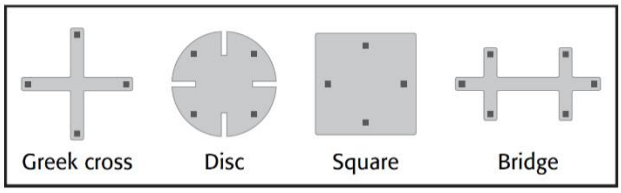

(especially for Hall's effect measurements)).

Fig. 1. Forms of the sample (darker dots indicate contacts).

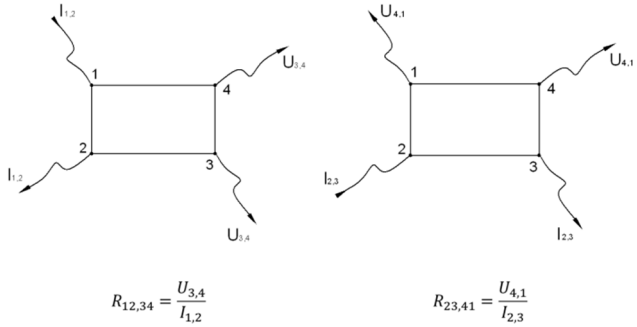

Fig. 2. Connections for measurement.

From a theoretical derivation we obtain a formula:

$$\exp\left(\frac{-\pi d}{\rho} R_{12,34}\right) + \exp\left(\frac{-\pi d}{\rho} R_{23,41}\right) = 1$$

12 Experimental part

12.1 Measurement of rectangular sample

To check if the method is applicable for measurements of a rectangular sample a measurement circuit was built. A low-noise opamp was used to gain the output voltage. Then the formulate was solved numerically using WolframAlpha®. After analyzing the inaccuracies the results are comparable with given values.

For copper plate: $\rho = 1.85 \cdot 10^{-8} \Omega m$

When: $\rho_{Cu} = 1.72 \cdot 10^{-8} \Omega m$

12.2 Measurement of circular sample with a hole

Fig. 3. The circular plate used for experiments.

For examining the influence of holes on the results obtained using this method, a circular plate was

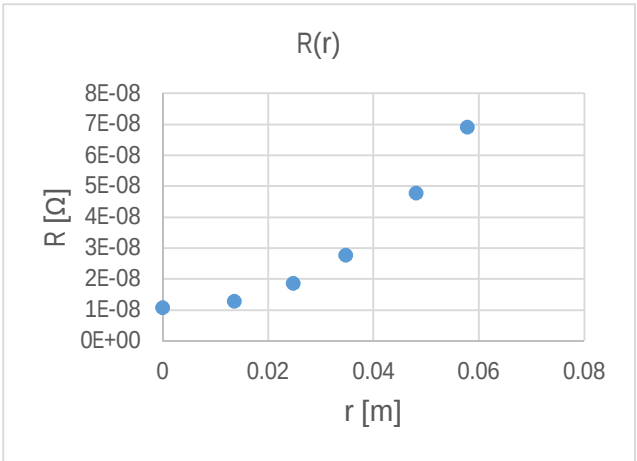

made and several circles where step-by-step etched on its surface. The dependency is shown below:

13 Conclusions

- After analyzing the inaccuracies of measurements the results are comparable with expected values;
- A hole in the sample causes the value of calculated resistivity to increase.

14 Future research

- Simulation of current distribution in the plate;
- Study on the influence of holes in the plate on the results of measurements;
- Determination of correction coefficients for different holes.

15 References

- L. J. van der Pauw. Philips Techn. Rev. 20, 220–224 (1958);
- D. W. Koon and C. J. Knickerbocker. What do you measure when you measure resistivity? Rev. Sci. Instrum. 63, 1, 207-210 (1992).

How does a laboratory have room on a chip?

Batiz Orsolya Bernadett[1]

Tóth Anna Borbála[2], *Holczer Eszter*[2], *Fürjes Péter*[2]

Apáczai Csere János High School, Cluj-Napoca/Romania, bbbotty@yahoo.com
HAS Centre for Energy Research – Institute of Technical Physics and Materials Science (MTA EK MFA)

Introduction and purpose of the study

I started working on this project during the summer of 2015 in a science camp organized by the MTA EK Institute of Technical Physics and Materials Science in Budapest. I participated in an on-line competition in which 23 students were selected to attend the camp. With my 22 colleagues we worked in different laboratories for a week, where our project leaders supervised our activity. In February 2016, I returned to Budapest to continue my experiments, as I couldn't find the equipment needed for them in Cluj-Napoca. My project leaders guided me in using the laboratory infrastructure again, and assisted me in doing the experiments.

In summer, I personally got to work in the microfluidics laboratory, where I got to make my own lab-on-a-chip. The purpose of my study is to experimentally characterise the specific behavior of a microscale lab-on-a-chip system and to establish adequate explanations of the revealed physical phenomena of fluids in microfluidic structures.

Methods of investigation

In order to start the investigation, I had to prepare the chip. Firstly, I designed the mask-layout (plan of the fluidic channels) for manufacturing lithographic mask on computer. Then, I coated a silicon wafer with special photosensitive layer. I lit the coated wafer by UV light through the mask and since I used negative tone photoresist, the radiated region of the coating was polymerised and became non-removable. After that, I poured polydimethyl-siloxane (PDMS – Dow Corning) [1] on the wafer applied as moulding replica and waited until it polymerized [2]. I peeled, cut and punched the PDMS to form uniform chips, and then I bonded the chips onto glass slides by using oxygen-plasma activation.

I made four different chips in two sets, depending on the experiments planned. One of the mask-layouts is presented in Fig. 1. Basically, the chips made on the same set have only minor differences, because they were used to test the different aspects of the same experiment. I applied inverted fluorescence microscope (Zeiss AxioVert A1) [3] with camera to record photos and I processed them by Zeiss Zen [3] and Image J [4] image analysis softwares. I performed experiments regarding continuous flow and droplet-based microfluidics, also.

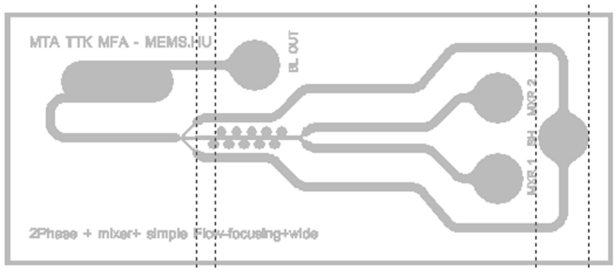

Fig. 1. Mask-layout of one of the chips I made

The continuous-flow microfluidics [5] can describe the behavior of mixed liquids having similar viscosity. In the first experiment I tested how a fluid can be focused to a certain size in a micro-channel. I used water as sheath fluid and diluted fluorescent human serum albumin (HSA – Sigma Aldrich) [6] solution as sample liquid. I analyzed the width of the HSA stream as function of the sheath flow-rate.

In the second experiment I tested the mixing process of two fluids in continuous flow and droplet based microfluidic system. I used fluorescently (quinine) painted liquid [7], and water for continuous mixing and silicon oil (a fluid with high viscosity) as sheath flow for droplet generation. In this case the two fluids would not mix with the oil due to their different viscosity. I made fluorescence intensity profiles and compared the mixing effects in continuous streams and droplets.

My first experiment regarding droplet-based microfluidics [8] focused on the generation of droplets. Droplet-based microfluidics analyzes the behavior of liquids with different viscosity, as water and oil. I examined the diameter dependence of the droplets on the oil flow rate, in order to determine the optimal rate of the sheath fluid applicable to form droplets with uniform size.

The second experiment here was also the mixing of two fluids, but in this case, the mixture was formed in micro-droplets. The intensity profiles I made show that mixing in droplets is more efficient than in a simple laminar system. After making the intensity profiles, I also calculated the relative concentration distribution in the droplet.

Results of experiments

In continuous-flow microfluidics the experiment with liquid focusing showed that the higher the speed of the water, the narrower the HSA beam gets. The graph below shows the width of the focused liquid depending on the rate of the water and HSA speed. The HSA speed was constant, firstly 0,6 µL/s and then 0,4 µL/s, the speed of the water was changed by 0,2 µL/s firstly from 0,6 to 3 µL/s, then from 0,4 to 2 µL/s. So fluid-focusing to a certain size is possible on a chip as presented in Fig. 2.

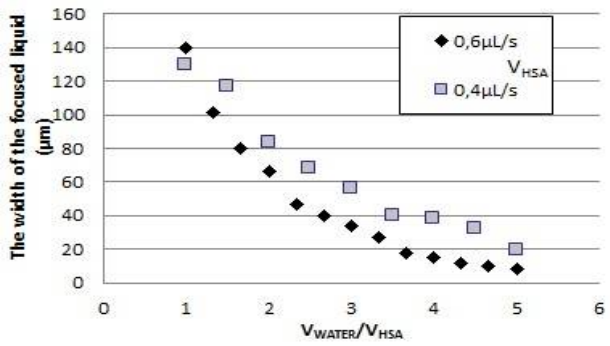

Fig. 2. Width of focused sample as the function of flow rate ratios

The second experiment with mixing two fluids of similar viscosity in a simple microfluidic system showed that this kind of mixing process is very inefficient due to the laminar flow, and extremely long mixing distance is needed.

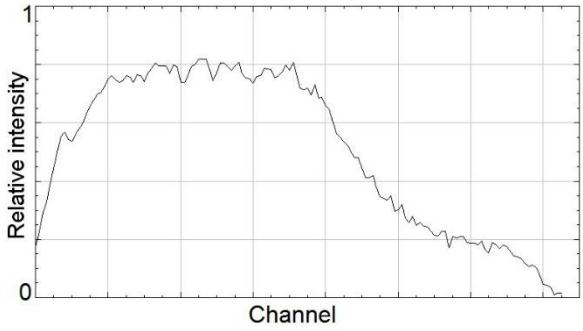

Fig. 3. Relative concentration distribution of the fluorescent sample in straight channel.

The first experiment I made regarding droplet-based microfluidics shows that the higher the flow-rate of the oil, the smaller the diameter of droplets. We can determine the optimal rate of the sheath fluid for proper sized droplets to be formed. I calculated the average droplet-diameter from the diameter of approximately 25-30 droplets (Fig. 4).

The second experiment here showed (Fig. 5) that the mixing process in a droplet is much more efficient than in laminar flow systems. Mixing fluids or stirring solutions to enhance homogeneity or to accelerate a chemical reaction is easier and faster due to the extremely small size of the droplets (pL).

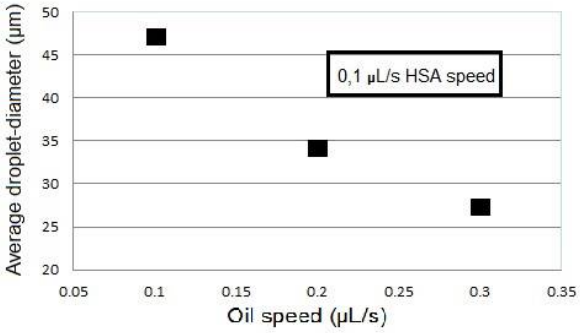

Fig. 4. Droplet diameter as the function of oil flow rate

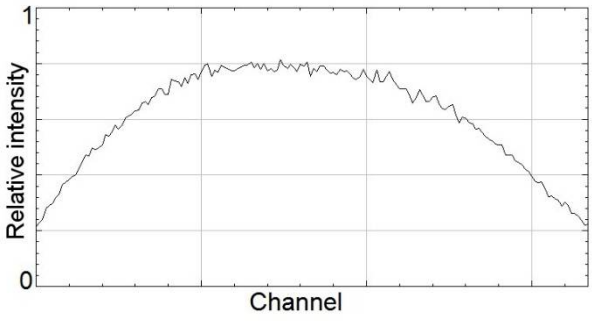

Fig. 5. Relative concentration distribution of the fluorescent sample in micro-droplets

Conclusion

I proved that a laboratory can really exist on a chip containing fluid-focusing, droplet generating microfluidic systems or even nanoreactors.

Fluids can be focused to a certain size, depending on their flow rate in the channel system.

Proper-sized droplets can also be formed depending on the flow rates.

Mixing of fluids is critical in microscale, due to laminar flow, yet faster inside the droplets due to the extremely small amount of reagents.

Lab-on-a-chip systems are a great improvement in research, because this way the micro-scale analysis and processing of fluids is made possible and it can be applied in physical, chemical, biomedical fields as well.

References

[1] http://www.dowcorning.com

[2] Whitesides, G. M., Nature, 2006, **442**, 368-373.

[3] http://www.zeiss.com/microscopy/

[4] http://imagej.nih.gov/ij/

[5] https://en.wikipedia.org/wiki/Microfluidics

[6] http://www.sigmaaldrich.com/

[7] https://pubchem.ncbi.nlm.nih.gov/compound/Quinine

[8] Shia-Yen The, Lab Chip, 2008, **8**, 198-220

The Measurement of Electrical Signals in Plants

Filip Lupaș, Andrei Colhon, Dragoș Tuluc, Georgiana Pușcaș, Farauanu Emanuel
"Emil Racoviță" National College

Our Purpose

During the last hundred years scientists have managed to measure the stimulus-induced systemic change in membrane potential, also known as variation potential[1]. Usually the voltage output from the electrodes attached to the plant is passed to a high-impedance two channel amplifier. Such devices are usually too big for carrying around, and as our first objective was to use plants in the wild as live sensors for collecting data about the pollution, precipitation quantity or potential fires, we chose to build our own custom-made portable measurement device so that we would be able to use it anywhere on the field. After some trial and error, we have managed to achieve building the needed device.

Method of Realization

Our homemade electrometer is a high impedance device used to measure the surface potential on leaves. The full features of this device are:

- 100TOhm input impedance
- aluminum case
- BNC input terminals
- two stage adjustable gain (10-10000)
- auto zero leveling
- SD card slot for recordings
- live data feed through USB

The electrometer is built using high quality components, in order to minimize the overall temperature over time drift. We need to remember that this device is used for long time measurements, therefore any change in temperature could induce incorrect data. We chose BNC connectors for easy compatibility with other cables and electrodes. The auto-zeroing function is mainly used to ease later data processing (no hysteresis is applied) and the SD card feature is used in case of remote measuring, where no PC or power are available (this device can run from a standard 9V battery).

Our device uses a CMOS buffer for each channel, in order to keep the total input bias current to a minimum (10fA). The internal construction is floating on ceramic supports to prevent any leakage of current through the printed circuit board or other components. A differential amplifier is used afterwards in order to get the voltage difference between the electrodes, value which will be amplified later by the second stage amplifier; it represents the absolute value of the transmembrane potential. This value is then taken by an ADC and converted into a digital signal. This is done to maintain the quality of the signal over long cables. At the end, a computer is connected via USB to analyze and store the data. During the experiment, several conditions need to be accomplished to ensure relevant data.

- wounding must be reproducible
- leaves must be fixed and undamaged
- the plant should be watered the day before the experiment
- temperature and light intensity must not fluctuate

Results of the preliminary Experiment

We did a set of measurements using a potentiostat, in order to see the form of the signal that we wanted to obtain through measuring with our own device. We have used platinum wires as electrodes, KCl to facilitate the contact between the leaf and the electrode, and of screened wires to avoid unwanted noise. The software which was used to make a live graph from the received data of the potentiostat does not allow the recording of incoming signal, so we had to use screen capture software to obtain the graph. The graph was plotted using the potential variation derived by time on the Y axis and the time itself on the

[1] **"Characterization of the Variation Potential in Sunflower"** by Bratislav Stankovik, Tadeusz Zawadzki, and Eric Davies

X axis. The results were immediate, as soon as we induced pain into the plant, using a variety of stimuli the variation potential could be observed in real time as the graph was plotted. One of the first details that resulted from our measurements was that the potential variation rose if our stimuli was more intense. This provoked a question about the possible correlation between the intensity of the harmful stimuli and the stimulus-induced systemic change in membrane potential. Our main obstacle in determining this correlation was the fact that we were not sure about the precision of our collected data. Therefore we are waiting to do our second set of experiments using the device we have built, as it still needs some small adjustments.

Correlation between a Natural Dielectric Lens and a Transmitarray Lens

Chua Xian Wei[1,*]
Chia Boon Khim Kerrell[2], *Chia Tse Tong*[2], *Tan Guoxian*[1]
[1]*Raffles Institution,* [2]*DSO, Singapore, *chua_xian_wei@hotmail.com*

1 Introduction

Conventional dielectric lenses rely on accumulation of phase delay during wave propagation to produce a desired wavefront. By considering the required phase delay at each lens position, an 'equivalent' transmitarray can be obtained. This paper has adopted a 'proof-of-concept' approach in correlating the performance of a conventional and transmitarray lens, both operating at 8 GHz. Such transmitarray lenses find useful applications in satellite communication, automotive radar and imaging systems, due to their characteristics of high-gain, lightweight, easier fabrication and low-profile.

2 Design Methodology of Natural Dielectric Lens

Firstly, the design of a conventional spherical biconvex lens is proposed using geometric optics. By considering the phase delay experienced by a wave passing through a dielectric lens and the thickness function of the lens, the required phase delay as a function of the lens position is derived.

3 Design Methodology of an 'Equivalent' Transmitarray Lens

Secondly, to design a corresponding transmitarray antenna, the unit cell element is first designed. A square loop element is chosen due to stability of frequency response under various incident angles. A concentric ring is added to maximize phase shift per layer. The geometrical model of the double square ring element is shown in Fig. 1. The gap S between the inner and outer rings was varied to obtain a design S-curve with a slow rate of phase increment with respect to the change in the geometrical dimensions in the unit cell element. Four identical layers, separated by an air gap and each backed by a dielectric substrate, as shown in Fig. 2, were required to achieve a 360° phase range.

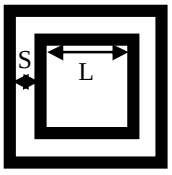

Figure 1. Design parameters of unit cell

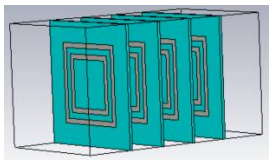

Figure 2. Four identical layers in a unit cell

The unit cell periodicity was kept at $\lambda_0/3$ = 12.5 mm to reduce grating lobes and sensitivity to incident angles. The simulation was run with finite integration technique (FIT) in CST Microwave Studio. A normal incidence plane wave was used to illuminate the unit cell element, and unit cell boundary condition was used to simulate an infinite array. The transmission *phase* and *magnitude* of the unit cell element as a function of L, the dimension of the innermost ring, are plotted in Fig. 3 and 4. L of the innermost ring was chosen to be between 0.983 and 4.904 mm, to correspond to the gentler part of the S-curve while maintaining transmission loss below 2.32 dB.

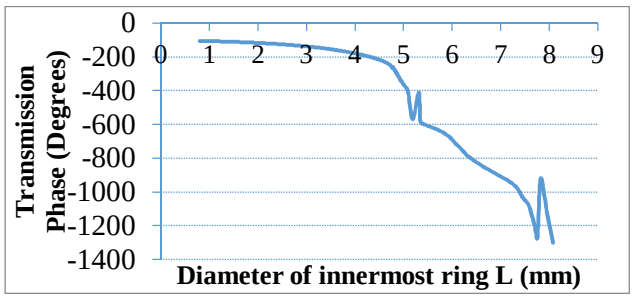

Figure 3. Transmission phase against L of innermost ring

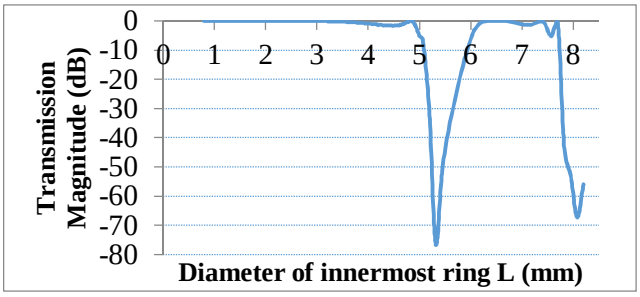

Figure 4. Transmission magnitude against L of innermost ring

The transmitarray is then designed by discretizing the ideal phase profile in the natural dielectric lens and

considering the phase shift at the centre of each unit cell.

4 Correlation and Comparison of Performance of Both Lenses

The simulation results of the *phase* and *amplitude* plots of the E-field for both the natural dielectric lens and transmitarray in the $x = 0$ plane are presented in Fig. 5 and Fig. 6, respectively. Both lenses are illuminated by an electric dipole placed at the focal point.

The results show the transmitarray mimics the dielectric lens in focusing, though with a greater spread of energy, while having the merits of a flat and thin profile, lightweight and easier fabrication. This provides a methodology in designing artificial dielectric lenses using periodic array.

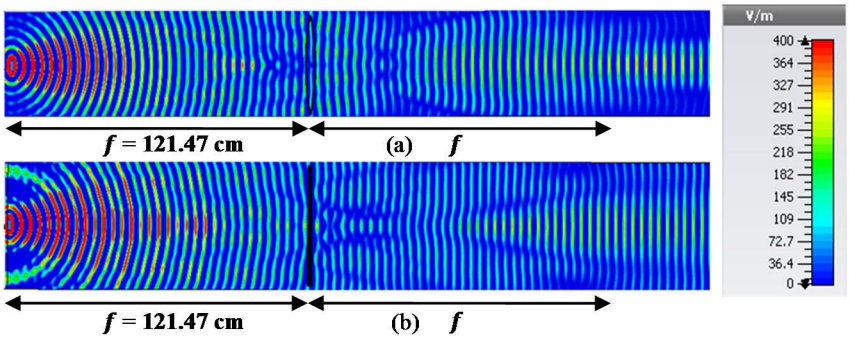

Figure 5. Phase plot of E-field of (a) natural dielectric lens and (b) transmitarray at $x = 0$ plane

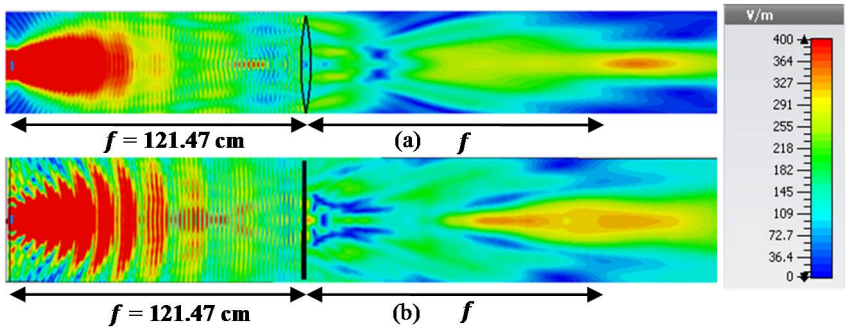

Figure 6. Amplitude plot of E-field of (a) natural dielectric lens and (b) transmitarray at $x = 0$ plane

5 Discussion of Simulation Results

To explain discrepancies in the results, the validity of infinite array and normally-incident plane wave assumptions used in the simulation of unit cell elements, as well as the following factors, are discussed: (1) coupling between neighboring elements changes towards edge of the transmitarray, thus altering approximate phases; (2) diffraction at lens edges due to finite size of transmitarray; (3) oblique incident angles affecting transmission magnitude and phase of edge elements.

To discuss transmission losses due to lens reflection, the reflection magnitude against L of innermost ring of the transmitarray was plotted. For our transmitarray, there is greater reflection for centre elements and multiple reflections between each of the 4 layers. We suggest that an advantage of the transmitarray approach is that the reflection magnitude can be determined from the simulation of the unit cell and incorporated as another design parameter.

Lens aberration is also discussed. A flat transmitarray is advantageous over conventional dielectric lenses as it does not show spherical aberrations due to lack of curved surfaces. Chromatic aberration of the transmitarray is investigated by plotting a 3D plot of the phase delay at various lens positions for other frequencies, using the S-curve of the unit cell. It is shown that as operation frequency decreases, focal length increases, similar to the phenomenon in traditional dielectric lenses.

6 Future Extensions

For future extensions, fabrication and measurement of our transmitarray is proposed, to allow for comparison with simulation results. We suggest that ohmic and dielectric losses will lead to even smaller radiation

efficiency than simulated, and manufacturing tolerances will result in phase errors in wavefront compensation. We also propose the use of an equivalent-circuit model to analyse our unit cell element, in order to design broader bandwidth and multiple bands transmitarrays.

7 References

[1] Nematollahi, H., Laurin J.J., Page, J.E., Encinar, J.A. (2015, April). Design of Broadband Transmitarray Unit Cells with Comparative Study of Different Number of Layers. IEEE Transactions on Antennas and Propagation, 63(4), 2946-2957.

[2] Zainud-Deen, S.H., Hassan, W.M., Malhat, H.A. & Awadalla, K.H. (2015, February) Radiation characteristics enhancement of dielectric resonator antenna using solid/discrete dielectric lenses. Advanced Electromagnetics, 4(1).

[3] Kaouach, H., Dussopt, L., Sauleau, R. & Koleck, T. (2009, March). Design and demonstration of an X-band transmit-array. 3rd European Conference on Antennas and Propagation, 1191-1195.

[4] Zhou, S., Wang, Z., & Feng, Y. (2012, May). Optimal Design of Wideband Microwave Absorber Consisting of Resistive Meta-Surface Layers. Journal of Electromagnetic Analysis and Applications, 4, 187-191. doi:10.4236/jemaa.2012.45025

[5] Wang, Y., Deguchi, H. & Tsuji, M. (2012, July). A broadband flat lens based on aperture-coupled patch FSSs with four-pole resonant behaviour. 2012 IEEE Antennas and Propagation Society International Symposium, 1-2.

[6] Silver, S. (Eds.). (1949). Microwave antenna theory and design. IEEE Electromagnetic Wave Series.

[7] Erdil, E., Topalli, K., Zorlu, O. & Toral, T. (2013, April). A reconfigurable microfluidic transmitarray unit cell. 2013 7th European Conference on Antennas and Propagation, 2957-2960.

[8] He, Y. & Eleftheriades, G.V. (2014). Rotated infrared antenna transmitarray for the manipulation of circularly polarized wavefronts. EPJ Appl. Metamat. 2014, 1(8). doi: 0.1051/epjam/2015002

[9] Rajagopalan, H., & Rahmat-Samii, Y. (2011, August). Reflectarray Antennas: An Intuitive Explanation of Reflection Phase Behavior. General Assembly and Scientific Symposium, 2011 XXXth URSI, 1-4. doi:10.1109/URSIGASS.2011.6050485

[10] Goodman, J. (2005). Introduction to Fourier Optics (3rd ed.).

[11] Hecht, E. (2002). Optics (4th ed., pp. 149-165). San Francisco: Addison Wisley.

[18] Abdelrahman, A.H., Nayeri, P., Elsherbeni, A.Z., Yang, F. (2015, July). Bandwidth Improvement Methods of Transmitarray Antennas. IEEE Transactions on Antennas and Propagation, 63(7), 2946-2957.

RUNNING SPEED MEASURED BY USING THE SIGNAL GENERATED FROM OSCILLATING MAGNET IN COIL

Mr.Thatthep Rukpanich
Asst. Prof. Dr. Worawat Meevasana, Mr.Nateethorn Nuchklang, and Mr.Worapot Bothpiboon
Rajsima Wittayalai School, Nakornratchsrima, Thailand, thatthep8436@hotmail.com

1. Introduction:

Oscillating magnets in coil will induce to generate the electrical signal. Moreover, Different magnet-oscillating pattern will generate different pattern of signal.

In this research work, we analyze the electrical signal generated from the movement of the magnet in coil which attaches to one shoe. When running, the magnet will oscillate and the electrical signal measured by oscilloscope shows a unique pattern which can be effectively converted to the running speed.

2. Objective:

The purpose of this research work is to create a device for measuring the running speed by using the generated signal from electromagnetic induction principle.

3. Methodology:

We separate our experiments into 2 parts:

1st Experiment: "The best number of magnet"

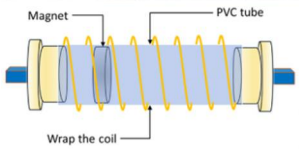

We wrapped a long wire around the PVC tube; the two ends were then connected to a multimeter. Then the device was put on a shaking machine. Then we measured the generated voltage differences generated due to the induction when put a different number of magnets into the tube.

Finally, we selected the best number of magnets which gave the highest voltage under the same condition, i.e. the device would give the highest efficiency. We then used this configuration for the 2nd experiment.

2nd Experiment: "Signal and the running speed"

We attached the same device in the 1st experiment (i.e. the magnet inside the electrical coil) to a running shoe and then connected the two ends of the wire to an oscilloscope.

After that, we got on a treadmill that we can adjust the velocity. Then we record the signal on the oscilloscope while running and analyze the signal software Igor Pro.

How a device can measure the running speed:

- Consider to find the EMF from oscillating magnet in a round of coil

$$\varepsilon(z) = \frac{d\Phi}{dt} = \frac{d}{dt}\int B_{av}(z)dA$$

$$= \frac{dz}{dt}\int \frac{dB(z)}{dz}dA$$

$$= v_z \int \frac{dB(z)}{dz}dA$$

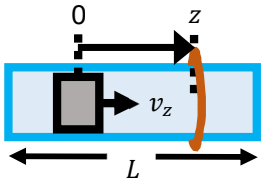

The equation show that $\varepsilon(z) \propto v_z$(speed of magnet)

- Consider to find the EMF from oscillating magnet but in the continuous coil

$$\varepsilon_{all} = \int_{l-L}^{l} n\,\varepsilon(z)dz$$

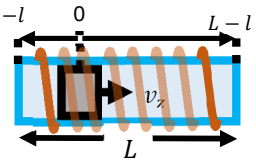

If the running speed (V) increase, the speed of magnet (v_z) will increase as well.

In a round of coil and the continuous coil, the equation show that $EMF \propto$ speed of magnet. Speed of magnets will actually depend on running speed. So, we can know the running speed from measuring the EMF.

Results:

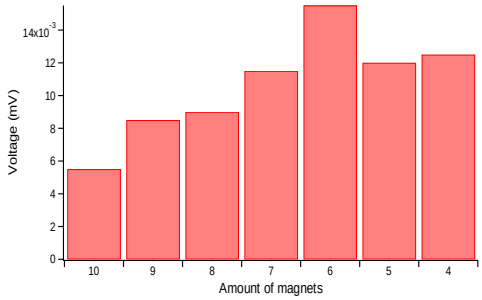

Figure 1: Voltage measured and number of magnets

In the first experiment, we find how many magnets give the highest voltage from the oscillating magnet in coil. When there are a few magnets, it has higher speed but the magnetic field is weak. Vice versa

when there are many magnets. As shown in Graph 1, it turned out that 6 magnets optimize these two effects and give the highest voltage.

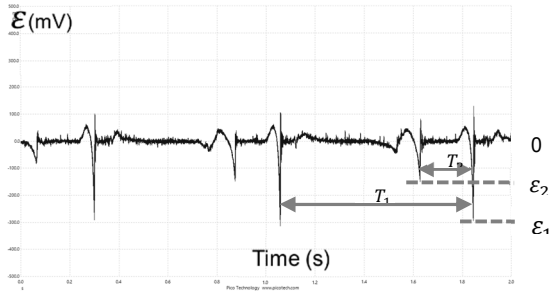

Figure 2: Electrical signal measured from running 4 km/hr.

In the second experiment, when running, the pattern of the electrical signal will be generated as shown in Graph 2. When the running speed varies, the signal still shows a similar pattern but the magnitudes of variables$(T_1, T_2, \varepsilon_1, \varepsilon_2)$ will be varied accordingly. Different speed, signal shows the similar pattern, but different magnitudes.

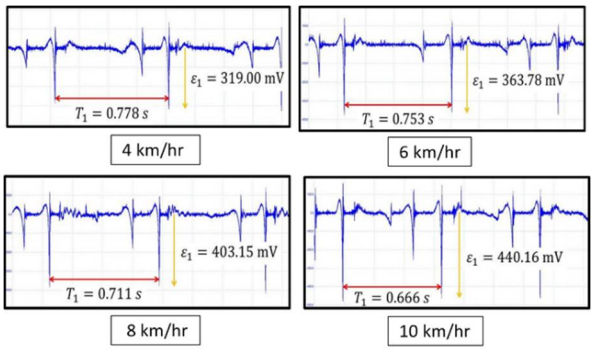

Discussion:

The highest voltage (ε_1 in Graph 2) generated while running increases correspondingly upon increasing the running speed, as shown in Graph 3.

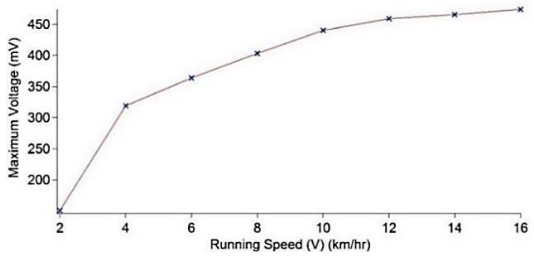

Figure 3: The relationship between Maximum Voltage(ε_1) and Running Speed(V)

However, the relationship is not linear, which is inconvenient to use. So, we create the empirical model for this usage.

With trial and error, we also find that the empirical model using the formula $\frac{\varepsilon_1}{\sin^2\left(\frac{2\pi T_2}{T_1}\right)}$ also corresponds well with the running speed(V) as shown in Graph 4. This may use to predict the running speed from the signal better.

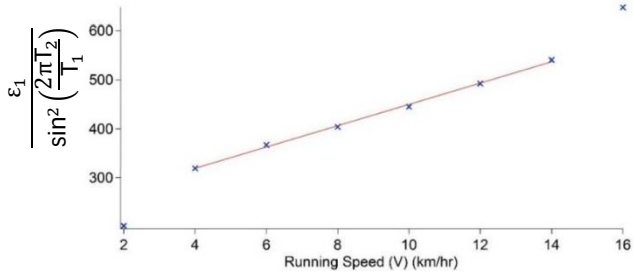

Figure 4: The relationship between $\frac{\varepsilon_1}{\sin^2\left(\frac{2\pi T_2}{T_1}\right)}$ and Running Speed(V)

Conclusion:

In this work, when a strong magnet oscillates inside a coil while running, there is a pattern of signal corresponding to the running movement.

The experiment and empirical models analysis show that, the linear relationship can be used to predict running speed in the range between 4 and 14 km/hr.

The created device can generate the signal that can be used to measure the running speed efficiently.

Such device may also be used to investigate other kinds of movements in other applications e.g. movement therapy, and movement-triggering device.

References:

1. Serway RA, Jewett JW. Physics for scientists and engineers with modern physics. 9th ed. Boston: Cengage Learning; 2013.
2. Halliday D, Resnick R, Walker J. Fundamentals of physics. 10thed. New Jersey: John Wiley & Sons; 2013.
3. Young HD, Freedman RA. University physics with modern physics. 13th ed. Boston: Addison-Wesley; 2011.
4. Neil Zhao. Full-Featured Pedometer Design Realized with 3-Axis Digital Accelerometer [Internet]. 2011[cited 2015 Feb 14]. Available from: http://www.analog.com/library/analogdialogue/archives/44-06/pedometer.html

Acknowledgements:

This project was supported by the Ministry of Science and Technology through the Science Classroom in University Affiliated School (SCiUS) (Suranaree University of Technology and Rajsima Wittayalai School)

DEVELOPMENT AND CHARACTERIZATION OF

OPD – OLED HYBRID DEVICE SYSTEM

Özgür Ülker & Güven Çömezoğlu

Alper Bayram

İzmir Private Fatih Science High School /Izmir/Turkey /aalperbayramm@gmail.com

1. INTRODUCTION

In this day and age, increasing the efficiencies of the electronic devices and decreasing their energy consumptions, have great importance. Since it can be composed new device – architecture combinations, semiconductor devices have quite high development potentials in this context. Organic semiconductors attract the attention thanks to the supply of more material varieties compared to inorganic semiconductors and their ability for being turned into thin film. OLED, OPD, OSC and OTFT are the examples of nano – applications that organic semiconductors are used in.

2. PURPOSE

Semiconductor materials are used in many different areas from screen technologies to photovoltaic devices. OPD and OLED are one of important application areas of semiconductor materials. In our literature researches, it has been seen that PFE [poly(9,9-dioctyl-fluorenyl-2,7-yleneethynylene], which is an organic semiconductor, was used in OLED applications as light emitting layer. Besides; the usage of ZnO NPs (nanoparticles) in the active layer of the optoelectronic devices, makes a positive contribution to the carry of charges and enables device to be run also under feedback.

In our project; we aimed to develop new generation OPD – OLED hybrid device system, which has PFE/ZnO NPs based active layer, with a low cost of production. In accordance with this purpose;

- Determination of the usability of materials in device, by UV-Vis Spectrophotometer, Fluorescence Spectrophotometer and Atomic Force Microscope (AFM),
- Optimization of the appropriate volume – ratio of the molecules that form the active layer,
- Execution of the preliminary preparations required for the production of the device (substrate cleaning, preparation of the solutions, removal of ITO with acid),
- Production of the device (coating processes),
- Execution of the electrical characterizations of developed device under feedforward and feedback and interpretation of the results

processes were aimed to be performed respectively.

3. METHOD

Firstly, the active layer materials were characterized using UV – VIS Spectrophotometer, Photoluminescence Spectrophotometer and Atomic Force Microscope within the context of experimental studies.

a) **b)**

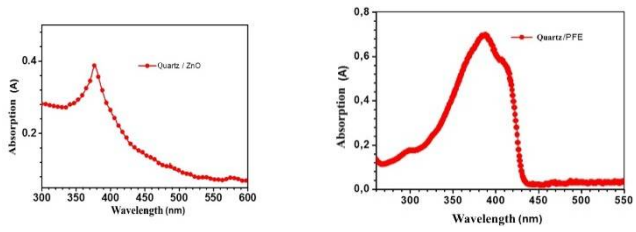

Figure 1. Absorption curves of **a)** ZnO and **b)** PFE thin films prepared on quartz glasses.

a) **b)**

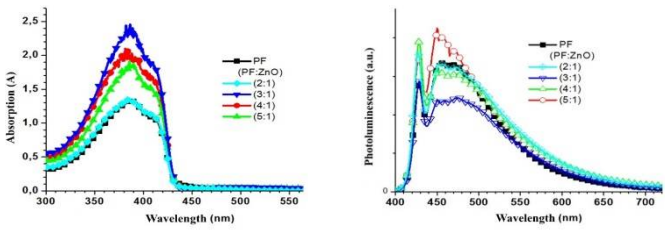

Figure 2. a) absorption, **b)** photoluminescence curves of (PFE:ZnO) prepared with the volumetric ratios of (2:1), (3:1), (4:1) and (5:1).

a) **b)**

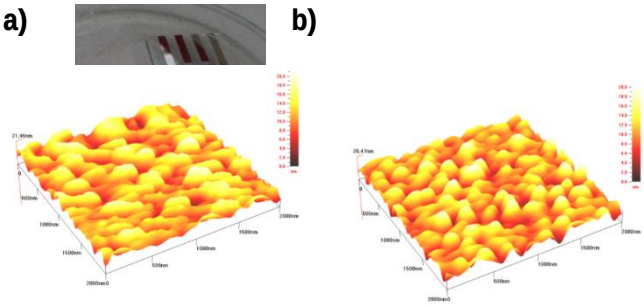

(3:1) RMS: 3.1 nm (25 ºC)/(3:1) RMS: 3.0 nm (60 ºC)

Figure 3. AFM images of the thin film prepared with (3:1) (PFE:ZnO) ratio at **a)** 25 ºC , **b)** 60 ºC.

For the preparation of the device, firstly the ITO layer which is cut 3cm x 3cm, was etched with acid in such a manner that ITO left only at the center in the form of band 1cm x 3cm.

And then, PEDOT:PSS material was coated on ITO, whose cleaning process had been previously done, at 3000 rpm for 1 minute with spin coater and substrate was kept at 100 ºC for 30 minutes at vacuum furnace for removing the humidity.

The PFE:ZnO NPs solution was coated at 1500 rpm for 1 minute on ITO/PEDOT:PSS. Following this, ITO/PEDOT:PSS/PFE:ZnO was annealed at 60 ºC, which is the glass transition temperature of the organic polymer of the active layer, for 15 minutes at vacuum furnace.

Finally, Al was coated with low coating speed, (0,4 Å/s) as the cathode material.

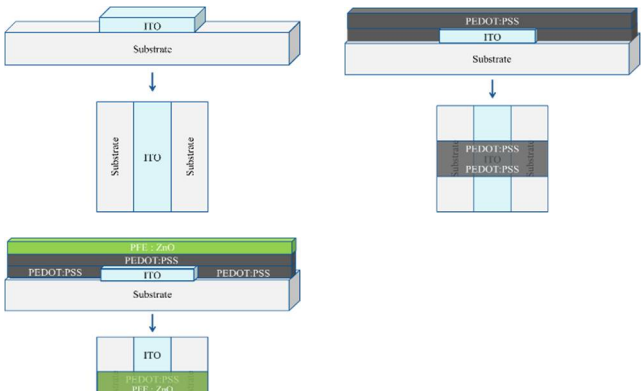

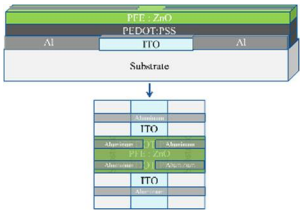

Figure 4. The demonstration of the device structure after each production step.

Figure 5. The images of OPD – OLED hybrid device systems.

4. RESULTS AND CONCLUSION

4.1. Investigations in OPD Hybrid Device System

The electrical characterizations and interpretations of the electricity signal obtained with feedback are explained below.

a) **b)**

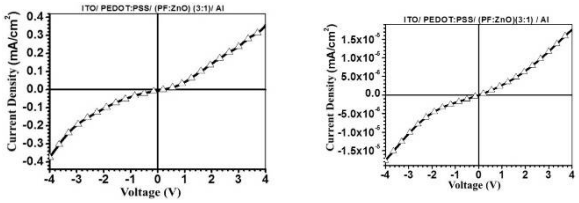

Figure 6. Current density – voltage curves of OPDs obtained **a)** under radiation with 365 nm wavelength and 1 mW/cm^2 intensity, **b)** in the dark.

When the photocurrents and dark currents are examined, it can be seen that OPD photocurrents are 10^4 times higher than dark currents (Figure 6). And these results approve that OPD can work efficiently under the light.

4.2. Investigations in OLED Hybrid Device System

The electrical characterizations and interpretations of the light obtained with feedforward are explained below.

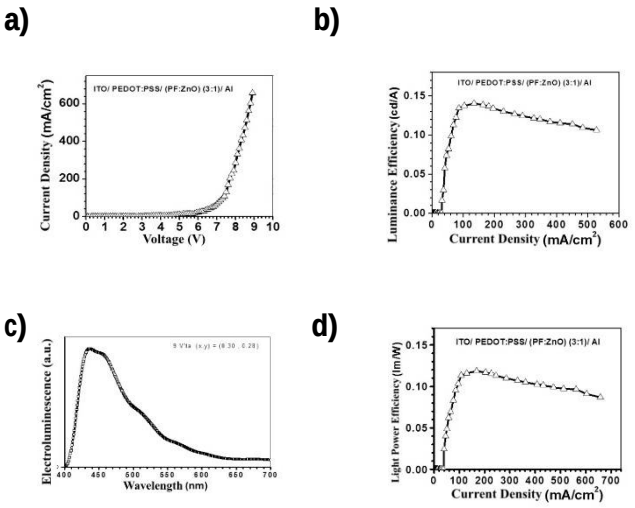

Figure 7. a) Current density responses of OLEDs to voltage, **c)** electroluminescence – wavelength curve **b)** luminance efficiency, **d)** light power efficiency responses of OLEDs to current density.

- ✓ The "Hybrid" layer, which consists of polymer: inorganic nanoparticle mixture, was used in the active layer of ITO/PEDOT:PSS/Active Layer/Al device architecture.
- ✓ Because our OLED – OPD device system can run under both feedforward and feedback, it is named as "Hybrid" in this respect too.
- ✓ Our system was successfully provided to be run, which is the essential success criterion of the project.
- ✓ Since our system has no equivalent product in market, it has not been able to be compared with such a product.
- ✓ Besides; it was been able to be obtained light from device under feedforward, and it was occurred current densities that could compete with the results of similar studies in literature. Thus, the project has achieved its objective.

5. REFERENCES

1. Ali, G. M.,& Chakrabarti, P. (2010). Effect of thermal treatment on the performance of ZnO based metal-insulator-semiconductor ultraviolet photodetectors. Applied Physics Letters, 97(3), 031116.

2. Aouaj, M. A., Diaz, R., Belayachi, A., Rueda, F., & Abd-Lefdil, M. (2009). Comparative study of ITO and FTO thin films grown by spray pyrolysis. Materials Research Bulletin, 44(7), 1458-1461.

3. Belhaj, M., Dridi, C., & Elhouichet, H. (2015). PFE: ZnO hybrid nanocomposites for OLED applications: Fabrication and photophysical properties. Journal of Luminescence, 157, 53-57.

Investigation of Polarization Dependent Magneto-Optical Properties of DNA- Magnetic Liquid Mixture

Hüseyin Kutluay ÇAKADUR

Meltem Gönülol Çelikoğlu

İzmir Private Fatih College /Izmir/Turkey/g.meltem@gmail.com

6. INTRODUCTION

Magnetic nanoparticles combining with DNA lead to the design of various nano-hybrid structures that have unique magnetic properties and biological diversities. Therefore it is very important to understand DNA-magnetic nanoparticles interaction properties. These structures are used for carrying the drug to a certain region inside the live being, forming highly sensitive and selective DNA sensors, diagnosing genetic diseases, determining viruses that cause infection, diagnosing epidemics and their prevention and control and for identification purposes in criminal cases (Tuan and Hai, 2009; Pershina et al., 2014; Tiwari et al., 2015). Therefore it is very important to understand DNA-magnetic nanoparticles interaction properties.

Electrochemical DNA sensor is a promising technique for simple, fast, on-site virus detection. However, the low sensitivity is still a challenge for this method. In a study by Tuan and Hai (2009) shows to improve the sensitivity by magnetic enrichment of the DNA concentration before measuring DNA concentration by the DNA sensor.

7. PURPOSE

In light of the aforementioned studies, I have developed the hypothesis that DNA molecules magnetic fluid combination may show different magneto optic properties for the single stranded, double stranded DNA molecules. I aimed to analyse the optic properties related to polarization under the magnetic field with the experimental apparatus of the magnetic fluid that contains DNA.

In line with this objective, I aimed to;

- Create the experimental set up where the measurements will be conducted,
- Ensure the homogeneous combination of magnetic fluid with DNA molecules and their production so that they do not damage the DNA,
- Obtain a single stranded DNA molecule from a double stranded DNA,
- Examine the optic properties of double and single-stranded DNA molecules added inside the magnetic fluid under magnetic field and determine the differences between these.

8. METHOD

I aimed to analyse the magneto-optic properties related to polarization under the magnetic field of the magnetic fluid that contains DNA in this study. For this purpose, in order to learn how the DNA can be obtained, the banana's DNA was extracted. Magnetic nanoparticles were synthesized and magnetic fluid was formed. In order to take the measurements, the experiment apparatus was set up and magnetic fluid's measurements were made. In order to ensure the combination of double helix DNA with the magnetic fluid, trials were performed with different surface coating materials and as a result, the pH of the magnetic fluid was made suitable for the dissolution of DNA inside the fluid without any damage to the DNA In order to take measurements with the single stranded DNA, double helix DNA was denatured and a single stranded DNA was obtained.

Figure: Synthesize magnetic nanoparticles and fluid

Magneto-optic features of the magnetic fluid samples which do not contain DNA,

contain double helix DNA and single stranded DNA are examined under the magnetic field and they were compared to each other.

9. RESULTS AND CONCLUSION

Magneto-optic properties of double-stranded, single-stranded and without DNA liquid samples due to polarization were examined. On double-stranded DNA - magnetic liquid structure, as a result of magnetic nanoparticles combining to DNA, as the amount of the DNA is higher the change according to the polarization is observed to decrease. On single stranded, the formation of chain structure was quite less, therefore the change due to the polarization was already decreased. As a consequence on single-stranded, the formation of chain structure is blocked. As a result of the differences on the light transmission, with the experimental setup prepared the double-stranded and the single- stranded DNA including magnetic liquids were separated. Also, with the improvement of the experimental setup, a basic and portable prototype is developed. Addition to improved prototype, matching results with the previous experiments done with the experimental setup were observed.

The magneto-optic properties for the magnetic liquids containing double-spiral and single-stranded DNA were not researched before. Besides the homogenous DNA magnetic liquid structure obtained by several workouts in this study and supports the uniqueness and originality of the study as well.

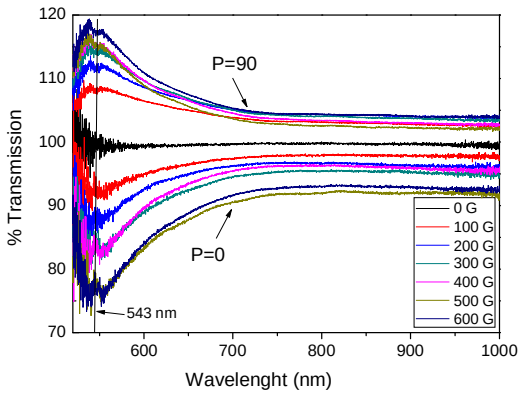

Figure: Transmission spectrum of reference liquid, which contains oleic acid and ethanol, under different magnetic field values for perpendicular and parallel polarizations to magnetic field.

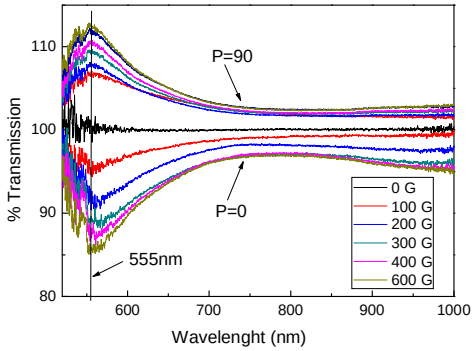

Figure: Transmission spectrum of magnetic liquid that contains 15mg DNA under different magnetic field values for perpendicular and parallel polarizations to magnetic field.

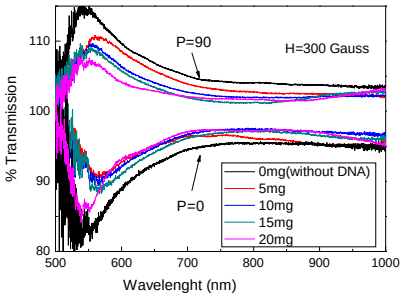

Figure: Transmission spectrum of magnetic liquid that contains various quantity of DNA under 300G magnetic field and for perpendicular and parallel polarizations to magnetic field.

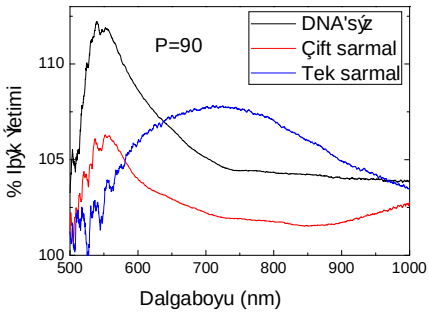

(a)

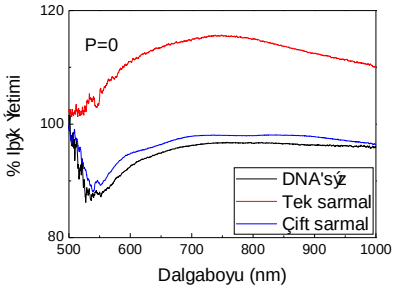

(b)

Figure: Transmission spectrum of magnetic liquid that are without DNA, 20mg double- stranded DNA and single- stranded DNA under 100G magnetic field. a) P= 90 polarization, b) P=0 polarization

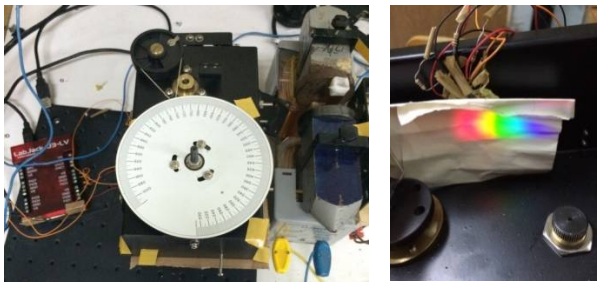

Figure: Prototype of the system

REFERENCES

1. Avgin I., and Huber D. L. (2014). Magnetic Properties of Dipolar Chains in Ferrofluids, Braz J Phys, 44, 219–222.

2. Pershina A. G.,Sazonov A. E., Filimonov V. D. (2014). Magnetic nanoparticles - DNA interactions: design and applications of nanobiohybrid systems, Russian Chemical Reviews, 83(4), 299

3. Serway R. A.,Beichner, R. J. (2000). Physics for Sci. Eng (Trans. Ed.:Prof Dr. Kemal Çolakoğlu), Brooks/Cole, Belmont.

4. Tiwari A. P.,Ghosh S. J. And Pawar S. H. (2015). Biomedical applications based on magnetic nanoparticles: DNA interactions, Anal. Methods, 7, 10109

5. Tuan M., A., and Hai N. H. (2009). DNA enrichment by functionalized magnetic nanoparticles for on-site and fast detection of virus in biomedical application, Journal of Physics: Conference Series, 187, 012059

6. Zhao Y.,Ying Y., andWang Q., (2014). Theoretical Research on Microstructure and Optical Properties of Magnetic Fluid Composed of Rod-Like Shape Nanoparticles, Ieee Transactions On Magnetics, 50, NO. 6, JUNE 2014.

EXPERIMENTAL STUDY OF DYNAMIC CHARACTERISTICS OF FLUID FLOW

Alexander Olevskyi
Sydorenkov Eugene
Dnipropetrovsk school № 19

Introduction

Fluid transportation systems are used in science, technology, daily life and other areas of human activity. The effectiveness of such systems is characterized by fluid flow rate, which in turn depends on the dynamic flow characteristics, namely speed, dynamic viscosity and character of the flow. Real liquids have a feature that their viscosity is not constant, but changes its value depending on transportation conditions.

Purpose of the investigation

In the present research work the aim is to investigate experimentally the above dynamic flow characteristics of Non-Newtonian Fluid using capillary viscometer with variable parameters. For laboratory experiment a solution of sodium chloride in various concentrations was passed through syringe needles which were used as viscometers. To study the dependence of dynamic characteristics of fluid flow on the transportation conditions electronic viscometer model and electronic blood model were used, because for research of blood in vitro in medicine extra additives and anticoagulants are used, which affects the research results. Models used in the research provided an opportunity to explore multiple dynamic flow parameters in different conditions of transport simultaneously. In vitro such studies have significant limitations caused by the parameters of viscometer and the accuracy of measurements. To simulate fluid flow in the viscometer with parameters changing, software complex «SolidWorks» was applied.

Results of the experiment

From the results of the laboratory tests the dependence of the dynamic viscosity on the solution concentration, "critical" values interval of sodium chloride concentration in the solution in which the interaction of molecules most notably affects the effective dynamic viscosity of the fluid were experimentally defined. The presence of this interval of values was not mentioned in the investigated sources of information. In the view of the authors, it is possible to use this result in the medicine . Research of dependence of this interval on the temperature is promising.

D, sm	**1**		**0,5**		**0,25**	
L, sm	**η, Ps**	***v*, m/s**	**η, Ps**	***v*, m/s**	**η, Ps**	***v*, m/s**
0	0,085	7,89	0,068	4,45	0,059	2,2
2	0,076	7,97	0,058	4,7	0,042	2,75
4	0,067	8,08	0,047	5	0,035	3,1
6	0,063	8,2	0,043	5,05	0,032	3,3
8	0,06	8,27	0,039	5,2	0,031	3,5
10	0,055	8,35	0,036	5,45	0,03	3,6

Conclusion

Experiments conducted with the help of electronic viscometer made it possible to conclude that a gradient of velocity and viscosity of the fluid in small diameter vessels is high , which coincides with the real picture of the flow of blood through the capillaries and arteries. This result can be used in the design of the transportation systems for liquids and gases. At the same time "critical" size of thrombus in the vessel or obstacles in the transport artery was defined. Theoretical calculations of the "critical" size of a blood clot in the carotid artery coincide with the results of the pilot study. The author has created a model of "collapse" of the vessel on "critical" values. The mechanism of "collapse" can be used to control special mechanism to prevent the excess fluid flow in the case of emergency in its transportation systems.

Air conditioner "CheapCold"

Andrew Bezmen
Supervisor:Roman Lopatkin
Sumy specialized school № 7, Sumy, Ukraine, abezmen@mail.ua

Introduction

In the twenty-first century humanity is suffering an era of global warming, so a sharp rise of temperature in summer, this is a huge problem, which makes the world to research and implement new technologies in this direction. The person spends 30% of the life at work and nearly 60% at home, so the question arises, how to make work in the office and the rest at home were comfortable and productive even on hot days?

Theoretical part

Air conditioning is a device that allows to ensure thermal comfort, in other words optimal conditions for good health, rest and high working capacity. But, modern air-conditioning is inherent in the huge number of unsolved problems, among which are: a large value, a high level of noise, huge energy consumption, complex structure, expensive and exceptionally professional service, complex installation works, the use of certain environmentally contaminated components.

Therefore, the development of air conditioner, which solves all the drawbacks, is very actual scientific and technical task.

In the process of development we have set ourselves the main aims of the study:

1. To review the scientific literature.
2. To study the theory of the thermosyphon.
3. To conduct the calculations of separate elements of construction.
4. To calculate the heat loss of the room.
5. To build a real model of the air conditioner.
6. To conduct the experiments.
7. Patented and put into production the development.

Experimental part

The working models of conditioner and the experimental room were created for experiments. The air conditioner consists of power supply, thermosyphon, which essentially is the main part of the design and connects the internal and external air-conditioner unit. Separately the internal unit consists of an inner radiator, fan, air filter and water tank. In turn, the external unit consists of an external radiator, fan and a special device, which delivers the capillary water from the internal unit to the external in order to cooling the hot side of the thermosiphon. All data and physical quantities are monitored and processed in real-time software-hardware complex, developed in the Institute of applied physics of NAS of Ukraine.

Fig. 1. The working model of air conditioner.

Fig. 2. The working model of the experimental room.

Conclusion

The advantages of thermosyphon air conditioner are a high efficiency, unrealistically low price and optimal productivity,the absence of noise and great energy efficiency. It is also quickly achieve and support set temperature. The individual achievements are absence of compressor, freon and almost all the complex components of construction that in modern air conditioners. It is easy in installation and service, use only ecologically clean components, and an endless working life.

Discussion

In present experimental researches of "CheapCold" conditioner are conducted, on the basis of which it will be possible to do positive conclusions and its further introduction in real conditions and sizes.

References

1. Ляху Л. В. Теорія кодиціонера: довідник / Л. В. Ляху . - К.: Наук. думка, 1979. - 768 с.
2. [Електронний ресурс]. – Режим доступу: http://housea.ru/index.php/car/58539.

Droplets on Liquid Surface

Grigorchuk Maksim

Introduction

XXI century is characterized by fast technological progress, especially in the computer and electronic engineering, robotics and medicine. Recently, more an interest to the "drop on the layer". The essence of this system is that a drop of water soap solution, which is on the same soap solution water in contact with the surface, which ranges, then at a certain oscillation frequency of the surface, the drop can not break down very long.

This system can be effective in medical diagnosis that is performed on the structure of the track, which remains after the evaporation of a drop of blood. You can use the system "drop on the layer" as a micro reactor for the implementation process of self-assembly of nanostructures in the

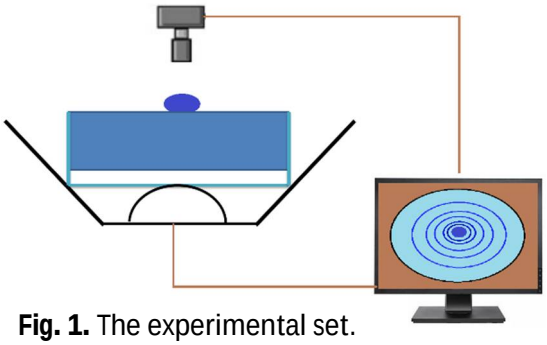

Fig. 1. The experimental set.

process of evaporation on the pillow drops of colloidal nanoparticles.[1] You can also use the system to cool the solids, by evaporation drops set on their surface.

Theory

Why the drop did not destroyed? The drop is not destroyed through an air layer between the drop and soapy water. Sound vibrations transmitted drops dynamics and therefore she oscillates vertically, she "jumps". Just a drop of water fall on it right away and jump between it and the water formed a layer of air. Therefore a drop will no touch with soap solution, and therefore will not drop collapse. If the speaker is not varied, drop still had some time to air layer. But due to

Experiment

We elaborated a device where a drop "lived" more than an hour. We hooked up the speaker to the computer, which was installed to play on the

Fig. 2/ The group of drops.

dynamics of different sound frequencies. Then we put vessel on a speaker into which we poured soapy solution. (Fig. 1)

We threw back drop of soap solution. If you throw a few drops, then formed groups who will move erratically (Fig. 2). If any of these groups face, all drops will be dissolved.

Results

The paper studies droplet which stand on a dynamic surface. During the execution of this work has been clarified that the optimal frequency of 177 Hz. We also found that a drop is not destroyed because of the air cushion beneath it, which is replenished through the fluctuation of dynamics. Using "drop on layer" in medicine will make much more accurate blood tests and not very costly way. The use of this system for cooling by evaporation of solid surfaces will provide lower cooling costs.

References

1. Molacek, Jan, and John W. M. Bush. “Drops walking on a vibrating bath: towards a hydrodynamic pilot-wave theory.” Journal of Fluid Mechanics 727 (July 28, 2013): 612-647 – 37 c.

2. Restoring Superhydrophobicity of Lotus Leaves with Vibration-Induced Dewetting, Jonathan B. Boreyko and Chuan-Hua Chen

3. Driving forces of the solute self-organization in an evaporating liquid microdroplet /L.V. Andreeva, A.V. Koshkin, P.V. Lebedev-Stepanov et al. // Colloids and Surface cal and Engineering Aspects. – 2007. – Vol. 300, - 3 Spec. Iss. – P. 300–306.

4. Andreeva L.V., Koshkin A.V., Lebedev-Stepanov P.V., Petrov A.N., Alfimov M.V. Driving forces of the solute self-organization in an evaporating liquid microdroplet.

The interaction of drops of soap solution with a vibrating surface

Maksim Grigorchuk

Introduction

XXI century is characterized by high speed os scientific and technological progress, especially in computer and electronic engineering, robotics and medicine. Recently, more and more interest is to the system called "a drop on a layer". The essence of this system is that a drop of water-soap solution, which is on the same soap solution, is in contact with the vibrating at a certain frequency surface, and this drop can not be destroyed for a very long time.

This system can be effective in medical diagnosis that is performed on the structure of the track, which remains after the evaporation of a drop of blood. You can use the system "a drop on a layer" as a micro reactor for the implementation process of self-assembly of nanostructures in the process of evaporation on the pillow drops of colloidal nanoparticles. You can also use the system to cool the solids, by evaporation of drops installed on the surface.

Theory

Why is the drop not destroyed? The drop is not destroyed through an air layer is between the drop and the soapy water. Sound vibrations are transmitted to the drops and therefore they oscillate vertically, or simply they "jump". As a drop of water falls on the surface and between the soap water and the drop forms a layer of air. Therefore a drop will no touch soap solution, so drop will not collapse. If the speaker does not vibrate, the drop still remains for some time on the air layer. But due to lack of vibrations the air layer will not be replenished, so the drop will collapse almost immediately.

play different sound frequencies on the dynamics. Then we put a vessel on the speaker into which we poured soapy solution. (Fig. 1)

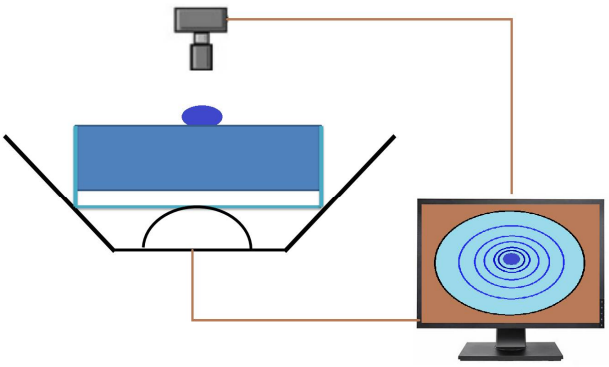

Fig. 1 Our device

We threw the drop on the soap solution. If you throw some drops, then they form groups, which will move erratically (Fig. 2). If any of these groups jostle, all drops will be destroyed.

Fig. 2 The group of drops

Results

The paper studies a droplet which stand on a dynamic surface. During the fulfilment of this project, has been clarified that the optimal frequency is 177 Hz. We also have found that a drop is not destroyed because of the air layer beneath it, which is replenished through the fluctuation of dynamics. Using the system of "a drop on a layer" in medicine, it will make much more accurate blood tests and not in a very costly way. The usage of this system for cooling of solid surfaces will provide lower cooling costs by evaporation.

References

1. Molacek, Jan, and John W. M. Bush. “Drops walking on a vibrating bath: towards a hydrodynamic pilot-wave theory.” Journal of Fluid Mechanics 727 (July 28, 2013): 612-647 – 37 c.
2. Restoring Superhydrophobicity of Lotus Leaves with Vibration-Induced Dewetting, Jonathan B. Boreyko and Chuan-Hua Chen
3. Driving forces of the solute self-organization in an evaporating liquid microdroplet /L.V. Andreeva, A.V. Koshkin, P.V. Lebedev-Stepanov et al. // Colloids and Surface cal and Engineering Aspects. – 2007. – Vol. 300, - 3 Spec. Iss. – P. 300–306.
4. Andreeva L.V., Koshkin A.V., Lebedev-Stepanov P.V., Petrov A.N., Alfimov M.V. Driving forces of the solute self-organization in an evaporating liquid microdroplet.

The Rolling Disk Investigation

Humenuk Mykola

Paul Pshenichka

Liceum №1, Chernivtsi/Ukraine, veremchukmukola@gmail.com

Introduction

Rigid-body dynamics studies the movement of systems of interconnected bodies under the action of external forces. The assumption that the bodies are rigid, which means that they do not deform under the action of applied forces, simplifies the analysis by reducing the parameters that describe the configuration of the system to the translation and rotation of reference frames attached to each body. This excludes bodies that display fluid highly elastic, and plastic behavior.

Experimental part

Fig. 1. The experimental setup.

If you put a loop, a ring or a ball on a rotating surface, it may not fall off of it as you would expect, but stay on the surface for a certain period of time due to its movement. To make our setup we used a smooth plastic surface and a metallic ring. The surface was rotating at 75 rounds per minute, which was the highest speed we could get. This made the ring to move closer to the center of the surface due to the centripetal force.

Theoretical part

We consider the dynamics of ring, which is rolling on horizontal surface, to explain the effect “Rotation on the disk”. We made a hypothesis, that situation, when ring is rolling on a static surface, is the same situation, when ring is rolling on the rotating surface.

Comparison of the theoretical dependence between the oscillation period and ring's radius and experimental measurements are shown in fig. 2

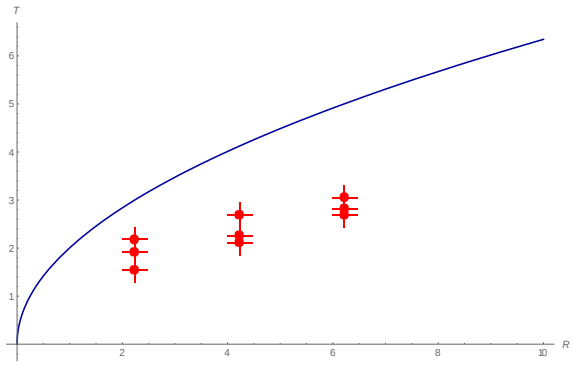

Fig. 2. Blue line – theoretical dependence between the oscillation period and ring's radius. $T = 2\pi\sqrt{\frac{R}{g}}$

Red points – experimental measurements.

The dynamics of rigid body system is described by the laws of kinetics and by the application of Newton’s second law (kinetics) or their derivative from Lagrangian machanics. The solution of these equations of motion provides a description of the position, the motion and the acceleration of the individual components of the system and overall the system itself, as a function of time.

Conclusion

The solution of the problem may help in understanding different qualities of rigid bodies. The formulation and solution of rigid body dynamics is an important tool in computer simulation of mechanical system. This is why we find the further investigation of this problem very important.

References

1. Eshbach's Handbook of Engineering Fundamentals By Ovid W. Eshbach, Byron pg. 9.

2. Oxford Technical Solutions Inertial Navigation Guide.

3. E. v. Hinueber (iMAR Navigation) (2011). "Design of an Unaided Aircraft Attitude Reference System with Medium Accurate Gyroscopes for Higher Performance Attitude Requirements".

Candle in weightlessness,

or metalcutter for the astronaut

Mykola Muzychenko

Supervisor*: Bilous Svitlana Yurivna*, the head of the department scientific-research experimental laboratory of The National Centre "Minor Academy of Science of Ukraine", Ph.D.

Zaporizkii technical lyceum, Zaporizhya, Ukraine, sp_muzychenko@ukr.net

1. The Aim of work

To work out the mathematic model of flame burning in the weightlessness and to mare original metalcutter construction from improvised means; to explore features of burning and describe the flame's charateristics of the device.

2. Methods of the research

The methods are: theoretical, mathematical, design, experimental, estimative on the basis of the physical model.

3. Theoretical part

It`s no convention in the weightlessness and the opened flame looks like a scope. Spherical shape of the flame is stationary when oxygen flow is equal to hydrogen and combustion products flow. The authors first offered mathematic model of this process. This model was described by such equation.

$$\frac{\partial C}{\partial t} = 0 = D\left(\frac{\partial^2 C}{\partial r^2} + \frac{2}{r}\frac{\partial\ C}{\partial r}\right) - kC\ + k_1 C_1 \quad (1)$$

Boundary conditions of the problem are:

$$\alpha_1 C = \alpha_2 C_2 \qquad (2)$$

$$-D\frac{\partial C}{\partial r} = -D_2\frac{\partial C_2}{\partial r} \quad (3)$$

C- the concentration of combustion products (D-the diffusion coefficient)

C_2-the hydrocarbons concentration around the wick (D_2-it`s diffusion coefficient)

The Mathematica Program (Fig.1) solved equation.

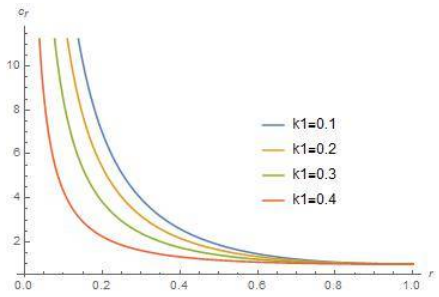

Fig.1. Dependence of combustion products concentration from the distance of the scope center (diffusion coefficients has different values)

4. Experimental part

For the research of the effectiveness of this device we have made some researches of the flame by means of sounding it with the help of thermocouple and also we have discovered the dependence of temperature of the flame from the pressure in air flow.

The theoretical estimation of pressure in the flame were made and the quantity for the highest temperature inside the flame we experimentally determined.

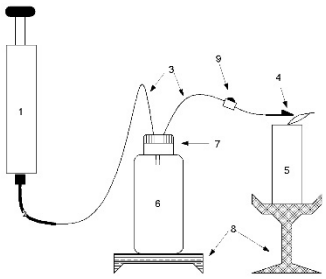

1-pump; 2,3-tube system for blood transfusion; 4-needle of the syringe;

5. Results

The results of our research are interesting from the point of the construction itself, accessibility of its components and opportunity to collect a workable device in a short period of time. With the help of this device one can melt and cut metals using a concentrated flame of the candle, which can be put into practice and can be used in the state of imponderability during space flights.

6. References

1) Karapetyants M. Chemical thermodynamics.— M.:"Chemistry", 1975.

2) Ksandopulo G. Chemistry of the flame. M.: "Chemistry",1980.

3) Aramanovych IG, VI Levin "Mathematical physics equation" - M .: Nauka, 1982 - 386 p.

The Bouncing Ball

Iryna Olar
Paul Pshenichka
Lyceum №1, Chernivtsi/Ukraine, irka.olar@gmail.com

Introduction

The subject of this paper is to investigate the nature of a bouncing ball. A rigorous analysis of the bounce of a ball is complicated by several factors, one being that in practice, a relatively soft ball can easily squash to half its original diameter and also squash asymmetrically. Specificity of collisions consists in their intensity and rapidity. The impact forces, from a physical point of view, are the co-called responses to deformations occurring around the area of interaction and expanding in waves throughout a body. Despite some complicating factors, the bounce of a ball can be analyzed at an elementary level using a combination of elementary mechanics and experimental data on the force wave forms.

The characteristics of a collision

The energy may be dissipated in the ball during the collision as a result of internal friction, or energy may be lost as a result of a permanent deformation of the ball or the surface. Alternatively, energy may be stored in the ball as a result of its compression and subsequently dissipated after the rebound either in internal modes of oscillation or by a slow recovery of the ball to its original shape. When two hard solid objects collide, acoustic waves are generated in the place of impact. The deformation of the objects and their subsequent separation are associated with the propagation of these acoustic waves through the objects and their reflection from the surfaces.

Computer modelling

Computer model of the bouncing ball is taken from Wolfram Demonstration Project library and assumes that if the tangential and normal components of velocity are u and v before a bounce, they are k·u and -k·v after the bounce, where 0<k<1. It has been generalized so that the reflected components are f·u and -e· v, where f is the tangential coefficient of restitution and e the normal coefficient of restitution. There may be a reason to assume f=e, but e is the usual coefficient of restitution, and f seems to be a frictional effect. Obviously, friction would affect rotation, which is ignored.

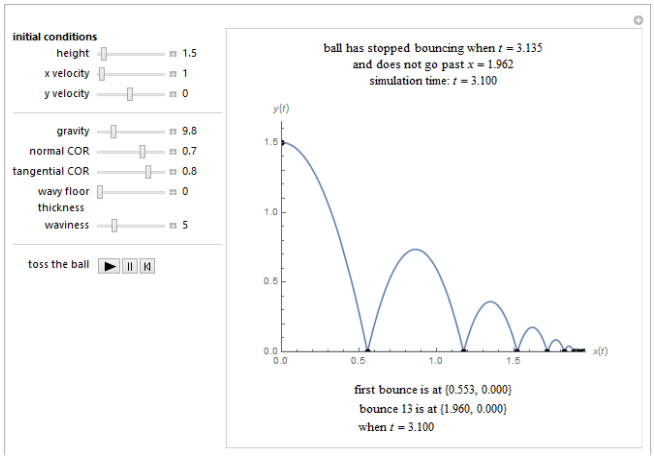

Fig.1. Screenshot of the computer model.

The coefficient of restitution for balls made of different material s

The collision of any objects is always accompanied by a loss of energy. Newton was the first to recognize that such collisions can be conveniently described in terms of the coefficient of restitution (e) defined in the case of a head-on collision as the ratio of the relative speed of the objects after the collision to the relative speed before the collision. The COR was measured for four balls of different masses and made of different materials. It has been investigated that the coefficient decreases as the mass increases and vice versa. However, this principle works exclusively for materials whose structure is fundamentally identical.

Conclusion

If the colliding bodies are not force response rigid they may have small but significant transient deformations which persist through the collision duration. Yet these deformations might either die out well before the bodies attain any appreciable overall displacements/rotations or suitably average to zero on such time. The thicker the surface is, the more time it takes for acoustic waves to fade out. The height to which a ball will bounce depends on the height from which it is dropped, what the ball is made out of (and if it is inflated, what the pressure is), and what the surface it bounces from is made out of.

References

Levi-Chivita T., Amal'di U. Kurs teoreticheskoj mehaniki. Tom 1, chast' 1: Kinematika, principy mehaniki. M.-L.: NKTL SSSR, 1935.
Fizika tverdogo tela: jenciklopedicheskij slovar'. Tom 1. Bar'jahtar V.G.

Leidenfrost Effect Investigation

Taras Kuzyk

Paul Pshenichka

Liceum №1, Chernivtsi/Ukraine, kuzyktaras@yahoo.com

Introduction

A common demonstration of the Leidenfrost effect can be observed when a frying pan is heated to a high temperature, and then some water is sprinkled on it. The effect is seen when the water droplets don't vaporize quickly, but instead "float" on the pan's surface and "run around" chaotically. This happens due to the vapor layer that forms between the droplet and the hot surface, which then inhibits the heat transfer, thus extending the life span of the droplet and making it float. Although this effect has been well-known since 18th century, there is still a lack of empirical data and theoretical understanding of it. The goal of this work is to investigate the Leidenfrost effect experimentally, and further advance the understanding of it.

Experimental part

Two main experiments were performed to investigate this effect (each consisting of multiple iterations of the experiment). In the first experiment, the relationship between the lifespan of water droplets and the pan's temperature was investigated. It demonstarted a definite onset of the Ledienfrost effect occuring at 200°C, which also resulted in the longest lifespan. With a further increases in temperature, the lifespab decreased fairly linearly.

The second, and most intersting, experiment was aimed at investigating the Leidenfrost effect with hydrophobic surfaces and different shapes of objects. Similar experiments were performed to the one described above, but this time the metal ball was covered in a water resistent coating, which turned the surface of the ball hydrophobic. It was found that the Leidenfrost effect could be achieved at lower temperatures this way. When the experiment was performed with a metal rod instead of a ball, the effect could not be achieved at any temperature regardless of whether it was coated with the hydrophilic substance.

Theoretical part

Our experiments demonstrated that there is a difference in the effect between hydrophobic and hydrophilic surfaces. Hydrophobic surfaces seem to induce the effect at a lower temperature. We believe that this may be explained by a phase transition of hydration. A similar effect has been demonstrated with a binary system of methyl-heptane. In such experiments at certain temperatures, the system exhibits a phase transition of hydration, which is reflected by its optical properties, which in turn are analysed using laser beams.

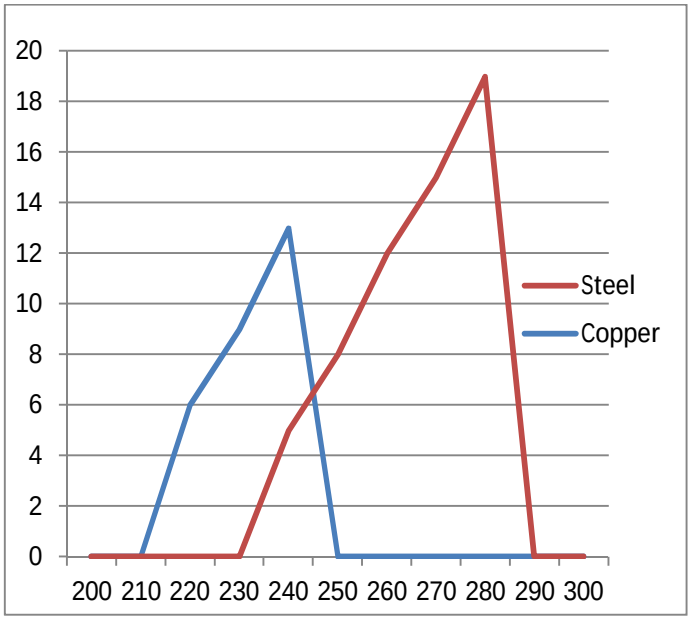

Fig.2 Lifespan of the vapour layer vs. metal ball temperature.

Conclusion

The Leidenfrost effect is still a relatively uninvestigated phenomenon, and with our

experiments we hope to advance the understanding of it both empirically and theoretically. The experiments have revealed that with hydrophobic surfaces, the Leidenfrost point can be lowered, which may be important in applications of this phenomenon (one of which could be in reducing drag on ships or other marine vessels). Also, it is clear that the shape of the object matters significantly, which remains to be further investigated and understood. It raises a question of whether there is an optimal shape to produce and sustain the Leidenfrost effect.

References

1. G. S. Landsberg, “Elementarniy uchebnik fiziki”, 1978

2. S. G. Illina, Thesis from X Russian physical conference, 1999, p.170

3. http://www.nature.com/news/how-to-boil-water-without-bubbles-1.11400

4. Jearl Walker, Boiling and Leidenfrost’s effect, 2009

Investigation of the behaviour of the small droplets on the surface of hydrophobic liquid

Vitalii Yurko

Supervisors: Dr. Volodymyr Kurnosov, Ph.D. Student Uliana Nyemchenko

Educational Centre of Youth Gifts Development in Karazin Kharkiv National University,

Gymnasium № 45, Kharkiv, Ukraine, E-mail: vetas12jen@gmail.com

Introduction

Frequency, Hz	Average lifetime of droplet,s
20	25
45	180-240
60	130

Hydrophobic (or Ultrahydrophobic) liquids are those liquids, the surface of which is extremely difficult to wet. If we drop some soup solution on the surface, the contact angle for such liquids exceeds 150°. This phenomena is also referred to as the Lotus effect. Thus, the droplet, which falls down on these kind of surfaces can fully rebound like an elastic ball. Such droplets can exist for quite a long time under certain conditions. The theory of liquids mentioned above was first described by Tomas Young in 1805.

The purpose of the investigation

The main goal of our research is investigation of behavior of the soapy water droplet, which is formed on top of the same soapy water solution, being in dynamic motion state.

The object of the research are droplets placed on the surface of soap solution, which oscillates due to the sound waves resonance. During our research, the following *tasks have been set*: to describe the droplets and the surface, mentioned above; to examine the factors (amplitude, frequency, and soup solution concentration), which might effect the lifetime of the droplets, chaotic responses; to give theoretical explanation of the observed phenomena, which can be seen in the picture below

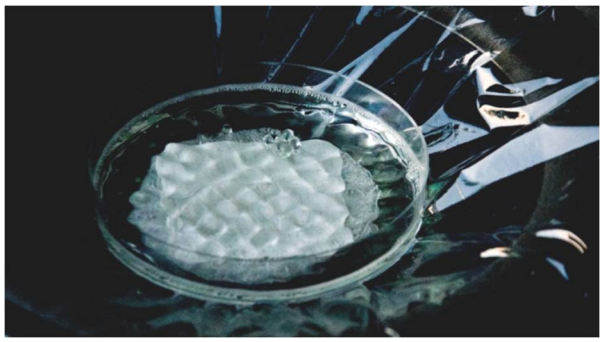

Pic.1 Floating droplets on the vibrating surface

Method of the investigation

To accomplish the tasks of our research, the following methods have been used: theoretical analysis of the literature data and internet information about soap bubbles and droplets; experimental setup, which was developed and created for the investigation; theoretical explanation of the observed phenomena.

Results of the experiment

There have been some stages in our research. Firstly, the liquid has been put on the Petri dish, which was put on top of the loudspeaker. The range of frequencies varied from 20 to 100 Hz. The phenomenon was obtained in the first attempt. The experimental setup has been arranged and modified. After literature analysis has been done, the two ideas to explain the observed phenomenon were found:

1) Electrostatic repelling

2) Air flow under the droplet. (When the droplet going down, then air under droplet pushing up one, and it is repeating for some time.)

Conclusion

The behaviour of the droplets on the surface of vibrating soap solution is an impressive phenomenon to investigate. According to the literature analysis, the experimental device has been constructed and designed. It gives an opportunity to obtain the dynamical effect of droplets, floating over the soap solution surface. It was observed with different oscillation frequencies and explained.

References

1. Pavlov-Veryovkin V.S. Soap antibubbles // Chemistry and life, No. 11, 1966.

2. Ivanov I.B., Platikanov D.N. Colloids. L.: Chemistry, 1975.

3. Ya.Ye. Geguzin // Droplet. M.: Nauka, 1977.

4. Goran Romme “Soap bubbles in art and education”

5. *Young, T. (1805). "An Essay on the Cohesion of Fluids".*

Internet sourses:

https://youtu.be/KZ5ZLPWasrM

https://youtu.be/OU3953k7tIQ

Investigation of the behaviour of the small droplets on the surface of hydrophobic liquid

Vitalii Yurko

Supervisors: Dr. Volodymyr Kurnosov, Ph.D. Student Uliana Nyemchenko

Educational Centre of Youth Gifts Development in Karazin Kharkiv National University,

Gymnasium № 45, Kharkiv, Ukraine, E-mail: ***vetas12jen@gmail.com***

Introduction

Hydrophobic (or Ultrahydrophobic) liquids are those liquids, the surface of which is extremely difficult to wet. If we drop some soup solution on the surface, the contact angle for such liquids exceeds 150°. This phenomena is also referred to as the Lotus effect. Thus, the droplet, which falls down on these kind of surfaces can fully rebound like an elastic ball. Such droplets can exist for quite a long time under certain conditions. The theory of liquids mentioned above was first described by Tomas Young in 1805.

The purpose of the investigation

The main goal of our research is investigation of behavior of the soapy water droplet, which is formed on top of the same soapy water solution, being in dynamic motion state.

The object of the research are droplets placed on the surface of soap solution, which oscillates due to the sound waves resonance. During our research, the following *tasks have been set*: to describe the droplets and the surface, mentioned above; to examine the factors (amplitude, frequency, and soup solution concentration), which might effect the lifetime of the droplets, chaotic responses; to give theoretical explanation of the observed phenomena, which can be seen in the picture below

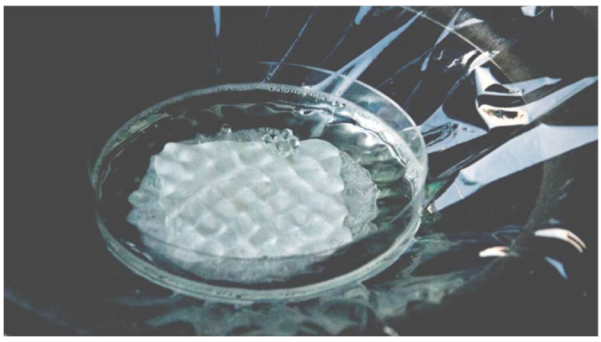

Pic.1 Floating droplets on the vibrating surface

Method of the investigation

Frequency, Hz	Average lifetime of droplet,s
20	25
35	120-180
60	130

To accomplish the tasks of our research, the following methods have been used: theoretical analysis of the literature data and internet information about soap bubbles and droplets; experimental setup, which was developed and created for the investigation; theoretical explanation of the observed phenomena.

Results of the experiment

There have been some stages in our research. Firstly, the liquid has been put on the Petri dish, which was put on top of the loudspeaker. The range of frequencies varied from 20 to 100 Hz. The phenomenon was obtained in the first attempt. The experimental setup has been arranged and modified. After literature analysis has been done, the two ideas to explain the observed phenomenon were found:
1) Electrostatic repelling

2) Air flow under the droplet. (When the droplet going down, then air under droplet pushing up one, and it is repeating for some time.)

Conclusion

The behaviour of the droplets on the surface of vibrating soap solution is an impressive phenomenon to investigate. According to the literature analysis, the experimental device has been constructed and designed. It gives an opportunity to obtain the dynamical effect of droplets, floating over the

soap solution surface. It was observed with different oscillation frequencies and explained.

References

1. Pavlov-Veryovkin V.S. Soap antibubbles // Chemistry and life, No. 11, 1966.

2. Ivanov I.B., Platikanov D.N. Colloids. L.: Chemistry, 1975.

3. Ya.Ye. Geguzin // Droplet. M.: Nauka, 1977.

4. Goran Romme “Soap bubbles in art and education”

5. *Young, T. (1805). "An Essay on the Cohesion of Fluids".*

Internet sourses:

https://youtu.be/KZ5ZLPWasrM

https://youtu.be/OU3953k7tIQ

The Relation Between Colour and Surface Structures on Butterfly Wings

Vossa van der Vegte

Trevianum Scholengroep, Sittard, The Netherlands, vossa98@hotmail.com

1 Introduction

Nature provides us with a wide range of beautifully coloured organisms, ranging from plants and flowers to birds and insects. Butterflies are generally recognized as the order of insects that exhibit the most diverse patterns and colours. Butterflies belonging to the family of the Morphinae are famous for their characteristically brilliant metallic-like blue color. The view angle-dependent blue color does not originate from dyes or pigments, but is caused by the special interaction between light waves and sub-micron surface structures on the wings of this butterfly. This type of colouring is called structural color or iridescent color.

2 Purpose of the investigation

The aim of this study is to answer the question: "How does the *Morpho peleides* creates its iridescent blue color ?".

3 Method of the investigation

To answer the above research question five different sub-questions and hypotheses were defined and subsequently tested via experiments. In the experiments, the iridescent *Morpho peleides* was compared to a non-iridescent white *Pieris rapae*.

Morpho peleides

Pieris rapae

The sub-micron surface structures on the wings and wing scales were studied with Light microscopy (LM) and Scanning Electron Microscopy (SEM). The reflectance spectrum of the top side of the *Morpho* wing was measured with micro-photospectroscopy. This spectrum was compared with theoretical calculations [1] of the reflectance spectrum using light interference in an optical multilayer structure model to describe the observed microstructure on the wing scale. The dimensions of the microstructures as measured by SEM were used to model the multilayer structure. To further prove the validity of an optical multilayer structure to describe the blue color of the *Morpho*, the view angle-dependence was studied with photography and compared with theoretical calculations. Additionally, the colour change dependency on the refractive index of the medium was studied by applying liquids with different refractive indices to the wings. The observed color changes were compared with predictions obtained from the theoretical model for multilayer interference. Infrared light reflection from the wings was studied with IR-photography.

4 Results of the experiments

The microscopy study revealed specific lamellar nanostructures on the length ridges of the wing scales of the iridescent blue *Morpho*. These lamellar structures are absent on the non-iridescent *Pieris rapae*. The wing scales of the *Pieris rapae* show pigment beads in between the length ridges [2].

The lamellar structure on the length ridges can be modelled as an optical multilayer structure in which light interference can occur [3]:

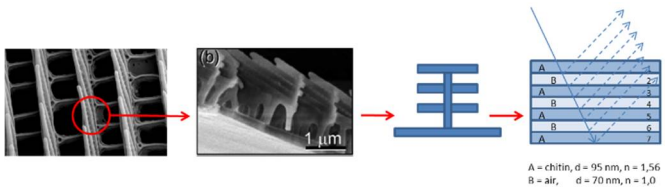

Figure 1. Model of the lamellar structure on the wing scale depicting an optical multilayer

The reflectance spectrum measured on the blue wing of the *Morpho* reveals strong reflections in the UV, blue and IR wavelengths. This reflectance spectrum measured shows good correlation with a calculated reflectance spectrum using the theory of interference of light waves in an optical multilayer.

Based on the constructive interference of light waves in this multilayer, the angle dependence of the reflected wave length can be calculated:

$$2\,(n_a d_a \cos\theta_a + n_b d_b \cos\theta_b) = m\lambda$$

Equation 1: wavelength at which maximum constructive interference occurs in an optical multilayer

The equation was found to describe the optically observed colour shift from blue to violet when the viewing angle increases. This viewing angle-dependent colour change is not observed for the non-iridescent *Pieris rapae*.

From equation 1, it is clear that the wavelength at which maximum constructive interference should occur, also depends on the refractive index of the medium. When the medium in which the wing is present, is changed from air (n=1) to ethanol (n=1.36) or p-xylene (n=1.56), the colour changes from blue to green to brown. Moreover this colour change is qualitatively predicted by calculations of the respective reflection spectra using the theory of interference of light waves in an optical multilayer. Again, the non-iridescent *Pieris rapae* does not show a colour change when the medium is changed.

Next to reflections at UV and blue wavelengths, the reflectance spectrum measured on the blue *Morpho* also exhibits a strong reflection peak at Infrared (IR) wavelengths. This specific reflection was clearly visualized using IR photography.

5 Conclusions

The answer to the research question on how the *Morpho peleides* creates its iridescent blue color is the following:

The view angle-dependent brilliant blue colour of the *Morpho peleides* originates from constructive interference in lamellar nanostructures on length ridges on its wing scales which resemble an optical multilayer structure.

6 References

[1] Filmetrics (2014): ”Reflectance Calculator”, https://www.filmetrics.com/reflectance-calculator

[2] Stavenga, D. G. et al, (2004) : butterfly wing colours: scale beads make white pierid wings brighter. Proc. R. London., 2004, 271, 1577-1584

[3] Kinoshita, S., Yoahioka, S. (2005): Structural colors in nature: the role of regularity an irregularity in the structure. Chem. Phys. Chem., 2005, 6, 1442-1459

Flow Dependency of Electrolytic Resistance

Arthur Admiraal

Supervisor: Rutger Ockhorst

Northgo College, Noordwijk, the Netherlands, arthuradmiraal@hotmail.nl

1 Introduction

Although the effects of the electrolyte concentration on the conductivity of a solution have long been understood, and the electrical characteristics of such a solution have been modelled extensively, there is no research known to the author examining flow-dependent electrical behaviours of electrolytic solutions.

If a flow-dependent effect on the resistance of electrolytic solutions exists, it could have a number of useful applications. For example, it could be exploited to design inexpensive miniature non-mechanical ultra-low power flow sensors, which enable novel applications, such as flow speed sensing arrays. Furthermore, it may be a factor to consider in fields such as process control and impedance spectroscopy. Because of these reasons, this paper examines such flow-dependent effects.

2 Theory

The electrical behaviour of the electrolytic solution is mostly determined by the formation of electrical double layers and faradaic currents.

In a flowing solution, double-layer formation may be hampered, which would lead to an increase in current, and thus a lower resistance.

3 Methods

A test setup, as illustrated in figure 1, was constructed out of two reservoirs connected by some tubing to a measurement chamber, consisting of a PVC tube in which two electrodes were placed, using some flanges. These electrodes were connected to a digitally controllable lab power supply and an oscilloscope, measuring both the voltage over and – using a current amplifier – the current through the solution. A pump pumped a NaCl solution through the setup.

The flow rate was calculated from the trend in weight measured by the scale under container 2 and the concentration was calculated from the electrical behaviour of the solution.

Using this setup, transient responses of electrolytic solutions were gathered in the presence of various amounts of flow at multiple concentrations.

The electrical behaviour of a known equivalent circuit was determined. This model was then fit to the experimental data. From this fit, equivalent component values could be calculated. These were then compared.

4 Results

As expected, the resistance decreased ever more with higher flow speeds. The charge time of the double layers did also vary with flow speed, which was unexpected.

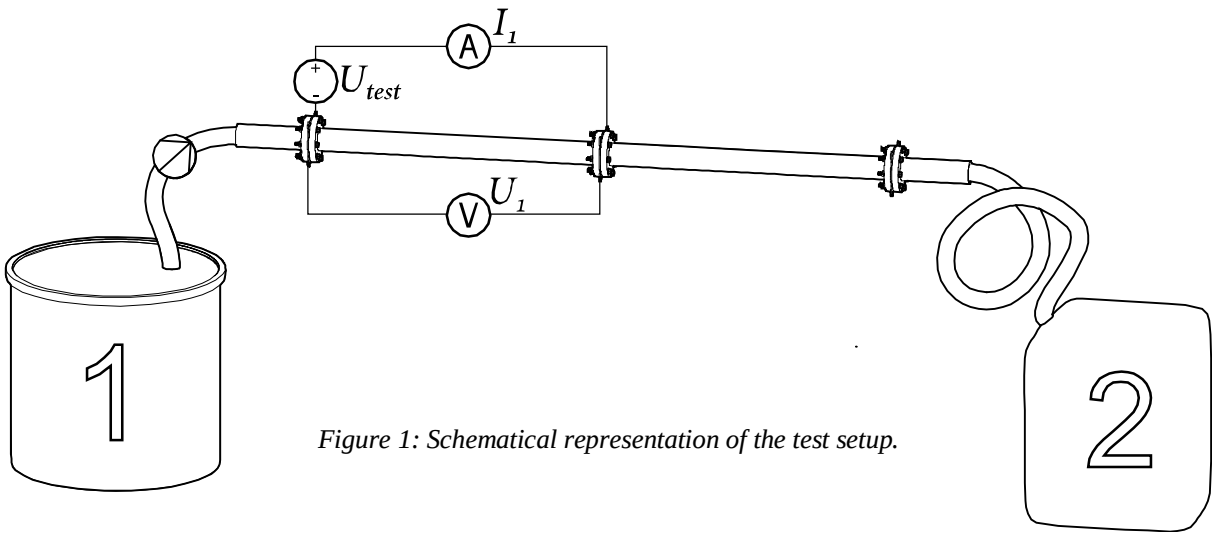

Figure 1: Schematical representation of the test setup.

Thermoelectrical generator

Nekrasov Andrei Evgenievich

Supervisor: Tikunov Anatoli Sergeevich

Lyceum №1502, Moscow/Russia, an-32010@yandex.ru

Today, the problem of using the heat of waste gases becomes more important than ever. Waste gases are hot gases, which after some useful output are just throwing away. This only makes an additional burden on the environment. However, there are some ways to use their energy. One of them is a Seebeck element. Unitary Seebeck element is a pair of semiconductors, one with p-type of conductivity and the other with n-type. It produces electricity from the temperature difference. It is a thermoelectric Seebeck effect – the conversion of heat directly into electricity at the junction of different types of wire. This effect is reversible – the opposite is the Peltier effect: the presence of heating or cooling at an electrified junction of two different conductors. It means that we can make a thermoelectrical generator and use the heat of waste gases to get electricity.

Before starting my work, I have set the following tasks:

- To research a method of producing electricity from the heat of waste gases through the Seebeck-Peltier element.
- To invent a thermoelectrical generator to get a cheap electricity.
- To find places where this generator can be used.

For the experiment, I bought a Peltier element and developed an experimental installation.

It contains a radiator, Peltier element (30 mm * 30 mm), a heat insulation plate, a metal cylinder as a heat conductor and a metal plate for equable heat distributing. As the source of heat, I use an industrial dryer or alcohol stove.

I had been measuring the current, voltage and temperature difference with an ammeter, voltmeter and a universal measuring device – LabQuest Vernier.

After few experiments, I found a dependence of power from temperature difference and made a graph.

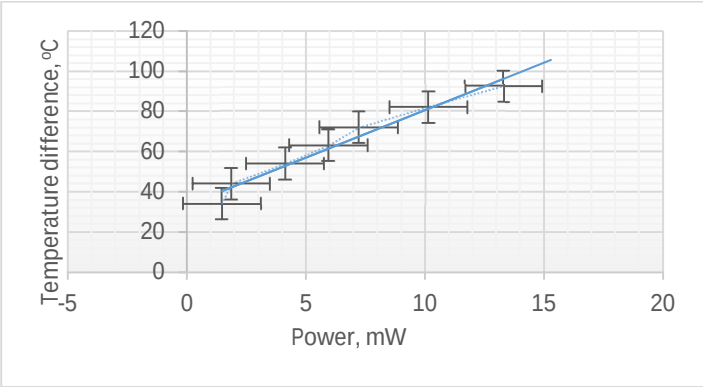

The dependence of the power from temperature difference is the same that the producer gives. It means that I can use characteristics of Seebeck element from this producer to do calculations.

So where can we use this generator? We can use it in places where hot gases have already done some work and now they are throwing away. These places are condensing gas boilers, gas boilers, diesel boilers and exhaust pipes of cars.

To determine the output power it is sufficient to know the dimensions of one Seebeck element (40 * 40), the dimensions of the place (a * B, where a - height, B - base perimeter) where the generator will be located, the exhaust gas temperature (t) and the output of one Seebeck element at this temperature (P0). To determine the payback time (T) the price of 1 kWh (5, 09 rubles for Moscow) and the price of one Seebeck element (250 rubles) should be known.

Seebeck element number N in the generator is defined by N = a / 40 + B / 40.

Total generator power P: P = N * P0.

Generator payback time T is equal to the price of the generator (number of elements Seebeck, multiplied by the cost per item) divided into the cost of electric power: T = N * 250 / (5.09 * P), or

T = N * 250 / (5,09 * P0 * N) = 49,1 / P0, where P0 is expressed in kilowatts.

The outside temperature is taken as 0 ° C

I found information about places where this generator can be used and accounted the cost of the generator, total generator power and payback time for each place using these formulas.

Condensing gas boilers

N = 700/40 + 730/40 = 17 + 39 = 56

P = 56*0,5 = 28 Вт = 0,028 kW

Cost – N*250 = 14000 rubles

T = 14000/(0,028*5,09) = 98000 hours

Diesel boilers

N = 920/40+502/40 = 36

P = 36*3,44 = 123,84 Вт = 0, 123 kW

Cost– N*250 = 9000 rubles

T = 9000 / (0,123*5,09) = 14400 hours

Gas boilers

N = 855/40+735/40 = 39

P = 39*3,1 = 120,9 Вт = 0, 121 kW

Cost – N*250 = 9750 rubles

T = 9750 / (0,121*5,09) = 15800 hours

Exhaust pipes of a car

N = 100/40+376/40 = 12

P = 12*2,52 = 30,24 Вт = 0, 03 kW

Cost – N*250 = 3000 rubles

T = 3000/ (0,03*5,09) = 19600 hours

As a result, I have designed an experimental setup and after few experiments, received a graph of the dependence of the power from the temperature difference to the Peltier element. Considering measurement error, I approximated the graph in a linear relationship. I have created a device that converts thermal energy emitted into the atmosphere, into electrical energy, that helps conserve electricity, and calculated its economic benefits for different application areas.

We can say with confidence that in the near future electric Peltier-Seebeck element will become an integral part in energy conservation.

Producing of holographic pictures my mechanical way

Andrei Rasputnyi
Supervisor: Baiazitov Ivan
AESC MSU, laboratory LANAT, Moscow/Russia, science@aesc.msu.ru

The work is dedicated to the producing holograms by mechanical way. Such a hologram is made by use of a piece of plastic material and scratching the circles of the same radius on its surface. If we want to make straight line, we should place the centers of these circles on a straight line. And I set a goal to create some pictures using such method.

The Fig.1 shows that there are always two rays of light which lie in a plane that is perpendicular to the plane of the picture with circle. So we will observe the light points instead of the entire circle.

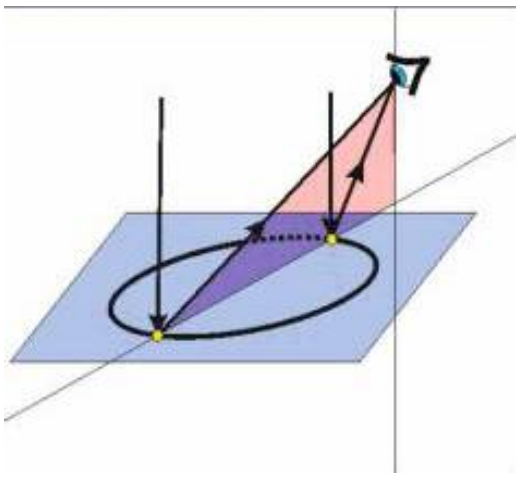

Fig.1

At first stage I reproduced straight line in any direction (not only horizontal or vertical). I had to draw circles of different radii if I needed to get the slopping line. After that I could do such simple three-dimensional bodies as cube and tetrahedron.(Fig.2)

Fig.2

At second stage I developed the method tj reproduce the curves lines. I began to make circle line. But it turned out that I got some kind of ellipse. To correct this defect I tried to scratch other second order curves such as ellipse and parabola instead of circles. As a result I get figure which looks like a real circle.

And the last detail is shadows. This will be very necessary for the portraits. They can be achieved using straight lines, which lies closely to each other

The light method for capillary waves investigation

Vladimir Shulgin
Supervisors: Klim Sladkov and Alisa Dorofeeva
AESC MSU, laboratory LANAT, Moscow/Russia, science@aesc.msu.ru

1 Introduction

The waves on the water surface can be treated as the capillary waves, if the value of the surface tension forces are greater than the gravity forces. These waves usually have short length (less than 3 millimeters).

2 Method of the investigation

I studied the behavior of capillary waves that have been excited on the surface of liquid jet. Capillary waves can be obtained in various ways. I use the water jet impact upon the obstacle that was a smooth liquid surface. Also I used a hard surface as an obstacle, but the results were slightly different. Due to the impact, the swell arisen along the jet, that was slightly visible by the naked human eyes. In order to make the swell noticeable I decided to highlight jet by the laser pointer (pic 1,2).

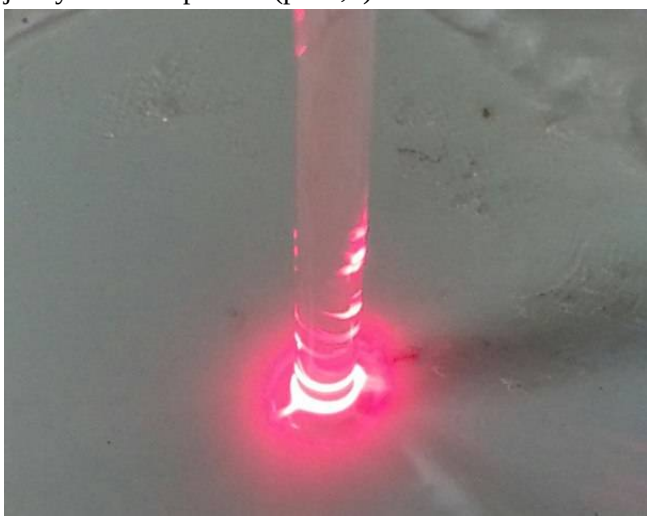

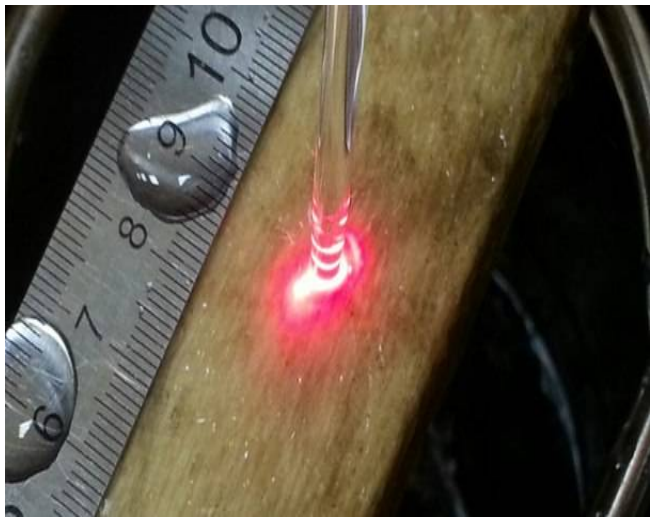

Pic 1,2. Photographs of the capillary waves on the water jet have been visualized by laser light. The light forms bright rings along the waves.

After the waves were visualized I began to study the phenomena. I investigated the dependences of the rings on the diameter of the jet, the speed of water, Different liquids and the obstacles were used. The method of investigation was based on the measuring of the light rings parameters that are linked with the characteristics of the waves.

3 Theory

Capillary waves are described by the velocity

And wavelength

where σ – liquid surface tension coefficient, ρ – density of the liquid, –jet's radius.

I observed the standing rings, consequently, the capillary wave moves upward relative to the jet with the velocity that is equal to the fall speed. In my experiment , where h – height of the jet source.

4 Experiment

I designed the installation and conducted a number of experiments with different parameters of the jet. I have discovered how the distance between the rings (i.e., wavelength) depended on the jet velocity and diameter.

5 Conclusion

: I have investigated the dependence of capillary waves on the jet parameters. Theoretical and experimental data were in coincidence within the experimental errors.

experimental errors.

Control over circular hydraulic jump by rotation.

Kirill Smirnov
Evgeny Mogilevskiy

Advanced Education Science Center Lomonosov Moscow State University, Moscow/Russia, k.smirnov-33@yandex.ru

Introduction

The hydraulic jump is a phenomenon of rapid change of velocity and height of a free surface flow. Everyone sees it in a kitchen sink, when a water jet hits the rigid surface, then thin film flows radially, and at some distance its height suddenly rises. Thin films are used for cooling, coating, absorption, and other processes. Interchange rates are different in one for thin and fast film and for thick and slow layer. That is why control over position of jump is an effective way to change reaction conditions.

Shallow-water theory of circular hydraulic jump was developed by T. Bohr et al (T. Bohr, P. Dimon, V. Putkaradze, J. Fluid Mechanics 1993, vol. 254, pp 635-648). They derived governing equations and obtained scaling for the hydraulic jump radius.

We investigate hydraulic jump on a rotating surface. In this case centrifugal force accelerates the flow and pushes the jump away. Our aim is to add rotation to the shallow-water theory, construct an experimental setup and check our theoretical conclusions.

Theoretical model

Circular steady vertical jet of incompressible liquid falls onto horizontal disk. The axis of the disk coincides with the axis of the jet. The disk rotates with constant angular velocity. The liquid spreads radially over the disk. If the jet velocity is big enough then there is thin film flow right after the area of hitting. The flow is fast, so its velocity is greater than speed of small disturbances propagation (the flow is supercritical). Due to viscosity flow slows down and drops out of supercritical regime. At this point the jump is observed.

Theory is based on conservation laws. Following the cited paper of Bohr, we derive differential equations for velocity as a function of radius. These equations contain one non-dimensional number: , where is angular velocity of the disk, is a characteristic radius, is a characteristic liquid velocity. For (no rotation) our equations coincide with known ones. For small values of equations have a singular point, which mean that jumps can occur. If is greater than certain critical value this point disappear, and continuous flows are possible.

Experimental setup

In our setup water goes from wide reservoir through 4 mm diameter tube and is directed vertically. Typical flow-rate of water is 20-30 ml/s. The jet hits Plexiglas disk of radius of 10 cm. Scale marks are printed on the disk surface. The disk is connected to a motor with variable rotation rate. We use rotations up to 0.33 Hz. A camera is located above the disk and takes pictures of the jump. We measure the dependence of the jump radius on the flow rate and angular velocity. We also made tests to examine effect of the disk radius.

Results and discussion

For fixed value of the flow-rate we find critical value of angular velocity, when the jump goes away from the disk. Typical critical value is about 0.25 Hz, which is close to theoretical prediction.

We find the effect of disk radius: the jump is closer to the axis for smaller disk. Possible reason of this fact is surface tension on the disk edge.

Conclusion

We study the film flow over rotating disk and theoretically and experimentally show two regimes of flow (jumped and smooth). The angular velocity of the disk is a crucial parameter of the system; the rotation rate has a critical value, which separates the regimes. This result can be used for designing of chemical reactors, heat exchangers etc.

cje chemical reactors, heat exchangers etc.

Why Two Wheeled Suitcases Turn Over Under Certain Circumstances

Sara Eyvazi
Supervisors: Hassan Bagheri Valoujerdi, Nona Izadipanah
Emam Mohammad Bagher High School, Tehran/Iran
Accepted and edited by: Araian Young Innovative Minds Institute, AYIMI, www.ayimi.org , info@ayimi.org

1 Introduction

When two wheels suitcase is pulled along, under certain circumstances it can wobble side to side so strongly to the limit that it may turn over. Can it be suppressed or intensified by changing of the luggage packing?

2 Basic Information

Here, the suitcase has been presumed as a rigid object. So, the following two forces are considered as the most effective forces in the existed torque of suitcase:

1. The hand force

2. The force of suitcase load

Hypothesis 1: The suitcase is in balance condition
Hypothesis 2: The suitcase is not in proper stability

Mass of center, spin factor: Due to that the suitcase contain is not in balance condition by improper packing, thus the mass of center is not positioned on any of three axis ( ) as it is asymmetrical.

Axis: The length of resistant arm is more than mover arm, Therefor, the resistant force is increased and existed torque is around axis. So, the stack of bags falls from the person who takes it.

Axis: If the mass of center is shifted to sides due to way of packing, it could leads to rotation of suitcase around axis. In this case ,if the center of mass to be kept away from any of wheels, thus, the torque lever is increased and existed torque is around axis and consequently suitcase turns round while it is being pulled.

-Uneven Surfaces

Axis: When one wheel is placed on the steep surface and other is stood on the ground vertically, so, suitcase rotate around axis while it is being pulled on slop, therefore, torque is generated on the one wheel.

Axis: Load force vector inclines to shift the center of rotation axis and therefore is more vertical in proportion to rotation axis by increasing of packing load.

3 Conclusion

We can optimize this phenomenon by changing the package. If the load of suitcase are so packed that the center of mass is placed at the lowest height and the minimum distance from three axes and the same distance from them and stand in the middle of luggage, it can reduce the ttorque of suitcase. Also, if the objects placed on the sides of suitcase, it will make a balance in baggage that prevents it gets crazy.

References

- R. H. Plaut," Rocking instability of a pulled suitcase with two wheels". Acta mechanica 117, 1-4,165-179(1996)

- S.Suherman, R.H.Plaut, L.T.Watson and S.Thompson," Effect of Human Response Time on Rocking Instability of a Two-wheeled suitcase", J.Sound and Vibration 207, 5,617-625(1997)

Prop-plane

AliakseiBarysevich
Supervisor: MikitaSyravatnikau, ViktarBeliautsou, Zharnasek Mikhail
Minsk State Regional Lyceum
Minsk/Belarus alexwelgum@gmail.com

Prop-planeis an absolutely unique flying vehicle. Prop-plane combines the advantages of a plane and a helicopter. It is much faster, more maneuverable and more economical. Moreover, it has an ability to hover in one point. The prototype doesnot require any runway to take off or land. It just takes off vertically and then flies forward like an airplane. Prop-plane has two propellers on the both sides of the fuselage which rotate in opposite directions. It also has wings which can be easily folded.

First, the engines are perpendicular to the ground,and the wings are folded which allows the prop-plane to take off vertically. When the prop-plane is at a certain height, one engine turns parallel to the ground, and the other one gets back into the fuselage, while the wings turn parallel to the ground. Then the prop-plane continues flying like an airplane.

It is noteworthy that the engines are able to rotate not only parallel to the fuselage but perpendicular to it. It makes the aircraft more maneuverable.

It is expected that the prop-plane will be able to fly at a speed of up to 300 km/h, carrying anadequate load of up to 2kg. Note that a quadcopter of the same size will fly the distance of 15-20 km, whereas the prop-plane will fly 100 km, because it uses the wings.

In the future,I am going to enlarge this model to the size of an airplane which will be able to participate in different rescue missions, carry people and heavy loads.

Geneces – Cloud EcoSystem

Uladzislau Hadalau

Supervisor: Uladzimir Zhuk

State Institution of Education "Secondary School №11 the town of Slutsk", Minsk/Belarus, zix-studio@yandex.by

1 Current problem and introduction

Today the hardware and software capabilities of portable devices (such as smart phones and tablets) are extremely limited in comparison with, for example, a home PC.

I have developed a cross-platform software for the realization of the cloud ecosystem with virtualization of most modern operating systems. The ecosystem means the hardware and software environment of the user, which becomes a "cloud" due to the use of remote computing power. This software can enable any user to go beyond hardware and software limits of the device he/she uses.

2 Realization

The main aim of the Geneces project is to bring the speed of cloud computing to its native use case as close as possible, even the user uses mobile internet connection. For that purpose, I developed two special remote control protocols: «Office Edition» and «Gaming Edition» protocols and configured the hypervisor and the remote server OS. When creating remote protocols, I introduced some algorithms to increase the speed of interaction between the remote server and the client device.

2.1 «Office Edition» protocol:

The following components and algorithms have been introduced forfast work of the «Office Edition» remote control protocol:

- **«Smart» transfer of the changed image sectors.** The essence of this algorithm is to transfer only the changed parts of the image. Parts can be transferred by rectangles of different sizes according to the principle «the smallest quantitative and qualitative composition of the image packages».
- **Dynamic change between compression JPEG (graphic representation) and ZLIB (text),** based on the analysis of the above sectors. It was experimentally established that these types of compression are best suited for sectors with text and image, respectively.
- **Smart distribution of network speedsbetween sessions of running remote control protocols.**
- **Automatic adaptation of the resolution of the remote screen.** For example, if you connect your smartphone to Geneces, remote operation system instantly configure the screen resolution like on your device.
- **Possibility of interaction client USB and USB OTG devices with a remote operating system.** This capability enables you to use the USB-input devices or USB-drives in the remote operating system.

2.2 «Gaming Edition» protocol:

For the implementation of the protocol has been taken a part of the "Office Edition" protocol, which is responsible for the client-server interaction. x264 and x265 library with embedded algorithm «Motion compensation» were used for image transfer. This protocol also works cross-platform, but

requires the client device faster access to the Internet. When using the mobile Internet is enough quality of 3G or 4G (preferred).

3 Conclusion

The use of the Geneces system enables to increase a computing power of the device by several times. For example, a typical tablet computer with moderate technical characteristics can have a power of a modern PC. The users of the Geneces project can develop the potential of their devices by using mobile internet technologies. These technologies are developing rapidly worldwide. In most developed countries, the third and the fourth generation of mobile communication systems have already been introduced. Thanks to these technologies, it is possible to implement this project in the mode of comfortable use. One of the main advantages of the Geneces project is complete server automation. Users need to make just a few clicks to switch from one operating system to another one. They have a large selection of various modern operating systems. As a result, the cost of a modern compact device, such as a smart phone, a tablet or an ultrabook, becomes much lower because the cost of components in desktop variations on remote servers is much lower than those in mobile solutions.

Construction of a flame spectrometer

Philipp Kessler
Jonas Gaiser and Augustin Harter
Supervisors: Jo Becker, Simon Gaiser
Friedrich-Schiller-Gymnasium Ludwigsburg,
Tamm/Germany, philipp_kessler@gmx.net

1 Introduction

Spectroscopic analysis is one of the most used methods for qualitative and quantitative analysis in several science areas, like chemistry or astrophysics. Each element emits a specific spectrum (when excited), which characterizes it. By splitting up this emitted light of excited samples, it is possible to distinguish the different spectra of the compounds and to draw conclusions on the substances in the sample. Combined with a flame, which excites the atoms of the sample, a simple and precise method for analyzing samples of alkali and earth alkaline metals results.

The aim of this project is the construction of a flame spectrometer, which can determine the compounds and the concentration of unknown samples consisting of alkali and alkaline earth metals. The spectral resolution and the photosensitivity of this device have been optimized.

2 Measuring setup

Fig. 1: Measuring setup

The sample is obfuscated pneumatically and guided into the flame. The excited atoms emit light, which gets into the optics of the spectrometer, where it is collected by two plano-convex lenses and projected on a self-made adjustable slit.

After passing the slit it is parallelized with a camera lens and split up by a diffraction grating. The measurement of the light is done by an image sensor from a DSLR camera. With the obtained data a plot can be created (Fig. 3) and the single compounds of the sample can be analyzed. Later, a program can match the determined wavelengths with a database and identify the compounds of the sample.

3 Results

The spectrometer reaches a very good spectral resolution, about 0,3 nm. This is apparent from measurements in which the both Sodium D-lines can be observed. These have a wavelength difference of only 0,6 nm.

Due to this, the distinction of several spectra is accurate and allows a precise qualitative measurement.

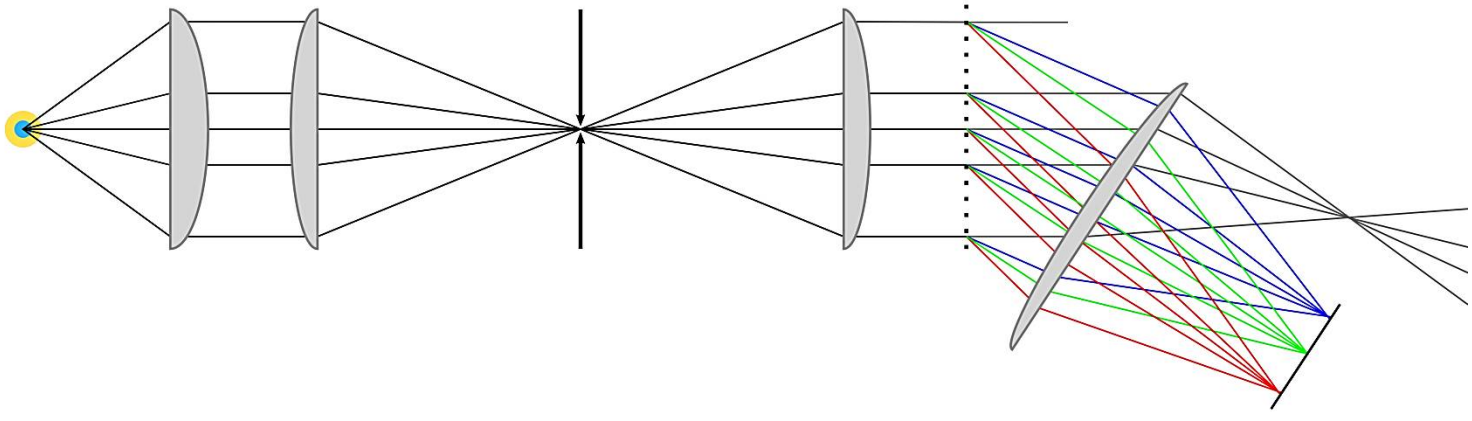

Fig. 3 shows the plot of the analysis of a sodium/strontium sample, in which the different compounds can be distinguished well, although the wavelength of sodium (589 nm) and strontium (606 nm)[1] are rather close to each other (about 17 nm).
The dependence of concentration and light intensity passes over from linear growth in nearly logarithmic growth, as suggested in Fig. 4. That means that quantitative measurement is possible, at least in lower areas of concentration (< 1 g/l).

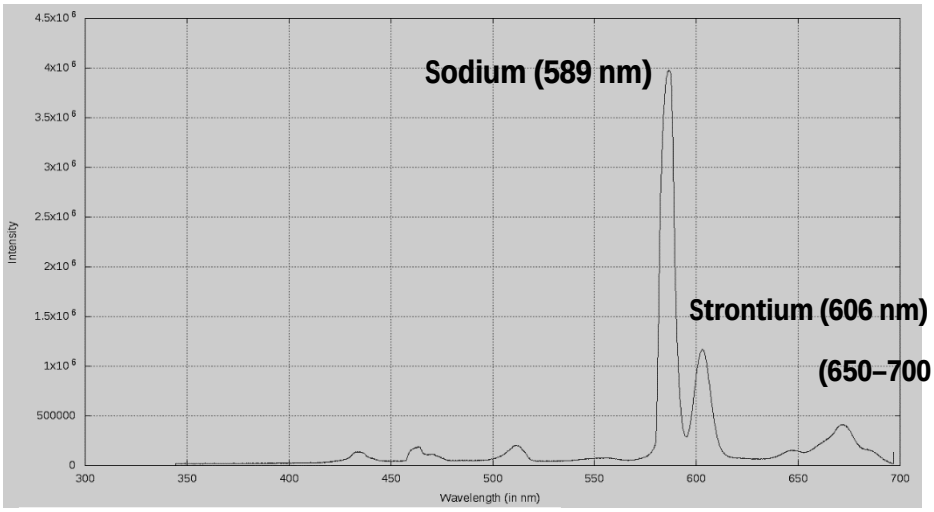

Fig. 3: Plot of a sodium/strontium sample

Also, very low concentrations can also be determined. Concentrations of lithium, which fall below 0,2 mg/l can still be determined.

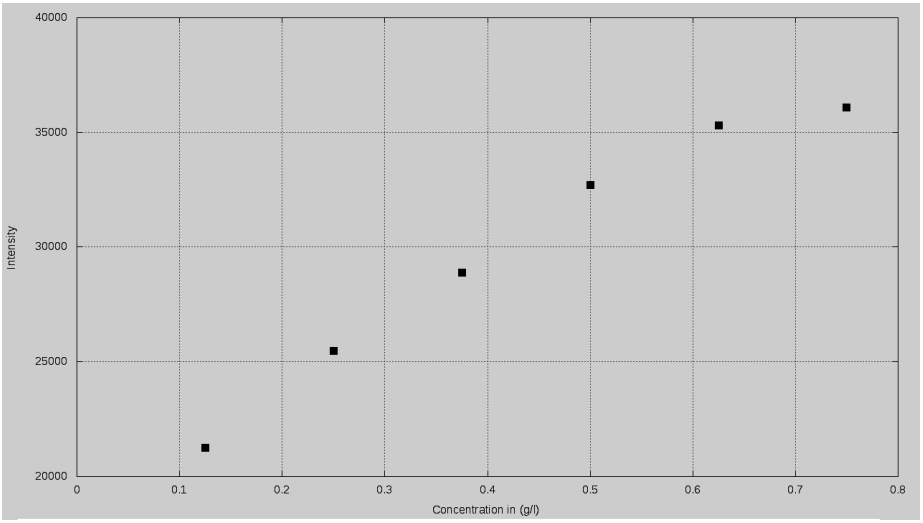

Fig. 4: Plot of the intensity several lithium samples with various concentrations

4 Conclusion

In conclusion it can be said that this spectrometer reaches a good spectral resolution, which allows a precise qualitative measurement. The quantitative measurement is also possible and allows the use for accurate chemical analyzes.

Particularly the high spectral resolution, as well as the adjustable slit, shows the far advanced optimization.

5 References

[1] http://physics.nist.gov/PhysRefData/Handbook/element_name.htm

[1] Strontium also emits in the range of 650-700 nm

ABSTRACT

OCa Application to Reduce Weight

Isabela Pu Dwi Andini (Puput)
animeisabela@gmail.com
Ida Ayu Dewi Susiani, S.Pd. , M.I.L
Trinitas High School, Bandung, Indonesia

ICYS 2016

SHORT INTRODUCTION

Most of all people prefer to have a thin body, but in this modern era- where all food becomes more and more delicious and harder to deny- and more over because of the technology, some people become lazy to do exercise, this can cause an increase in obesity disease. But not all of the Technologies are bad for Humans, take an example, for the problem above, I can make use of our technology, to make a reminder or a control how to make our body ideal with OCa Application in Android by looking at the calories in our bodies.

RESULT

The formula used in an application OCA is taken from several sources that have been experienced in calculating the calories in the human body. After the survey, it showed that 70% of respondents managed to lose weight in two weeks, so it can be ensured that the application OCA can accurately calculate the number of calories.

CONCLUSION

Using these applications regularly, users can know the calories and an ideal weight and lose weight by 5% of respondents in two weeks. To support weight loss still in balance and composition of the foods eaten, we can take the benefit from OCa application.

PURPOSE

The purpose of the application is to make people who use this application be able to control their calories in their bodies, so they can make a weight loss, and still stay healthy through the process of weight loss.

EXPERIMENTAL METHOD

Calorie is everything when it comes to how much weight you lose, if you consume less than you burn over time you lose weight. The opposite is also true. If you consume more calories than you burn, you gain weight. So In OCa App, this App calculated user's calories first, and then when users do an activity, it will calculate whatever the users add or burn calories in their body.Using Android Studio and SQLite to make the program,

KEYWORD

Calories, weight, Obesity, Food, Development

REFERENCE

1. MACKENZIE, B. (1997) *Your Ideal Weight* [WWW] Available from: http://www.brianmac.co.uk/idealw.htm [Accessed 15/8/2015]
2. Murphy, Mark L.(2011). Android Programming Tutorials [PDF]. CommonsWare. Available from : https://commonsware.com/AndTutorials/AndTutorials-3_1-CC.pdf [Accessed 4/8/2015]

Boolean Chaotic Encryption (BCE)

Wilbert Osmond

Chandra Kusuma High School, Indonesia - wilbertosmond@hotmail.co.id

One of the greatest breakthroughs in mathematical computation in this century has been the realization that even the simplest of dynamical systems may behave extremely unpredictable. Chaos theory exhibits a great sensitivity to initial conditions that a mere slight of difference on the input, will result to a widely diverging output. Chaotic computation literally scrambles bits that it appears to be nonsense and static, regarding to its high frequency and increasing speed in bifurcation within its chaotic regime. This is what encryption finds chaotic computation most useful to conceal messages, by thoroughly destroying the relationship between its input and output. Despite its seemingly randomness, it has a deterministic nature, regarding its fractal self-similarity from iterations, also helps the necessity of decryption. Another important factor that has to be considered is its speed, which is inversely proportional to its strength. This is why I have decided to apply the mathematical and exploited chaotic equation, which its simplicity is to assure the speed effectiveness and its dynamical unpredictability for the strength effectiveness, to encryption. However, converting mathematical chaos theory into an electronic circuit has also found itself troubles.

Boolean networks consist of randomly connected nodes, each of which has a binary state: on or off (1 or 0), which simplify the treatment of highly nonlinear systems. The state space of deterministic boolean networks with synchronous update is, however, finite, and thus, they cannot exhibit chaotic behaviour, as defined by an exponential sensitivity to initial conditions. One way of recovering non-periodic behavior is to update the state of the Boolean elements in an, at least seemingly, random order, in which chaos theory can be utilised. The chaotic binary state, I hypothesise, can be projected into logic gates electronic circuit for encryption.

For its efficient security assurance, further security analyses are to be carried out. First, avalanche effect analysis, to verify its exhibition of chaos' most prominent feature that is its sensitivity to initial conditions by how the input value should produce a completely different and widely diverging output even a single bit is altered. Subsequently, for its determination of chaotic region, its bifurcation diagram is to be shown as the visual analysis; whereas for the mathematical analysis, the Lyapunov exponent is to be tooled. Last but not least, time complexity to guarantee how fast mode of communication it can be. On the other hand, the practical prove as to if the encryption works, will be carried out in a simulator program.

Keywords*: chaos theory, encryption, boolean algebra, security analyses*

Abstract, **Identity-based authentication for Cloud Computing.**

Petar Bubinski
Supervisor: Elizabeta Stojilkova
SOU ”Vanco Prke” Vinica, Dimitar Vlahov n.6,
bubinskipetar@gmail.com

Cloud Computing is a newly-developed technology for complex (distributed) systems which defines services of massive proportions that are shared between numerous users. This term may also be defined as a way of using computational resources in which dynamically scalable and often virtualized resources can be provides as a service via the Internet. Many companies deliver services by means of the Cloud. The most known are: Google (Google Drive), Microsoft (Microsoft SharePoint), Salesforce.com etc.. There are three main models of service in Cloud Computing: Platform as a Service, Infrastructure as a Service and Software as a Service. IaaS is the basic model, and every higher model is abstracted from the details of the lower models. Other models of service include: Strategy as a Service, Collaboration as a Service, Business process as a Service, Database as a Service etc.. There are also three main types of Clouds: Private, Public and Hybrid Cloud. The Private Cloud is a Cloud based infrastructure which is operated for one organization individually, whether it is operated internally or by a third side and hosted externally. The Hybrid cloud is a mixture of the previous types of Cloud.

In the case of providing secure user access and secure data transfer in a technology like Cloud Computing, the authentication is a very important issue. Most simply said, the authentication is identification plus verification. An identification is a procedure in which the entity provides a certain identity, while verification is the procedure by which means that the claimed identity is confirmed. Therefore, the credibility of an authentication procedure relays on the accuracy of the verification used. The Hybrid type of Cloud is the most vulnerable one when the security identification and secure transfer of data are concerned. The authentication protocol that is used recently in Cloud Computing is SAP (SSL Authentication Protocol). The SSL authentication is a mutual authentication process in which both sides authenticate each other by means of verifying the provided digital certificate. In technical terms this may apply to the Client (a web browser or a client application) and the server (a web-site or a server application) in which case the server also authenticates itself to the client via verification of the digital certificate which is published by a certification authority (CA).

The Identity Based Authentication protocol is a new and experimental way of securing the users data and credentials. The Identity based authentication consists of an Identity Based Encryption method and an Identity Based digital Signature. The authentication protocol is analog to a TLS that uses a RSA algorithm for the key exchange.

When those two methods are compared, the SSL authentication has shown not to be appropriate for Cloud computing due to its Public Key Infrastructure implementation and immense calculations that are brought in by the digital certificates, which are excluded in the Identity Based Authentication scheme. In this context we will explore an authentication scheme that looks into the hierarchical structure and an authentication that supports the same structure in the Hybrid Cloud. This authentication is the Identity-Based Authentication for Cloud Computing (IBACC).

SMART HOME

Ferencz Albert and Róbert Budai
Júlia Geváld and László Bárdos
Apáczai Csere János, Cluj-Napoca/Romania, xaviferi123@gmail.com

Introduction

The so called „Smart Home" project was founded aproximately 5 moths ago. The main purpose of this project, as its' title says, is building a home which is totally supervisable through our smartphones. Our system is based on a Raspberry pi 2, and will be presented on a wooden scale model. SmartHome can thank its existence to smartphones, so the guard application was written in android, for android smartphones. In the past, this application used to be replaced by a website hosted by an Apache server. Unfortunately, the website brought up several problems, and its hosting took up a large amount of processing power. The attempt to use two raspberries would have seemed like solving the problem, but in reality, it only brought up more problems in communication. Porting to android widened our range of possible upgrades, and offered a larger problem solving opportunity.

First of all, the most problematic element of the website was the MySQL database. This database had more than ten tables, filled up with thousands of lines. These tables stored every single data from lamp switching to temperatures. Surely, the database was more efficient in storing the data, but was really backfiring at its speed, taking more than 1 second to read the last lamp switching data. Giving up the possibility of storing the data, the MySQL database was replaced by python socket servers. These servers are responsible for everything, from data sendig to picture taking. Currently, the SmartHome system has the following features: Lamp-, relay switching, movement detection, IP Camera, bell, bell camera, door-, window state detection, music player, thermostat handling and last but not least, a log-in module. Every feature is hosted by a server, which are all run on the raspberry, besides the login-server, a.k.a. "Main Tunneler", which is hosted on an external server 24/7, and makes the users home accessible from wherever exists an internet connection. Every user has its own personal User Account(s), which stands of a username and password.

Login module/activity

This is the module that shows up, whenever the user decides to launch the so called "Smart Security" application on their smartphones. Once open, a logo, two text areas and a button appears. These text areas will contain the username and password typed in by the user. When the button is clicked, the Java activity in the background connects to the data server, the main tunneler, and sends a login request. If the username exists, and the password is correct, the login procedure will succeed, and the user will be redirected to the next platform, else, the user will be notified of the failure and shown an error message.

Sensors

The scale-model contains several sensors, such as magnet-sensors, above the door and the window. Through these elements we can follow the status of doors and windows, if they are opened or closed. Two temperature-sensors are built in as well, which digitally transmit the temperatures both from outside and inside. The temperatures are visualized in Celsius on your phones' display. Besides these, the security of our system is also very important. The Infra-Red motion-sensors are monitorizing every movement is the house, or in this case, in the scale-model. These data, more precisely the date, the exact time, and the place of the movement is appearing in every case on the display of your phone. In order to present the lamp switching feature, we have built in LEDs which represent high capacity consumers. These LEDs function only on 3.3 V, but this can be solved easily by a so called relay, which is able to control 220 V by using just 3.3 V. Our modell contains one of this as well.

Security Alerter

The security alerter is responsible for notifying the user about every transgression. Enabling this feature starts the SmartHome Notification server. If the security alerter is enabled, every movement, window-, door-opening will trigger a notification, and the application will notify the user about the transgression. The bell also takes part of the security alerter feature, although this cannot be dis- or enabled. In case of bell ringing, the user will be notified about the event, and will be sent a picture of whoever was standing in the door at the time of the bell ringing.

The "Command Room"

The “Command Room” is the main activity of the application. This is the activity that the users get redirected to if the login procedure was successful. This consists of several ImageViews, which redirect to the activity set to them, for example a lamp stands for lamp switching, the musical note stands for the music player and so on.

The “Thermo-Room”

Today, every home has a separate heating system with a thermostat. With the help of this element and our system, the regulation of our home’s temperature can be easily solved through our smart-phones. By clicking on the thermostat, the user gets redirected to the “Thermo Room”. This is the room, which consist, of a thermostat, and a “+” and a “-“ button. Clicking on these we can reduce, or increase the base temperature set to the room.

The “Camera Room”

By clicking on the camera, the user is shown a list of available IP cameras. Clicking on one of the available cameras, triggers a new activity, which instantly shows up. This consists of a livestream, four arrows, and a save button. By pressing the arrows, the users can move the camera. This offers a 360° view coverage of the room. By pressing the save button the user can save the that present moment.

The Website

To make our system more userfriendly, we made a webpage for costumers. The aim of this webpage is to help new users to create their own SMART-Home system. Right after opening the webpage, the new user has to enter his or her username and password. After this step the webpage displays a 20x20 table, on which the user can build the specific home using walls, doors and other basic things. This can be done on 5 floors. After this, every sensortype or controllable element can be put down and be named as the owner wants. When the user finishes desiging his SMART Home the user my click ont he GENERATE button which generates a file, consisting of the numbers of the elements and their names. This .txt document has to be uploaded to an online server, using the same website. From the server the SMART-Home system gets the file and then „et voilà”, the system is totally complete, with the users preferences.

Conclusion

In conclusion, we succeded in creating a cheap, but trustworthy system, and we also widened our knowledge in programming and engineering.

Bibliography

https://docs.python.org/2/library/socket.html

https://docs.oracle.com/javase/7/docs/api/java/net/Socket.html

„Java a mindenapi kenyerünk” – Simon Károly

Side Note

The physical side of the project was mainly assambled by my must be mentioned partner, Róbert – Mihály Budai, who has done all the cabling and sensor mounting, and also, he designed the website! The programming side was mainly written by me. Our work can hardly be separated!

Thank you for your attention accorded.

Io – The SmartCar

Student: Coţop Ruxandra Anca

Supervisor: Coţop Carmen Viorica

Nicolae Bălcescu High School, Cluj-Napoca, Romania

3.1.1 The purpose of the investigation

Have you ever woke up in the morning and wonder how would it be if you would have your own personal autonomous robot? Well I have and ever since I tried to create it. So, the purpose of this investigation is to demonstrate the creation of an innovative prototype for an autonomous car which is automatically controlled by an embedded electronic system containing a smart logic behind for driving the mechanical components, as well as an intelligent mobile app for the users' interface, all integrated in a smart car called "Io". Environment sensing, trajectory planning and feedback is supported through continuous monitoring and smart control of dedicated sensors.

Method of the investigation

When I started working on this project I have found out from my research the fact that car producers like Lexus, Mercedes, Audi or Nisan have already thought of this. They have hundreds of people that are coming up with ideas and they almost realised to create a driverless car. Though they have been working on this for over 8 years they didn't manage to make a total autonomous car.

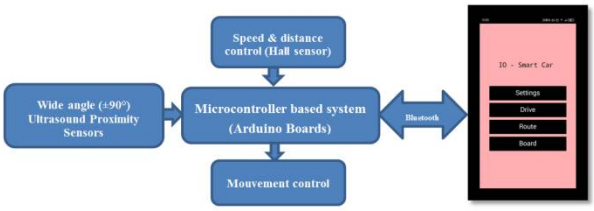

So, with this in my head I have tried to create a prototype for such a car. My idea of what it should be like can be seen in the scheme above. Though it sounded pretty easy in theory, the practical implementation has required to overcome a number of hardware and software challenges.

The first one I faced was the fact that in order to create a smart car the most important thing to do is to make it autonomous. To do that, the processor needs to know exactly where the robot is at any time. The solution I found for this problem was to add a Hall Sensor to one of the wheals along with two magnets. This way the robot is able to measure the distance it made since it started moving and to calculate the speed of the car at any moment. This two can be done using two simple formulas (the distance = number of rotations*length of the wheal; speed = distance/time).

Next thing on my list was for the robot to be able to turn on/off its lights only when needed, in order to save some energy. For this I used a photocell and some LEDS as lightning. After this was done I figured that a real car has signalisation lights and I attached some more LEDS for this.

The third thing is the fact that a smart car should never hit an obstacle no matter the direction it comes from. So I attached 4 Ultrasonic Proximity Sensors that have a wide angle(±90°), thanks to the 4 ServoMotors that they are attached to.

To control all this components I had to use two Arduino boards that use a I²C protocol to communicate one with the other. Besides this, to command the master board I attached a HC-06 bluetooth module. Using it the two Arduinos get a command from a smart phone and turn it into an action.

The mobile application was created using MIT App Inventor and it has more options like: driving the car, creating a new route, set the bounds of the route etc.

Results of the experiment

The prototype seems to be acting pretty good in the tests I made. I measured some of its parameters and the only problem I seem to face till now is that the batteries don't last more than one hour, but this can be fixed by changing the alimentation.

Conclusion

The experimental set-up and the tests have shown that "Io" is a reliable test bed for a future generation of smart cars and autonomous robots.

The evolution of the climatic characteristics under the influence of solar radiation

Student: Varvara Dragos

Coordinating teacher: Teodorescu Gabriel

"Avram Iancu" Theoretical Highschool

Abstract

During the last few years, the study of climatic changes has become an intensely scrutinized and debated topic within the scientific community in the field. The importance given to recent climate changes is due to the fact that they produce negative effects on natural ecosystems and on society, being caused by the global warming. The increase of the air's minimum and maximum average temperature has been confirmed by numerous studies from different regions of the world.

The object of research

The evolution of climatic characteristics (temperatures) near the city of Cluj-Napoca is determined by the solar radiation influence (length of Sun brightness, SSN, Wolf number and solar cycles). Their knowledge has applications in architectural systematization, photovoltaic systems and plant growth patterns. The study refers to the problems of the climate variability system of the given area. The phenomena that occur during CMEs are quantified by the number of sunspots or the Wolf number. We tested the studied parameters using the Meteotest software.

Materials and Methods

The climate in the area is influenced by radiation-related, dynamic and physical-geographical factors, being specific to the North-Western region of the country. The characteristics under analysis were: air temperature, time-length of Sun brightness and the number of sunspots. The meteorological station of Cluj-Napoca is situated at approximatively 46047'N/23034'E at a height of 414m.

By using mathematical statistics in order to identify the most suitable trend, we tested that square linear model, the exponential model and the polynomial model. We calculated r^2, the determining coefficient, the absolute average percentage error, the absolute average deviation and the square average deviation. `Data were taken from:` http://www7.ncdc.noaa.gov/IPS/mcdw/mcdw.html; http://www.meteoromania.ro; The Exploratorium's Guide to Sunspots; RWC Belgium World Data Center for the Sunspot Index; NASA Solar Physics Sunspot Cycle page and Table of Sunspot Numbers by month since 1749 CE

Conclusions

The variation in air temperature points to clear tendencies towards the increase of this variable due to solar activity and these tendencies have proven to be significant from a statistical point of view.

By employing statistical analysis we tested the various models and the relationship between temperature, time-length of Sun brightness and the number of sunspots, in relation to the solar cycles.We highlighted the periods of excessive or insufficient amounts of annual average solar radiations and temperatures in comparison with the multi-annual average. We have tested the homogeneity of time sequences regarding global solar radiation throughout the period of solar cycles by using the normal standard homogeneity test (TOSN).

Length of Sun brightness – x (1989, 2000) [*]

Temperature – y (1993, 2006, 2015) [**]

Number of sunspots - z [**]

Level of significance - [*,**,**]

The climatogenetic factor that influences and determines the formation and evolution of the processes in the terrestrial atmosphere is represented by the sun (the parametres being solar radiations, time-length of Sun brightness and the number of sun spots).

According to the data gathered during the period under analysis we have noticed that the polynomial model, the square model and the linear model (according to values of r^2) are the most suitable for the evolution, time-length of Sun brightness and temperature. According to the standard homogeneity test, the temperature exhibits increasing tendencies although solar radiation manifests slightly decreasing tendencies and the number of sunspots is rising. According to the regression line there was no indication of significant variations with regard to the sequences of data, although some oscillation was present, yet the statistical models become much more complex.

We attribute the increasing temperature to solar activity and it is not uniform, but subject to significant variations function of solar cycles. By using the Pearson correlation we have pointed out that there is a solid link between the parametres under analysis. Temperature variations registered in recent years, variations from the multi-annual average temperatures, are the result of solar radiation activity and natural climatic changes. The process by which the Sun exerts its influence cannot, however, be clearly outlined.

There is a correlation between Wolf number and atmospheric nebulosity causing temperature variations, so that a high number of sunspots (CMEs), determines minimal nebulosity and very high temperatures, and vice-versa.

The effect of solar activity on the decrease or increase of insolation weathering becomes manifest through changes in temperature, there being a correlation between temperature and Wolf number. By testing software such as Meteotest (data at international level) with regard to the parametres under analysis we have discovered that some variables are either overrated or underrated in what concerns their value, but they fit according to existing data, there being either a positive trend (for temperatures and sunspots) or a negative one, for the number of insolation weathering hours and thus for global solar radiations. The increase in atmosphere temperature also comes as a result of anthropic causes which lead to climatic changes and high temperature oscillations from the annual average.

Consequently, it may prove impossible to classify the real causes of oscillation in some climatogenetic parametres, as their root may be either in solar activity or in pollution.

The Computer Program for Solving Tsume-Shogi

Student: Aleksandr Suppes

Supervisor: Dmitry Shtukenberg

Laboratory of Continuous Mathematical Education, Saint-Petersburg, Russia, suppes98@mail.ru

The purpose of the investigation

Shogi is a Japanese chess-like game. However, unlike chess, humans still beat computer in shogi. So, the problem of developing programs playing shogi is of a great interest in Computer Science. The program developed is able to solve some sorts of tsume-shogi problems (the forced checkmate problems).

4 Brief description of tsume-shogi

5 Shogi in general resembles European chess, however it has several important differences. The game is played on 9*9 field, the pieces are weaker than the chess counterparts (e.g. knight has only 2 fields, where it can go, in comparison with 8 fields of chess knight), but these details are not very important for computer and do not make the game more complicated. The major difference is that pieces taken from the enemy are not removed from game, but can be taken “in hand”, and later any of them can be placed at any position on the field. This increases the number of variants and makes computer analysis of position much more complicated.

6 As in European chess, shogi has a big volume of different debut strategies, problems etc. One of the most important shogi problems is tsume shogi: problems on forced checkmate. In this kind of problems you need to checkmate your partner, and each your move is to be done with check. Analysis of tsume shogi is much simpler than that of shogi game in general, so we choosed this problem to simplify our task.

7 Description of the program developed

8 The program developed is able to solve any tsume shogi problem. The algorithm searches the solution by traversing the tree of possible moves. The program has user-friendly interface, able to draw and edit shogi positions in graphical form.

Conclusion

We developed a program that can solve some shogi-related problems. The program is not very fast (this is due to the number of variants that should be analyzed in shogi position), and it poses a challenge to improve the speed of the program.

MINIMUM VOCABULARY LANGUAGE PRACTICALITY AND DESIGN: M

Matija Čupić
Supervisor: Nikola Srzentić

Regional Centre for Talented Youth Belgrade II, Belgrade, Serbia, matija.cupic.97@gmail.com

1. Introduction

Today, the majority of programming languages have vocabularies between 20 and 100 words. Ones with 30 to 50 make up the most of that majority. The 80 to 100 segment is populated mostly by *.NET* languages due to their extra contextual keywords, while the 50 to 80 interval is very sparse. At the other end of the spectrum, languages with less than 25 keywords are practically non-existent. Esoteric turing tarpits are the only representatives. They provide very little practicality and are often used only as a proof of concept or as an example.

Archaic languages, such as *ANSI COBOL* and *SystemVerilog* have a relatively high amount of keywords. Their vocabulary size is multiple times larger than of any modern language, having more than 300 reserved keywords.

Exploring the practicality of minimal keyword languages beyond turing tarpits is the purpose of this research. The goal is creating a practical implementation of a programming language as well as developing a specific IDE supporting the minimal-vocabulary notion.

9 2. Method of investigation

Data about keyword density was extrapolated from the specification of some of the most popular languages.

Samples were taken from a selected few of the most active public GitHub repositories to form the basis for the analysis of the relationship between the keyword count, size of the project and popularity of the language.

9.1 2.1. M Language

- 4 data types: number, string, boolean, list. All of them are nullable
- Expressions: addition, multiplication, power (raising a number to a certain power), equality and relational
- Unary operators of boolean negation and negative number prefixing
- 4 built-in functions: println (prints text in a new line), print (prints text), assert and size (returns the size of a list)
- Dynamically typed variable system with flexible assignment and lookup
- User defined functions
- 3 control flow statements: if and the for and while loops
- Variable scope: all control flow statements have their own scope (unknown variables are looked up in the parent scope); functions have a separate private scope

The language itself distinguishes two valid syntax flavors: "compact" and "expanded" versions. The "compact" has only several characters and is designed to be as compact as possible. The latter is C-like and is designed to be familiar to most people.

ANTLR was used as a parser generator. It serves both as a lexer and a parser and is in almost every way superior to the outdated YACC/LEX toolchain which was the alternative.

9.1.1 2.1.1. Lexer

During the design process the exact value of keywords fluctuated between 8 and 14, in the end finally setting on 11 (4 are scope identifiers). There was a dilemma about scoping in the language. Two options were present: implicitly and explicitly defining scopes. The implicit scope option was chosen because it allowed the language to be even more compact removing the need for scope symbols (tokens). Being unable to define custom variable scopes further simplifies the language and reduces the possibility of memory leaks.

9.1.2 2.1.2. Parser

Every *M* script is treated as a block of code. It consists of one or more statements with each being terminated by a semicolon. The statements can be recursive and are designed to be as flexible as possible. They can consist of one or more statements, as well as of only variables.

9.1.3 2.1.3. Abstract Syntax Tree

Instead of representing the lexer recognized tokens in a flat list, the language builds an Abstract Syntax Tree (AST). This approach allows not only better flow manipulation and easier interpretation but also provides good debugging capabilities of both the language and scripts written in it.

9.1.4 2.1.4. Interpretation and evaluation

Since *M* is designed to be dynamically typed, a generic value type which gets checked and operated at runtime is implemented. It's later broken down to the appropriate value type (number, string, boolean or list).

Every value belongs to a scope. Scopes can be nestable. When execution exits a scope it independently handles releasing reserved resource

while prioritizing scopes which are leafs in the scope tree structure

A *function* class was created to encapsulate a series of statements which represent a user defined function. It resolves the self-scope autonomously.

Script interpretation is implemented using a *visitor pattern*. This means that the syntax tree is abstracted from the implementation, providing added flexibility. Every statement is a node in the AST and the variables themselves are leaf nodes. The nodes are visited by the *walker* which walks upon nested statements if any, or interprets and evaluates the statement if there aren't any.

The *M* language breaks on the first occurrence of an exception in runtime.

9.1.5 2.1.5. Interoperability

The language is designed to lean on the class libraries of the platform it's being executed on, meaning it can access any function already in the "host" language (C#, Java, Python, JavaScript) library. This research is oriented towards implementation in the Android OS.

2.2. M – IDE

9.1.6 2.2.1. Design

MIDE itself is designed to be as compact and practical as possible. It splits the screen into two segments: the code view, and the input entry method.

CodeView has two distinct modes that can be seamlessly switched to and from by swiping. One mode displays the "extended" version of the code in C-like syntax, while the other offers a more compact version which is less human readable but much more compact.

The IME adopts a design similar to the code view and has two swipeable modes. The "smart" and "dumb" code entry modes.

9.1.7 2.2.2. Functionality

The CodeView compact mode shows the code in compact form by using only a limited number of symbols to denote keyword tokens, making it more esoteric but useful in environments which have limited view space.

The "dumb" IME shows only the symbols allowed in the language. Depending on the CodeView mode, that might be the keyword list or the symbols used to represent them.

On the other hand, the "smart" IME shows several buttons representing contextual groups of tokens. Different tokens are entered by pressing buttons a different amount of times. This design further optimizes the experience for the mobile platform and produces a more practical, clutter-free UI.

10 3. Results

The uniqueness of the language is seen in its one of a kind specification and tie-ins with other platforms. The unique design is synthesized from the results of the analysis of the impact of language vocabularies in other languages.

It's designed to be used alongside its companion app, the MIDE. Together they offer an elegant way of writing small projects with minimal effort by reducing the amount of code needed to enter and by providing a "smart" IME. It also allows the developer to use some of the already written Android libraries. The language is ideal when developing small proof of concept projects in the smallest timeframe possible, or when unable to use your laptop or desktop PC, but having the need to test something.

11 4. Conclusion

From the analysis of the research results it can be concluded that there is practicality to be found in minimal vocabulary languages, if executed properly. Their use is not limited to just being esoterical turing tarpits.

While severely lacking in many aspects, compared to languages with higher keyword density, it can be seen that they are capable of being used for creating quick "gists", proof of concept projects and especially when developing on a limited platform – mobile.

The research can be further extended by improving the IDE offering better debugging capabilities and other functionality.

12 5. References

[1] P. Naur; Programming languages, natural languages, and mathematics; Copenhagen University 1975

[2] G. Winskel; Formal Semantics of Programming Languages; The MIT Press 1993

[3] H. Abelson, G. Sussman, J. Sussman; Structure and Interpretation of Computer Programs; The MIT Press 1996

[4] F. Turbak, D. Gifford, M. A. Sheldon; Design Concepts in Programming Languages; The MIT Press 2008

[5] R. Harper; Practical Foundations for Programming Languages; Cambridge University Press 2012

GAME SUIT

Uroš Filipović
Supervisor: Nikola Srzentić
Regional Centre for Talented Youth Belgrade II, Belgrade, Serbia, uros@programmer.net

1. Introduction

Human-machine interface is field of computer science that researches new ways for people (users) to interact with computers and reverse. Now days scientist are researching virtual reality, EEG sensors, in field of medicine interface for control of robotic wheelchair and visualization of medical data in virtual environment. Based on previous researches I came up with the idea of making the Game Suit. The role of Game Suit is to increase the feeling of immersion while playing a game by simulating in game haptic feeling. It can also collect data while the player is playing the game and process it and display it in game or on the suit. So it increases interaction between human (player) and computer (game).

2. Method of work

Game Suits parts are Arduino, TENS signal generator, electrodes, pulse sensor, relays, bluetooth module and displays. Arduino MEGA 2560 is controlling all the parts of the suit. TENS (Transcutaneous electrical nerve simulation) signal generator makes signal witch stimulates muscles. TENS signal is a high voltage pulse that is spread by the electrodes and activates mussels. Relays path the signal to stimulate the right muscle. Smart phones or PCs connect to the Game Suit and send data via bluetooth using HC-06 bluetooth module, so it is easier for player to move around without worrying about pulling out cables. Games connect to the suit using my API for Unity 3D game engine. API support both Android and Windows platform. Because Unity does not support bluetooth on Android I wrote Android native plugin to allow my API to use bluetooth.

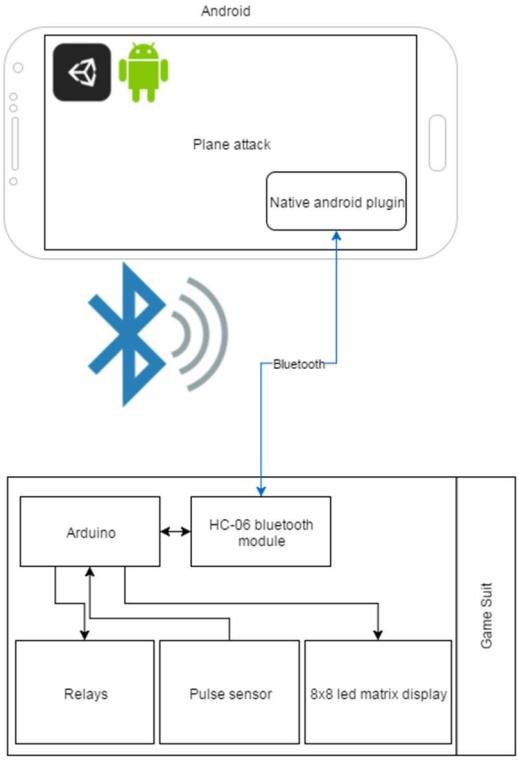

Picture 1 - Connection between Unity Android game and the Game Suit

For games that don't support API can use application that connects to SQL base or connects to the game using the TCP socket and gathers data and sends it to the suit. I have made a plugin for Counter Strike Global Offensive that stores hitbox information on the SQL base. Game Suit interface application connects to the SQL database and as described gathers and sends data do the suit.

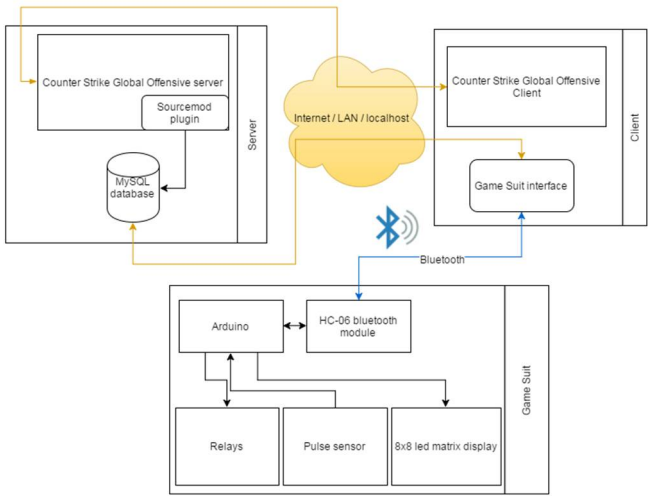

Picture 2 - Connection between Counter Strike Global Offensive game over the SQL base

3. Result of work

Player would put on the suit and connect it via bluetooth, and run a game. Suit will immerse player in virtual world in field of physical feeling. Suit will measure players stress and change the way the suit works. It will also send that data to the game and it will react differently based on the value. Game could display it for example blur the screen if player has stressed out or activate other functions of the suit like vibrating motors or display something on 8x8 display.

4. Conclusion

The whole idea is to engage research in field of connecting machines with human body where machines can generate some signals and control some pats of human body. In future that kind of suit could control lower limbs so the user could walk again. Future versions of the Game Suit would have conductive fabric witch will replace uncomfortable wires and electrodes. Conductive fabric allows much more electrical power lines and much more flexibility unlike using classical electrical wires.

5. References

[1] Lukic, P, Zunjic, A. Ergonomic and Electronic Designing of Muscle Stimulator. 2010.

[4] Tello, Richard JMG, et al. "Development of a Human Machine Interface for Control of Robotic Wheelchair and Smart Environment." IFAC-PapersOnLine 48.19 (2015): 136-141.

[5] Krapichler, Christian, et al. "Human-machine interface for a VR-based medical imaging environment." Medical Imaging 1997. International Society for Optics and Photonics, 1997.

Abstract: Tin based Oxides and Sulfides as Anodes for Lithium-ion Batteries

Bruce Wen Ke Zhen, [1], Dr M. V. Reddy[2],*
[1]Raffles Institution,[2] National University of Singapore, Singapore, [*]wen.kezhen@gmail.com

1. The purpose of Investigation

Lithium-ion batteries (LIBs) are important as a portable source of electrical energy. However, the graphite anode present in the commercial LIB has a low practical capacity of 300-320mAh g^{-1}. Tin based materials SnO_2 and SnS have attracted huge attention for anode research due to their high theoretical capacities of 791mAh g^{-1} and 782mAh g^{-1} respectively, easy preparation through extraction from cassiterite ore, and high energy densities. However, these materials still suffer from poor cycling performance, especially when cycled above 1.0V. Therefore, the aim of the research is to prepare SnO_2, SnS, via novel methods to obtain anode materials with both high capacity values and good capacity retention.

2. Method of Investigation

Preparation temperature and preparation chemicals are identified to be key factors to affect capacity and capacity retention of anode materials. Based on literature studies, a novel method of preparing SnO_2 using $SnCl_4$ at a low temperature of 180℃ via the molten salt method (MSM) is adopted. To find the optimal cycling performance, a wide range of temperatures, 150 ℃ to 240 ℃, is chosen in the preparation of SnS material using the solvothermal method.

From the prepared samples, several methods of characterization were carried out: X-ray diffraction to determine the purity of the samples, Scanning Electron Microscopy to find out the morphology and particle size, Cyclic Voltammetry to understand the reaction mechanics and potentials, as well as Galvanostatic Cycling to obtain the capacity and capacity retention values.

3. Results of the experiment

Galvanostatic cycling studies in Fig. 1(a) show that prepared SnO_2 material exhibits a high reversible capacity of 1056mAh g^{-1}, and a capacity retention of 44.9% over 50 cycles. Hence, significant capacity fading is still noted. However, this has still been found to be a significant improvement from literature on SnO_2 nanoparticles.

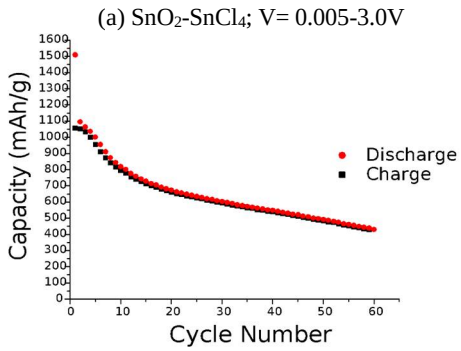

***Fig. 1(a): Galvanostatic Cycling**: Capacity against Cycle Number plot of SnO_2-$SnCl_4$, cycled from 0.005 to 3.0V, current rate: 100 mA g^{-1}*

Among the range of the temperatures studied, SnS prepared at 180℃ via the solvothermal method showed unprecedented electrochemical performance, as seen in Fig. 1(b). The prepared SnS material displayed a high reversible capacity of 1131mAh g^{-1}, and a very promising capacity of 1066mAh/g after 30 cycles. Thus good capacity retention of 85.3% is achieved over 30 cycles. The capacity values obtained are approximately 3 times the practical capacity of graphite anode material.

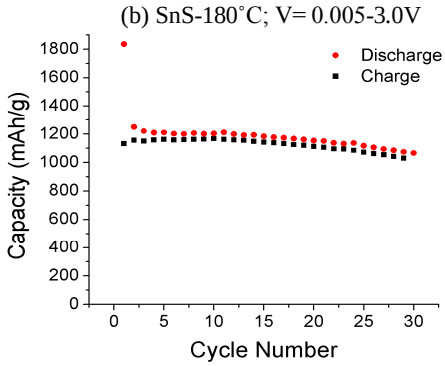

***Fig. 1(b): Galvanostatic Cycling**: Capacity against Cycle Number plot ofSnS-180℃, cycled from 0.005 to 3.0V; current rate: 60 mA g^{-1}*

Analysis of the above good results are conducted via the Scanning Electron Microscope (SEM) technique and Cyclic Voltammetry studies.

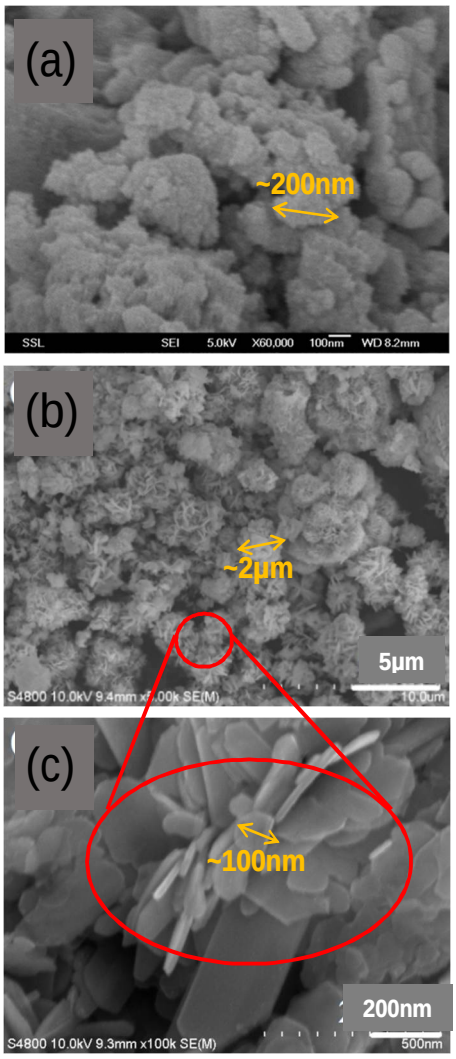

***Fig. 2: SEM Images**: (a) SnO_2-$SnCl_4$; Bar scale: 100nm, with magnification of 60000x (b, c) SnS-180 ℃; Bar scales: 10µm and 500nm respectively, with different magnifications of 5000x and 100000x respectively; Numbers above bar scale represent length of white line.*

The SEM image in Fig. 2(a) of SnO_2 above show agglomerations of particles in the nanometre range. The SEM imagesin Fig. 2(b) and (c) indicate that the prepared SnS exhibits a structure consisting of microspheres constructed via nanoflakes. The high capacity values of both SnO_2 and SnS may thus be attributed to the nano-sized morphology, which results in greater surface area to volume ratio and hence improved cycling performance. Furthermore, the special nanoflake structure seen in Fig. 2(c) suggests that even better morphology has been obtained for SnS. This results in better contact during Li-cycling and thus reduced capacity fading, explaining the good capacity retention seen in Fig. 1(b).

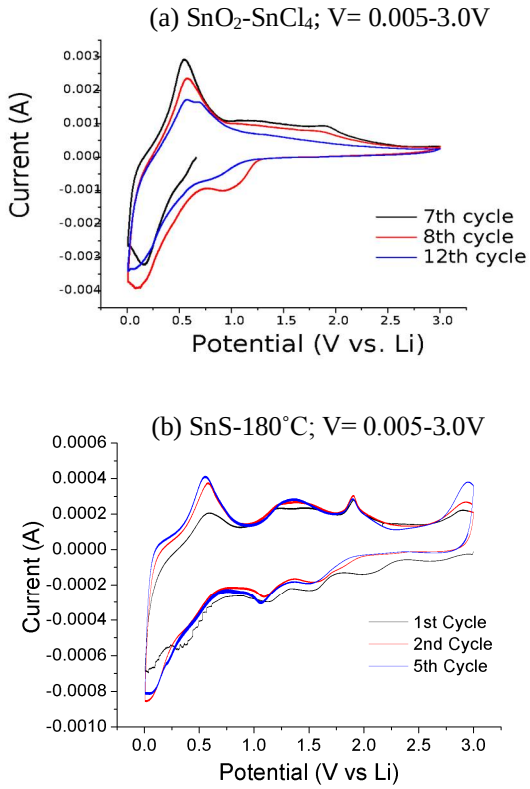

***Fig. 3: Cyclic Voltammetry**: (a) SnO_2-$SnCl_4$, cycled from 0.005 to 3.0V; (b) SnS-180 ℃, cycled from 0.005 to 3.0V; Scan Rate: 0.058mV/sec*

The spectacular results shown in SnS-180˚C can be further explained via cyclic voltammetry studies. There are unique peaks noted at 1.3V, 1.8V and 3.0V in Fig. 3(b) not present in Fig. 3(a), representing formation reactions that take place leading to additional capacity for SnS material. The noteworthy morphology as seen in Fig. 2(b) and (c) is a likely cause for the subsidiary formation reactions taking place.

4. Conclusion

Both SnS and SnO_2were successfully prepared and shown to have high capacity values and good capacity retention at optimal preparation temperature.

The results for SnS prepared at 180˚C is especially notable. Through a simple synthesis process without surfactants, we have attained unique microsphere-nanoflake morphology that results in superior capacity, and most importantly, successfully reduced capacity fading to only 14.7% over 30 cycles in the higher voltage range of 0.005-3.0V. The capacity and capacity retention values surpass past research into SnS material. Given the large capacity of the prepared tin based anode materials, cheap cost of material extraction, simple preparation, and high energy density, tin oxides and sulfides are very promising materials as anode.

5. References

1. Nazri, G.-A.; Pistoia, G. 2003. Lithium Batteries: Science and Technology.(Eds), Lithium Batteries: Science and Technology, Kluwer Acad Publ., New York, USA.

2. M.V. Reddy, G.V. Subba Rao, B.V.R. Chowdari. 2013. Metal Oxides and Oxysalts as Anode Materials for Li Ion Batteries, Chem. Rev. 113, 5364.

3. K. Ozawa. 2009. Lithium Ion Rechargeable Batteries (ed.), Lithium Ion Rechargeable Batteries, Wiley-VCH.

4. Reddy, M., Tse, L., Bruce, W., & Chowdari, B. 2014. Low temperature molten salt preparation of nano-SnO2 as anode for lithium-ion batteries. Materials Letters, 231-234.

5. M.V. Reddy, L.Y.T. Andreea, A.Y. Ling, J.N.C. Hwee, C.A. Lin,S. Admas, K.P. Loh, M.K. Mathe, K.I. Ozoemena, B.V.R. Chowdari. 2013. Effect of preparation temperature and cycling voltage range on molten salt method prepared SnO_2, Electrochim. Acta 106, 143.

6. Li, Y., Tu, J., Huang, X., Wu, H., & Yuan, Y. 2006. Nanoscale SnS with and without carbon-coatings as an anode material for lithium ion batteries.Electrochimica Acta, 1383-1389.

7. Tripathi, A., & Mitra, S. 2015. The influence of electrode structure on the performance of an SnS anode in Li-ion batteries: Effect of the electrode particle, conductive support shape and additive. RSC Adv., 23671-23682.

8. Son, D., Kim, E., Kim, T., Kim, M., Cho, J., & Park, B. 2004. Nanoparticle iron-phosphate anode material for Li-ion battery. Appl. Phys. Lett. Applied Physics Letters, 85(24), 5875-5875. doi:10.1063/1.1835995

9. M.S. Park, Y.M. Kang, G.X. Wang, S.X. Dou, H.K. Liu. 2008 The effect of morphological modification on the electrochemical properties of SnO_2 nanomaterials, Adv. Funct. Mater. 18, 455.

10. M.S. Park, G.X. Wang, Y.M. Kang, D. Wexler, S.X. Dou, H.K. Liu. 2007. Preparation and electrochemical properties of SnO2 nanowires for application in lithium-ion batteries, Angewandte Chemie-International Edition 46, 750.

11. Kim, H., & Cho, J. 2008. Hard templating synthesis of mesoporous and nanowire SnO2 lithium battery anode materials. Journal of Materials Chemistry J. Mater. Chem., 771-771.

12. Chao, J., Wang, Z., Xu, X., Xiang, Q., Song, W., Chen, G., Chen, D. 2012. Tin sulfide nanoribbons as high performance photoelectrochemical cells, flexible photodetectors and visible-light-driven photocatalysts. RSC Advances RSC Adv., 2746-2746.

13. I.A. Courtney, J.R. Dahn. 1997. Key factors controlling the reversibility of the reaction of lithium with SnO_2 and Sn2BPO6 glass, J. Electrochem. Soc. 144, 2943.

14. R. Retoux, T. Brousse, D.M. Schleich. 1999. High-resolution electron microscopy investigation of capacity fade in SnO_2 electrodes for lithium-ion batteries, J. Electrochem. Soc. 146, 2472.

15. T. Brousse, R. Retoux, U. Herterich, D.M. Schleich. 1998. Thin-film crystalline SnO_2-lithium electrodes, J. Electrochem. Soc. 145, 1.

Artificial Intelligence Supported Learning

Furkan ŞAHİN & İrfan AKARSU

Hüsnü TURHAN

IşıklarAir Force Military High School, Bursa/Turkey, turkcan32@gmail.com

1. Purpose

Interactive education system has many advantages when compared to the classical education given in schools.[1] On the other hand, there are disadvantages in interactive education system and the most important disadvantage of interactive education is its failure in flexibility.[2] While one can understand a specific topic through visual presentations, other can understand it via auditory materials. In brief, each person can understand differently. For that reason, it is not expected humans to understand things in the same way. In our study, it has been tried to solve interactive education system's flexibility problem by personalization of systems thorough artificial intelligence applications. Thanks to the artificial intelligence applications learning activities are tried to be more active and effective.

2. Methods

In order to carry out our aim, interactive education system (IES) which has both teacher and student interface has been coded. Php language has been chosen because of its appropriateness in system coding and having many sources at present. For display, responsive and eye catching theme has been designed by using HTML and JavaScript. IES has security recording system against SQL inject and XSS attacks.

2.1 Student Pages

2.1.1 Starting Page

All registered students are directed to this page and in this page their intelligence types are determined thorough assessment questions and tests. Then results are saved and students are provided with personal education.

2.1.2 Lessons Page

It is the page that students get their lectures. While lecturing, it is being controlled whether students can understand the lecture or not by interpreting students gestures and face expressions with artificial intelligence via webcam. Students' present levels are interpreted by processing front camera sources and system creates output considering processed sources. In website, the lectures given students are being kept in XML pages as dynamically. So it is easy to change course contents anytime.

2.1.3 Tests Page

In tests page students could take a test about each content they got and evaluate themselves. By assessing students' scores with classification algorithms, it is determined whether students understand the issue.

2.1.4 Profile Page

It is the page showing students IDs and lectures they button up.

2.1.5 Question-Answer Page

In this page, students can ask their questions or anything they could not understand. These questions can be answered by both students and teachers. If questioner finds a satisfying answer, he can verify by pointing it (like Stackoverflow).

2.2 Teacher Pages

2.2.1 My Students Page

This page has been built for teachers to observe their students' improvements. Hereby teachers have opportunity to give useful suggestions to their students.

2.2.2 Material Sharing Page

This page is designed for teachers to make lectures more effective by sharing their experiences and materials between themselves.

2.2.3 Forum Page

In order to answer students' questions, authorization for Question-Answer platform has been given to teacher accounts.

2.3 Gamification

In this interactive education system which aims to boost the level of success, gamification which is common in these days has been used. This method is generally used by children and both entertaining and enjoyable lectures are designed for teaching.

2.4 Artificial Intelligence

Artificial intelligence applications are used in our system's two different departments.

2.4.1 Classifying Results

By considering the results of final tests of lectures that students take and comparing with other students' results, thanks to the machine learning and classifying algorithms artificial intelligence has been used for evaluating students level properly.

2.4.2 Emotion Recognition

In order to get the highest efficiency in lectures, students present gestures and facial expressions are processed during lecture by using visual data captured by user authorization needed front camera. In this way, facial expressions such as losing attention, unhappiness, confusion, nervousness, happiness etc. are observed and the system is equipped with giving output about current conditions.

3. Results

In our school the topic 'programming' has been given three different classes by using traditional, interactive and artificial intelligence supported learning (AISL) methods and then students are taken tests related given lecture. The grades 70 points and over are considered successful. When the results are evaluated, Artificial Intelligence Supported Learning (AISL) which is supported with personalized interfaces and artificial intelligence applications is seen as more successful than traditional method and other interactive education systems. It is observed that artificial intelligence supported learning environment increases learners motivation and their success. Thanks to these artificial intelligence applications more flexible and effective learning environments can be developed for student.

	Rate of Success (%)
Traditional Learning	65
Interactive Learning	78
AIS Learning	92

Studies are continuing to enhance the success of AIS learning. 'Triumphs' tab page can be added to profile page in order to make the system more attractive and entertaining. In this way, children's enthusiasm to lectures can be increased.

4. Conclusion

When we tested our project that we have studied for over one year, it has been observed that students' perception and learning levels are determined properly, students complete the lectures successfully and reach the expected level in exams. This study contributes to the design and development of efficient learning environments.

5. Reference

Berge, Z. L. (2002). Active, İnteractive, And Reflective E-Learning. *The Quarterly Review of Distance Education* 3 (2): 181–190

Bates, A.W.T. (2005). *Technology, E-learning and Distance education*, Routledge, New York.

LITHIUM-ION BATTERY PRODUCTION USING NEW GENERATION NANOMATERIALS BY ELECTROSPINNING METHOD

Güler Selin Sunar & Gülce Afacan

Alper Bayram

İzmir Private Fatih Science High School /Izmir/Turkey /aalperbayramm@gmail.com

1. INTRODUCTION

Energy is the ability to perform a work. The energy demands of societies are directly proportional to the development of industry and technology. In order to seize the contemporary living standards, as well as economic growth, it is essential to produce energy in a constant, safe and cost-effective manner. Today, lithium-ion batteries from among battery systems developed for the purpose of storing and utilizing electrical energy have wide spread fields of application with their high capacity and energy density as compared to other batteries. The latest studies have been focused on the usability of nanomaterials for the optimization of the capacity of lithium ion batteries which are currently in use.

2. PURPOSE

Based on the researches conducted, development of batteries with high energy density, long cycle life, designed with innovative battery materials, having safe and wide operating temperature ranges has been foreseen. In our project we hypothesized that the efficiency of the batteries could be increased by using $LiCoO_2$ and $LiCoO_2/TiO_2$ nanofibers in lithium ion batteries as cathodes.

In our project we aimed to analyze the usability of the new generation metal oxide composite nanofibers which we produce through electrospinning method within the cathodes of the lithium ion batteries. In accordance with this purpose;

- Production of $LiCoO_2$ and $LiCoO_2/TiO_2$ composite nanofibers by electrospinning method,
- Characterization of the produced nanofibers by SEM (Scanning Electron Microscope), XRD (X-Ray Diffraction), TGA (Thermogravimetric Analysis),
- We aimed to realize in phases the processes of preparing button batteries $Li/LiCoO_2$ and $Li/LiCoO_2/TiO_2$ half-cells and performing battery capacity tests.

3. METHOD

3.1. Lithium Cobalt Oxide ($LiCoO_2$) Nanofiber Production

In line with our target the polymer solutions were prepared with stoichiometric which are indicated in the table.

Table 1. The amount of materials used in the production of nanofibers.

Chemicals	Amount (g)
PAA	0.8696
LiOH	0.0215
$Co(OH)_2$	0.08344
Distilled water	10

Than the solutions were transformed into nanofibers by electrospinning method.

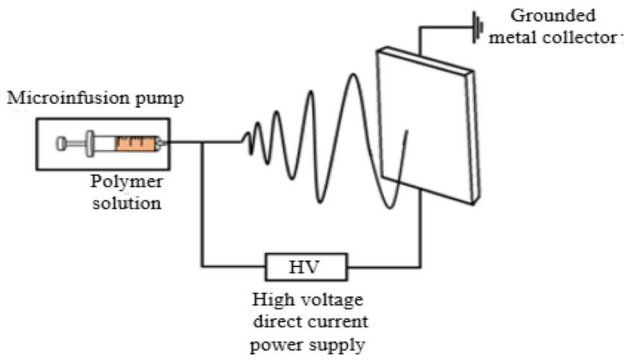

Figure 1. Schema of electrospinning

Table 2. Parameters of electrospinning

Mixture	**PAA/LiOH/Co(OH)$_2$/H$_2$O**
Feed Rate	1 ml/hr
Voltage	13 kV
Collector-needle distance	19 cm

The polymers within the structure were removed by controlled heat treatment.

3.2. Lithium Cobalt Oxide / Titanium (IV) Oxide ($LiCoO_2$ /TiO_2) Nanofiber Production

In order to produce $LiCoO_2$/TiO_2 nanofiber, was taken from PAA/LiOH/$Co(OH)_2$ solution which was prepared in the previous phase and TiO_2 colloidal solution.

Table 3. The amount of materials used in the production of $LiCoO_2$ **/** TiO_2 nanofibers.

Chemicals	**Amount (g)**
LiOH/$Co(OH)_2$/PAA	4
TiO_2	0.958

Than the solutions were transformed into nanofibers by electrospinning method.

Table 4. Parameters of electrospinning

Mixture	**PAA/LiOH/Co(OH)$_2$/TiO$_2$**
Feed Rate	1.5 ml/hr
Voltage	15.5 kV
Collector-needle distance	18.5 cm

The polymers within the structure were removed by controlled heat treatment.

3.3. Utilization of Produced Nanofibers in Lithium-Ion Batteries as Cathode Active Material

3.3.1. Preparation of Cathode

Production processes were continued until the amount that shall be used in the electrodes of lithium-ion batteries was acquired. When the production was completed, nanofibers were mixed with the necessary connectors and half-cell lithium-ion button batteries production in the stuffy atmosphere of argon was effectuated in accordance with the formation stages of lithium-ion button batteries and the battery was subjected to electrochemical tests.

Table 5. The amount of materials used in the production of cathode.

Active Material-Nanofibers	80 mg
Carbon Super P	10 mg
PVDF (Polyvinylidene fluoride)	10 mg
NMP (1- methyl 2- pyrrolidone)	0.7 ml

3.3.2. Production of the Battery

Afterwards other battery components were assembled in accordance with the diagram.

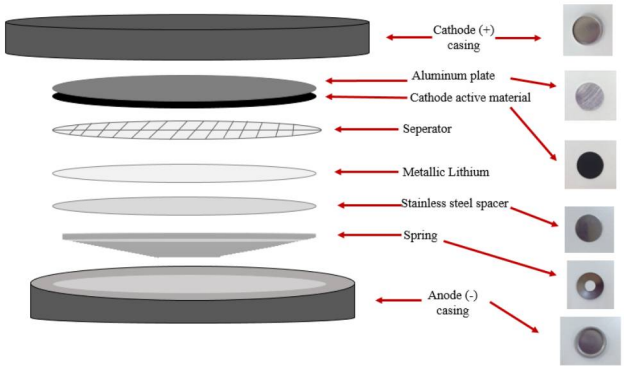

Figure 2. Structure of half-cell lithium ion button battery

4. RESULTS AND CONCLUSION

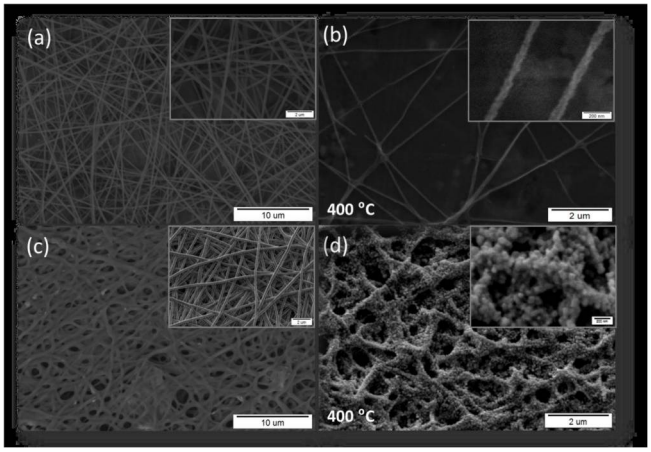

Figure 3. Scanning electron microscope images of the fibers before and after the calcinations (a) PAA/LiOH/$Co(OH)_2$, (b) $LiCoO_2$, (c) PAA/LiOH/$Co(OH)_2$/TiO_2, (d)$LiCoO_2$/TiO_2

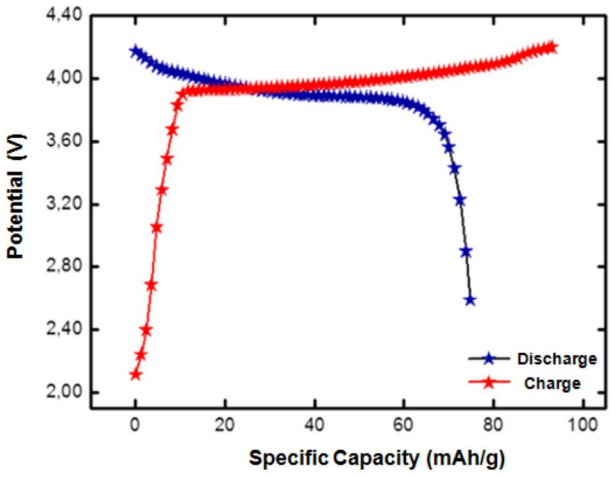

Figure 4. Charge-discharge curve of Li/$LiCoO_2$ button battery

According to the material characterization processes conducted; it was proved by XRD (X-Ray Diffraction) analysis that $LiCoO_2$, $LiCoO_2$/TiO_2, $Li_2CoTi_3O_8$ nanofiber materials were produced by electrospinning method and the loss of mass due to change in temperature was specified by TGA (Thermo-gravimetric Analysis). Additionally, according to the results of SEM (scanning electron microscope) analysis when the fiber diameters of the nanofibers obtained are observed it was seen that the nanofibers having desired features have been produced and the material production phase was completed with success. It is observed that electrochemical test results of lithium-ion batteries prepared by the produced nanofibers

have reached the capacity values which can compete with the results of similar studies that have been reported in the technical literature.

As a result, due to the mechanical stability of the produced nanofibers and because they increase crystallization, the utilization of lithium ion in the batteries as a new generation material and putting in practice such material demonstrates the authenticity of the study.

5. REFERENCES

1. Buchmann, I. (2001). Batteries in a portable world. Richmond: Cadex Electronics.

2. Dhameja, S., (2001) Electric vehicle battery systems, Newnes.

3. Nair, N. K. C.,&Garimella, N. (2010). Battery energy storage systems: Assessment for small-scale rerenewable energy integration, energy and buildings, 42(11), 2124-2130.

4. Scrosati, B. (2000). Recent advances in lithium ion battery materials. Electrochimica Acta, *45*(15), 2461-2466.

5. Zhang, X.,Ji, L., Toprakci, O., Liang, Y., &Alcoutlabi, M. (2011). Electrospun nanofiber-based anodes, cathodes, and separators for advanced lithium-ion batteries. Polymer Reviews, 51(3), 239-264.

Roses Guido Grandi or outline flower petals in polar coordinates

Dmitry Nuzhdin

Supervisor*: Stegnienko Marina Ivanovna,*

Informatics and Mathematics Lyceum-General Educational School of I-II stages of Dzerzhinsk city council of Donetsk region, Ukraine, nvklicey@yandex.ua

1 Introduction

The polar coordinate system specifies points on the plane two numbers - angle and distance. Putting these coordinates is very natural, because the location of any point on the earth's surface for a stationary observer is conveniently determined using this distance from the observer point. Due to polar coordinates some curves can be quite simply described polar equations, whereas equations in Cartesian coordinate system would be much more difficult. The most famous polar curves include: polar rose, Archimedean spiral, snail Pascal.[1]

2 Object of study

The object of this study is Polar Rose. Its geometry equation described by the Italian Guido Grandi in the 18th century. "Roses" Guido Grandi amaze correct and smooth lines, but their shape is not a whim of nature - they are due to specially selected mathematical dependencies.[2] Family of "roses" is described by the equation in polar coordinates ρ (φ) = a * sin (kφ), where a and k - some permanent. Setting parameter k = c / b ratio of positive integers can be closed curves, which under certain conditions are transformed into delicate flower petals or outlet and can serve as elements of decoration or ornament.

3 Purpose of the work

Objective: to classify and identify the main features of appearance schedule "roses", given in polar coordinates the equation ρ (φ) = a * sin (kφ), depending on the values of the parameters k and a.
The subject of the study is the appearance of the graphics functions ρ (φ) = a * sin (kφ).[3]
Objective: To meet with the polar coordinate system; create a project among the Microsoft Visual Studio 2010 for plotting polar curves Parametric equations; trace properties schedules when choosing certain values of the parameters k and a; hypothesize in general.

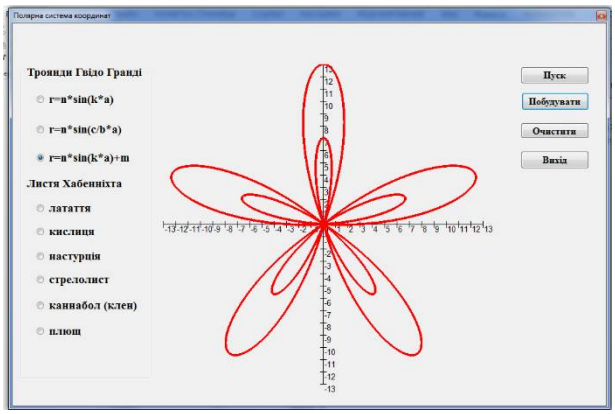

4 Conclusions

During the project we have considered various forms of "roses" Guido Grandi for different values of k for the equation ρ (φ) = a * sin (kφ).
For integers k there have been found the formula counting of the number of petals (for even k: m = 2k, for not paired k: m = k), shown only point of intersection and conclusions about the location of petals.

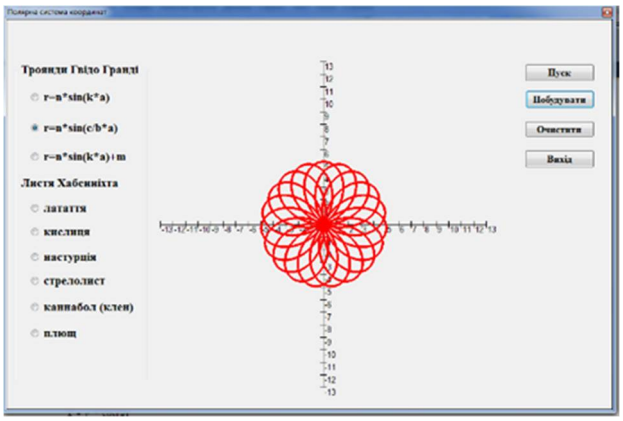

Fig. 1 Screenshot of the program

We have been able to formulate the rule for counting the number of petals rational and irrational k. Define the look dependence graph of ρ (φ) = a * sin (kφ), and the parameter (larger value and, the longer the petals), and also the number of intersections petals for rational and irrational k (Fig .1, Fig. 2).
During the research we have received a variety of forms of "roses" Guido Grandi, ich give their imagination to use. We have studied the use of polar coordinates in various areas of life and science.

Fig. 2 Screenshot of the program

5 References

[1] Zawadzki IA, Zabolotnyi RI basics of visual programming; textbook, publishing group VNV, K: 2009.
[2] SS Byushhens Dyfferentsyalnaya Geometry; Publishing House tehn.-teoret. lit. 2008.
[3] Savelova AA Flat curves. Systematics, properties, applications (directory) under. Edited by AP Norden State Publishing physical - mathematical literature, Karl: 1960

Mykola Muzychenko, the pupil of 10th form

Supervisor: Bilous Svitlana Yurivna

(Ph. D., branch director of National Center

"Minor Academy of Sciences of Ukraine")

Zaporizkii technical lyceum, Zaporizhzhya, Ukraine

CANDLE IN WEIGHTLESSNESS, OR METALCUTTER FOR THE ASTRONAUT

1. Aim of the work

To work out the mathematic model of flame burning in the weightlessness and to make original metalcutter construction from improvised means; to explore features of burning and describe the flame's characteristics of the device.

2. Methods of the research

The methods are: theoretical, mathematical, design, experimental, estimative on the basis of the physical model.

3. Theoretical part

It`s no convention in the weightlessness and the opened flame looks like a scope. Spherical shape of the flame is stationary when oxygen flow is equal to hydrogen and combustion products flow. The authors first offered mathematic model of this process. This model was described by such equation.

$$\frac{\partial C}{\partial t} = 0 = D\left(\frac{\partial^2 C}{\partial r^2} + \frac{2}{r}\frac{\partial\ C}{\partial r}\right) - kC\ + k_1 C_1 \quad (1)$$

Boundary conditions of the problem are:

$$\alpha_1 C = \alpha_2 C_2 \quad (2)$$

$$-D\frac{\partial C}{\partial r} = -D_2\frac{\partial C_2}{\partial r} \quad (3)$$

C- the concentration of combustion products (D-the diffusion coefficient)
C_2- the hydrocarbons concentration around the wick (D_2-it`s diffusion coefficient)
The Mathematica Program (Fig.1) solved equation.

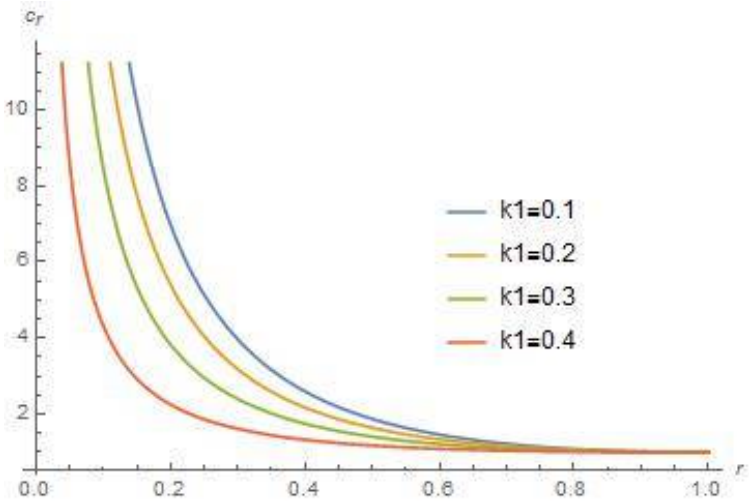

Fig.1. Dependence of combustion products concentration from the distance of the scope center (diffusion coefficients has different values)

4. Experimental part

For the research of the effectiveness of this device we have made some researches of the flame by means of sounding it with the help of thermocouple and also we have discovered the dependence of temperature of the flame from the pressure in air flow.

The theoretical estimation of pressure in the flame was made and the quantity for the highest temperature inside the flame we experimentally determined.

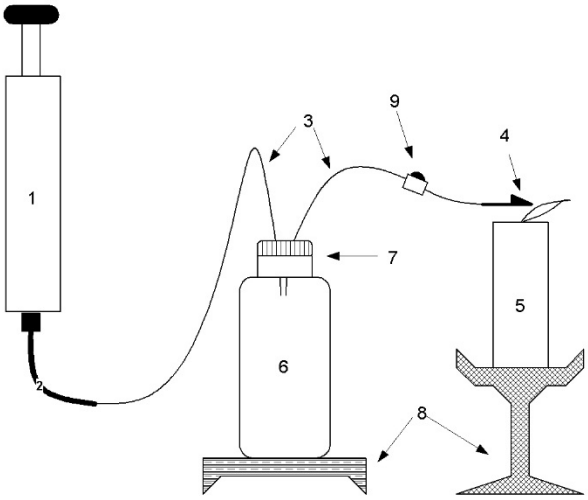

1-pump;
2, 3-tube system
for blood transfusion;
4-needle of the syringe;

5. Results

The results of our research are interesting from the point of the construction itself, accessibility of its components and opportunity to collect a workable device in a short period of time. With the help of this device one can melt and cut metals using a concentrated flame of the candle, which can be put into practice and can be used in the state of imponderability during space flights.

6. Literature

1) Карапетьянц М.Х. Химическая термодинамика / Михаил Христофорович Карапетьянц.-М.: Химия,1975. – 584 с.
2) Ксандопуло Г.И. Химия пламени / Георгий Иванович Ксандопуло.-М.: Химия, 1980.-37 с.
3) Араманович И.Г. Уравнения математической физики / И. Араманович, В. Левин. – М. : Наука, 1989. – 286 с.

Jesper Provoost & Evert Guliker

Willem de Wit

Corlaer College, Nijkerk, The Netherlands, wdewit@corlaercollege.nl

1. About our research project

Our project is called 'FlowPed – new urban mobility'. We came up with this project in June 2015, because we wanted to gradually solve big global issues with our own technological solution. Specifically, we were looking for a way to solve urban mobility issues. The main research question of our project was: *"How can we create a reliable, realistic and user-friendly technological solution for the current urban mobility issues?"*

Our research project is quite unique, since we used a variety of important aspects to create our own product. These aspects are as follows:

- Research about urban environments
- Technical development
- Business operation
- Marketing

The reason for us to create such a diverse project, was our strong opinion that a great technological solution cannot be successful without factors like business studies, marketing and societal research. Our goal was clear: we wanted to make a product that would be ready for actual deployment in big cities by 2016. As of today, FlowPed has been a fairly successful project, with multiple companies and authorities interested and amazed by our solution.

2. Method of the investigation

Since we incorporated multiple aspects into our project, we used a variety of investigation methods. First, we wanted to investigate the actual mobility issue in big cities. As our basic principle for the project, we used New York City because of its known mobility issues and its open data. We used multiple official surveys of the New York City Transportation Department and the City of New York about transportation habits to investigate the urban issues. Based on the results of this research, we drafted a list of advantages and disadvantages about the current New York City transport system. By having a lot of brainstorming sessions and inspiring moments, we came up with a solution for every disadvantage and an improvement for every advantage. Based on all these elements, our own product came to life.

Of course we wanted to know whether or not our business would be profitable. Based on actual New York City tax rates and competitive prices, we created our own business model. We took every expense into consideration and calculated the break-even point for our business. To attract customers, we also came up with a marketing plan by analyzing our target audience and their habits. We also looked at logo trends from other companies all over the world. Because our goal was to create a realistic and profitable product, we decided to ask feedback from relevant companies and authorities all over the world. As a result, we got in touch with the City of Vienna, and a startup accelerator in Lisbon. They were very interested in our idea, and they wanted to collaborate with us in the near future. For us, that was the moment when we knew we were on the right track, except for a few small issues.

Then, we started thinking about the prototype of our product. Our goal for the prototype was to be able to show others how our product works and how easy it can be used. We came up with entity-relationship diagrams (ERD) and data flow diagrams (DFD) to sketch the functions of the system. We also compared different methods for building the prototype, like programming languages and computer platforms. Factors such as user-friendliness and security were also very important during this process. The physical aspects of the system were designed by making 3D models and getting feedback from potential users.

3. Results of the investigation

The results of the experiments were very important during the creation of FlowPed. In our project, we used a modular approach, which means that we constantly used our previous results for the next step of the project. First, we discovered that the magnitude of mobility issues in New York City is huge. Actually, official surveys showed that 67% of the New York inhabitants use the car as their primary way of transport (*figure 1*). We found out that 68% of the New York drivers only use the car for distances less than 3 miles. As a result, New York drivers have to deal with 53 hours of traffic jams on a yearly basis.

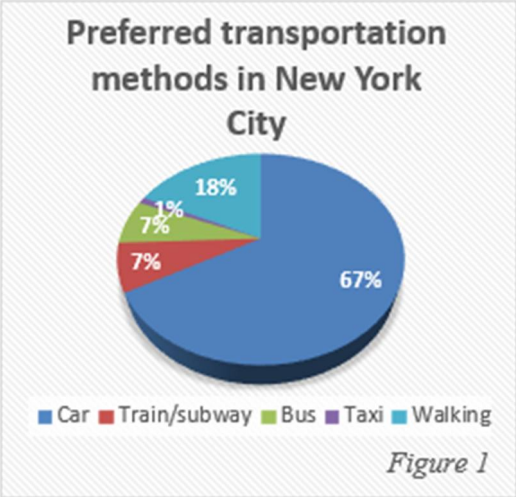

Figure 1

The advantages and disadvantages of the current urban mobility situation could be based on the previously mentioned results. The most important advantage is the huge impact of mobility on the New York City economy. The biggest disadvantages turned out to be traffic problems and CO_2-emissions. Of course we came up with many more (dis)advantages, but we will not mention them in this abstract.
Based on the advantages and disadvantages, we came up with our own product that solved all disadvantages and improved the advantages. By coming up with an existing solution for every disadvantage, the result was a comprehensive and final concept. Our concept is a technological rental system where people can rent one-person smart vehicles to move from one VEP (vehicle exchange point) to another. We asked companies to give feedback on our concept, and as a result two European authorities offered us to collaborate on our product in the future. To prove that our concept could actually become successful, we composed an actual economic forecast. To be able to attract customers, we came up with an attractive and fair price formula. It turned out that we needed to rent our vehicles at least 7,6% of the day to reach our break-even point.
It is very important for a tech startup to launch an effective marketing campaign. We found out that there are two vital components of a successful marketing campaign: a name and a logo. The name of our product became 'FlowPed', based on the words 'moped', 'flow' and 'pedestrian'. Based on current logo trends, we designed our own logo. The FlowPed logo can be seen in figure 2 below.

FLOWPED

Figure 2

Building the prototype was the hardest part of our whole project. We ended up using five different programming languages: Swift, PHP, JavaScript, HTML and C++. The most important component of FlowPed is the mobile application (figure 3), which we developed for iOS using Xcode and Swift. This app is connected to a VEP (vehicle exchange point) through a MySQL database. A prototype VEP was built by us using multiple Arduino's, a magnetic lock, an RFID-reader and an ultrasound sensor. Because all these components are perfectly adapted to each other, a FlowPed user can rent a smart vehicle with his/her smartphone. The VEP was designed by ourselves using SketchUp. The prototype VEP can be seen in figure 4.
To guarantee the safety of our customers and vehicles, we took multiple clever measures. First, we installed GPS-trackers in the vehicles. In our online vehicle management panel, we can now find the real-time location of our vehicles. This way, we can trace stolen or vandalised vehicles. To prevent digital crime on our platform, we used multiple techniques. Most importantly, we protected ourselves against SQL-injections and DDoS-attacks. Without proper protection, the core of our system would be very vulnerable for these kinds of attacks.

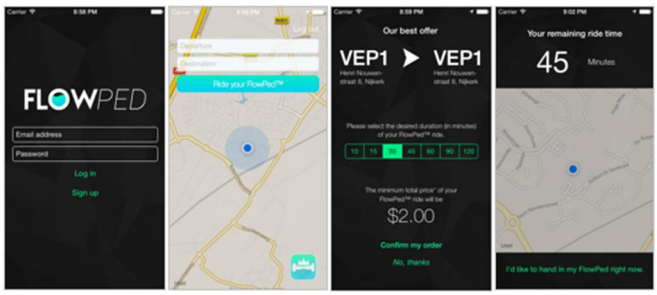

Figure 3


Figure 4

4. Conclusion

The conclusion of our project was that we have actually created a product that partially solves the urban mobility problem. In the first stages, the classic research methods were very important for us to come up with a suitable concept. After that, the purpose of the research was mainly to make a good

business plan and to find the best way to build a prototype. This means that our project can be summarized in three key elements: doing research, designing and building. The final product (in other words, the prototype) can be seen as a result of the initial research.
We did not only find out about written facts and theories (like traffic data), but we also learned soldering, programming and assembling. This shows how versatile our project actually is.
We can safely conclude that we have made a technological product which is profitable, user-friendly, functional, safe and reliable. With this product, city inhabitants can easily rent a one-person smart vehicle with their smartphone. By spreading VEPs all over the city, FlowPed creates a whole new transportation network within the city. This product is completely unique and is completely designed and built by ourselves.

Measurement of the solutions concentration using a laser

Danila Deyankov

Supervisor: Andrey Isachenko

Summer School LANAT, fn@lanat.ru

13 A brief statement of the problem

The main purposes of my project are: 1) to create a laser construction, which can be used to measure the concentrations of various solutions of copper sulphate; 2) to develop a program for its automation. Additional purposes: to enter calibration of the solutions with different colored compounds in the program data base and to improve the program.

14 Theory

Measuring concentrations of solutions of various compounds is an important tool in analytical chemistry, which has a great practical use. Nowadays the most accurate and the fastest ways of measuring concentrations of different solutions are instrumental methods of analysis, which can be classified into the following:

1) Potentiometry is method for determination of various physical and chemical quantities, based on the measurement of the electromotive force (EMF) of reversible electrochemical cells. In other words, it is the dependence of the equilibrium electrode potential of the activity of ion concentrations determined, described by the Nernst equation.

2) Conductometry is a set of electrochemical analysis methods based on the measurement of electrical conductivity solutions. Conductance-measuring analysis is based on the change in concentration of a substance or chemical composition of the medium in the interelectrode space; it is not associated with an electrode potential, which is usually close to the equilibrium value. Conductometry includes direct analysis methods (used, for example, in salimeter) and indirect (for example, in gas analysis) using AC or DC (low and high frequency), as well as chronometric, low and high frequency titration.

3) Mass spectrometry analysis is a method of research material, based on the determination of the ratio of mass to charge ratio of ions formed during the ionization of interest of the sample components. This is one of the most powerful ways to identify high-quality materials, which also allow the quantitative determination. We can say that mass spectrometry is a "weighting" of molecules in the sample.

4) The emission spectrum, emission spectrum, emission spectrum is the relative intensity of the electromagnetic radiation of the object of study on the frequency scale.

Usually we research the radiation in the infrared, visible and ultraviolet range from the highly heated material. The spectrum of the radiation substances is either in the form of horizontal color bands which is result from the object beam splitting prism, or as a graph of the relative intensity, or in tabular form.

5) X-ray analysis and methods based on the measurement of radioactivity are instrumental methods of elemental analysis, based on a study of the spectrum of X-rays that have passed through the sample or emitted by them.

15 Main results

I have developed hardware and software system using microcontroller Arduino Uno. Acting model of the laser system is created. The software is written using engineering programming environment LabVIEW. In addition, the general skills with microcontrollers are obtained. Thus, the fully functioning laser system capable of measuring the concentration of copper sulfate solutions is assembled.

16 Conclusion

I have created a portable compact device, which can compete with spectrophotometer in all qualities but not accuracy. In addition, the device has a lower price than spectrophotometer. The standard spectrophotometer costs from 430 dollars to 4.000 dollars. While my device costs only 200 dollars. Even with the trade margin (≈ 50%), my machine will cost less than a standard spectrophotometer.

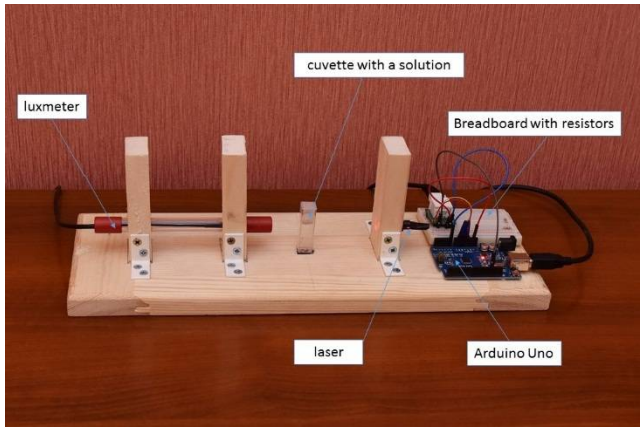

Dragonflies as indicators of the status of water bodies

Ihar Plotnikau
Belarus

It is well known that some of the inhabitants of water bodies can serve as living indicators of water purity. In many literature sources on bioindication of water bodies dragonflies are also referred to as indicators of water purity as they are amphibiotic animals, the larvae of which lives in water. However, we could not find any specific evidence of physical or chemical parameters of water and in what extent they affect richness of dragonfly species, or specific species. That is why the aim of our work was to establish the relationship between species richness of dragonflies that live in different types of water bodies, and physical and chemical parameters of water quality.

Authors data served as a base of our scientific work. Data was collected during field seasons of 2012-2015 years. Dragonflies were caught with entomological scoop-nets. Some species were determined by photos. Dragonflies larvae was caught with hydrological scoop-net. Also we were counting the presence of exuviae. Physical parameters of water (electrical conductivity, total mineralization and temperature) were determined using the TDS-meter and the pH-meter , water sampling was made using glassware in 1-1.5 m from the bank, at a depth of 20-30 cm in different parts of water bodies. For each of the water bodies analyzes were performed with three or fourfold replications, including chemical analyzes. From the chemical characteristics of water we have determined the amount of oxygen dissolved in water, the presence of phosphate and nitrate ions. For chemical analysis, we used a field lab. Analyses were performed immediately after sample collection on the banks of water bodies, in the first half of the day with similar weather conditions. To estimate the species richness of dragonflies on water bodies we used Margalef's index. That way takes into account not only the number of species in water body, but also their number in a sample. To establish whether there is a significant correlation between the physical and chemical parameters of water and species richness of dragonflies we carried out correlation. We used the Spearman's rank correlation.

During the research work we examined 21 water body: 4 rivers, 3 flooded peat extractions, 5 lakes, 2 reservoirs, 7 ponds. For physical and chemical analysis we selected 11 water bodies, with different species diversity and presumably the physical and chemical parameters of water. 100 gatherings were performed, noted about 2,500 instances of dragonflies. 47 species were found in general. In water bodies where water analysis was made, 43 species were registered. Analysis on the lakes near villages Dubeni and Bytcha showed very low levels of total mineralization of water, that means the amount of dissolved impurities in these water bodies is minimal. On Loshitsa reservoir revealed heavy pollution of water body with phosphates and, in consequence, water was blooming. Nitrates are revealed in 9 out of 10 reservoirs, but their concentration is minimal. The water temperature near the shore of standing water bodies generally higher than on the rivers. On Staroborisovskoe reservoir pH of water has alkaline environment, and indicators exceeded 9 units. Same high indicators were in 2014 at Loshitsa Reservoir. The only water body with a slightly acidic environment of water is a lake near the Bytcha village. Obtained data shows that there is significant strong positive connection with water temperature and average negative connection with indicators of total mineralization and electrical conductivity between the number of species and species richness index. Some species of dragonflies may be bio-indicators of some physical and chemical parameters of water. Such species include Anax imperator and Anax parthenope that inhabit water bodies with low levels of total mineralization and electrical conductivity. Indicator species of water acidity include Epitheca bimaculata that prefers ponds with an alkaline environment, and peat-loving species that live at water bodies with a slightly acidic reaction of water or close to neutral: Coenagrion hastulatum, Leucorrhinia caudalis , Leucorrhinia pectoralis, Leucorrhinia rabicunda, Leucorrhinia albifrons, Sympetrum danae.

That way we confirmed our hypothesis that some species of dragonflies can serve as living indicators of some physical and chemical parameters of water, and found a new method of bioindication.

Geziel Gontijo de Ávila

Guilherme Weber

Escola Estadual Querência, Querência/Brazil, gezielotavio@hotmail.com

An Epidemiological Approach About Youth and Drugs

Purpose: Due to anatomical and physiological changes, the teenagers are the most vulnerable group found in society. This vulnerability occurs in the physical and behavior mode, this leads us to worry with young people get involved with legal and/or illegal drugs. Based on this, we seek to outline an epidemiological profile of these teenagers, treating the risks and the contact with drugs. Knowing the profile of young high school students, and their access to legal and illegal drugs we try to describe the main risks of teenage in order to map out effective measures that can promote the removal of these teenagers from the risk zone, also, this research can be used by governors to trace strategies to combat drugs used by teenagers.

Methodology: After we accomplished a literature review, we decided making a questionnaire aiming at data. It has developed asking some personal questions, such as age, gender, education, and in a second part, several behavior questions: how many times take cigarettes, how many times drank alcohol, how many times used illegal drugs. We decide to study city of Querência, because it is a typical city in development, located in the center region of Brazil. Querência is a city with very young people, 20 percent of the population aged 10 to 19 years, the population surveyed in question. After we organize the data and prepare comparative graphs between factors, such as, age and education, the to a more didactic view. The main researched drugs are: alcohol, tobacco, energy, hookahs (legal) marijuana, cocaine, steroids, crack, other drugs (illicit).

Results:

The questionnaire was made in 268 volunteer, these 142 girls, 26 with 14 years old, 59 with 15 years old, 36 with 16 years old, 16 with 17 years old, 4 with 18 years old and 1 with 19 years old and 126 boys these 22 with 14 years old, 46 with 15 years old, 31 with 16 years old, 20 with 17 years old, 6 with 18 years old, 4 with 19 years old and 2 with 20 years old. The questionnaires were applied to all high school classes of all city schools in question, regardless of shift, type and school address. Questionnaires showed us the following results:

Graphic 1 - Number of students, sex and age

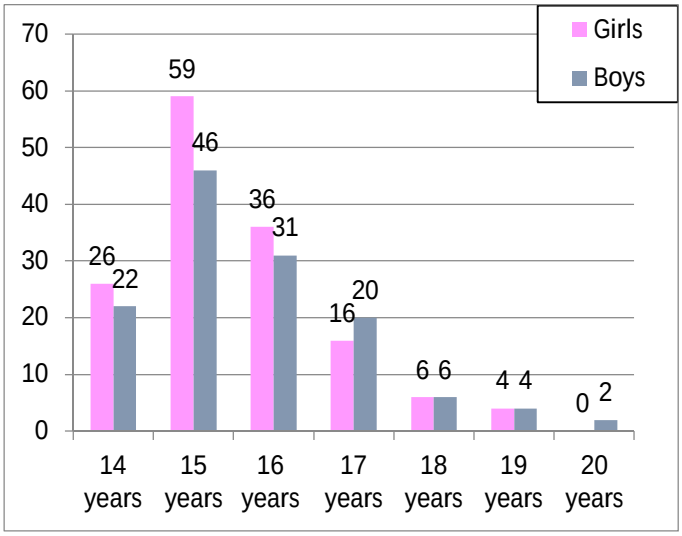

The use of illicit drugs was reported by 19 boys and 7 girls, representing 9.7% of the total, however, only 2 boys reported using these drugs weekly and 1 reported daily use.

Regarding the use of alcohol we found that 72 (50.8%) of the girls have already used alcohol at least once in life, this group, 55 (78.6%) reported use of drinks up to 3 times a month . Already in boys, we found that 72 boys, 57.1% have already made use of alcohol, however, of these 42 (41.7%) reported use of drinks up to 3 times a month.

Regarding the use of cigarettes for any kind, like thatched cigars, handmade cigarette, smoking pipes, among others, show us that only 7 girls (4.9%) reported having smoked any of the products listed, and of these, 5 (71.4%) reported smoke less than 3 times a month.

The group of boys brought us the following result: 21 (16.6%) reported having smoked any of the products

listed, and of these 14 (66.6%) reported smoking less than 3 times a month.

About other licit drugs such as energy drink and narghile, we found that 54 (38%) girls have already used, but 41 (75.6%) answered that use up to 3 times a month. In the other group we found that 56 (44.4%) boys reported having used, but 46 (82.1%) answered that use up to 3 times a month.

Graphic 2- Use of drugs

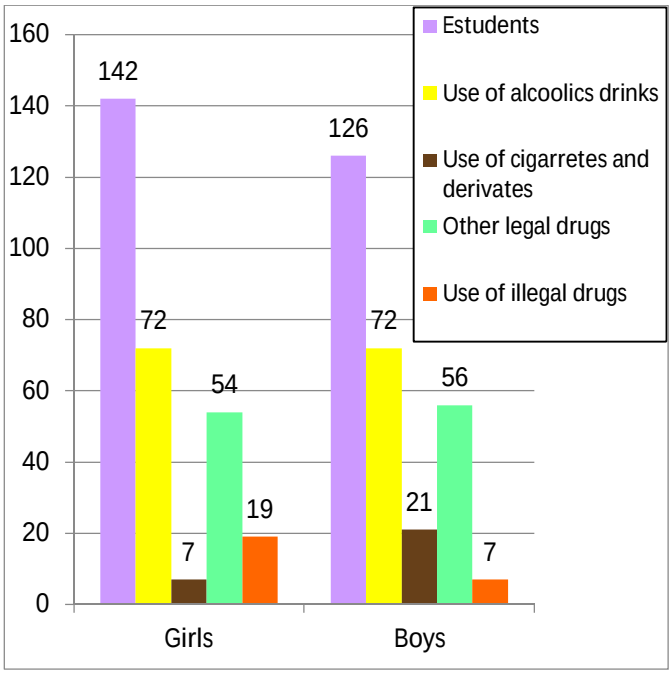

Conclusion: From this research, we can to map a profile about the young people and your access to legal and illegal drugs, with it, we are looking for a ways to reduce this data and turn this city a ´´free zone´´ drugs. Also, we demonstrated that the city of Querência has very useful data for regional and national analysis, since it is a typical town in development and can serve as a basis for further research in this area.

Ricky Wochner

Guilherme Weber

Escola Estadual Querência, Querência/Brazil, rickywochnerl@outlook.com

Campylobacter: An Invisible Evil

Purpose: *Campylobacter* is a bacteria genus that is among the most common causes of bacterial infections in humans worldwide. These bacteria can affect people of all ages, locations and social classes. Based on this, we accomplished this research project in order to expose information such as symptoms, treatment and consequences of this very common infection to the general population.

Methodology: After we accomplished a literature review, we opted to approach these main subjects: Definitions about *Campylobacter*, main way of infection, epidemiology of the infection, infection transmission, symptoms and signs and the different ways that the disease can affect the population. During the project development, we have searched references and information from different sources, such as books, scientific magazines, Scielo articles and google academy. All the information has been checked in other security sources in order to avoid mistakes in the research.

Results: This research resulted in the creation of a project with a rich content about *Campylobacter* as well as diseases caused by these bacteria, making this research a source of information for the general population. From this disclosure, we expect to hold an awareness about this invisible evil that affects so many people. The main data collected with this research are: Detailed classification of the main subspecies of *Campylobacter,* describing their morphology and differences between species, furthermore, define important characteristics to facilitate the choice of medicines against infections. In the definitions, we found relevant aspects about this genus, it is curved and has a flagellum that provides its movement and assists in their fixation to the gastrointestinal tract. The most important subspecies of *Campylobacter* is *campylobacter jejuni*, this subspecies represent 99% of food infections. The other subspecies combined represent less than 1% of annual infections. In addition, *campylobacter jejuni* is the most common pathogenic bacteria to cause diarrhea. This subspecies is considered the leading cause of the " traveler's diarrhea". Due to their needs for temperature, oxygen and acidity, the birds' and mammals' intestines are the perfect place for the development of these bacteria. According to the CDC (Center for Disease Control and Prevention of the USA), this is the main cause of food infections and affects 13 per 100,000 people each year and is estimated to affect 2.4 million people per year in the whole world, representing approximately 0.8% of the world population. The main way of spread of infection is from the consumption of animal products, such as milk, viscera and meat in general, which tend to be contaminated at the slaughter, when they are exposed to contact with feces or contaminated sites. The infection proceeds in two ways: The infection can be self-limited by the body, without causing symptoms or causing symptoms very lightweight; or more accentuated, causing symptoms such as diarrhea, vomiting, nausea and abdominal pain. In general the disease is combated by immunological defenses, without causing great damage to the patient, however, in more severe cases may cause dehydration, fainting and cause death.

Conclusion: Considering the above, it is clear that the *Campylobacter* infections are the main cause of foodborne, and must be handled carefully, because they may lead to death, moreover, prophylaxis is simple, cheap and accessible and should be stimulated widely in order to reduce the incidence of this disease, as well as reduce unnecessary costs with their treatment.

The preparation of a non-cytotoxic compound for surface coating of gold nanorods

Jan Zelený

RNDr. Linda Schmutzerová, doc. PharmDr. Kamil Musílek, Ph.D., PharmDr. Michal Novotný, Ph.D.
RNDr. Alena Uhríková, Ph.D.

The First Private Language Grammar School, Hradec Kralove, Czech republic
zeleny.jan@psjg-hk.cz

1 Introduction

Gold nanorods have, in recent years, gained more and more attention in fields such as medicine or biochemistry. This is due to the fact, that they display a wide variety of potential applications. In practice, however, these are greatly limited by the presence of a highly cytotoxic compound, known as

CTAB (cetyltrimethylammonium bromide)

which, during their industrial preparation, forms a double layer on the surface of the nanorods and which is necessary in order to stabilise them in solution. Simultaneously this compound acts as a bridge between the particles themselves and any compound one may wish to attach to them (e.g. drugs, radiotherapeutic compounds etc.).

If gold nanorods are to become widely used, without them presenting any health hazards, this compound needs to be replaced by another, which, whilst retaining the same function, will lack the unwanted cytotoxic properties of CTAB.

This research was devoted to synthesising a surfactant which would meet these exact requirements.

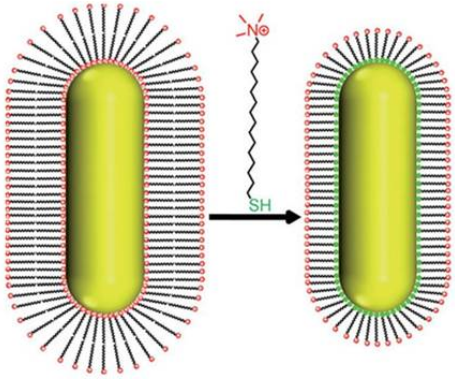

Figure 1: CTAB being replaced by MTAB on the surface of a gold nanorod – Source: Vigderman 2012

2 Method of investigation

The compound prepared during this project was

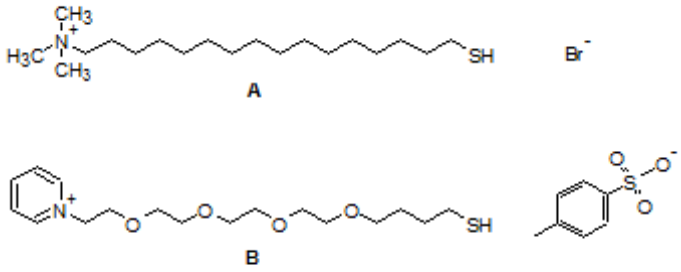

Figure 2: Comparison of MTAB (A) and 16-mercapto-3,6,9,12-tetraoxahexadec-1,16-diyl-1-pyridinium-p-toluenesulfonate – Source: Vigderman 2012

structurally based on a molecule named MTAB, the preparation and properties of which were described and published in a research paper by Leonid Vigderman, Pramit Manna and Eugene R. Zubarev named

Quantitative Replacement of Cetyl Trimethylammonium Bromide by Cationic Thiol Ligands on the Surface of Gold Nanorods and Their Extremely Large Uptake by Cancer Cells.

The synthetic approach used to prepare the intended compound was designed by modification of the original process, described in Vigderman's publication.

3 Experimental procedure

The synthetic approach consisting of nine individual steps was carried out in the laboratories of the Faculty of Science of the University of Hradec Králové under the supervision of the consultants listed above. Each of the nine steps was divided into four sub-steps:

- chemical reaction leading to the generation of the desired intermediate product
- processing of the acquired crude reaction mixture
- final purification
- TLC and NMR testing

The chemical compound obtained by this procedure was named **16-mercapto-3,6,9,12-tetraoxahexadec-1,16-diyl-1-pyridinium-p-toluenesulfonate**. As seen below, it presents a modified version of the original molecule – MTAB (A).

4 Results

After a collaboration with the University of Hradec Králové, which lasted for approximately one and a half years, and after several alterations of the synthetic approach we succeeded in isolating 50 mg of 16-mercapto-3,6,9,12-tetraoxahexadec-1,16-diyl-1-pyridinium-p-toluenesulfonate, which was a hitherto unknown and undescribed compound. The properties and applicability of this molecule are currently subject of further research.

5 Conclusion

The required compound has been successfully isolated. It is a yellow, oil-like, treacly liquid with a distinct butter-like malodour which is caused by the toluenesulfonate group in its molecule.
If further testing proves its supposed lack of cytotoxic properties, it will be a highly valuable expansion of the hitherto small number of such chemicals and will thus not only help improve the applicability of surface-coated gold nanorods but also serve as a starting point for the preparation of other, perhaps more advanced, surfactants

6 Sources

Alaaldin M. Alkilany Pratik K. Nagaria, C. R. (2009). Cellular Uptake and Cytotoxicity of Gold Nanorods:Molecular Origin of Cytotoxicity and Surface Effects. *Small Journal* .

Aneta J. Mieszawska, W. J. (2013). Multifunctional Gold Nanoparticles for Diagnosis and Therapy of Disease. *Molecular Pharmaceutics* .

Boisselier, E., & Astruc. (2009). Gold nanoparticles in nanomedicine: preparations, imaging, diagnostics, therapies and toxicity. *Chemical Society Reviews* .

Leonid Vigderman, P. M. (2012). Quantitative Replacement of Cetyl Trimethylammonium Bromide by Cationic Thiol Ligands on the Surface of Gold Nanorods and Their Extremely Large Uptke by Cancer Cells. *Angewandte Chemie* .

Leonid Vigderman, P. M. (2011). Supporting Information - Quantitative Replacement of Cetyl Trimethylammonium Bromide by Cancer Cells. *Angewandte Chemie*.

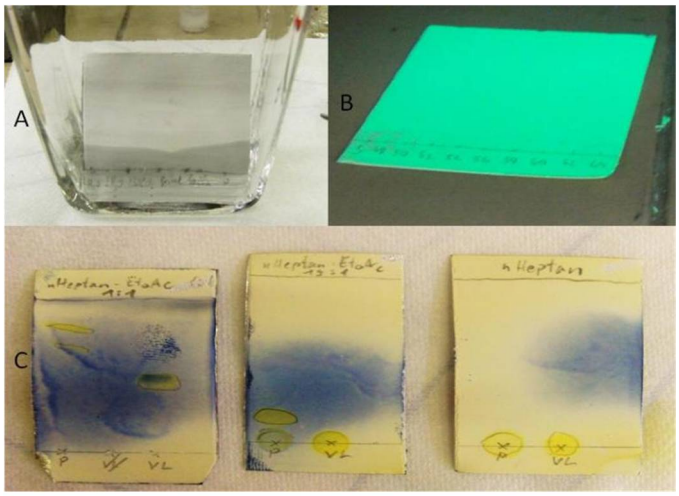

Figure 3: Thin layer chromatography (TLC) testing of the final product – Source: photographed by author

Figure 4: Nuclear magnetic resonance (NMR) testing of the final product – Source: http://www.emory.edu/NMR (illustrational)

Comparison of cytotoxicity of antidote substances used to treat organophosphate poisoning

Natálie Živná

RNDr. Linda Schmutzerová, Ph.D., Mgr. Petr Jošt

The First Private Language Grammar School, Hradec Kralove, Czech republic, arnesis90@gmail.com, Department of Toxicology and Military Pharmacy, Faculty of Military Health Sciences, University of Defence, Hradec Kralove, Czech republic

7 Introduction

Weapons of mass destruction, especially chemical warfare agents, belong to the most feared group of weapons. They persist in the environment for several years. Nerve agents are one of the most significant chemical weapons. They are known for being highly toxic and being absorbed through various ways of exposure, predominantly by the skin and respiratory tracts. For these features they can be misused in armed conflicts or terroristic attacks.

The intoxication of nerve agents is based on inhibiting an essential human enzyme acetylcholinesterase (AChE), which controls transmission of an electrical signal along neurons. The therapy of poisoning by nerve agents is based on the recovery of inhibited AChE by the oxime AChE reactivators.

The aim of my project was to assess the toxicity of chosen AChE reactivators *in vitro* on human liver cells HepG2 using the clonogenic assay. Using this method I was able to determine IC_{50} values for comparison of toxicity of these compounds. Based on these values I compared each structure of the reactivator with its toxicity value. Then I described the relationship between toxicity and chemical structure and identified potentially toxic structures in molecules. These results can bring very important information for development of new less toxic AChE reactivators for organophosphate intoxication treatment.

8 Methodical part

Clonogenic assay

Clonogenic assay *in vitro* is a method based on a principle that single cell which survives a chemical treatment is able to form a visible colony (of at least 50 cell clones) during long term incubation.

a) Plating cells to 6-well panel

- I plated cells HepG2 to a 6-well panel in number 1000 cells per each well, in 2 ml of culture medium.
- I performed all experiments in triplicate for each sample.
- I placed cells containing panels to CO_2 incubator to attach overnight.

b) Cell treatment by AChE reactivators

I tested 7 different AChE reactivators. I calculated the amount of the reactivator required for the preparation of working solutions.

- I dissolved the reactivator in the culture medium and then I prepared concentration series by the serial dilution in ratio 1:1.
- To each well I added 1 ml of the corresponding reactivator solution to achieve the final tested concentration.
- The cells were then left to cultivate for 2 weeks.

c) Fixation and staining of colonies

After a 2-week-long cultivation the cells were washed by phosphate buffered saline and covered in a fixating and staining solution to make the colonies visible for counting.

- The solution consists of 0.5% crystal violet and glutaraldehyde 6%.
- After 30 minutes I washed the solution out of panels by immersing to distilled water.

d) Colony counting and IC_{50} calculating

After staining I left the dried panels in a chamber with 40°C air temperature.

- I took a photo of the panels with the stained colonies and analyzed it using Fiji® software.

- I counted the cell colonies in each well.
- Using GraphPad Prism 5.0v software I calculated the toxicity index IC_{50} and standard error of mean (SEM) for each tested concentration.

9 Results

9.1 Cytotoxicity of tested reactivators

In my project, I tested seven AChE reactivators to analyse their cytotoxicity to human liver cells HepG2. Using statistical software I calculated IC_{50} values obtained from the clonogenic assay. The structural formulas are shown in Picture 1.

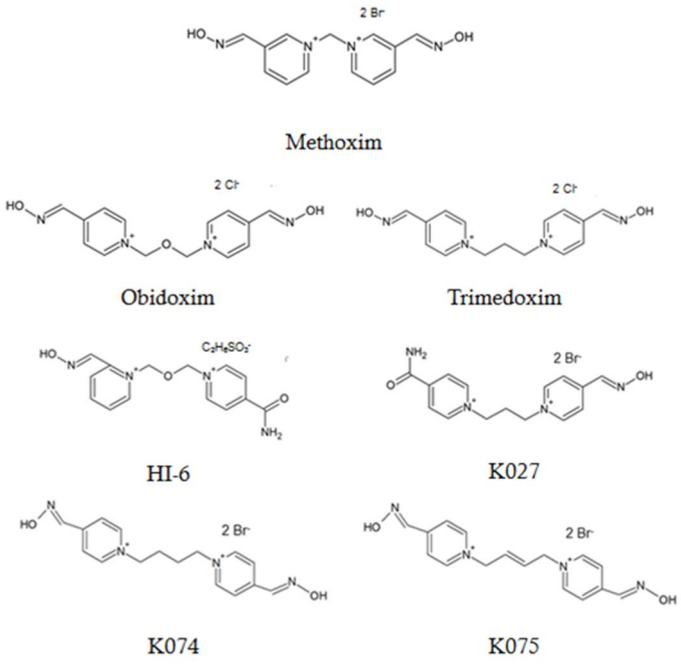

Picture 1: Structures of tested AChE reactivators

To get these values, it was necessary to optimize the concentration range to obtain sigmoidal dose-response curve (Picture 2). The line in the point 50% crosses the curve in the concentration of the tested reactivator, which causes death of 50% cells in comparison with control cells.

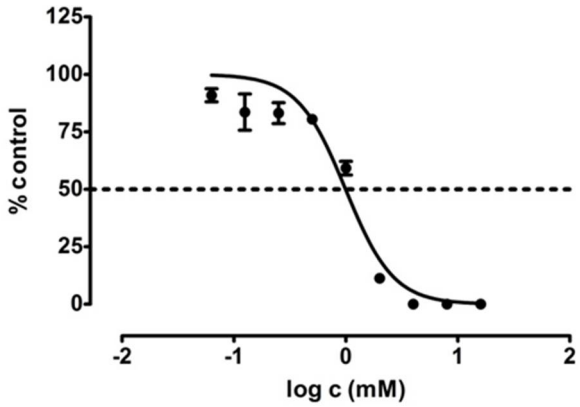

Picture 2: Sigmoidal dose-response curve for K027

In the following Table no. 1 there are summarized names of the tested reactivators and their toxicity (IC_{50}).

Compound	IC_{50} ± SEM (µM)
Methoxime	56.62 ± 6.61
Trimedoxime	292.7 ± 18.08
Obidoxime	6.54 ± 0.36
HI-6	18.94 ± 3.27
K027	253 ± 33.37
K074	20 ± 0.85
K075	32.14 ± 3.10

Table 1: IC_{50} of tested reactivators

9.2 Structure – toxicity relationship

By the analysis of the structure – toxicity relationship it was possible to find several structural elements of molecules in Picture 1, which leads to an increase of cytotoxicity to HepG2 cells.

I found out that the carbon linker chain length 1C (Methoxime) and 4C (Trimedoxime) in the reactivator molecule is less toxic than 3C linker (K074). Presence of two oxime functional groups in molecule (Trimedoxime) dampens toxicity in comparison with

one oxime- and one carbamoyl- group in molecule (K027).

We also found out the difference in toxicity in case of presence of multiple bounds in a carbon linker chain. The multiple bounded (K075) is slightly less toxic than single bound (K074).

10 Conclusions

In summary, I compared seven reactivators of AChE. On these compounds I evaluated and compared cytotoxicity using determination of IC_{50} value. According to the toxicity and structures I determined several structure elements, which led to an increasing toxicity of the tested compounds in comparison with an analogical chemical structure of other reactivators.

The results of my project could give base data for an improvement of a design of new, less toxic and safer AChE reactivators used to treat organophosphate poisoning.

Influence of temperature on growth rate of the house cricket (*Acheta domesticus*)

Lora Pevec
Supervisor: Romana Halapir Franković, prof.
V. Gymnasium, Zagreb/Croatia, E-mail: lorapevec@gmail.com

1. The purpose of the investigation

House cricket (*Acheta domesticus* L., 1758) is one of the three most common commercially available cricket species used for various purposes, primarily as food for exotic pets (Figure 1). Because of its wide usage it is grown on farms or improvised house hatcheries, wherein it is important to ensure the best possible conditions for faster development. The aim of this study was to investigate if the different temperatures influence growth rate of the house cricket reared in a house hatchery.

Figure 1. Usage of house crickets. Most commonly, house crickets are used as food for exotic pets, e.g. chameleons.

2. Material and methods

Two groups of house crickets, each containing 15 individuals, were included into the study. One group was reared at an average temperature of 31°C, and the other at 24°C (Figure 2). The length of crickets was measured every five days until the end of their growth and development (Figure 3). Total growth rate and growth rate for each period between two measurements were calculated. The life expectancy was also considered.
The differences between groups were calculated using the Mann Whitney test or the Kruskal-Wallis test as applicable, and they were considered to be significant at probability values of $p < 0.05$.

Figure 2. Study terrariums. The 15 W light bulb heated terrarium (left) assured an average temperature of 31°C, while at the unheated terrarium (right) an average temperature was 24°C.

Figure 3. Measuring the length of crickets. Smaller crickets were measured using a millimetre paper (upper panel), and larger ones were placed inside a test tube and measured by a ruler (lower panel).

3. Results

The ultimate length averaged 27 mm after 30 days for crickets reared at 31°C, and 26 mm after 55 days for

crickets reared at 24°C. The difference between the two groups was significant ($p < 0.0001$) at all time points (Figure 4). Comparing the lengths achieved by male and female crickets, the difference was significant only between those reared at 31°C (26 mm vs. 28.5 mm; $p < 0.0105$) (Figure 5).

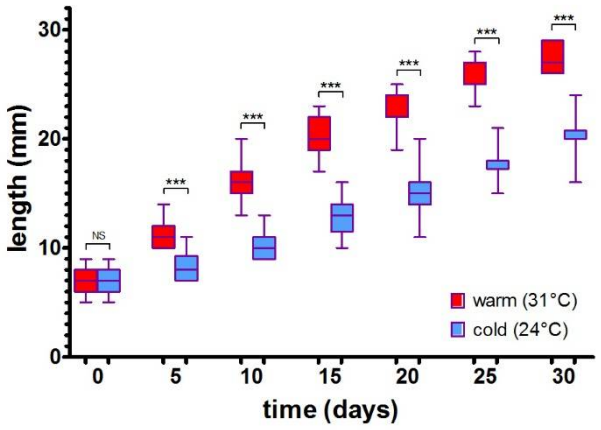

Figure 4. Length of crickets. The lengths of 15 crickets reared in the heated terrarium - warm (31°C) (red) and 15 crickets reared in the unheated terrarium - cold (24°C) (blue) at the beginning of the experiment (0) and at six following time points (5, 10, 15, 20, 25, and 30 days).
The significance levels: NS - not significant, * - < 0.05, ** - < 0.01, *** - < 0.001.

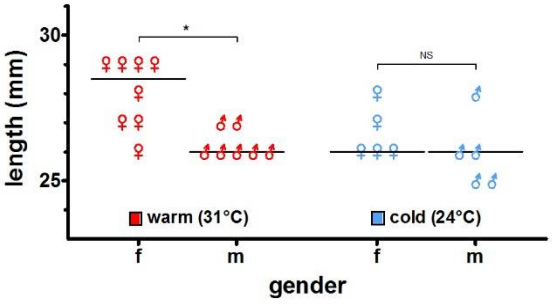

Figure 5. Ultimate length of male and female crickets. The lengths of 8 females (f) and 7 males (m) reared in the heated terrarium - warm (31°C) (red) as well as 5 females and 5 males reared in the unheated terrarium - cold (24°C) (blue) at the end of their development (30 days for 'warm' vs. 55 days for 'cold').

The significance levels: NS - not significant, * - < 0.05, ** - < 0.01, *** - < 0.001.

Total growth rate was 0.67 mm/day for crickets reared at 31°C, and 0.35 mm/day for crickets reared at 24°C. The growing period consisted of two phases in both groups of crickets, and those phases were characterized by faster and slower growing rates, respectively (Table 1). The life expectancy averaged 65 days for crickets reared at 31°C, and 128 days for crickets reared at 24°C (Figure 6).

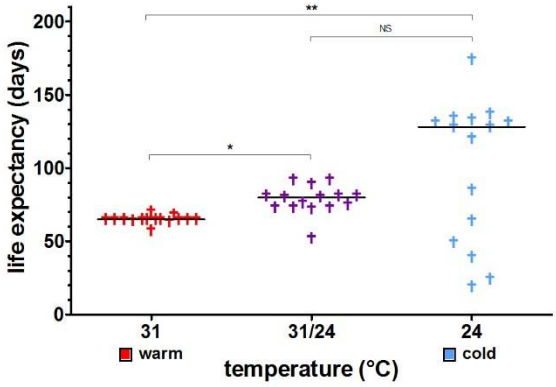

Figure 6. Life expectancy of crickets. The life expectancy of 15 crickets reared in the heated terrarium - warm (31°C) (red) and 15 crickets reared in the unheated terrarium - cold (24°C) (blue). Also shown is the life expectancy of 15 crickets reared in the heated terrarium until the end of their development (30 days) and then transferred to the unheated terrarium - (31°C/24°C) (purple).
The significance levels: NS - not significant, * - < 0.05, ** - < 0.01, *** - < 0.001.

4. Conclusions

Higher temperatures (~31°C) positively affected development of crickets in terms of their faster growth and greater final length. This was particularly true for females, as they outgrew males reared in the heated terrarium. The growing period of all crickets consisted of two phases, characterized by faster and slower growing rates, respectively. Contrary to positive effect on the development of crickets, their expected lifetime was shorter at higher temperatures.

GROWTH RATE (mm/day)	PERIOD	0 - 5 days	6 - 10 days	11 - 15 days	16 - 20 days	21 - 25 days	26 - 30 days	31 - 35 days	36 - 40 days	41 - 45 days	46 - 50 days	51 - 55 days	TOTAL
				0,85*		24 mm	0,30**						
	warm (31°C)	0,80	1,00	0,80	0,80	0,20	0,40						0,67
	cold (24°C)	0,20	0,40	0,60	0,40	0,60	0,40	0,40	0,40	0,20	0,20	0,00	0,35
					0,43*				24 mm		0,13**		

* a phase characterized by faster growing rate
** a phase characterized by slower growing rate

Table 1. Growth rates of crickets. The growth rates of 15 crickets reared in the heated terrarium - warm (31°C) (red) and 15 crickets reared in the unheated terrarium - cold (24°C) (blue) calculated for each period between two measurements and for the total duration of growth (30 days for 'warm' vs. 55 days for 'cold'). Average rates of two different growth phases in both groups are also shown - a phase of faster growing (*), observed during the first 4 and 8 periods in 'warm' and 'cold' terrariums, respectively, as well as a phase of slower growing (**), observed during the last 2 and 3 periods in 'warm' and 'cold' terrariums, respectively. Those phases were separated by the same average length of 24 mm in both groups of crickets.

Defining Polyphenols in some Sorts of Georgian Grapes

Mariami Vardosanidze & Nino Kerdikoshvili

Supervisors: Medea Toloraia & Guranda Gabunia

Georgian-American High School, Tbilisi, Georgia, info@gahs.edu.ge

Introduction

Polyphenols and anthocyanins are plant pigments that have powerful antioxidant properties. There are more than 8000 polyphenolic compounds, which are separated by a variety of plant organs. Their quantity depends on the degree of maturity of the plant and the environmental conditions.

Red, purple and black colour of the fruit plant indicates the presence of polyphenols and anthocyanins in them. Fruit such as: tomatoes, black rice, cranberries, currants, raspberries, blackberries, red beans, pomegranate, cocoa powder, grapes and others contain polyphenols.

Purpose

The purpose of our work was to determine main parameters of grapes, polyphenols and anthocyanins in such white and colourful sorts of Georgian vine that have not previously been studied in this direction, as well as to estimate their oenological potential.

Materials and Methods

Varieties of the research grapes were taken from the Viticulture and Wine Institute (Agrarian university of Georgia) from the village of Skra collection vineyard (Gori region) in 2015 during the vegetation period (in the fall). 8 sorts of grapes were taken for research: Dondghlabi Mtsvane, Kapistoni Tetri, Krakhuna, Tsitska Kloni, Tsolikouri, Samarkhi, Ojaleshi, Saperavi. 6 bunches for each variety, which were divided by 3 repetitions (2 bunches in each repetition). The following parameters have been studied for carpological analysis: colour and weight of grain, weight of skin, grape stone, bunch, quantity of grape stone in grain, length and width of grain. Skin and grape stones were fixed separately for each repetition in acidified ethanol (70% Et, 29% H2O, 1% HCI (38%)) solution. In order to study grape stones and skin extracts, define total anthocyanins and polyphenols phenotyping method was used worked out within the project COST action FA1003 “East-West Collaboration for Grapevine Diversity Exploration and Mobilization of Adaptive Traits for Breeding” for oenocarpological estimation of adapted varieties (Rustioni et al. 2014).

Total anthocyanins were defined in mg/kg grapes, by using spectrophotometers in equivalent of Malvidini 3-0 glucoside. Total polyphenols were determined in skin and grape stone extracts separately mg / kg of grapes (+) in equivalent of catechins. Defining total polyphenols in white grape varieties was conditioned by winemaking rules of Georgia (Kakhetian and Imeretian), where chacha was also involved.

Results and Generalization

Carpological parameters indicated a significant variability in the studied varieties (Chart 1). As shown on the chart, The grain weight varies from 1,6 grams to 2,3 grams. Out of this the smallest grain was for Kapistoni Tetri and the biggest for Samarkhi sort. Samarkhi sort had the biggest bunch weight (321,8), and Saperavi Tsiteli sort had the smallest (124,3).

Total anthocyanins were studied in 2 colourful sorts and its content was Ojaleshi 1312,4 mg/kg, Saperavi 1087,3 mg/kg.

Saperavi (2582,5 mg/kg) showed the highest content among skin extracts of the studied sorts. Samarkhi sort (680,1 mg/kg) is characterized by the lowest content of polyphenols in skin among white grape sorts, whereas Dondghlabi Mtsvane has the highest content (2115,5 m/kg).

As the study shows, number of polyphenols extracted from generally all grape stones are significantly less than skin. The number of polyphenols in grape stones of white grape sorts varied from 12,8 to 111,0 mg/kg, the number of polyphenols in grape stones of red grape sorts were Ojaleshi – 48,8 mg/kg, Saperavi – 56,4 mg/kg.

Chart 1. Carpological parameters of Georgian vine sorts

Sort	Grain Colour	Grain Weight (g)	Skin Weight (g)	Number of grape stones in grain	Weight of grain stone (mg)	Grain length (mm)	Grain Width (mm)	Bunch weight
Dondghlabi Mtsvane	White	2,3	0,63	2.3	46,4	14,5	14,3	144,7
Kapistoni Tetri	White	1,9	0,59	2,7	27,5	12.8	13,1	130,0
Krakhuna	White	2,3	0,41	2,7	41,2	15,6	14,3	128,3
Samarkhi	White	1.6	0,84	3,3	60,1	16,6	14,9	321,8
Tsitska, Kloni	White	1,9	0,49	2,4	48,2	13,9	13,7	154,5
Tsolikouri	White	2.3	0,44	2,2	59,8	14,9	14,4	184,7
Ojaleshi	Red	2,1	0,65	2,8	49,3	14,1	13,8	165,5
Saperavi	Red	1,8	0,46	1,7	39,3	14,1	13,0	124,3

Conclusion

According to the study, Georgian vine sorts are characterized by significant variability of carpological and biochemical signs. Such diversity is particularly interesting for characterizing technological potential of single, less widespread sorts. Biochemical parameters depend on the degree of grape maturity, environmental conditions and agro-technical practice. But if we take into consideration the fact that the studied sorts were taken from the same collection, where same conditions apply to all sorts, we may conclude that the difference between numbers of total anthocyanins and polyphenols is conditioned by genetic properties of sorts.

References

Maghradze, D., Popescu, C.F., Cola, G., Abashidze, E., Aroutiounian, R., Brazão, J.; Coletti, S., Cornea, V., Dejeu, L., Dinu, D., Eiras Dias, J.E., Fiori, S., Goryslavets, S., Ibáñez, J., Kocsis, L., Lorenzini, F., Maletic, E., Mamasakhlisashvili, L., Margaryan, K., Mdinaradze, I., Memetova, E., Montemayor, M.I., Muñoz-Organero, G., Nemeth, G., Nikolaou, N., Raimondi, S., Risovanna, V., Sakaveli, F., Savin, G., Savvides, S., Schneider, A., Schwander, F., Spring, J.L., Pastore, G., Preiner, D., Ujmajuridze, L., Zioziou, E., Maul, E., Bacilieri, R.,

Failla, O., 2014: First results of the European Grapevine collections' collaborative network: validation of a standard eno-carpological phenotyping method. Vitis 53 (4), 219–226.

http://zdorovyda.ru/polifenolyi-v-produktah-moshhnaya-zashhita-ot-bolezney-stareniya-ili-pochemu-nuzhno-chasto-est-granatyi/

http://xn----9sbghaihfc5cza6m.xn--p1ai/18/6/1/

http://ru.wikihow.com

http://infofoodsupplements.ru/topic/47-antioksidanti-polifenoli-i-flavonoidi/

http://themindfulbeauty.com/?p=1565

Investigation of biological and environmental effects of nano- and microparticles

Hanna Brüggemann, in collaboration with Veronika Kienle and Clara Heilker

Supervisor: Daniela Bernlöhr

Wieland-Gymnasium, Biberach/Germany, hanna.brueggemann@t-online.de

11 Introduction

Plastic contamination is an increasing environmental problem. Not only big plastic fragments are problematic but also small pieces of plastics, named microplastics. These are particles smaller than 5 mm in diameter. They get into freshwater rivers and also into oceans through cosmetic articles and plastic packaging. Sewage works can not completely filter out the microplastics so that they contaminate the drinking water. We looked for a method to extract particles from water.

But also other tiny fragments named nanoparticles are a problem for the environment. Nanoparticles are smaller than 100 nm. They are used in many different ways in industry and households, for example, for special coatings, although their consequences are not always checked consequently. We investigated the impact of nanoparticles on human cells to check if they have a detrimental influence.

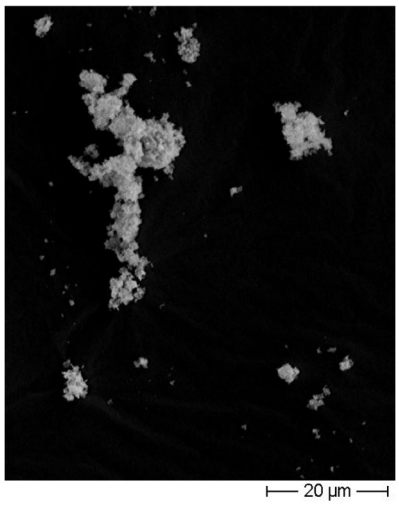

Fig. 1: TiO_2 nanoparticles show agglomeration as seen under a scanning electron microscope

12 Methods of the investigation

In the first step we extracted microplastics to analyse their characteristics. We tested different filters and also the centrifuge and plankton grids to extract microparticles from shower gels and toothpastes. We tested these particles with different studies on concentration, size and polarity. With the data of the different characteristics we tried to find a standard method to extract microplastics from water. In addition, we took samples in a sewage work to check how many particles are released into the environment by reason of inadequate separation. We analysed the components of the samples with infrared spectroscopy in attenuated total reflection. In continuing steps we checked the influence of these small particles on cells. Due to the fact that even smaller particles have probably more influence we used nanoparticles for this part. We analysed the influence of nanoparticles to human and animal cells to determine if the particles influence the viability of cells. For this experiment we used human tumour cells and hamster ovary cells. After contamination with the nanoparticles we took samples after two, four and 24 hours and used the viability measure and an apoptosis assay to check these samples on apoptosis (programmed cell death) and viability. Furthermore the toxicity of nanoparticles to luminous bacteria was tested.

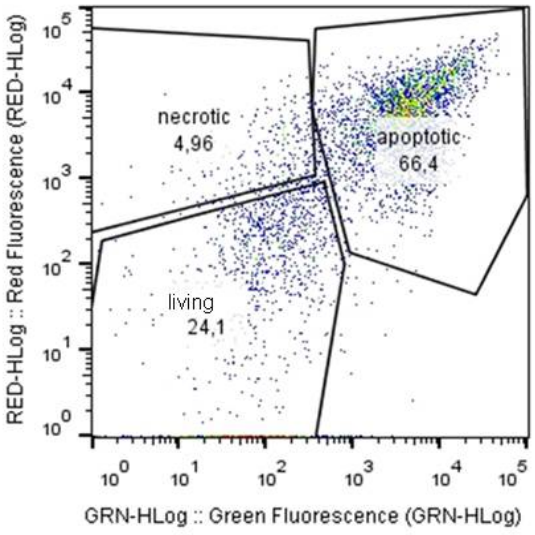

Fig. 2: Results of the apoptosis assay with TiO_2 which show the fractions of apoptotic, necrotic and living cells.

13 Results of the experiments

The results showed that microplastics and nano-particles are in many cosmetic products and the fraction of microparticles in, for example, a typical shower gel is surprisingly high with 3.7 %. We could see that microparticles and nanoparticles have different characteristics dependent on the components. That is the reason why it was not easy to find a standard method for extraction. Our studies showed that the centrifuge and the plankton grid are the best methods for extraction of microplastics. The samples of the sewage work showed that there were microplastics in the cleaned water. Most of them were so tiny that you can not see them by visual inspection. The viability measure showed that many nanoparticles have a detrimental influence to cells. Also the apoptosis increased through the influence of nanoparticles. The toxicity measure indicated similar results with a reduction in luminous intensity. They showed that nanoparticles are in part highly toxic for bacteria.

14 Conclusion

We successfully separated microplastics from shower gels and toothpastes and found a method to extract microparticles from water. Our investigations identified microplastics in cleaned water from the sewage work, so we can say that microplastics are a big problem because they are released into rivers and oceans. We saw that nanoparticles have negative influence on human and animal cells and, in addition, they are toxic for luminous bacteria.

15 References

[1] LUWG: Umweltschutz im Alltag – Mikroplastik, Mainz 2014

[2] Mechsner, Julia: Mikrokunststoffe, Mainz 2014

[3] Regmann, Sascha und Heckhausen, Angelika: Micro-Beads - Auswirkungen von Kunststoff-Mikropartikeln auf die marine Umwelt, Herne 2014

[4] https://www.test.de/Nanoteilchen-Das-sollten-Sie-wissen-4445980-0/

Golden Algae Army Combats Osteoporosis and Bone Fractures

Ariadni Papadopoulou

Anatolia College

ariadnipd@yahoo.com

Dr. Matthew Julius, Professor of Biology

Saint Cloud State University

Saint Cloud, Minnesota

Abstract

Pleurochrysis carterae is a unicellular marine algae covered with interlocking calcite plates, called coccoliths, which produce bioavailable calcium. The ability of *Pleurochrysis carterae* to perform biologically-directed calcification is very important to the evolution of the medical field since calcium is the most predominant mineral in bone. It provides structure and strength and promotes bone growth. Magnesium is another mineral essential to the structural development of bone. Strontium is a trace mineral vital for normal bone formation, strength and mineralization, which decreases the risk of non-vertebral bone fractures, increases bone mineral density, prevents and combats osteoporosis.

This experiment investigated uptake of magnesium and strontium by *Pleurochrysis carterae* and the incorporation of those metals into its calcium carbonate cell wall.During a period of 10 days, two different *Pleurochrysis carterae* cultures were grown. One was kept as the controlculture while the other was treated with 10 micrograms of magnesium and 10 micrograms of strontium. A culturing apparatus provided sterile air and dispensed oxygen and carbon dioxide produced by the algae. Cultures were sub-sampled every day at 2:00 pm (12:12 light/dark cycle). Two biological endpoints were selected so as to determine whether algae's physiology was altered. Dry weight measurements helped us assess algae's growth rate. A mineral analysis using a Scanning Electron Microscope examined calcium, strontium and magnesium content of *Pleurochrysis carterae*in order to explore whether it could be a suitable resource for mass production of magnesium, strontium and calcium supplements which could alleviate the large percent of people suffering from mineral deficiency, low bone density and osteoporosis.

Finally, we examined the economic viability of investing in the production of such supplements and the potential economic and social benefits while discussing why they outweigh the benefits of magnesium and strontium supplements already available on the market.

PACAP prevents the effects of mechanical load in chondrifying cell cultures

Flóra Veres
Supervisors: Tamás Juhász M.Sc., Ph.D., Zsolt Krakomperger M.Sc., Ph.D.
Kossuth Lajos Teacher Training Grammar School of the University of Debrecen

1. The purpose of the investigation

Pituitary Adenylate Cyclase Activating Polypeptide (PACAP) is an endogenous neuropeptide distributed throughout the body. PACAP influences development of various tissues and exerts protective function during cellular stress, inflammatory processes and apoptosis. However, little evidence is available on its role in the function and development of skeletal elements. Activation of PACAP receptors (PAC1, VPAC1, VPAC2) can regulate divers signalling pathways from which the canonical signalling connection induce the activation of PKA and/or MAPK system [1], which is one of the cascades involved in mechanotransduction[2]. It is also known the activation of PACAP signalling pathways decrease the expression of Hedgehog signalling such as Sonic Hedgehog (SHH) and Indian Hedgehog (IHH) which are responsible for the regulation of hypertrophic differentiation of cartilage and also regulated by mechanical stress [3]. On the basis of these data I attempted to clarify the possible role of PACAP in cartilage formation and its function during mechanical stress of chonrifying cells.

2. Methods of the investigation

Chondrogenesis was investigated in high density cell cultures established from chondrogenic cell of limb buds of chicken embryos in 22-24th of Hamburger-Hamilton developmental stages. Mechanical stimulation was carried out by a self-designed bioreactor that exerted uniaxial intermittent cyclic load transmitted by the culture medium as hydrostatic pressure and fluid shear to differentiating cells. The loading scheme (0.05 Hz, 600Pa, for 30 min) was applied on culturing days 2 and 3 during final commitment of chondroprogenitor cells. Administration of the PAC1 receptor agonist PACAP1-38 (the full version of PACAP neuropeptide which contains 38 amino acids) happened in 100 nM concentration continuously from day 1 of culturing. Cartilage differentiation was visualized by acidic Dimethyl-methylene Blue (DMMB) and Toluidene Blue (TB) staining. Collagen type II. content of the extracellular matrix was monitored with ^{3}H-prolin incorporation. RT-PCR was used to follow mRNA expression and protein expression was detected by Western Blot.

3. Results of the experiment

Administration of both the PAC1 receptor agonist PACAP1-38 and mechanical stimulation augmented cartilage formation (Figure 1) and stimulated collagen production. Mechanical load increased the expression of Collagen type X., marker of hypertrophic differentiation of chondrocytes and PACAP addition attenuated this elevation.

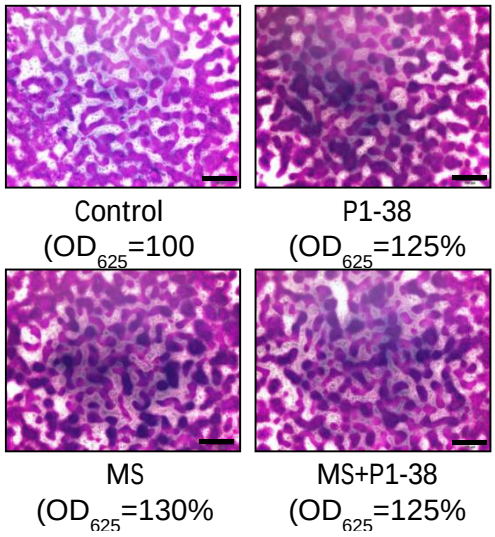

Figure 1.Metachormatic staining of High Density cell cultures on day 6th of differentiation

Purple colour represents the extracellular matrix of hyaline cartilage. Optical density (OD) of resolved TB staining was measured on 620 nm. Significant differences are considered as P>0.005.

As the proof of endogenous activation PACAP signalling mRNA and protein expression of PACAP and PAC1 receptor also increased during mechanical load. PACAP administration diminished the level of SHH and IHH, but the mechanical load elevated the protein expression of these molecules. I have also proven that the downstream target of Hedgehog signalling, the Gli1 transcription factor, appeared in a higher expression during mechanical

induction, which was reduced by PACAP addition (Figure 2).

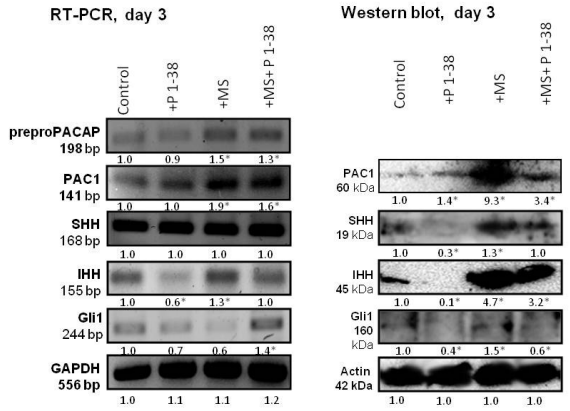

Figure 2. mRNA and protein expression of signalling molecules

RT-PCR and Western blot was used to detect expression changes of signalling molecules. Optical Density (OD) was determined with ImageJ. GAPDH and Actin were used as inner control.

4. Conclusion

The observation imply the therapeutical perspective that PACAP might be applicable as a natural agent exerting protecting effect during joint inflammation and may promote cartilage regeneration during cartilage degenerative diseases of articular cartilage[4]. These experiments will make us better understand the steps of mechanotransduction and further experiments may come up with some results which clarify the complete process of PACAP signalling and cartilage regeneration.

5. References

1. Vaudry, D.; Falluel-Morel, A.; Bourgault, S.; Basille, M.; Burel, D.; Wurtz, O.; Fournier, A.; Chow, B. K.; Hashimoto, H.; Galas, L.; Vaudry, H. Pituitary adenylate cyclase-activating polypeptide and its receptors: 20 years after the discovery. *Pharmacol. Rev.* **2009,** *61* (3), 283-357.

2. Juhasz, T.; Matta, C.; Somogyi, C.; Katona, E.; Takacs, R.; Soha, R. F.; Szabo, I. A.; Cserhati, C.; Szody, R.; Karacsonyi, Z.; Bako, E.; Gergely, P.; Zakany, R. Mechanical loading stimulates chondrogenesis via the PKA/CREB-Sox9 and PP2A pathways in chicken micromass cultures. *Cell Signal.* **2014,** *26* (3), 468-482.

3. Juhasz, T.; Helgadottir, S. L.; Tamas, A.; Reglodi, D.; Zakany, R. PACAP and VIP signaling in chondrogenesis and osteogenesis. *Peptides* **2015,** *66*, 51-57.

4. Juhasz, T.; Matta, C.; Katona, E.; Somogyi, C.; Takacs, R.; Gergely, P.; Csernoch, L.; Panyi, G.; Toth, G.; Reglodi, D.; Tamas, A.; Zakany, R. Pituitary adenylate cyclase activating polypeptide (PACAP) signalling exerts chondrogenesis promoting and protecting effects: implication of calcineurin as a downstream target. *PLoS. One.* **2014,** *9* (3), e91541.

ICYS_2016_abstract India (Life Science - Indian Herbs - Turmeric)
Maanvi Mudgil
Ms. Sudha Chand
St. Mark's Senior Secondary Public School, Meera Bagh , New Delhi ,India
stmarksmb@saintmarksschool.com

Purpose of Investigation

There are a number of problems that we face in everyday life like increased bacterial growth due to pollution, harmful effects of chemical based cosmetics, growing adulteration in food products etc. All these gave me a good reason to investigate on turmeric because it is believed to have excellent antibacterial properties. Turmeric, in India, is used to heal sores. It is also used as a cosmetic product for enhancement of skin and countering the problem of acne and pimples.

(turmeric as an underground stem)

Moreover, it is also considered auspicious and holy in India and has been considered important in various ceremonies. Haldi ceremony is an important ceremony observed during Hindu weddings. A paste of turmeric is applied to the bride's and groom's body few days before the wedding. It is believed that application of turmeric softens the skin and adds a natural glow to it. This is one of the reasons why it was used as a beauty product in ancient times.

(*Haldi ceremony during weddings)*

All these fascinated me very much, hence this investigation. The aim of the experiment was to find out how good is turmeric as an antibiotic and how does it affect our skin when used as a cosmetic product. On the same lines some cosmetic products like moisturizer and face cleanser using turmeric are also made after performing the experiment. Due to the extensive use and sale of turmeric and turmeric powder in the market many issues related to adulteration of turmeric powder have come up so another experiment was performed to check the presence of adulterants like metanil yellow in turmeric powder.

Method of Investigation

Checking the affect of turmeric on bacterial growth**.**

1) A turmeric paste is prepared using half tablespoon turmeric powder and one tablespoon distilled water.

2) An agar petridish is taken and is swabbed with a sample of human saliva.

3) A second petridish is prepared in the same way and turmeric paste is added to it.

Checking the presence of adulterants like metanil yellow in turmeric powder

1) About ¼ tsp of turmeric and distilled water are added to a test tube. Shake the test tube well.

2) A few drops of HCl are added to the sample

3) If the colour of the sample changes pink then it indicates that the sample contains the adulterant metanil yellow.

Results of the experiment

After performing the first experiment bacterial count of the sample is noted at an interval of two days each.The petridish sample treated with turmeric showed a fall in bacterial count.

In the second experiment we observe that the colour of the turmeric sample changes to pink when HCl is added to it as it contains the adulterant metanil yellow.

Conclusion

From these experiments we can conclude that turmeric can be used as a mild antibiotic as it helps in inhibiting the growth of bacteria, it can act as a good substitute for chemical cosmetics and can help us to counter the problem of acne and pimples also. Moreover many adulterants like metanil yellow are present in the turmeric powder sold commercially so one must be cautious of it and try and use good quality of turmeric powder for enjoying its benefits.

Reference

http://www.turmeric.co.in

http://www.whfoods.com

Effectiveness of Coat Button Plants in Eliminating Foot Odor

Maria Immaculata Tania Suradja

Vonny, S.Si

Santa Laurensia High School, Indonesia, taniasuradja@gmail.com

1. Introduction

Body odor has always been displeasing and a bother, yet is a common problem for everyone, particularly during their teenage years. Body odor may be hard to avoid as it is caused by hormones that appear especially during puberty. People tend to avoid others who give of a foul odor, hence making people find lots of ways to prevent the emergence of odor from their body. One of the most common parts of the body where odor emerges is on the feet.

Oftentimes, body odor appears when sweat is produced. In feet sweat, bacteria, such as *Bacillus subtilis*, can be found as it digests and produce foul-smelling gas. Eliminating the bacteria that produces the acid would eliminate body odor. Hence, the use of antibacterial agent may solve this.

Nowadays, many natural resources such as plant extracts are often used for antibacterial agents. Coat button plants (*Tridax* procumbens) are wild plants that grow abundantly, yet it is often used for medicinal purposes, meaning that it has lots of useful substances in it. Therefore, coat button plants may be a candidate for the elimination of bacteria that cause of foot odor.

According to the problem stated above, a research has been started with the title "The Effectiveness of Coat Button Plants (*Tridax procumbens*) as an Antibacterial Agent towards Bacteria Found on Feet (*Bacillus subtilis* and *Staphylococcus spp.*)". Through this research, another usage of wild plants is proposed for antibacterial purposes.

2. Problem Statement and Purpose

Foot odor is a problem faced by lots of people and is often sought to be eliminated. Coat button plants are also abundant and not much used. Hence a solution is needed in order to solve the foul-smelling odor and the abundance of wild plants.

The purpose of this research is as stated below.

1. Study antibacterial activity of coat button plants extract towards bacteria *Bacillus subtilis*
2. Identify bacteria found on the feet
3. Determine whether the extract may work on other bacteria on feet

3. Research Methodology

The antibacterial test data was obtained quantitatively through pour plate method and agar disk diffusion method. The bacteria identification was done qualitatively through observations and tests.

Coat button plant extract was obtained by using all parts of the plant through soxhlet with ethanol. Different concentrations of the extract (25%, 50%, 75%, 100%) were then made.

Antibacterial test was then done on *Bacillus subtilis*. The test was done with pour plate method by agar disk diffusion. Clear zones that appeared were then measured. Part of the clear zone was then inoculated to determine bacteriostatic or bactericidal antibacterial agent.

Bacteria sample was taken from feet and inoculated in nutrient broth. Bacteria were then grown on agar plate to form colonies. Bacteria were identified by gross colony, agar slant, gram staining, and catalase test. Each colony was then inoculated.

Antibacterial test was done on each colony through spread plate with agar disk diffusion method. Clear zones were then measured and analyzed.

4. Result and Analysis

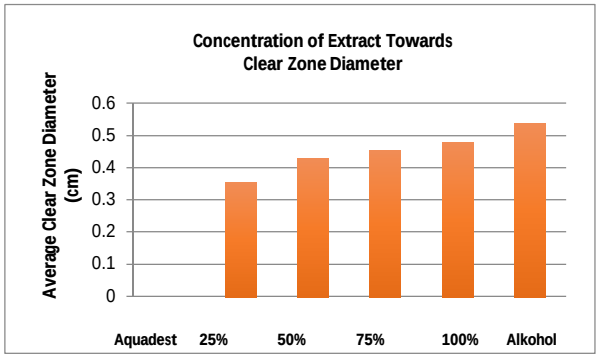

Fig 1. The average clear zone diameter of each concentration and control of antibacterial test on *Bacillus subtilis*

Clear zones formed surrounding all the extracts, proving that the extract does have antibacterial activities. Among the extracts, the 100% concentration had the largest clear zone. A trend was seen that the higher the concentration, the larger the clear zone, though the difference is not significant, indicating that antibacterial activity only differs slightly. Yet the extracts were still below alcohol meaning that it did not reach lethal doses.

Swab taken from the clear zone was found to be able to grow again, meaning extract works as bacteriostatic antibacterial agent.

Based on its components, coat button plant extract may work as it messes up protein, alters the outer membrane, inhibit enzyme activity, permeability of cell membrane, and synthesis of bacteria cell.

Through identification, the bacteria taken from the feet formed colonies and can be classified as Staphylococcus that are also known to be found in feet.

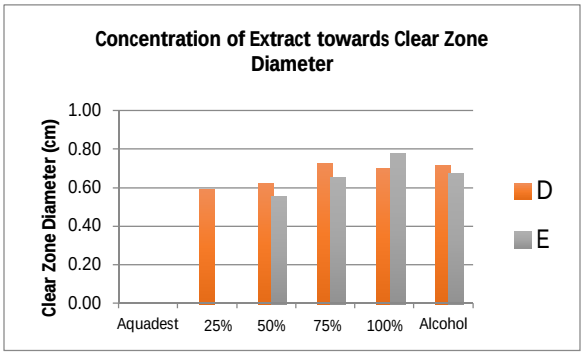

Fig 2. The clear zone diameter of each concentration and control of antibacterial test on Staphylococcus D and E

The extract only worked on 2 types of Staphylococcus found and yet not with a clear trend of clear zone diameter result. This shows that the extract does not work on all types of bacteria and that it might be due to media that does not support maximum growth of all bacteria.

5. Conclusion and Recommendation

Based on our research titled "The Effectiveness of Coat Button Plants (*Tridax procumbens*) as an Antibacterial Agent towards Bacteria Found on Feet (*Bacillus subtilis* and *Staphylococcus spp.*)" a few conclusions were withdrawn as follows.

1. *Tridax procumbens* extract can work as a bacteriostatic agent towards bacteria *Bacillus subtilis*, with the 100% concentration as the most effective
2. *Staphylococcus spp.* Can also be found on the feet.
3. Coat button plant extract can work as an antibacterial agent towards several types (not all) of bacteria found on feet

As this research was done within a limited amount of time and facility, hence we recommend a few suggestions for the next researchers studying this topic.

1. Use statistics on clear zone results
2. Redo antibacterial test with repetition

Antibiotics Based from Insect

Potency of Various Insect Species in Bali as an Antibotic

PutuAgastyaSatryana, KadekAdindyaPradnya

Dra. Ni NyomanYuniati, M. Pd

SMA Negeri 1 Denpasar, Denpasar-Bali/ Indonesia, p.agastya.1@gmail.com

1. Introduction

Antibiotics are chemical substances produced by fungi and bacteria, which had a lethal efficacy or inhibit the growth of bacteria.The ability of antibiotic drugs as antibacterial encourages excessive use of antibiotics with improper dosage. As a result, the development of antibiotic resistance by bacteria process is now beginning to emerge. Antibiotic resistance condition is characterized by the lost of its efficacy for some diseases caused by bacteria.

Effort to find an active substance that is antibacterial continues to be done.Insects have been used as the first standard traditional medicine of various ethnic groups around the world for wound healing.Based on that information, Reseacherinterested in investigate the potential of maggots or larvae of the green bottle fly (*Luciliasericata* (Meigen)), coconut caterpillars or larvae of the red palm beetle (RPW) (*Oryctesrhinocherus* L.), Kroto (mixture of larvae and pupae of ants (*Oecophyliassmaragdina*)) and larvae of silkworms (*Bombyxmori*) to be employed as a source of antibiotics.

2. Problem Statement

There is no research comparison about maggots or larvae of the green bottle fly (*Luciliasericata* (Meigen)), coconut caterpillars or larvae of the red palm beetle (*Oryctesrhinocherus* L.), Kroto (mixture of larvae and pupae of ants (*Oecophyliassmaragdina*) and larvae of silkworms (*Bombyxmori*) to be employed as a source of antibiotics.

3. Purpose of the Research

The purposes of this study include were **(1)** to review the potency of insect producing antibiotic published in scientific papers; **(2).**To identify the types of insects and their larvae (maggots or larvae of the green bottle fly (*Luciliasericata* (Meigen)), coconut caterpillars or larvae of the red palm beetle (RPW) (*Oryctesrhinocherus* L.), Kroto (*O. smaragdina*) and larvae of silkworms (*Bombyxmori*) with the most potential to produce antibacterial or antibiotic substance.

4.Research Methodology

Coconut caterpillars (*Oryctes rhinoceros* L), Kroto (*O. smaragdina*), Maggots (*Luciliasericata*), and silkworm (*Bombyxmori*) were collected from sources available in Bali such as abattoir, cadaver, (maggots; collection of Biomedical Lab Vetereinary Faculty of Udayana University), rotten coconut tree (coconut caterpillar), bird markets Denpasar (Kroto), and Agro silkworm, SibangKaja Village Badung Regency (silkworm). Various scientific papers on natural antibiotic from insect are reviewed.

Research has been conducted in the Microbiology Lab of Faculty of Medical Udayana University. 25thJanuary – 12thFebruary ,2016. This study used an experimental method of completely randomized design, which consists of six (6) treatments, namely:P-0: NaCl physiologic (negative control), P-1: Penicilin-Gentamycin suspension of 25.000µgpenicillin and 25.000 µg Gentamycin/milliliter (positive control),P-2: Maggots(*Luciliasericata(Meigen*)),P-3:Kroto(*O. smaragdina*), P-4: Coconut Caterpillars (*Oryctes rhinoceros L*), P-5:Silkworm(*Bombyxmori*). Each of bacteria contain 6 kinds of treatment and there are 4 plates for each bacteria so the total of research objects on both plates of *Escherichia coli and Staphylococcus aureus*are 192, So Each treatment was repeated four times.

A total of 10 grams of all insect larvae was crushed to a final concentration of 100% with physiological NaCl. Grinding is done using micro-pastel. After grinding, the suspension of hemolymph was centrifuged at a speed of 10,000 RPM for 5 minutes. Supernatant was taken and stored in sterile Eppendorf tubes and frozen until testing is done.

Gram negative bacteria of *Escherichia coli* and Gram-positive of *Staphylococcus Aureus* grown in agar were provided by Microbiology Lab of Faculty of Medical Udayana University. Antibacterial activivity was tested in Mueller Hinton agar. The presence of inhibition zone was observed and measured.

Six (6) filter disks were submerged in each plate

(positive and negative controls as well as four insect larvae suspensions). The disks were than applied in the surface of Mueller Hinton agar plate with *Eschericia coli* and Streptococcus sp. The plates were incubated in 37°C overnight. The presence of inhibition zone was observed and measuredby vernier caliper.

5. Results& Analysis

Observation of the inhibition zone diameter is shown in Graph 1. As shown, the suspension of the silkworm extract had shown the widest inhibition zone diameter towards gram negative bacteria Escherichia Coli compared to the other treatment except P-1 Inhibition zone is the widest towards gram negative bacteria *Escherichia Coli* but Silkworms extract also showed the widest inhibition zone after the P-1 which also followed by the other extract with their own inhibition zone itself

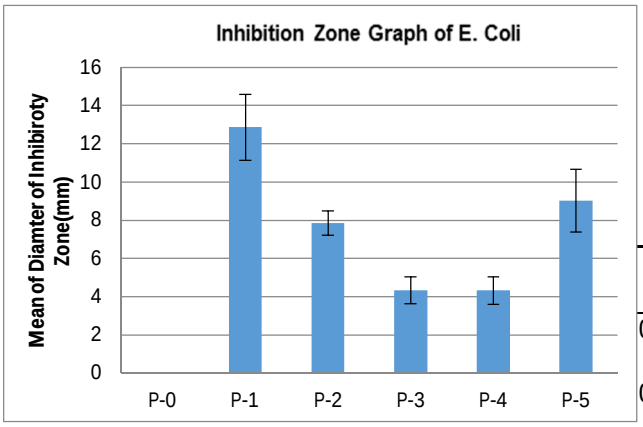

Observations	16	16
Hypothesized Mean Difference	0	
Df	15	
t Stat	22.11493959	
P(T<=t) one-tail	3.6594E-13	
t Critical one-tail	1.753050356	
P(T<=t) two-tail	7.31881E-13	
t Critical two-tail	2.131449546	

Graph 1. Mean of Inhibition Zone Diameter of Escherichia Coli (millimeter)

Observation of the inhibition zone diameter is shown in Graph 2. As shown, the suspension of the silkworm extract had shown the widest inhibition zone diameter towards gram positive bacteria Staphylococcus aureus compared to the other treatment except P-1 Inhibition zone is the widest towards gram positive bacteria *Staphylococcus aureus* but Silkworms extract also showed the widest inhibition zone after the P-1 which also followed by the other extract with their own inhibition zone itself

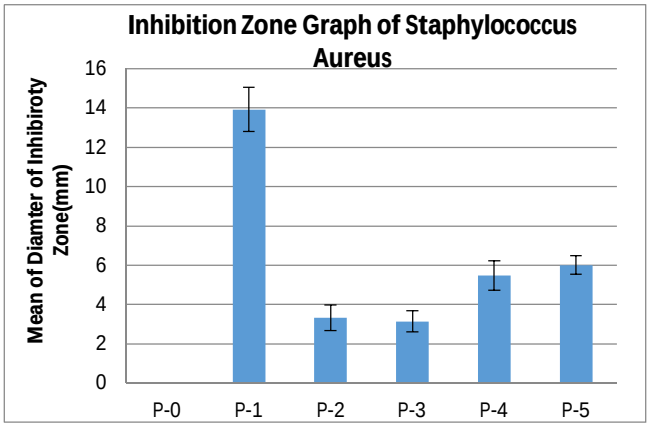

Graph 2. Inhibition Zone Diameter of *Staphylococcus Aureus* (millimeter)

From the graphic that shown above, we can take a conclusion which is each extract shown an inhibition zone and the significant of each data is very different because on this research, we want to know if there's a potency on each treatment and the data also showed that P-1 showed the widest nhibition zone than the other treatment but P-5 which is Silkworm extract showed a big inhibition zone towards each gram positive and negative bacteria.

6. Discussion

Table 1 Comparing with Control Negative in Escherichia coli

On the discussion, we discuss the data in statistic, as what it shows on the statistic we can conclude that the data is valid and there's a potency of each treatment can be use as antibacterial and antibiotic. Silkworm as an example, because silkworm has the biggest inhibition zone which showed that it's the most potential as an antibacterial also antibiotic than the rest of the treatment, after compared with the control negative on bacteria Escherichia coli, the

T stat showed the extract is statistically significant at $\alpha \leq 0.05$ due to no inhibition observed in the negative control of NaCl. Then the inhibition zone produced by the treatment must be due to the active compound contained in the extract.

Table 2. Comparing with Control Negative in Staphylococcus aureus

	Variable 1	*Variable 2*
Mean	6.0125	0
Variance	0.2105	0
Observations	16	16
Hypothesized Mean Difference	0	
Df	15	
t Stat	52.41903609	
P(T<=t) one-tail	1.04062E-18	
t Critical one-tail	1.753050356	
P(T<=t) two-tail	2.08123E-18	
t Critical two-tail	2.131449546	

On the discussion, we discuss the data in statistic, as what it shows on the statistic we can conclude that the data is valid and there's a potency of each treatment can be use as antibacterial and antibiotic. Silkworm as an example, because silkworm has the biggest inhibition zone which showed that it's the most potential as an antibacterial also antibiotic than the rest of the treatment, after compared with the control negative on bacteria Staphylococcus aureus, the T stat showed the extract is statistically significant at $\alpha \leq 0.05$ due to no inhibition observed in the negative control of NaCl. Then the inhibition zone produced by the treatment must be due to the active compound contained in the extract.

10.Conclusion.

The conclusion that can we gather from the paper is P2-P5 can be used as antibacterial also antibiotic, because all of the extract from the insect showed a inhibition zone on both of gram positive and negative bacteria which is Staphylococcus aureus and Escherichia coli, P-1 showed the biggest inhibition zone but P-5 which is Silkworms extract showed a big inhibition zone toward the bacteria itself, and the rest of the treatment also showed some inhibition zone which proved there's a potency for them to be an antibiotic

Effect of Eggplant Skin in the Process of Apoptosis in Cancer Cells

Hoda Seraj[a], *Fatemeh Afshari*[b]
Supervisor: Ensieh Olamafar, Ladan Ghotbi
Rahe Shayestegan High School, Tehran/Iran

Accepted and edited by: Araian Young Innovative Minds Institute, AYIMI, www.ayimi.org , info@ayimi.org

1 Introduction

The process of programmed cell death, or apoptosis, is generally characterized by distinct morphological characteristics and energy-dependent biochemical mechanisms. Apoptosis is considered a vital component of various processes including normal cell turnover, proper development and functioning of the immune system, hormone-dependent atrophy, embryonic development and chemical-induced cell death. Inappropriate apoptosis (either too little or too much) is a factor in many human conditions including neurodegenerative diseases, ischemic damage, autoimmune disorders and many types of cancer. The ability to modulate the life or death of a cell is recognized for its immense therapeutic potential.

1.1 The main Research

Cancer is a disease in which damaged cells do not cause apoptosis and uncontrolled cell division leading to the formation of malignant tumor.

Since the eggplant skin is rich in antioxidant- containing compounds causes the body's cells become resistant against premature aging and can also cause cancer cells to apoptosis. In this study the effect of alcoholic extract of eggplant skin on apoptosis of gastric cancer cells) AGS) and normal skin cells (FIB) was examined by MTT assay.

The MTT assay is a colorimetric assay for assessing cell metabolic activity. In this way, the yellow MTT salt becomes insoluble Formosan, which has a purple colour by dehydrogenase enzymes found in the mitochondria of active cells. The absorption of this compound is measurable after solution in DMSO at 570 nm. The results showed positive effect of eggplant peel extract on cancer cell apoptosis.

Refrences:

1-S. Elmore, "Apoptosis: A Review of Programmed Cell Death", NIEHS, Laboratory of Experimental Pathology, Research Triangle Park, North Carolina 27709, USA, Toxicol Pathol. 35(4): 495–516. 2007.

2- CELL CULTURE BASICS, www.invitrogen.com, handbook

3- http://www.cancerresearchuk.org/

Abstracts of 2016

The research of the level of pollution of atmosphere by the bioindicative method.

Karolina Savicka, Arina Skorochodova

Gimnazium of a name of F. Skoriny of the City of Vilnius

✓ 1. Introduction

The survey was carried out in the area of Vilnius Skorina School and in the nearby forest. The school is in the western part of Vilnius in the Karolinishkiu district. There is a road at the west side of the school , which average traffic intensity increases at the peak hours. There is a grove with installation of garages on the other side of the road.

2.Content

2.1.The purpose of the investigation

- Research of atmospheric pollution using the method of bio indication in the area of Skorina High School

Research tasks:

- to investigate the structure of lichen;
- to get acquainted with variety of lichen species within the school area;
- to assess the level of air pollution in the territory of Vilnius Skorina High School according to abundance of different morphological lichen groups.

Hypothesis: if we identify a sufficient amount of lichens, we can draw conclusions about the favorable ecological environment of the researched area.

2.2 Method of the investigation

- We created a map of the investigated area.
- We divided selected area into squares (10x10)m.
- We chose 5 trees in each square.
- We counted the amount of lichen species on each tree.
- All found species were divided into three groups: flat, leafy, branched.
- We assessed the tree trunk coverage with lichens. We put the strain of the measuring grid of 10x10 cm on a selected part and determined the area occupied by lichens.

2.3. Equations

The overall envelope counted by the formula : H=(100a+50b)/c

Relative index of atmosphere pollution ***(ARU)*** **=** $\frac{1F+2L+3B}{30}$

The higher index (ASU), the cleaner lichens growth area.

2.4. Results of the experiment

"Repression zone'' – poor lichens flora № 1, 2,3.(ASU: 0.2)

"Normal living zone"; points № 4, 5.(ASU: 0.36-0.46)

3.Conclusion

After revising graphs we can emphasize high indexes in the research facilities such as No 4, and No 5 School area. These items are mostly covered. Slightly lower

indexes are in objects № 1 A Park Near School and № 2 Roadside. In these objects lichens are in depressed state. The atmosphere is moderately polluted.

Indexes of object № 3 Grove threaten more. Branched lichens are not found here. There are some species of leafy and flat lichens. The biggest number of atmospheric polluters are found in this object.

4.References

1. A.A.Pleshakov«From the earth to the sky» - the atlas-determinant on natural study and ecology. Moscow "Education" of 2000

2. T.J.Ashihmina «School ecological monitoring»"Agar" "Rendezvous" of 2000

21 Century - How to Prevent the Youth from Getting Overweight and/or Obese

Damjan Pavlov, Vasilka Aleksova

Elida Angelova

VancoPrke, Vinica/Macedonia, damjanpavlov98@yahoo.com

Content

The 21st century has brought a great amount of inventions which literally changed the course of living for the people. However, it seems to have brought more disadvantages than advantages. I will not look into every single disadvantage but only on one – overweightness and obesity especially among the youth. Overweightness and obesity are defined as abnormal or excessive fat accumulation that may impair health. I put an emphasis on the youth. Why? Childhood obesity leads to adulthood obesity. The beginning, the root is what matters always and everywhere. If we teach our children the principles at an early stage of their lifetime we will make great progress – this will decrease the number of overweight and/or obese children annually. I do not implicate that everyone should have a mind-blowingly looking body but have normal weight and most of all be healthy. So, how do we do that?

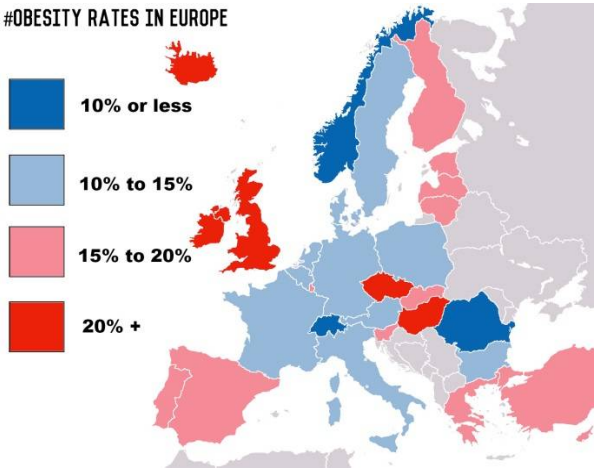

The purpose of the investigation

The statistics on obesity among young people is devastating and frightening. Childhood obesity has more than doubled in children in the past 30 years. The percentage of children aged 6–11 years in the United States who were obese increased from 7% in 1980 to nearly 18% in 2012. Similarly, the percentage of adolescents aged 12–19 years who were obese increased from 5% to nearly 21% over the same period. In 2012, more than one third of children and adolescents were overweight or obese. What's more dreadful are the following facts. One study showed that children who became obese as early as age 2 were more likely to be obese as adults. They are at risk for adult health problems such as heart disease, type 2 diabetes, stroke, several types of cancer, including cancer of the breast, colon, endometrium, esophagus, kidney, pancreas, gall bladder, thyroid, ovary, cervix, and prostate, as well as multiple myeloma and Hodgkin's lymphoma and osteoarthritis. Do you see how alarming and serious this is? But that's not it.

Overweightness and obesity do not only have an effect on your health but on your social life, your noosphere as well. Most of the people suggest that being obese is fine and something that shouldn't be dealt with but just let it be. I am not one of those promotors who get paid to promote some product or sell an idea. I was obese. I know perfectly well what's the feeling to be obese, and believe me it is not at all pleasant. I had been dealing with obesity since I was a child. Daily consumption of uncontrolled and most of all unhealthy food. I am a person known pretty well in the society I live and I have great reputation. I am a great student, I play the piano, I am an actor, I am mad for mathematics, physics and chemistry, I am a film and book addict, I draw.

I still do these things but back in the days when I was obese these skills were overshadowed by my outer appearance. Even though I have a strong character and attitude, I started getting depressed, worried, sad, self-destructive, nihilistic. Despite the negative feelings I started getting ill. Going to doctors, taking pills, my parents started getting worried. The moment when everything exploded was when I had a patellar dislocation. I was bedridden for 2 months and gained weight even more. When I finally looked at myself in the mirror I was so frightened that I wanted to escape from my own body. But no, I said

to myself – “Damjan this is it. It’s time for you to wake up.” The question was how to become “normal”. The answer came right up. One of Balkan’s most famous nutritionists Cveta Dineva. My parents and I went to her office and that’s when I started the battle.

Results of the experiment

After a year and a half I have thoroughly and completely changed my lifestyle. I weighed 116 kg and now I have reduced that weight to 92 kg. Without any artificial supplements, without any powder shakes I have naturally walked a road to being healthy and fit. Daily consumption of fruits, vegetables and a lot of water. I am still walking that road and will never stop. Why? Because this road is the way I live now. I have developed a programme to a lifestyle. That is why this programme is something which guarantees to be a success but not on its own. You have to be dedicated and strong. Not only have I changed the way I look on the outside buy I have encouraged other people who had problems with their weight to fight and face the problem. I was the one to actually break the ice in the area where I live. I achieved to considerably change the prejudice of other people towards people dealing with obesity. I achieved to raise the awareness of this problem on a higher level. Cveta Dineva and I had two appearances on two major TV channels in Macedonia.

They went amazingly well, the hosts were amazed by my experience and my incredible friendship with Mrs. Cveta.

Conclusion

Sadly, overweightness and obesity have become common and usual all over the world. To make matters worse, some mainstream artists use this matter as a promotional material saying that being obese is something that you should be proud of and stay that way. Unfortunately, this does function and people find shelter in these songs or music videos.

But is getting cancer, diabetes, cardiovascular diseases, hypertension, strokes something that you should be proud of? All the people who are dealing with this problem should take action and stand tall. Break free, make the first step and afterwards, things will run smoothly and successfully, of course if you keep to the principles this programme suggests. This programme is something that will make you go through a renaissance and become a new person, a person you truly are.People it’s time to wake up. It’s time to see with our eyes wide open. Overweightness and obesity are not something unstoppable. They are preventable. So, let’s break free.

Mrs. Cveta Dineva and Damjan Pavlov on the morning programme on

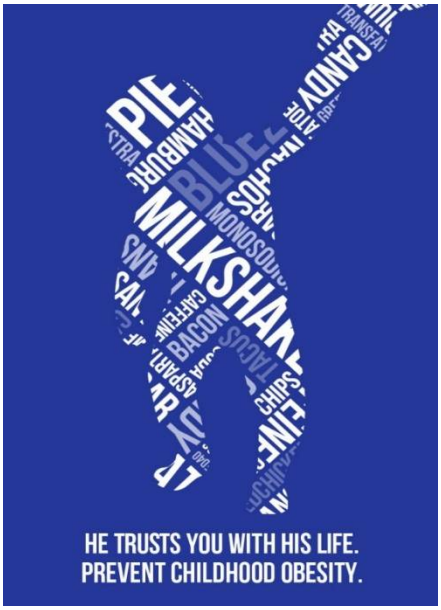

Understanding the human immune system

Jane Peshov,Bojana Vasevska
Elida Angelova
Vanco Prke , Vinica / Macedonia, jpeshov@yahoo.com

- Abstract

  Human immune system is a network of cells, tissues and organs that work together to defend the body from diseases. In order to function properly, the immune system must be able to detect a variety of foreign bodies. The human immune system is amazingly complex and it can't be easily explained. It is classified into many subsystems.

- The purpose of investigation

  The purpose of this study is to learn how our immune system works against pathogens and to learn how to preserve it. Knowing the basics of the immune system is a key factor to a healthy life.

- Method of the investigation

  Obtained information from a specialized personnel, data analysis and research.

- Result

  Eating plenty of fruits, vegetables and whole grains, getting enough sleep, reducing stress, avoiding alcohol and smoking and keeping up with annual vaccinations can help to preserve and maintain a strong immune system.

- Conclusion

  Why is our immune system important? Immune system is a system that keeps us safe from infections and diseases. Our immune system plays a crucial role in maintaining proper health. Every single breath that we inhale, every drop of water we drink or every bite of food we eat, all contains germs. Strong immune system fights against those germs and keeps us protected. People with weak immune system, might catch these diseases more easily.

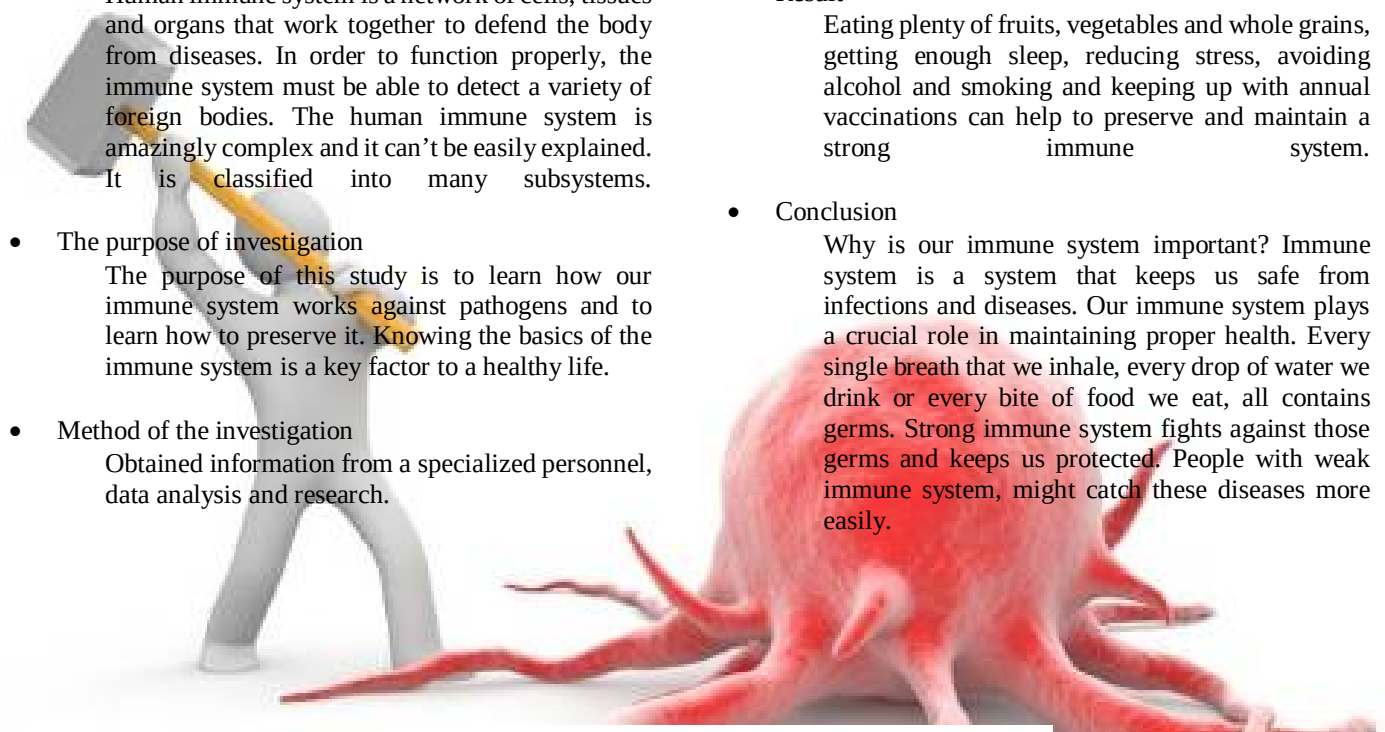

Example of immune system boosters

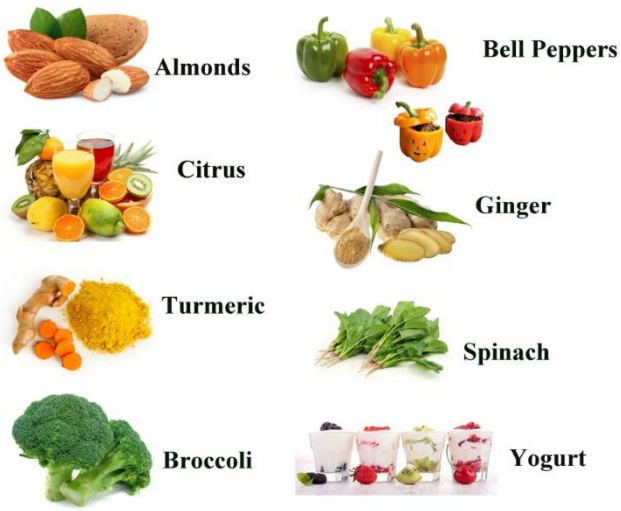

Which is the best killer of bacteria? Garlic, onion or honey?

Sara Trajkova, Kliment Angelov

Suzana Trajkova

Vanco Prke, Vinica/Macedonia, saratrajkova999@gmail.com

16 Introduction

It is widely known that garlic has the ability to fight against bacteria and viruses. The antimicrobial substance in garlic is called allicin. Allicin is contained in garlic from 0.3% to 0.5%. It is also discovered that honey has antibacterial effect. We are all aware that onion absorbs the bacteria but does it kill them? This project is designed to prove that garlic, onion and honey are, indeed effective in killing bacteria.

17 Method of the investigation

We have selected 4 strains of pathogenic bacteria isolated from different sites and Candida, isolated by tongue. They are planted on appropriate bacteriological base. Solution of garlic, onion, honey and antibiotic is added on the planted surface. After a period of incubation, the material is inspected and the zones of inhibition are measured. After analyzing the results, it is concluded that:

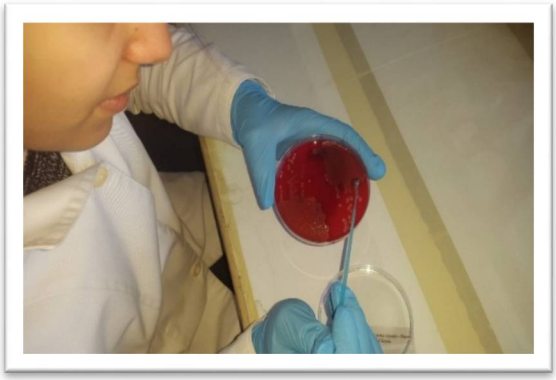

18 Results of the experiment

- Garlic and honey have antibacterial abilities.
- Onion has not antibacterial abilities.
- Garlic and honey act well on gram positive cocci – Streptococcus pyogenis group, on some E. Coli act better than an antibiotic and on Streptococcus aureus garlic is better than honey.
- Garlic and honey have excellent effect on fungus Candida

	Bacteria	Garlic	Honey	Onion	Antibiotic
1.	Streptococcus pyogenes	25mm	26 mm	0mm	25mm
2.	*Staphylococcus aureus*	25 mm	0 mm	0mm	30 mm
3.	*Enterococcus*	0mm	0mm	0mm	0mm
4.	Escherichia coli	10mm	18 mm	0mm	0mm
5.	Candida spp.	30mm	5 mm	0mm	/

4 Conclusion

Candida is often a result of too much taken antibiotics. Eating garlic and honey while taking antibiotics would prevent the development of infections with this fungus, and at the same time would increase the effect of the antibiotic.

ANTIOXIDANT EFFECTS OF STANDARDISED ETHANOLIC PHYLLANTHUS NIRURI EXTRACT AND ITS ACTIVE COMPOUNDS ON HYDROGEN PEROXIDE STIMULATED COLON CELLS

Hamsa Yogini A/P Ganesan1

[1]PERMATApintar[TM] National Gifted Centre, National University of Malaysia, Malaysia

ABSTRACT

Phyllanthus niruri has been used in modern medicine to prevent or treat multiple disorders such as diabetes, kidney stones and HIV. In Malaysia, Phyllanthus niruri is known as 'dukung anak' and is used traditionally for medicinal purposes. This research was conducted to investigate the antioxidant effects of standardised ethanolic Phyllanthus niruri extract and its active compounds on hydrogen peroxide-stimulated colon cells. This research aimed to prove that natural products can be used to mitigate risk of diseases, especially cancers. CCD18Co cells (fibroblast normal colon cells) were stimulated with hydrogen peroxide, H2O2 which decomposes into hydroxyl radicals which are highly reactive free radicals. Excess free radicals causes oxidative stress which can cause cell death, chronic diseases and aging. Besides that, excess free radicals also damage the DNA (deoxyribonucleic acid) which increases the chance of getting cancer. P. niruri extract, along with its constituent active compounds, mainly phyllanthin and hypophyllanthin were tested for their ability to prevent further DNA damage in H2O2-stimulated cells. Among the assays that were done to assess its ability were alkaline comet assay, DPPH assay, FRAP assay and GSH assay. Through alkaline comet assay, Phyllanthus niruri proved to have positive effects on preventing DNA damage in the stimulated colon cells while the DPPH, FRAP and GSH assay results showed that Phyllanthus niruri has antioxidant property.

KEYWORD: Phyllanthus niruri; Phyllanthus; antioxidant; oxidative stress; natural remedy

PREPARATION AND CHARACTERIZATION OF CARBON NANOPARTICLES FROM METROXYLON SAGU

Muhammad Adib Fadhullah Muhammad Lukman1

[1]PERMATApintar™ National Gifted Centre, National University of Malaysia, Malaysia

ABSTRACT

The acid hydrolysis of Native sago (Metroxylon sagu) starch at 40°C was monitored for 7 days. The yield of sago starch was reduced from 15 g (100%) to 2.94 g (19%) when the hydrolysis rates were increased to 80.4% on the seventh day. X-ray diffraction results show a gradual increase in crystallinity of hydrolysed sago starch compared to the native starch and the starch changed from C-type to A-type. FE-SEM micrographs showed that hydrolysis starch owned round shape and rough surface with size diameter of 125-257 nm. In addition, DSC analysis shows the melting enthalpy (J/g) was reduced to 2.49 J/g. Starch nanoparticles were further used to prepare carbon nanoparticles by refluxing with nitric acid for 1 hour. The obtained carbon nanoparticles show round shape with size diameter of 30-35nm. Carbon nanoparticles show a peak at 392 nm under UV-visible spectra which indicates the presence of C=O bond. X-ray diffraction analysis showed that the carbon nanoparticles are in amorphous state. The prepared carbon nanoparticles owned fluorescence properties and it showed wide peak at 320 nm when excited with various energy protons. The fluorescence properties of carbon nanoparticles were confirmed under UV-lamp, where they showed light green ray under 365 nm of blue ray. Finally, this research enables the identification of less toxic property of the prepared carbon nanoparticles from sago starch.

KEYWORDS: metroxylon sagu, acid hydrolysis, fluorescence, carbon nanoparticle

Mycorrhizal associations - support for agriculture

Author: OȘAN CIPRIAN

Coordinating teacher: MÎNICAN LIGIA, GEORGESCU DUMITRU

Scientific Advisors: Univ. Asist. Sc.D. STOIAN VLAD

Univ. Sc.D. ROȘU CRISTINA

National College „Mihai Viteazul" Turda, Romania

1. Introduction

Increasing environmental concern demands that we employ ecological management, such as using organic inputs and managing soil-plant and microorganism relationships in the rhizosphere. In sustainable agriculture, soil and crop management systems are of vital importance for biological soil fertility. The establishment of functional mycorrizal symbioses improves the soil nutrient availability to plants.Symbiotic mycorrhizal fungi influence the terrestrial environment in different ways, either through direct interactions with the mineral or organic substrates that they colonize, or indirectly, via interactions with their host plants or other organisms.

The objective of this study was to examine the development of mycorrhizae associations in 3 types of sterile soil: a former industrial factory, a former garbage dump, extensively excavated area. We wanted to demonstrate the potential of adaptation of soil micro flora to plants.

At each location, three soil samples were collected at 0-20 cm depth during the winter of 2016. We studied the possibility of transferring all the mycorrhizae obtained in the laboratory, in these sterile soils. The physical, chemical and biological properties of a former industrial factory, a former garbage dump and an extensively excavated was studied. Preliminary results are presented in the following table:

Sample	Identified minerals
excavated area	quartz, feldspars, chlorite, muscovite / illite
former garbage dump	quartz, calcite, feldspar, chlorite, muscovite / illite, zeolite
former industrial factory	muscovite / illite, quartz, feldspar, calcite, chlorite, silicate K, Mg and Al

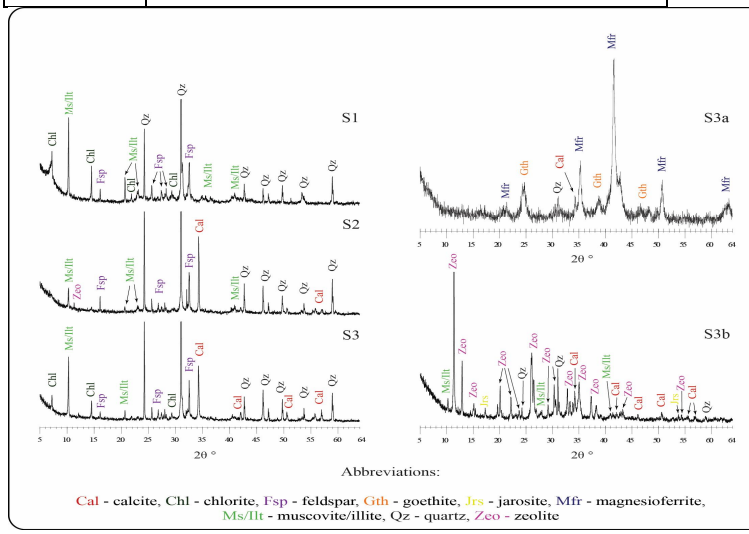

(X-RAY DIFFRACTION SOIL ANALYSIS)

2. Method of the investigation

Five *Triticum aestivum* and *Pisum sativum* seeds were sown into the sterile soil one week after germination to two plants per pot.

The chosen plants in order to be studied in the laboratory were: *Triticum aestivum* because it is a poacea and It has a reduced root system size (strong symbiosis are made) and with *Pisum Sativum* because it has a relatively well-defined root system and has the ability to enter into symbiosis with nitrogen-fixing bacteria.

We made insemination in laboratory of these two species in containers with soil fertilized so: 3 of each plant in soil with guano(N:P:K=10:3:1), 3 in soil with urea(N:P:K=20:0:0), and another 3 in soil with N:P:K=15:15:15. For our experiments, we use fertilizers in different proportions. Plants were maintained in laboratory conditions: 20° C, 60% humidity, natural lighting.

We studied the development of mycorrhizael associations in those 4 types of soil:

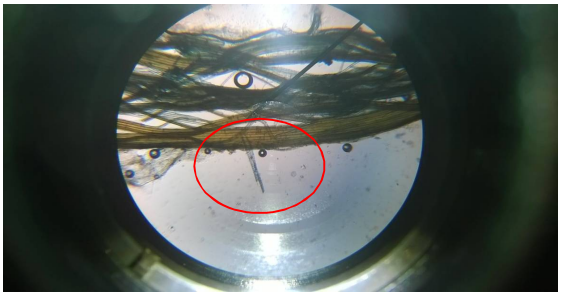

This survey is a comparative indicator of the mycorrhizal status of polluted soil versus that of unpolluted soil late in the growing season of the vegetation. Current studies involve isolation and assessment of potential of the mycorrhizal associations present in these polluted sites to infect plants and produce a positive effect on host plant growth in polluted soil. We also studied the correlation between the development of mycorrhizae and presence of heavy metals.

3. Conclusion

The extent to which interactions between mycorrhizal associations and other microorganisms influence different organic or mineral substrates is still unclear and further experiments are needed to distinguish between the activity of mycorrhizal hyphae themselves and facilitated mycorrhizal uptake of compounds mobilized by activities of other organisms.

The role of symbiotic mycorrhizal fungi in terrestrial ecosystems is fundamental. Many of the characteristic plant communities that dominate the major terrestrial biomes of the world do so today because selection has favored different types of symbiotic associations that are adapted to prevailing suites of soil, vegetation and climatic conditions characterizing these different environments. Comparative analysis of different systems will improve our understanding of responses to environmental and climatic perturbations. This knowledge is an important for future, sustainable management of terrestrial ecosystems.

References

Leigh, J. *et al.* (2008) Arbuscular mycorrhizal fungi can transfer substantial amounts of nitrogen to their host plant from organic material. New Phytol.

Hooker, J.E. *et al.(*2007) Polysaccharidies and monosaccharidies in hyphosphere of the mycorrhizal fungi *Glomus E3* and *Glomus tenue. Soil Biol. Biochem.*

Jackson, L. *et al.* (2008). Roots, nitrogen transformations, and ecosystem services. *Annu. Rev. Plant Biol.*

Ointment for acne treatment

Laura Atyim
Elisabeta Atyim
Kölcsey Ferenc National College
Satu Mare/Romania, lolatyim@yahoo.com

3.3.1 The purpose of the investigation

Provision of a preparation form of antiacne hydrogel based on the active ingredients from summer savory and wild thyme with antiseptic action. The puberty is accompanied by acne and blackhead skin which means not only an aesthetic problem, but you can easily win the war against pimples by using this hydrogel made with extract of summer savory or wild thyme.

3.3.2 Method of the investigation

I found a group of researchers from the Metropolitan University in Leeds, which established that an alcoholic extract with savory was more effective in acne treatment than other creams and lotions based on ordinary benzoyl peroxide. The use of tincture is really uncomfortable: it has short action because of the alcohol's evaporation, you cannot apply in effective amounts on different surfaces, it flows and leaves stain. As result I wanted to find a better preparation form to apply this extract, so I documented myself about opportunities and with the help of my coordinator professors we found out to realize hydrogel based on the savory extract, which is easier to apply on the skin and it has the wanted rheological nature. To expand the range of studied medicinal plants in acne control I can add thyme- as another efficient plant. This is similar to savory but it cannot be found in medical forms in specialty literature.

3.3.3 Results of the experiment

I created a comparative microbiological test of the two plant extract: I prepared a water-based infusion of savory and thyme. The extracts were contaminated for an hour respectively 24 hours with pathogenic bacteria. After an hour-contact with pathogenic bacteria (*Staphylococcus aureus hemolytic)* in the tea, I obtained a rich confluent culture. After the tea's 24 hour-contact with bacteria, the result was a significant decrease of colonies.

Staphylococcus aureus hemolytic

The formulation of the hydrophile ointment*:* The release and absorbtion of active ingredients from the ointments, depends on numerous factors, but the most importants are: the kind of ointment's base;
the ointment's release capacity in active ingredients; the physical-chemical properties of built-in substances.
As a result, to ensure a maximum efficiency at the place of application, an important phase in obtaining a suitable ointment is the choosing phase of the auxiliary substances and technologies.
The spreadability control was determined with the help of an Ojeda – Arbussa extensometer:

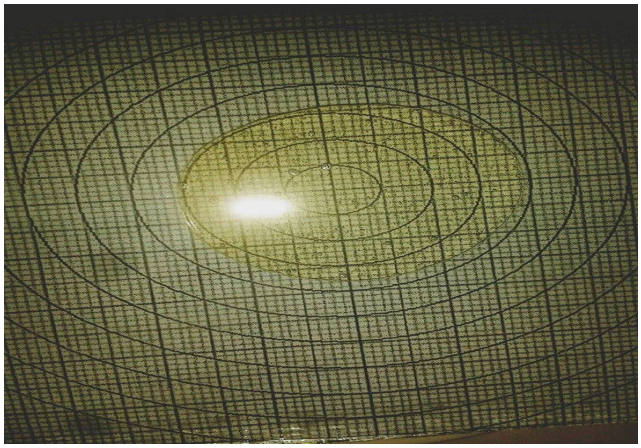

Form with thymus (hydrogel with sodium carboxymethylcellulose 4%)

Components	Concentration (g%)	Role in formulation
Extractum Thymus serpyllum	10,00	Therapeutic agent
sodium carboxymethylcellulose	4,00	Viscosity-increasing agent
Ethyl alcohol	10,00	Dispersant agent
Distilled water	to100,00	Vehicle

Hydrogel's extensiometrical curve with CMC Na 4% and with vegetal extract in comparation with Standard.

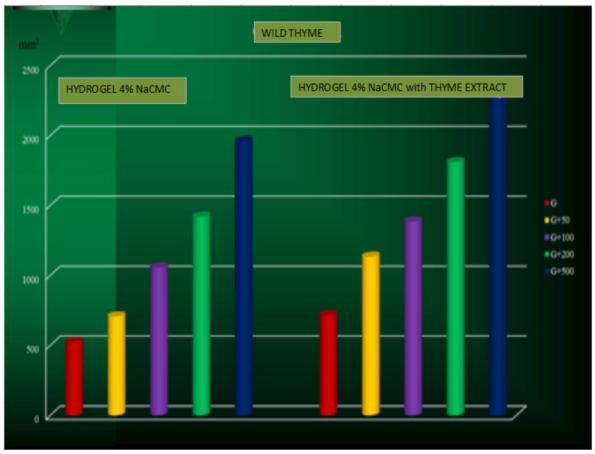

3.3.4 Conclusion

The hydrogels are washable, homogeneous , slightly opalescent. I formulated two antiacne preparations based on vegetal extract using as forming substance the sodium carboxymethylcellulose. After the control of the preparations I found out that the quality provisions match to every form respectively the physico-chemical and pharmocothechnical features.
Hydrogels adhere on the skin's level and allow a good release of active principles.They extand easily in thin layer and can be removed with simple washing.
Hydrogel with sodium carboxymethylcellulose 4% is optimal base to obtain an antiacne ointment.

Colloidal Silver - Rediscovering the Nanotechnology of the Past

Georgeta Pop

Liceul Teoretic "Pavel Dan", Campia Turzii

Coordinating Teacher: Ana Turcu

1. Introduction

Colloidal silver (electro-colloidal silver) is a tasteless, odorless, pure and natural substance. It is a very old antibacterial, anti-fungal, anti-viral, and anti-biotic without harmful side effects. The modern world has given up most of the practices used by our ancestors, being bombarded by the pharmaceutical industry and the chemical industry with various unnatural substances, some even toxic, to treat current problems linked to the health of humans, animals and the environment.

2. Purpose of the Research

The project aims to shed light on the rediscovery of the power of silver.

Used in a newer formula, as a result of many years of study, colloidal silver could be an environmentally-friendly replacement for many synthetic substances that harm our health and the environment.

3. Objectives

a) To inform people that our ancestors weren't polluting the planet with various toxic substances, instead they were using only natural substances.

b) To clarify the question: Why the modern world does not know about this form of silver?

c) To show the beneficial effects of colloidal silver, using our experiments.

d) To bring alternatives regarding the use and consumption of unnatural substances.

4. Methods

Water Experiment: We carried out tests on 4 different types of water, where we have identified through laboratory methods bacteria in water before and after the introduction of Colloidal Silver.

Redcurrant Experiment: Part of my redcurrants had Anthracnose (caused by a fungi) and Aphids (caused by insects). Knowing that silver has antifungal properties, I started a "treatment" which meant to spray them with colloidal silver.

Crops Experiment: I observed the development in the plant growth while using Colloidal Silver on beans, corn and grass.

Roses Experiment: Knowing that silver is responsible for some connections with the ethylene receptors of the plants, I want to see which plant withers quicker.

5. Results

a) The bacteria inside water die in a very short time after introducing a certain amount of colloidal silver in it.

b) Plant diseases such as Aphid Blister (*Eriophyes ribis*), Anthracnose (Ribis pseudopeziza fungus), can be prevented and combated by spraying them with colloidal silver.

Fig 1: a) b)

a) Spots caused by ***Eriophyes ribis.***
b) After 10 days of treatment

c) Increase in plant growth can be accelerated by administration of colloidal silver.

d) The life of flower bouquets in vases can be extended for at least two days with a small amount of colloidal silver.

Fig 2: Differences between test and control samples

6. Applications based on my results

a) During natural disasters, especially in tropical countries, it is an ideal and inexpensive way to sanitize water and put in place a disease prevention regime.

b) In farms, veterinary clinics and fisheries, water can be treated with colloidal silver to prevent infection with pathogens.

c) To disinfect work surfaces.

d) To disinfect water in swimming pools.

e) To clean toothbrushes, dental prostheses.

f) In agriculture, horticulture, colloidal silver can be used to accelerate plant growth or to slow down the process of wilting and also to protect plants from parasites.

g) Using Colloidal silver for food preservation.

References

[1] "Colloidal Silver for Plants and Agriculture." *Colloidal Silver for Plants and Agriculture*. Biophysica Incorporated. Web. May 2015. <http://www.biophysica.com/colloidal_generator/plants_colloidal_silver.html>.

[2] "What Is Colloidal Silver?" *Argint Coloidal Antiseptic Si Antibiotic Natural*. Salutifer. Web. May 2015. <http://salutifer.ro/ce-este-argintul-coloidal/>.

[3] Barwick, Steve. "The Ultimate Colloidal Silver Manual." *The Ultimate Colloidal Silver Manual*. Web. May 2015. <http://www.ultimatecolloidalsilvermanual.com/>.

[4] "Silver Safety Pyramid." *Silversafety.com*. Web. May 2015. <http://silversafety.org/pyramid.html>.

[5] Powell, Jim. "OUR MIGHTIEST GERM FIGHTER." *Science Digest* 1 Mar. 1978. Web. May 2015 <http://www.cs.kestar.com.au/scidi78.pdf>

[6] Maas, George. "Silver Particles: No Threat To The Environment." Web. May 2015. <https://www.purestcolloids.com/SilverNoThreat.pdf>

[7] Stack, Catherine. "Natural Health: The Benefits of Colloidal Silver." *Niagara Gazette*. 8 July 2011. Web. May 2015. <http://www.niagara-gazette.com/news/lifestyles/natural-health-the-benefits-of-colloidal-silver/article_e08c1c84-6967-544d-b349-680f72597eaa.html>.

Epigenetic Study conducted with the view of finding a cure for Allergic Asthma in Children

Radu Adrian Racovita

Supervisor: Daniela Samoilă, Prof. Dr. Ierima Alexandru, Ph D

"Vasile Alecsandri" High School, Galati/Romania, sracovita@yahoo.com

1. Introduction

I have chosen this topic because more and more children are suffering from allergic asthma, and, supposedly, in the next 5-7 years, one in two children will be allergic. Nowadays, children are more exposed to allergens like dust, air pollution and passive smoking. Considering that, at the time being, most of the children are not exposed to enough childhood's diseases in order to strengthen their organism, which, in addition to the fact that more and more mothers decide not to breastfeed their infants, there are a lot of aspects that will eventually result in a weak immune system. My research was carried in 2015 at the Emergency Hospital for Children "Sf. Ioan" Galati, in the Department of Allergology, under the guidance of Prof. Dr. Ierima Alexandru, Ph D. I was also aided by Professor William Cookson and Professor Miriam Moffatt from The National Heart & Lung Institute at Imperial College London.

2. The purpose of the investigation

The main goal of my research was to find out how the only existing medication works and how efficient it really is and, while to stressing the importance of the epigenetic developments. With the help of Prof. Dr. Ierima Alexandru Ph. D., I was able to look into the medicine that is supposed not only to reduce the hazardous effects of the disease but also treat it. This drug, that will be named X in the research, contains an active chemical, Omalizumab, which blocks the Immunoglobulin E (IgE), an antibody responsible with the allergic response.

3. Method of the investigation

First of all, I was granted access to the statistics regarding the number of asthma cases in children in Galati County from 2010 to 2014 (**Table 2**). The data was used to determine the evolution in numbers regarding the disease, as well as different aspects (e.g. gender or age) that influence the frequency of the allergy.

Subsequently, I was allowed to follow the evolution of three subjects, differentiated from one another by specific characters synthesized in the following table (**Table 3**), during the treatment with X.

The research was carried out for 315 days in which each patient received 13-15 doses of medication (after the 13th dose, the first patient's organism started rejecting the medication). The way their bodies reacted was analyzed and the data gathered was included in the following chart (**Figure 2**)

When all the data was gathered, I was able to tell that the drug used was not efficient enough, taking into account the high cost of the medication and the possible complications. Each subject presented a positive evolution throughout the analysis but their level of IgE was only decreased by 28-40 % after 13 to 15 doses. Good as the percentage might seem, the various possible side effects like anaphylaxis, pectoral angina or even cancer make one think that a better solution is to be found.

5. Conclusion

5.1. The existing medication needs improvement regarding its efficiency (considering the fact that to completely treat the disease a number of 40 to 45 doses are needed) as well as its cost (1200 Euros per dose).

5.2. A better solution, and, in my opinion, the most efficient treatment, would be the induced methylation of the 34 genes that code the synthesis of IgE. Although the exact loci of these genes are known, further research is needed in order for the procedure to be successful.

6. References

-Stoenescu M . 1991, *The allergic child*

-Stoenescu M . 1996, *The asthmatic child*

-Dr. Cutler E. W, 2011, *Life without allergies and asthma*

-Dr. Buckman R, 2004 *What you have to know about taking care of an asthmatic child*

-University of Medicine and Pharmacy "Gr. T. Popa" Iasi, 1998, *Pediatry-respiratory diseases, autoimmune diseases, hepatology*

	INTERNAL FACTORS					EXTERNAL FACTORS		OTHER FACTORS
	Age/ Gender	Atopy	IgE		Psychic	Allergens	Others	
			Total	Specific				
Subject 1	8yo/ Female	Both parents	2374(normal value <90)	>100(normal value <0.35)	Psychomotor agitation	Dermatofagoides Pteronissium and Farine	• Cat hair • Dog hair	• Allergic Rhinitis • Bronchitis • Allergic Rhinitis

YEAR	TOTAL	URBAN	RURAL	BOYS	GIRLS	1-14 YEARS	15-18 YEARS	
2010	1214	904	310	758	456	946	268	• Bronchitis • Allergic Rhinitis
2011	1141	848	293	661	480	1048	93	
2012	1171	874	297	707	464	1086	83	
2013								
2014								

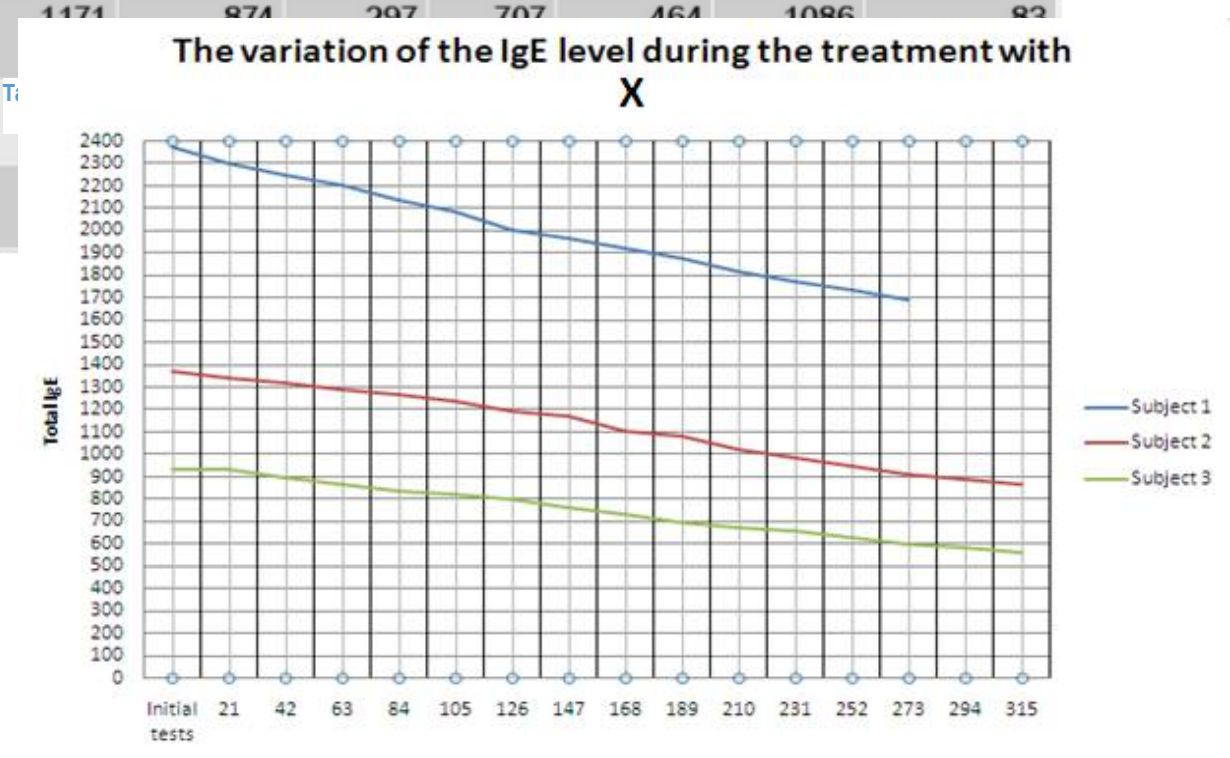

Figure 2-The variation of the IgE level during the treatment with X

Table 2-Number of cases-Galati County

ASTROCYTES INFLUENCE ON DIFFERENTIATION OF STEM CELLS FROM APICAL PAPILLA INTO MATURE NEURONS *IN VITRO*

Jovan Mitić
Supervisor: Andrej Korenić, PhD, Faculty of Biology, University of Belgrade
Regional Centre for Talented Youth Belgrade II, Belgrade, Serbia, Joxy97@yahoo.com

1. Introduction

A significant number of central nervous system (CNS) diseases occur as a consequence of degenerative changes which impact neurons and supportive cells in CNS. Therefore, one of the key objectives of neuromedicine is to find the ways to produce these cells *in vitro*, and subsequently graft them into damaged parts of CNS [1]. It is known that astrocytes, as the most numerous glial cells in CNS, besides the wide range of important functions, which are still to be examined, provide neurons with metabolic support [2]. Stem cells from apical papilla of tooth (SCAP) show a significant potential for osteogenic, chondrogenic, adipogenic and other differentiation pathways. Besides, these cells have an ability of neurogenic differentiation. Considering that they originate from neural crest of gastrula, it is interesting that these cells express some properties of immature neural cells even without neuronal induction [3]. The main hypothesis of this project is that astrocytes play an important role in neurogenesis, so their influence on stem cells could be used in co-culture in laboratory conditions to produce mature neurons [4]. **The aim** of this project is to examine to which extent astrocytes may influence the SCAP differentiation into mature neurons *in vitro*.

2. Material and methodology

For purposes of this research, primary astrocytic cultures isolated from post-natal cortex of *Wistar* rat pups, and SCAP from impacted human third molar tooth were used. Pieces of glass upgraded with paraplast wax balls and coated with poly-*L*-lysine were prepared for SCAP seeding. Astrocytes were seeded in Petri dishes. Cells were separately incubated in DMEM medium with 25mM glucose and 10% fetal bovine serum until they reached 60-80% of confluence after which they were placed into the same medium. The cultures were cultivated without direct mutual contact. After 24h, DMEM was replaced with Neurobasal serum-free medium in order to provide an adequate environment for neurons' development [5]. Cells were observed daily in order to visually determine morphological changes, after which they were subjected to immunocytochemical analysis. GFAP was used as an astrocytic marker, whereas β-III Tubulin was used as neuronal marker. Observations were conducted on confocal microscope with corresponding software package.

3. Results and discussion

Cell cultures have reached their confluence quickly which proves DMEM medium to be suitable for their proliferation. Astrocytes grew in monolayer until they fully covered Petri dish, after which they, expectedly, stopped with further divisions. SCAP were morphologically elongated and grew in monolayer too in all directions. First four days cells maintained their confluence, while only the fifth day differentiation beginnings could be observed in form of cellular extensions, when, based on current literature, it was expected that SCAP acquire morphology and interconnectivity of neuron-like cells [5]. It was determined that after chemically induced neuronal differentiation, SCAP expressed βIII-tubulin (unpublished data) which is considered to be the one of

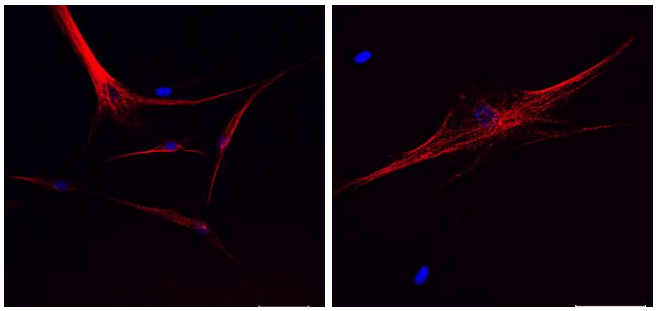

Figure 1. – Representative micrograph of βIII-tubulin immunocytochemistry staining of neuron-like cells

the basic neuronal markers, which was also expressed by cells differentiated in co-culture.

4. Conclusion

This project confirms stimulatory function of astrocytes in neurogenesis, which represents a significant contribution to the overall research of their numerous functions. Contribution is achieved in the field of SCAP research as well since they have been used in co-cultures with astrocytes for the first time. After only a week, SCAP developed into neuron-like cells which express neuronal markers. It was also observed that cells tend to establish connections, which points to the successful cultivation of neurons in laboratory conditions. Still, electrophysiological measurements are yet to be conducted in order to confirm that these neuron-like cells are actually functional, mature neurons, which could be used in

further research for finding therapy for neurodegenerative diseases.

5. References

[1] Tatullo, Marco, *et al.* "Dental pulp stem cells: function, isolation and applications in regenerative medicine." *Journal of tissue engineering and regenerative medicine* 9.11 (2015): 1205-1216.

[2] Korenić, Andrej. "The mechanisms of rat astrocytes survival in the medium without glucose and in hypoxic conditions *in vitro*." *PhD Thesis* (2015).

[3] Shakhova, Olga, and Lukas Sommer. "Neural crest-derived stem cells." (2010).

[4] Song, Hong-jun, Charles F. Stevens, and Fred H. Gage. "Neural stem cells from adult hippocampus develop essential properties of functional CNS neurons." *Nature neuroscience 5.5* (2002): 438-445.

[5] Zainal Ariffin, Shahrul Hisham, *et al.* "Differentiation of dental pulp stem cells into neuron-like cells in serum-free medium." *Stem cells international 2013* (2013).

IN VITRO BIOACTIVITY SCREENING OF LOWER ORGANISM EXTRACTS AGAINST BREAST ADENOCARCINOMA MCF-7 CELLS

Tamara Janković
Supervisors: Boris Pejin, PhD and Vesna Kojić, PhD
Regional Centre for Talented Youth Belgrade II, Belgrade, Serbia, tamara.jankovic.97@gmail.com

1. Introduction

Bioprospection has become dynamic scientific field that explores novel possibilities for the implementation of natural products [1]. The aim of this study was to screen *in vitro* antitumor activity of methanol extracts of selected lower level organisms against the breast adenocarcinoma MCF-7 cell line and to identify potential bioactive principle(s) of the most effective species.

2. Materials and Methods

The sponge *Ochridaspongia rotunda* (Arndt, 1937), the bryozoan *Pectinatella magnifica* (Leidy, 1851), the lichen *Usnea barbata* (L.) Mott. and the moss *Rhodobryum ontariense* (Kindb.) Kindb. were screened for the first time (Figure 1). Antitumor activity and antimutagenicity were determined by MTT and comet assays, respectively. Chemical composition of the most promising organism was estimated using Fourier Transform InfraRed spectroscopy (FTIR), UltraViolet-VISible spectroscopy (UV-VIS), Ion Exchange Chromatography (IEC) and Atomic Absorption Spectroscopy (AAS).

3. Results and Discussion

O. rotunda methanol extract was found to be almost 55-fold more selective against MCF-7 vs. MRC-5 (normal) cells, compared to doxorubicin (positive control) that highly affected both normal and tumor cells (Table 1).

Table 1. Antitumor activity of tested methanol extracts and doxorubicin (Dox)

IC_{50} (μg/mL)	*O. rotunda*	*P. magnifica*	*U. barbata*	*R. ontariense*	Dox
MCF-7	5.03	25.62	7.25	24.62	0.05
MRC-5	296.65	491.01	100.98	501.42	0.21

A 3.5-fold lower fragmentation of DNA molecule in the presence of the sponge extract (vs. doxorubicin) pointed out its good antimutagenic potential.
While both FTIR spectrum and meager content of simple phenolics (< 3.0 mg/kg, in a dried sponge material) practically excluded these compounds among the antitumor leads, the spectrum imposed the idea of sterol(s) (hydroxyl and methylene groups 3350.5 and 2927.6 & 2854.2 cm^{-1}, respectively) as possible key bioactive(s) (Figure 2) [2]. Furthermore, negligible contents of nitrites (< 0.1 mg/kg) and heavy metals (including one metalloid species) (< 2.3 mg/kg) are not likely to be responsible for the observed bioactivity.

A **B** **C** **D**

Figure 1. – **A.** *Ochridaspongia rotunda,* **B.** *Pectinatella magnifica,* **C.** *Usnea barbata,* **D.** *Rhodobryum ontariense*

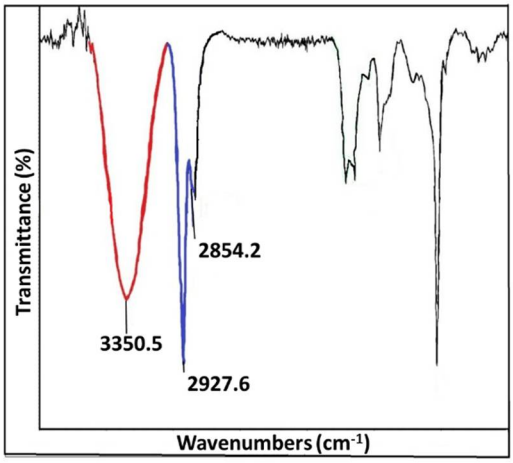

Figure 2. - FTIR spectrum of the sponge O. rotunda methanol extract

4. Conclusion

O. rotunda methanol extract may afford novel drug for breast tumor and/or inspire its design. Further research should include *in vitro* antitumor screens of the sponge extracts (using solvents of different polarity) on a vast number of cell lines, coupled with the relevant screens at *ex vivo* and *in vivo* conditions. *O. rotunda* aquaculture (*in situ* and *ex situ*) should also be formed, aiming to provide an optimal amount of biomaterial for the isolation and identification of the leading antitumor agents. Finally, the origin of these organic compounds should also be carefully addressed. Indeed, there is a chance that real producer(s) may be the sponge symbiotic microorganism(s), primarily some of its bacterial strain(s) [3].

5. References

[1] D.J. Newman and G.M. Cragg. 2012. Journal of Natural Products 75, 311-335.

[2] I.B. de Barros et al. 2013. Biochemical Systematics and Ecology 49, 167-171.

[3] T. Keller-Costa et al. 2014. PLoS ONE 9:e88429/ 1-e88429/15.

Mathematical Modelling of Sprouting Angiogenesis and its Implication on Tumour Growth and Treatment

Saw Khai Khai[1]
Koon Yen Ling[2], Chiam Keng-Hwee[2]
[1]Raffles Institution, [2]Bioinformatics Institute, A*STAR, Singapore

Introduction

Angiogenesis is the process by which new blood vessels develop from an existing vasculature. It plays a critical part in the onset of more than 50 diseases and is closely associated with the transition of benign tumours to a malignant one, making it a popular target in cancer treatment.

In angiogenesis, the cell at the front of the sprout becomes the tip cell, which leads the growth of a new vessel while the cells that follow become stalk cells, which build the body of the sprout. Endothelial cells release Vascular Endothelial Growth Factor-A (VEGF-A) in response to a hypoxic environment. The binding of VEGF-A to VEGF receptor 2 (VEGFR2) on the cell surface up-regulates Delta-like ligand 4 (Dll4) expression of the cell. Dll4 binds to Notch1 receptor on the neighbouring cell, inhibiting VEGFR2 and Dll4 but activating Jagged1 (Jag1).

In other words, Notch-Delta signaling forms a negative feedback loop, which causes the two cells to adopt different fates: the sender (high Delta, low Notch) becomes the tip cell while the receiver (low Delta, high Notch) becomes the stalk cell. Conversely, Notch-Jagged signaling forms a positive feedback loop which enables the two cells (both high Jagged, high Notch) to adopt a similar stalk cell fate. These maintain the required ratio between tip and stalk cells for the development of a functional blood vessel.

At the same time, Notch-Delta and Notch-Jagged signaling is also differentially regulated by glycosyltransferase Fringe, which glycosylates Notch such that it binds to Dll4 more favorably than to Jag1. It has been suggested that Fringe plays a stabilizing role and opens up another possible signaling pathway to be targeted in future cancer therapy.

In this paper, we develop a simple mathematical model to investigate the pattern-forming potential of a system in which lateral inhibition and lateral induction with feedback is mediated by Notch-Delta and Notch-Jagged signaling respectively between adjacent cells. We then review currently available drugs as possible angiogenic inhibitors in the treatment of cancer.

The Model

We model Delta-Notch and Jagged-Notch signaling as being characterized by just three parameters: the level of Notch activation, Delta inhibition and Jagged activation. The VEGF-A signal activates Delta, which interacts with its neighbors' Notch to suppress the neighbor's Delta, i.e., each cell is laterally inhibited via Delta/Notch signal. At the same time, the VEGF-A signal also activates Jagged, which interacts with its neighbor's Notch to induce the neighbor's Jagged, i.e., each cell is laterally activated via Jagged/Notch signal. We then run simulations and perform computational analysis of different Notch, Delta and Jagged regulations using Python.

Denoting the levels of Notch, Delta and Jagged activity in cell i by N_i, D_i and J_i respectively, we write:

$$\frac{dN_i}{dt} = L \times (pF\{D_i\} + qG\{J_i\}) - N_i + nN_i$$

$$\frac{dD_i}{dt} = v(H\{N_i\} - D_i) + dD_i$$

$$\frac{dJ_i}{dt} = v(I\{N_i\} - J_i) + jJ_i$$

where t = time. D_i/J_i denotes the mean of the levels of Delta/Jagged activity in the cells adjacent to cell i. F:$[0,\infty)\rightarrow[0,\infty)$, G:$[0,\infty)\rightarrow[0,\infty)$ and I:$[0,\infty)\rightarrow([0,\infty)$ are continuously increasing functions whereas H:$[0,\infty)\rightarrow[0,\infty)$ is a continuously decreasing function. L is the level of VEGF-A signal received by cell i. v is the ratio of the decay rates of Delta/Jagged and Notch activities. p and q are the ratio of Delta/Notch and Jagged/Notch activities respectively. n, d and j represent the regulation of Notch, Delta and Jagged respectively.

Results

Our computational analysis yielded 6 main findings:

i. Downregulation of Notch decreases tip cell formation, resulting in a more controlled angiogenesis and thus reduced tumour growth.
ii. Upregulation of Notch increases tip cell formation, resulting in a more extensive functional vasculature, contributing to a robust tumour angiogenesis.
iii. Downregulation of Dll4 increases tip cell formation. However, the cells exhibit a hybrid tip/stalk fate, forming a dense network of nonfunctional blood vessels, a hallmark of chaotic angiogenesis.
iv. Excessive upregulation of Dll4 decreases tip cell formation, leading to a more stable development of blood vessels.
v. Upregulation of Jagged leads to less distinct cell differentiation, but is not significant enough to destabilise the cell fate established through Delta-Notch interactions.
vi. Downregulation of Fringe destabilises the tip/stalk cell fate specification, but its significance in angiogenesis remains unclear.

Conclusion

The general reasons for tumour angiogenesis are over-activated Notch, which increases the formation of functional blood vessels; downregulated Dll4 and upregulated Jagged, which leads to chaotic angiogenesis; and downregulated Fringe, which results in indistinct phenotypes between tip and stalk cells.

From this, we isolated two possible strategies to inhibit tumour angiogenesis. First, we can inhibit the formation of tip cells to reduce the formation of functional blood vessels by repressing the Notch-Jagged pathway or over-activating the Notch-Delta pathway. Currently strategies to inhibit Notch activity include the use of γ-secretase inhibitors, anti-Notch1 monoclonal antibody, garcinol, as well as therapeutic delivery of miR-200c. Second, we can increase the formation of tip cells excessively to form a dense network of non-functional blood vessels by downregulating Delta while upregulating Notch. This can be achieved through anti-Dll4 monoclonal antibodies and Dll4-Fc.

While targeting Notch pathways to inhibit tumour growth appears promising, it is important to realise that Notch is involved in many development processes. Hence, aberrant Notch signaling might result in many unpredictable pathological consequences. However, as cancer diagnostics become more precise, there is a huge potential and possibility that future therapies will become more personalised in applying drugs to damaged signaling components on a case-by-case basis.

Finally, our findings highlight the significance of using computer-aided strategies to effectively elucidate complicated biological pathways for future drug design in our attempts to inhibit tumour angiogenesis.

References

1. Risau, W. 1997. Mechanisms of angiogenesis. *Nature, 386*(6626), 671-674. doi:10.1038/386671a0.

2. Carmeliet, P. & Jain, R.K. 2000. Angiogenesis in cancer and other diseases. *Nature, 407*: 249–257. doi: 10.1038/35025220.

3. Bray, S.J. 2006. Notch signaling: A simple pathway becomes complex. *Nat Rev 7*: 678-689.

4. Kopan R. & Ilagan, M.X.G. 2009. The canonical Notch signaling pathway: Unfolding the activation mechanism. *Cell, 137*(2):216–233.

5. Mukherjee, S. et al. 2014. STAT5-induced lunatic fringe during Th2 development alters delta-like 4-mediated Th2 cytokine production in respiratory syncytial virus-exacerbated airway allergic disease. *J Immunol, 192*(3):996-1003. doi: 10.4049/jimmunol.1301991.

6. Boareto, M. et al. 2015. Jagged–Delta asymmetry in Notch signaling can give rise to a Sender/Receiver hybrid phenotype. *Proc Natl Acad Sci, 112*: E402–E409.

FUNCTIONAL CHARACTERIZATION OF ICP35 IN WSSV (WHITE SPOT SYNDROME VIRUS)

Jamin Laoprasert
Dr. Pongsak Khunrae, and Ms.Nion Vinarukwong
Engineering - Science Classroom (KMUTT), Bangkok Thailand, min_21035@hotmail.com

1. Introduction

Shrimp farming is an important industry in Thailand. However, it has been greatly suffering from White Spot Syndrome Virus (WSSV) which causes 90 – 100% mortality in 7-10 days. ICP35 is WSSV's protein which has a crucial role for viral survival. In addition, the localization study of ICP35 revealed that ICP35 was resided in the nucleus of host cell [1]. Thus, we hypothesized that ICP35 may have the interaction with the DNA of host cell. However, the evidence showing the direct interaction between ICP35 and DNA has not been shown yet.

2. Materials and Methods

2.1 The purpose of the investigation

To investigate the function of ICP35

2.2 Method of the investigation

The ICP35 encoding gene was cloned into the E.coli expression vector (pET15b) and the recombinant ICP35 was purified by using Ni-NTA Gel Affinity Chromatography, then analyzed protein expression by using SDS-PAGE and investigated the interaction between ICP35 and DNA by using Electrophoretic Mobility Shift Assay (EMSA) and lastly modeled the structure of ICP35 by using Homology Modeling

2.3 Results of the experiment

The ICP35 was successfully expressed in high purity and also form itself into a dimer as shown in Fig1. The purified ICP35 was brought to incubate with DNA for an hour. Then the ICP35 was analyzed by EMSA. The result revealed that ICP35 could digest the DNA and was inhibited its function by EDTA which is a nuclease inhibitor as shown in Fig2.

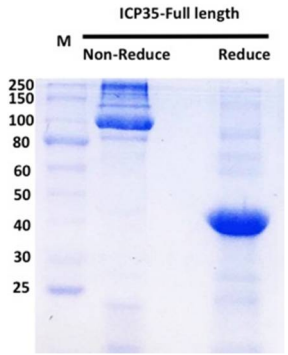

Figure 1. SDS-PAGE analys

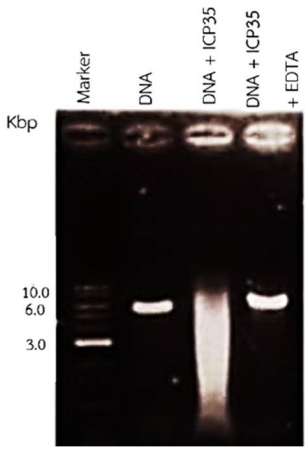

Figure 2. EMSA analysis

In addition, homology modeling suggested that ICP35 may adopt the structure from TREX and could form a dimer through the same mechanism as seen in TREX. Because several conserved residues playing an important role in dimerization in TREX are also found to reside at the interface of the ICP35 dimer as shown in Fig3.

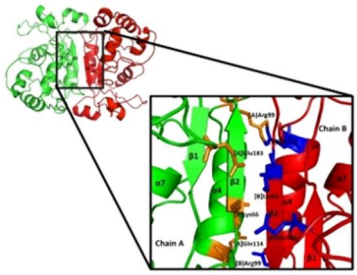

Figure 3. Homology Modeling

2.4 Conclusions

ICP35 is a DNA-binding protein having DNA digestion activity. In addition, we predicted that ICP35 may adopt structure from TREX and share similar DNA digestion mechanism as seen in TREX.

2.5 References

[1] Chen LL., and et al. (2002). Identification of a Nucleocapsid Protein (VP35) Gene of Shrimp White Spot Syndrome Virus and Characterization of the Motif Important for Targeting VP35 to the Nuclei of Transfected Insect Cells. Journal of Virology.

THE BYSTANDER EFFECT IN HUMAN LUNG CELLS AFTER SINGLE AND FRACTIONATED IRRADIATION WITH HELICAL TOMOTHERAPY SYSTEM

Nuttakrit Onuthai
Narongchai Autsavapromporn Ph.D., Tewin Moonwan
Yupparaj Wittayalai School, Chiang Mai, Thailand. nuttakrit_on@outlook.co

Introduction

Irradiation is the one of cancer treatments, by irradiating carcinoma cells. These cells must be damaged and become mitotic catastrophe. But since 1992 it was discovered that unirradiated cells which nearby the irradiated cells could exhibit irradiated effect and be damage like irradiated cells. This phenomenal is call **Bystander effect**. This project is contrasting on effect of techniques of irradiation and type of irradiated cell to survival of bystander cell. This studies will be helpful for selecting an irradiation technique for treatment and extrapolating damaged and effect due to radiation-induced bystander effect in the future.

Purpose of the investigation

Study and compare effect of irradiation techniques and types of irradiated cell to the growth and survival of bystander cells due to bystander effect

Methods

All cell culture was performed in a laminar flow cabinet for preventing bacterial contamination. MRC-5 and A-549 were grown in DMEM with FCS and incubated in a humidified 37°C incubator. The cells were put in full-filled water phantom. Irradiated using helical tomotherapy unit. Irradiated 2 Gy for 3 times separated with 24 hours for fractionation dose and 6 Gy continuously for single dose. After irradiation method, transfer irradiated medium to MRC-5 bystander cells culture flask, using medium exchange methods of Mothersill and Seymour (1997). All experiments were repeated four times.

Results

Irradiated medium	%PE Control	%PE 2 Gy	%PE 6 Gy
MRC-5	38.8±3.3	52.8±6.7	34.0±2.4
A-549	33.5±3.6	46.4±4.7	28.7±4.0

Table 1 showing PE for MRC-5 received medium from irradiated MRC-5 and A-549 cell lines

Irradiated med.	%SF 2 Gy	%SF 6 Gy
MRC-5	134.9±18.7	93.8±8.3
A-549	131.6±18.4	93.5±12.4

Table 2 showing SF for MRC-5 received medium from irradiated MRC-5 and A-549 cell lines

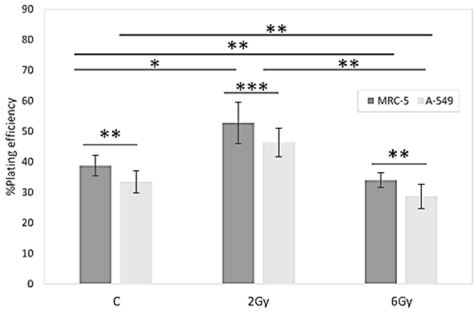

Figure 1 showing PF for MRC-5 received medium from irradiated MRC-5 and A-549 cell lines

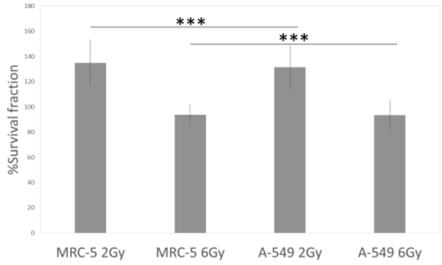

Figure 2 showing SF for MRC-5 received medium from irradiated MRC-5 and A-549 cell lines

Conclusion

Bystander cells received fractionated dose was significantly increasing growth rate but opposite result in cells received single dose (p-value < 0.15). And cells received medium from MRC-5 have exceeding growth related with cells received medium from A-549.

References

C. Mothersill and C. Seymore. 1997. Medium from irradiated human epithelial cells but not human fibroblasts reduces to clonogenic

survival of unirradiated cells. Int J. Radiat. Biol. 1997:421-427

R. K. K. Lam, Y. K. Fung, W. Han and K. N. Yu. 2015. Rescue Effects: Irradiated Cells Helped by Unirradiated Bystander Cells. Int. J. Mol. Sci. 2015, 16, 2591- 2609.

DEVELOPMENT OF A BIOCONJUGATE FOR REDUCING SERUM URIC ACID IN GOUT DISEASE

Ezgi BALKIR & Seray UĞUR

Ümit KARADEMİR

İzmir Private Fatih College /Izmir/Turkey / ukaraca2006@gmail.com

1. INTRODUCTION

Gout is a purine metabolism disorder caused by the level of serum uric acid in the blood exceeding the normal level that results in accumulated urate crystals in joints and their surroundings. Extremely severe pain is felt since such crystals affect joints, and life quality of patients deteriorates seriously. It is reported that gout cases have been doubled in the last two decades. Medication and apparatus used in its treatment do not provide definite treatment. They can be applied just after the first gout attack and help relieve instant effects only. Medical Technical Textiles is one of the most rapidly growing areas worldwide and intensively used areas in the treatment of different diseases. In our literature review, we found out that the uricase enzyme can break down uric acid crystals that cause the disease into allantoin, which is less harmful substances to the body. Based on this knowledge, we hypothesize that if uricase enzyme immobilized medical technical textile is developed, this textile can reduce the amount of serum uric acid in gouties.

2. PURPOSE

In our project, we aimed to develop a medical technical textile to remove uric acid crystals that are produced during the disease, through the wound area and blood; by means of enzymatic modification of PAN (Polyacrylonitrile) fabric with nitrilase enzyme, covalently immobilizing the uricase enzyme that breaks down uric acid to the modified fabric.

3. METHOD

We started the project by designing a medical technical textile product for removing of uric acids from blood and wound. For this purpose, Polyacrylonitrile (PAN) fabric was enzymatically modified with nitrilase enzyme, and the fabric prepared for reaction for uricase enzyme (EC 1.7.3.3.) immobilization. The project was carried out after forming various control groups and experiment groups.

Within the scope of the project, in order to produce a textile product including immobilized uricase enzyme. First we followed the given steps below;

- Enzymatic modification of PAN fabric with nitrilase enzyme,
- Activation of enzymatic modified PAN fabric and optimization of activation conditions,
- Immobilization of uricase enzyme to modified PAN fabric by covalent bonding and optimization of immobilization conditions,
- Characterization process of enzymatic modified PAN and uricase immobilized PAN by SEM (Scanning Electron Microscope) and ATR-FTIR (Attenuated Total Reflectance-Fourier Transform Spectroscopy),
- **Implementation of uricase immobilized enzymatic modified PAN fabric that we developed to horse blood and determination of its effectiveness in uric acid removal.**

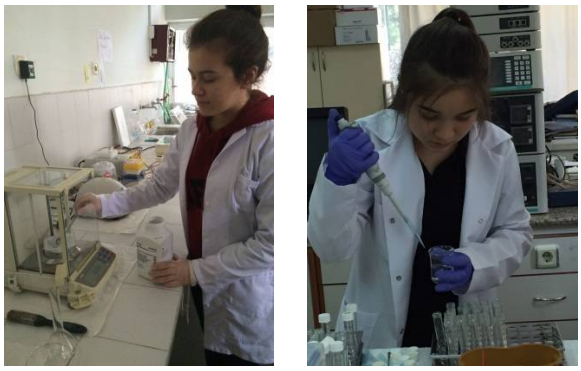

Figure: Enzymatic modification of PAN fabric and Uricase enzyme immobilization

4. RESULTS AND CONCLUSION

In our project, modification of PAN fabric was done enzymatically. In modification, nitrilase enzyme was used. After the modification, carboxylic acid groups were formed in the structure of the PAN fabric. Modification was examined by ATR-FTIR spectroscopy

and SEM devices. Uricase was covalently immobilized to the carboxylic acid groups obtained from the modification on EDC activated PAN fabric. Activities of the uricase immobilized PAN fabrics were given in results. Activity values of washing waters were recorded to be compatible with activity values of uricase immobilized PAN fabric. The immobilization process was proven by ATR-FTIR spectroscopy and SEM devices. Finally, the uricase immobilized fabric and uric acid removing in blood was examined, and it was seen that the fabric significantly affected the blood uric acid.

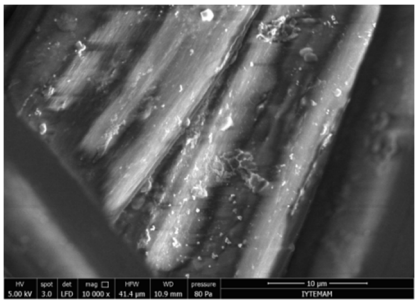

Figure: SEM images of uricase immobilized enzymatic modified PAN fabric

- ✓ As a result of enzymatic modification; free carboxylic acid groups were activated with the activating agent, EDC.
- ✓ Optimization of the activation with EDC was performed. During optimization;

1. Optimum amount of EDC was determined as 10mg.
2. Optimum buffer pH was determined as pH 4.
3. Optimum buffer concentration was determined as 100 mM.

- ✓ Optimization of the uricase immobilization was performed. During optimization;

1. Optimum buffer pH was determined as pH 5.
2. Optimum buffer concentration was determined as 10 mM.
3. Optimum amount of enzyme was determined as 0,3 U.
4. Optimum temperature was determined as 4°C.
5. Optimum stirring speed was determined as 250 rpm.
6. Optimum time was determined as 6 hours.

While activity of uricase immobilized fabric was 0,00173 U prior to optimization studies, the value rose up to 0,0165 U approximately increasing ten times as a result of the studies.

The product in the scope of this project was designed for gout. Therefore, uricase immobilized fabric was used on blood experiments at optimum conditions. As a result of blood experiment, 87,75% of uric acid was removed with uricase immobilized PAN fabric in 30 minutes. Thus, the uric acid level was reduced to reference values.

Our bioconjugate can be designed in a way to reduce uric acid concentration that causes gout. It can also be used for other diseases increasing uric acid concentration in blood. **Furthermore, this study reveals that several textile materials can gain different characteristics by using enzymes and microorganisms.**

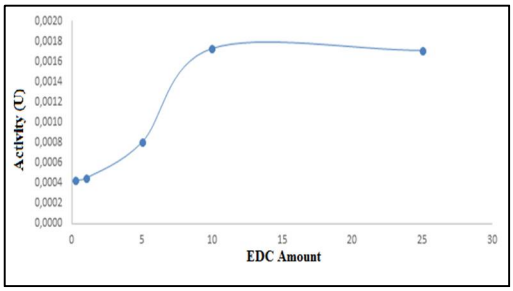

Figure: The effect of the EDC amount on activation of PAN fabric (Working conditions: activation buffer: pH 5 50 mM phosphate buffer)

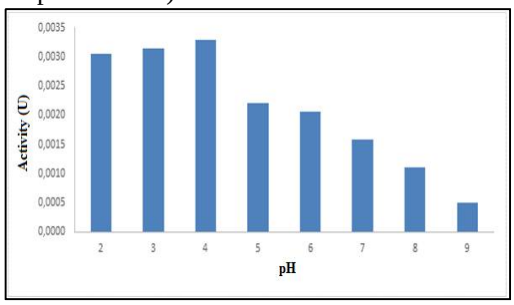

Figure: The effect of pH on activation of PAN fabric (working conditions: 10 mg EDC, buffer concentration 50 mM)

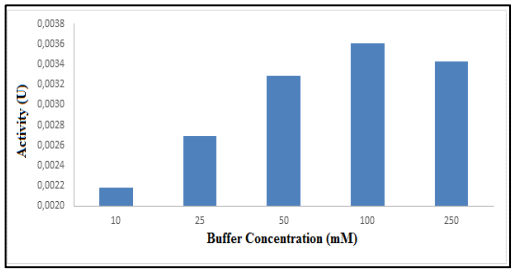

Figure: The effect of buffer concentration on activation of PAN fabric (working conditions: 10 mg EDC, activation pH 5)

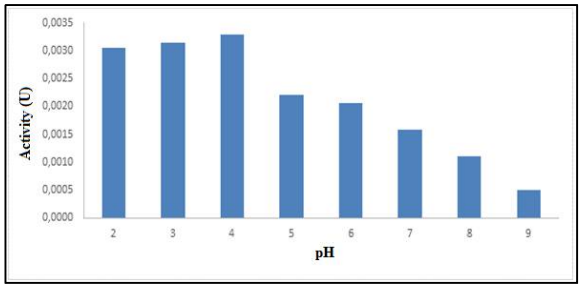

Figure: The effect of pH on activation of PAN fabric (working conditions: 10 mg EDC, buffer concentration 50 mM)

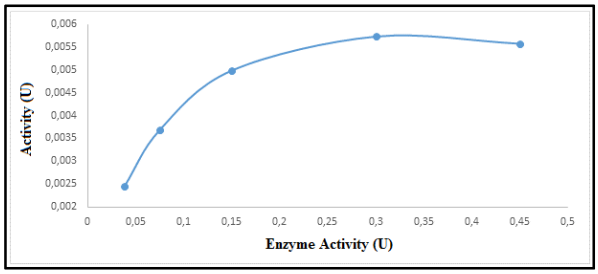

Figure: The effect of enzyme activity on uricase immobilization (working conditions: buffer pH 5, buffer concentration 10 mM, incubation temperature 25°C, stirring speed 150 rpm, incubation time 2 hours)

REFERENCES

1. Fischer-Colbrie, G., Herrmann, M., Heumann, S., Puolakka, A., Wirth, A., Cavaco-Paulo, A.; Guebitz, G. M. (2006). Surface Modification of Polyacrylonitrile with Nitrile Hydratase and Amidase from *Agrobacterium Tumefaciens*. *Biocatalysis and Biotransformation*, 24(6), 419-425.
2. Brook, R. A., Forsythe, A., Smeeding, J. E.; Edwards N. L. (2010). Chronic Gout: Epidemiology, Disease Progression, Tratment and Disease Burden, Current Medical Research & Opinion vol. 26 no. 12, 2813-2821.
3. Nuki, G.; Simkin, P. A. (2006). a Concise History of Gout and Hyperuricemia and Their Treatment. Arthritis Research and Therapy, 8(1),1.
4. Kumar, V., Misra, N., Paul, J., Dhanawade, B. R., & Varshney, L. (2014). Uricase-immobilization on radiation grafted polymer support for detection of uric acid using Ag-nanoparticle based optical biosensor. Polymer, 55(11), 2652-2660.

The study of antimicrobial properties of different sorts of Ukrainian beer

Kharkiv Academical Gymnasium № 45

Daria Cherednychenko

Supervisors: Dr Strilets Oksana, Gorbatko Galina

Introduction:

Beer is the third of the most popular drinks in world. Beer is one of available drinks, so that a great percent of beer consumers are teenagers, who can not afford other drinks. Despite of contain of alcohol, it is believed that beer has medical properties. Robert Koch, who found the causative agent of cholera, established, that beer has a positive influence into human health. So I was interested in studying the antimicrobial properties and influence of different sorts of beer on human normal microflora

The purpose of investigation:

The main goal of investigation is studying of the microbiological properties of the following sorts of Ukrainian beer such as infiltrated Chernihivske "Bila Nich", Chernihivske non-aclohol eco-beer, Rohan "Veseliy Monah" and Rohan traditional light beer;

The tasks of investigation are: to study and make analysis of literature about the topic of research; to study out antimicrobial properties of different sorts of beer;

Methods of investigation:

To accomplish the tasks of our research the following methods has been used:

Theoretical analysis of literature, making comparison of sorts of beer and generalization of literature sources;

Empirical methods: differential diagnosis method of coloring by Gram; sowing microorganisms on solid and liquid nutrient media; method of diffusion into agar; method of Koch;

Results of investigation:

Due to the tasks of investigation, the first experiment was the studying beer's antimicrobial functions, it was determined, that investigated sorts of beer has no antimicrobial properties. It is shown in table 1 below.

Antimicrobial properties of beer *(Table 1)*

Sort of beer	Microorganism culture			
	S.aureus	B.subtilis	E.coli	C.albicans
	Diapason of antimicrobial property, mm			
№1 – infiltrated Chernihivske "Bila Nich"	–	–	–	–
№2 – Chernihivske eco-beer without alcohol	–	–	–	–
№3 – Rohan "Veseliy monah"	–	–	–	–
№4 –Rohan traditional light beer	–	–	–	–

It is considered that the reason is preservatives, which can make the shelf life of beer longer than 3 days.

Quantity of lactobacillus colonies in nutrient media with beer

Due to result of second experiment, it was realised, that in all of the petri dishes the quantity of lactobacillus colonies in nutrient media with beer is higher than in control pattern without beer. The highest result was in example with infiltrated beer «Bila Nich» by Chernihivske. The smallest result was in petri dish with non-alcohol beer, but the quantity of lactobacillus colonies is higher than in control dish. It can be seen at table 2.

(Table 2)

Sort	Cultivation	Quality of calonies	Quality of lactic bacteries
Control	1:10	12	120
Infiltrated Chernihivske "Bila Nich" (№1)	1:10	36	360
Chernihivske non-aclohol eco-beer (№2)	1:10	17	170
Rohan traditional light beer (№4)	1:10	22	220

Conclusion

During the research it was studied microbiological properties of different sorts of beer such: Chernihivske "Bila Nich", Chernihivske non-alcohol eco-beer, Rohan "Veseliy Monah" and Rohan tradition light beer. Studying the antimicrobial properties, it was determined, that following sorts of beer has no influence on microorganism cultures. In next part of research that was studying quantity of lactobacillus colonies in nutria medias with beer it was found out that different sorts of beer has positive

influence into human organism and cultivating lactic bacteries.

References:

Yankovskiy D., “Microbial ecology of human”, 2005.

Yankovskiy D., “Microflora and health”, 2008.

Pirog T. “General microbiology”, 2010.

Volanskiy Y., Gritsenko I., Shirobokov V., “Studying of specifical activity of antimicrobial meds” Kyiv, 2004.

ANTIOXIDANT EFFECTS OF STANDARDISED ETHANOLIC PHYLLANTHUS NIRURI EXTRACT AND ITS ACTIVE COMPOUNDS ON HYDROGEN PEROXIDE STIMULATED COLON CELLS

Hamsa Yogini A/P Ganesan1

[1]PERMATApintar[TM] National Gifted Centre, National University of Malaysia, Malaysia

ABSTRACT

Phyllanthus niruri has been used in modern medicine to prevent or treat multiple disorders such as diabetes, kidney stones and HIV. In Malaysia, Phyllanthus niruri is known as 'dukung anak' and is used traditionally for medicinal purposes. This research was conducted to investigate the antioxidant effects of standardised ethanolic Phyllanthus niruri extract and its active compounds on hydrogen peroxide-stimulated colon cells. This research aimed to prove that natural products can be used to mitigate risk of diseases, especially cancers. CCD18Co cells (fibroblast normal colon cells) were stimulated with hydrogen peroxide, H2O2 which decomposes into hydroxyl radicals which are highly reactive free radicals. Excess free radicals causes oxidative stress which can cause cell death, chronic diseases and aging. Besides that, excess free radicals also damage the DNA (deoxyribonucleic acid) which increases the chance of getting cancer. P. niruri extract, along with its constituent active compounds, mainly phyllanthin and hypophyllanthin were tested for their ability to prevent further DNA damage in H2O2-stimulated cells. Among the assays that were done to assess its ability were alkaline comet assay, DPPH assay, FRAP assay and GSH assay. Through alkaline comet assay, Phyllanthus niruri proved to have positive effects on preventing DNA damage in the stimulated colon cells while the DPPH, FRAP and GSH assay results showed that Phyllanthus niruri has antioxidant property.

KEYWORD: Phyllanthus niruri; Phyllanthus; antioxidant; oxidative stress; natural remedy

PREPARATION AND CHARACTERIZATION OF CARBON NANOPARTICLES FROM METROXYLON SAGU

Muhammad Adib Fadhullah Muhammad Lukman1

[1]PERMATApintar[TM] National Gifted Centre, National University of Malaysia, Malaysia

ABSTRACT

The acid hydrolysis of Native sago (Metroxylon sagu) starch at 40°C was monitored for 7 days. The yield of sago starch was reduced from 15 g (100%) to 2.94 g (19%) when the hydrolysis rates were increased to 80.4% on the seventh day. X-ray diffraction results show a gradual increase in crystallinity of hydrolysed sago starch compared to the native starch and the starch changed from C-type to A-type. FE-SEM micrographs showed that hydrolysis starch owned round shape and rough surface with size diameter of 125-257 nm. In addition, DSC analysis shows the melting enthalpy (J/g) was reduced to 2.49 J/g. Starch nanoparticles were further used to prepare carbon nanoparticles by refluxing with nitric acid for 1 hour. The obtained carbon nanoparticles show round shape with size diameter of 30-35nm. Carbon nanoparticles show a peak at 392 nm under UV-visible spectra which indicates the presence of C=O bond. X-ray diffraction analysis showed that the carbon nanoparticles are in amorphous state. The prepared carbon nanoparticles owned fluorescence properties and it showed wide peak at 320 nm when excited with various energy protons. The fluorescence properties of carbon nanoparticles were confirmed under UV-lamp, where they showed light green ray under 365 nm of blue ray. Finally, this research enables the identification of less toxic property of the prepared carbon nanoparticles from sago starch.

KEYWORDS: metroxylon sagu, acid hydrolysis, fluorescence, carbon nanoparticle

How juggling influences the efficiency of working memory

Igor Wasilewski
Supervisor: Urszula Woźnikowska-Bezak
I Liceum Ogólnokształcące z Oddziałami Dwujęzycznymi in Katowice
Creative Group Quark, The Youth Palace in Katowice, Poland; email: wasyl21@gmail.com

1 Introduction

Several courses aimed at improving the efficiency of student learning have proposed juggling as a means of enhancing memory. In our research we aimed to find out if 3-ball juggling can influence the efficiency of working memory in a group of 16-year old high school students.

2 The method

We recruited a 40 high school students and assigned half each to a control group and an intervention group. Both groups were told to perform three one-stimulus (position) n-back tests of increasing difficulty: 1-back, 2-back and 3-back. The first set of tests was performed by both groups without juggling. After a week the test were repeated, with the intervention group performing a ten-minute juggling session prior to testing. Test score improvements between the first and second test were determined for both groups.

3 The results

The results are shown in table (1). The columns represent the value of the median for each test. The quartile bar represents the values of the first and third quartile.

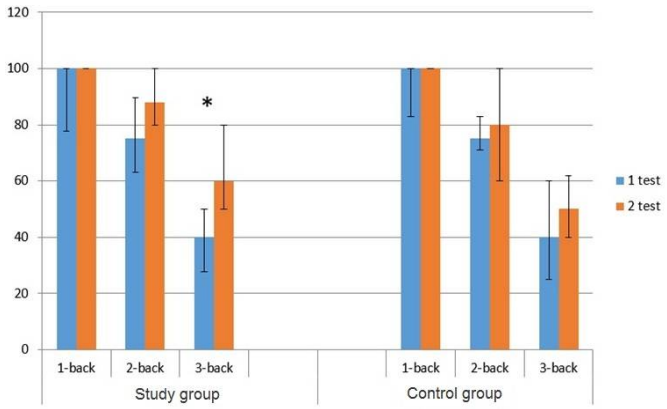

In the results of the 2-back test we can see that the intervention group experienced a greater improvement in test score than the control group. This improvement is even greater in the 3-back test, in which difference between the first and second test is 10 percentage points higher in the intervention group than in the control group. The sign test performed on each pair of n-back tests revealed that the study group had a statistically distinct improvement in the 3-back test (star above the graph).

4 The hypothesis

Juggling is a coordination-demanding skill. A study (1) conducted at Oxford University, demonstrated that long-term juggling training induces gray matter growth in a brain region called intraparietal sulcus. Because this region is responsible both for coordination and working memory, we may conclude that stimulating it through juggling causes it to work more efficiently in a working memory task provided after juggling.

5 Conclusions

The results of the experiment indicate that participants who performed a juggling session prior to the second test had a greater degree of improvement than the group that did not.

References

[1] Draganski, B. et al. ”Neuroplasticity: Changes in grey matter induced by training” *Nature* 427, 311-312 (2004).

The efficiency of iPSC-derived astrocytes using defined factors

Chagajeg Soloukey Tbalvandany and Dasha Mikhailovna Fedorushkova,
Department of Psychiatry, Erasmus Medical Centre, Rotterdam, The Netherlands, September 2015.

The purpose of the investigation

Psychiatric diseases, like schizophrenia, have proven difficult to study in the laboratory. Throughout history, scientists tried to find causes and cures of these diseases by studying neurons. Nevertheless, more scientists are seeing the importance of glia within the brain, such as astrocytes. Classical means of obtaining brain cells to conduct this kind of research, have their drawbacks. Finding the right models with which potential therapies could be tested or more insight into the pathophysiological process of these diseases could be gained, therefore remains a challenge.

Recently, the iPSC-method has emerged as a potential alternative. iPSCs are pluripotent stem cells, generated from mature somatic cells by the introduction of reprogramming factors. Like other pluripotent stem cells, iPSCs can be coaxed to differentiate into any cell type, by exposure to a combination of growth factors and cell culture conditions.

The iPSC-method offers the only known practical way of studying the development and function of live human brain cells and the possible effect of human genetic background on disease, since iPSCs capture the genetic diversity of the patient [1].

Nevertheless, there is little experience with and few data on this method. It was noticed that a specifically low amount of data is to be found on the efficiency of the iPSC-method. This leads us to our main research question: What is the efficiency of iPSC-derived astrocytes using defined factors?

The method we set out to study was previously used by Kondo et al. (2014) [2], which leads to our first sub-question: How do the results of this research compare to the efficiency of generating iPSC-derived astrocytes as stated in the research by Kondo et al. (2014) concerning quantification?

A larger positive ratio of differentiated cells is expected in our protocol, because of the use of different markers. Kondo et al. (2014) used Nestin, GFAP, GLT1/ALDH1, A2B5/CNPasae, and TUJ1/MAP2. Besides Nestin (neural precursor marker), GFAP (astroglial marker) and TUJ1 (neural lineage marker), the markers SOX2 (pluripotency marker), FOXG1 (neural progenitor marker) and S100B (astroglial marker) were used by us as well.

Comparing the results of the protocol as used by Bas Lendemeijer (PhD), whose research was conducted in the Erasmus as well, formed the second sub-question: How do the results of this research compare to the efficiency of generating iPSC-derived astrocytes by Lendemeijer concerning quantification?

A similar or smaller positive ratio of differentiated cells in our protocol is expected. The same protocols were used, but as Lendemeijer (PhD) is more experienced in said iPSC-method, the possibility of having a less efficient protocol should be considered.

Methods of investigation

As forming iPSCs from dermal biopsies is a lengthy process, the initial phases of our research were performed beforehand by Bas Lendemeijer (PhD).

Adherent cultures were maintained in NPC-medium, which was refreshed every other day. The NPC-medium consists of DMEM/F12, N2 supplements (added 1:100), B27-RA supplements (added 1:50), 1 ug/ml Laminin (added 1:1000), 20 ng/ml bFGF and 1% P/S.

NPCs were maintained at high density, grown on laminin-coated plates in NPC-medium and split approximately 1:4 every week with collagenase IV.

Cells were fixed in 4% PFA in PBS, washed multiple times with PBS, and primary antibodies were added: mouse Nestin, 1:200; chicken TUJ1, 1:100; rabbit GFAP, 1:200; rabbit SOX2, 1:200; goat FOXG1, 1:200; mouse S100B, 1:200;

The next day, cells were washed again with PBS and then added a mix which (in a 100 mL solution) consists of 70 mL miliQ, 5 ml 1M Tris, 0,9 gr. NaCl, 0,25 gr. Gelatine (dissolved in 5 mL MiliQ) and – after setting the pH to 7,4 – 0,5 mL 10% Triton.

Afterwards, the following secondary antibodies were added: Alexa donkey 488 anti-rabbit, Cy 3 donkey anti-mouse, Cy 5 donkey anti-goat and Cy 5 donkey anti-chicken; ratio 1:200. To visualize nuclei, slides were stained with DAPI. The day after, images were acquired using a Zeiss confocal microscope.

The amount of positive cells were quantified for the above mentioned markers by analysis with the cell counter of imageJ, expressed 'per DAPI%'. Cells were counted individually to ensure accuracy.

Results

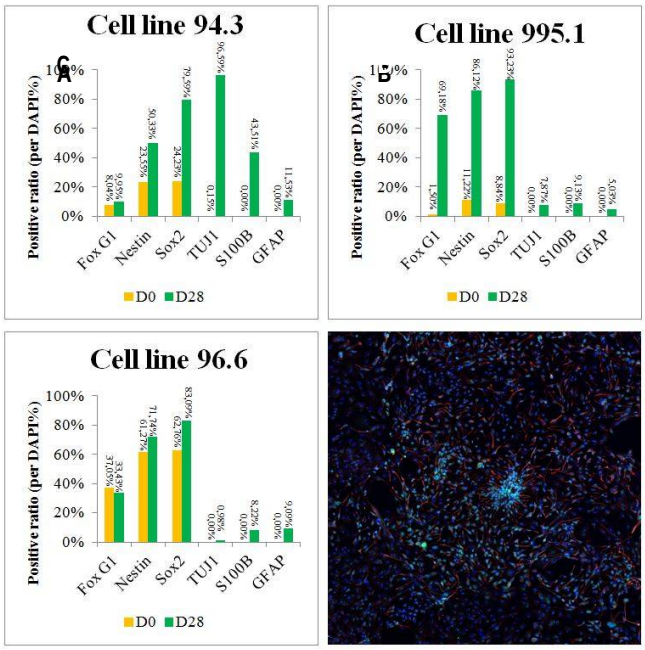

Figure 1: Results
(A-C) Graph of positive ratio of marker per DAPI% at D0 and D28 of cell line 94.3, 995.1 and 96.6, respectively.
(D) Representative image of cells, made with a Zeiss confocal microscope.

Afterwards, a mean of individual percentages was made. Statistical analysis of the raw data was done with a Student's t test, using Excel software. P-values <0.05 were considered significant.

Conclusion

Conclusion on main research question

In all cell lines at D28, SOX2 had an expression of 79,59% or higher and GFAP an expression of 11,53% or lower. All cells had a significant growth ($p < 0,05$) in the expression of SOX2 and GFAP. However, the growth of SOX2 from D0 to D28 was much higher than the growth of GFAP. Based on the functions of these markers, we conclude that the cells remain for the greater part in a pluripotent state. Therefore, the overall efficiency of making iPSC-derived astrocytes using defined factors is low.

Conclusion on sub-question I

We compared the mean results of the shared markers Nestin, GFAP and TUJ1 on D28 to the research by Kondo et al. (2014).

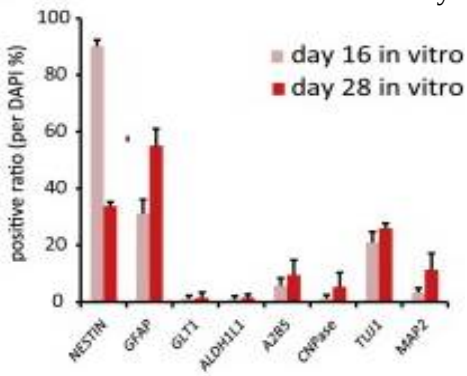

Figure 2: results by Kondo et al. (2014)
Quantification of hiPSC differentiation of the pictures seen on the right.

Nestin ($p > 0,05$) is, on the whole, expressed less in the cells from Kondo et al. (2014) at D28. GFAP ($p < 0,05$) is, on the whole, expressed more in the cells from Kondo et al. (2014) at D28. TUJ1 ($p > 0,05$) is expressed slightly less in the cells from Kondo et al. (2014) at D28. Based on the functions of these markers, the study by Kondo et al. (2014) is more efficient. This conclusion does not correspond with our hypothesis.

Conclusion on sub-question II

We compared the mean results of the shared markers GFAP, S100B and TUJ1 to the research by Lendemeijer. We will compare our D0 results with the D28 results of Lendemeijer.

At cell line 94.3, GFAP ($p < 0,05$) and S100B ($p > 0,05$) were expressed more in the cells of Lendemeijer. This applies to TUJ1 as well, to a lesser extent ($p > 0,05$).

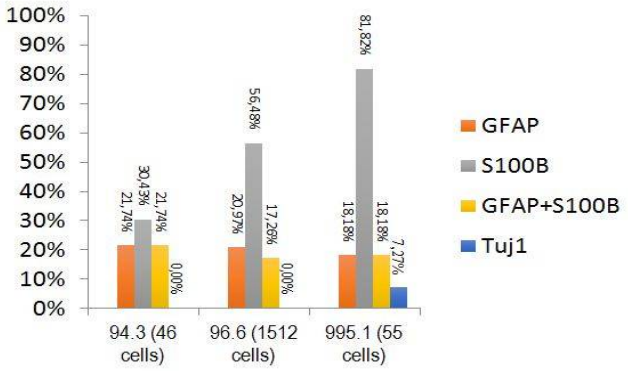

Figure 3: Results from B. Lendemeijer (PhD) – 'ASTRO DIFF high passage number NPC lines (passage 9)'

At cell line 96.6, GFAP ($p < 0,05$) and S100B ($p > 0,05$) were expressed more in the cells of Lendemeijer. TUJ1 ($p > 0,05$) was expressed equally in both studies (0,00%).

At cell line 995.1, no expression of TUJ1, S100B or GFAP was detected, forming a contrast with the findings of Lendemeijer.

To conclude, based on the functions of these markers, the research by Lendemeijer is more efficient. This conclusion corresponds with our hypothesis.

References

[1] R. Dolmetsch and D. H. Geschwind, "The human brain in a dish: The promise of iPSC-derived neurons," *Cell*, vol. 145, no. 6, pp. 831–834, 2011.

[2] T. Kondo, M. Funayama, K. Tsukita, A. Hotta, A. Yasuda, S. Nori, S. Kaneko, M. Nakamura, R. Takahashi, H. Okano, S. Yamanaka, and H. Inoue, "Focal Transplantation of Human iPSC-Derived Glial-Rich Neural Progenitors Improves Lifespan of ALS Mice," *Stem Cell Reports*, vol. 3, no. 2, pp. 242–249, 2014.

Growing plants on Mars

Research into abiotic factors and the possibilities for plant growth on the planet Mars

Author: Wouter van As
Supervisor: Drs. R. De Mooij
Norbertuscollege, Roosendaal, The Netherlands, wouter.van.as@home.nl

Introduction

In July 1969, Neil Armstrong and Buzz Aldrin were the first human beings place their footprints on the surface of the Moon. Now, almost 50 years later, mankind is preparing itself for a new adventure. An adventure even greater, more expensive and more prestigious than the Apollo moon programme. An adventure with the red planet as destination. Building a rocket to bring people to Mars is one challenge we have to face. However, feeding people during this 9 month journey and when they arrive on Mars is a much bigger issue. Sending rockets to Mars carrying only food is simply too expensive. Therefore, people should be able to cultivate their vegetables on the surface of Mars.

The purpose of the research

Growing plants on Mars is far more difficult than growing them on earth. The average temperature of -35 degrees Celsius at the equator with differences of -110 degrees and +30 degrees Celsius are extreme environments for all life types. Furthermore, the air pressure of Mars is almost 2000 times lower than our planet and radiation at the surface is sky-rocketing in comparison with earth. All those factors contribute to the fact that cultivation on Mars is impossible without proper protection. Therefore, plants should be grown in greenhouses.

Method of our research

For this research, soil was used that originally came from Mauna Kea, a dormant volcano on Hawaii. Here, you can find a basaltic soil similar to that found on the surface of the planet Mars. To make the soil useful for the experiment it first had to be adapted by the American space agency *NASA* in a specialised laboratory in Washington. In this way, the soil is almost identical to the soil on the surface of the planet Mars. The samples are very much loess 'lookalikes', only the ground is lacking many nutrients.

As an experiment, we compared the growth of plants in earth-like conditions with plants growing under Mars-like conditions. This is done with 5 different species: tomatoes (*Solanum lycopersicum* '*Moneymaker*'), red beans (*Phaseolus vulgaris* '*Berna*'), sweet corn (*Zea mays* convar. *Saccharata* '*Golden Bantam*'), courgette (*Cucurbita pepo* '*Black Beauty*') and radish (*Raphanus sativus* subsp. *Sativus* '*Ronde Half Rode Witpunt*'). This choice is based on the growing characteristics of each species.
For each species, 3 different groups where used:
- Group 1 in Martian soil;
- Group 2 in potting compost under the reduced light circumstances of the equator of Mars;
- A control group in potting compost with light intensity of equator of earth.

All plants have been growing for 50 days.

Figure 1: Experiment set-up

Results of the experiment

Most crop species grew well in the Martian soil. Also the plants which got the same amount of light as is present on the Martian surface thrived, although in both cases the plants generated less biomass than the control group. After 50 days, the red beans had grown the best and formed the biggest leaves to compensate for the reduced light as usual on Mars. The tomatoes didn't grow so well due to the lack of nutrients, especially nitrogenous substances, in the Martian soil and reduced light.

Figure 2: Red beans (Phaseolus vulgaris 'Berna') after 50 days (l.to.r control group, group 1, group 2)

After the 50-day growth period, we tested the organic material generated by the crops for heavy metals in the *Nutricontrol* laboratory because most species grew well. This analysis for the determination of the exact concentration of some heavy metals (mercury, arsenic, cadmium and lead) in crops grown in a soil similar to that found on the surface of the planet Mars was never previously carried out. This was done because the Martian soil contains lots of heavy metals. It is dangerous for humans when we get too much of them in our body. The results of the analysis showed that the percentage of heavy metals forming on the leaves is less that the 10% restriction of the European Union, which means the leaves should be edible. Finally, the results of the research showed that in the nutrient-poor soil of Mars, the nitrate concentration can be raised by the cultivation of the red bean. This plant is able to grow well in this soil and can convert nitrogen from the air into nitrate. Crops which need lots of nitrate (e.g. tomatoes) for a good growth can benefit from this and grew much better.

Figure 3: Tomatoes (Solanum lycopersicum 'Moneymaker') after 50 days (l.to.r control group, group 1, group 2)

Conclusions

According to the experiments done, plants should be able to grow on the planet Mars in a strictly controlled environment. Leaves collected from the plants are suitable for human consumption. Finally, we discovered that cultivating red beans is a good possibility to increase the nitrate concentration in the Martian soil and crops, which need lots of nitrate for a good growth, grew much better than first instance.

Acknowledgments and further research

Results of this experiment can also be linked to the earth instead of Mars. On our own planet, we also have many places where growing plants is very difficult or impossible due to a poor soil. Therefore, we should compare Mars with these places. As this research shows plants are able to survive in extreme conditions which can lead to a more effective food production for the future.

In May 2016, a group of scientists from Wageningen University (The Netherlands) under the leadership of Dr. Ir. W. Warmelink is going to do further research on this subject. Their focus is on testing the fruits from the species for heavy metals, to see if these parts of the plants are suitable for human consumption. They are also going to cultivate red beans in Martian soil because this specie grew well in this experiment under Mars-like conditions.

Investigating mutants of Chikungunya virus in IFNAR$^{-/-}$ mouse fibroblasts

Li Jiaqi[1], Lisa Ng Fong Poh[2]*

[1]Raffles Institution, [2]National University of Singapore, Singapore,[*] li_jia_qi_1998@hotmail.com

1 Introduction

Chikungunya virus (CHIKV) is a mosquito-borne alphavirus, transmitted mainly via the*Aedesaegypti*and *Aedesalbopictus*species[1, 2]. CHIKV has infected millions around the world since its re-emergence from East Africa in 2004. Symptoms of CHIKV infection include fever, myalgia, polyarthralgia, rashes and headaches. There have been many cases of chronic polyarthralgia, which can be severe and last for years [3, 4]. However, no effective vaccine or treatment against CHIKV currently exists.

As humans are the sole amplification hosts in urban CHIKV transmission, it is ideal to control virus spread through vaccination. However, there are no licensed CHIKV vaccines available. Possible vaccines developed from inactivated viruses, recombinant or chimeric viruses, and virus-like particles are unable to induce similar immune responses as that from natural CHIKV infection, and are expensive to produce [5–7]. Live-attenuated vaccines, meanwhile, are more similar to the wild-type strains, tend to be easier and cheaper to produce, and provide more durable immunity [8]. Here, we have explored an innovative approach of studying CHIKV to develop attenuated vaccines – by studying mutant strains.

In this investigation, we studied three mutant viruses with missense mutations in the non-structural protein region of the CHIKV genome. These mutations were selected as they are naturally occurring in the closely related Semliki Forest virus (SFV), and were shown to result in reduced virulence in SFV[9]. These mutations were induced in CHIKV, and the effects of the mutant CHIKVs were compared to the wild-type CHIKV (WT CHIKV) strain. Parameters studied included differences in infectivity, replicative potential and ability to induce immune responses, specifically the expression of interferon α and β, in WT and mutant CHIKVs.

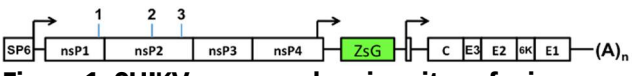

Figure 1. CHIKV genome showing sites of missense mutations in mutant CHIKVs.

Additionally, a key anti-viral responses in CHIKV infections is the type I interferon (IFN) response, which is strongly induced in nonhematopoetic cells such as fibroblasts. Upon infection with CHIKV, IFN α and IFN β are produced [10], which binds to the to IFNα/β receptor (IFNAR) to elicit the downstream responses to counter CHIKV infection [11]. To study the effects of mutant CHIKVs without interference from the type I IFN response, IFNα/β receptor knock-out (IFNAR$^{-/-}$) mousetail fibroblasts (MTFs) were used. This prevents the production of downstream anti-viral proteins, allowing for the different effects of the various mutants to be studied more accurately.

This investigation will allow insight into the mechanisms of infection by mutant CHIKVs, furthering the prospects of developing a live-attenuated CHIKV vaccine. If the mutations can cause reduced infectivity and replicative potential, while maintaining an immune response similar to natural CHIKV infections, they may be useful in developing a live-attenuated CHIKV vaccine.

2 Experimental Procedures

Primary cell culture of IFNAR$^{-/-}$MTFswas performed, followed byseeding and infection with CHIKV strains. Cells were harvested for RNA extraction and flow cytometryat time points of 0, 1, 3, 6, 12 and 24 hours post-infection (hpi). Flow cytometry was used to analyse the infectivity of WT and mutant CHIKVs, as the ZsGreen Tag in the CHIKV genomes allowed infected MTFs to be distinguished via the FITC channel of the BD FACS Cytometer (Cantos II). Viral RNA and total RNA were extracted, followed by quantitative real-time PCR to study viral load and gene expression respectively. The experiment consisted of 3 technical replicates.

3 Results and Conclusions

As hypothesised, the mutants displayed altered infectivity and replicative potential, and induced different levels of gene expression in the MTFs, compared to WT CHIKV. Specifically, mutant 1 showed lower viral replication and infectivity, and reduced expression of *IFN α.* This may be due to the mutation site being situated near the cleavage site between nsP1 and nsP2, thus resulting in slower cleavage and viral replication, reflecting lower vRNA copies and infectivity. Mutant 2 displayed lower infectivity but maintained the induction of type I IFN production, possibly due to the altered helicase and protease function coded by nsP2, which contains the missense mutation. The reduced infectivity of these two mutants suggests that they are weakened

viruses, showing great promise to explore for the development of a live-attenuated vaccine. The third mutant, mutant 3, displayed similar infectivity and replicative potential as the WT strain, but surprisingly, induced *IFN β* production by nearly 600-fold at 12hpi. As the anti-viral function of the type I IFN response is desired to counter CHIKV infection, it is thus ideal for the vaccine or treatment to stimulate higher IFN production. This makes the IFN-inducing properties of mutant 3 interesting to explore. Future developments and Implications

In the future, it is possible to study mutants with a combination of mutations, for example, mutations 2 and 3 together, to further understand the effect of these mutations on CHIKV infectivity and replicative potential. Eventually, a mutant strain could be developed with significantly reduced virulence, while maintaining the ability to induce similar or stronger immune responses in infected cells. This thus holds great promise for the development of an effective live-attenuated CHIKV vaccine.

4 References

[1] P. G. Jupp and B. M. McIntosh, "Aedes furcifer and other mosquitoes as vectors of chikungunya virus at Mica, northeastern Transvaal, South Africa.," *J. Am. Mosq. Control Assoc.*, vol. 6, no. 3, pp. 415–20, Sep. 1990.

[2] K. A. Tsetsarkin, D. L. Vanlandingham, C. E. McGee, and S. Higgs, "A Single Mutation in Chikungunya Virus Affects Vector Specificity and Epidemic Potential," *PLoS Pathog.*, vol. 3, no. 12, p. e201, Dec. 2007.

[3] D. Sissoko, A. Moendandze, D. Malvy, C. Giry, K. Ezzedine, J. L. Solet, and V. Pierre, "Seroprevalence and risk factors of chikungunya virus infection in Mayotte, Indian Ocean, 2005-2006: a population-based survey.," *PLoS One*, vol. 3, no. 8, p. e3066, Jan. 2008.

[4] F. Simon, H. Savini, and P. Parola, "Chikungunya: a paradigm of emergence and globalization of vector-borne diseases.," *Med. Clin. North Am.*, vol. 92, no. 6, pp. 1323–43, ix, Nov. 2008.

[5] N. L. Achee, F. Gould, T. A. Perkins, R. C. Reiner, A. C. Morrison, S. A. Ritchie, D. J. Gubler, R. Teyssou, and T. W. Scott, "A critical assessment of vector control for dengue prevention.," *PLoS Negl. Trop. Dis.*, vol. 9, no. 5, p. e0003655, May 2015.

[6] E. Wang, E. Volkova, A. P. Adams, N. Forrester, S.-Y. Xiao, I. Frolov, and S. C. Weaver, "Chimeric alphavirus vaccine candidates for chikungunya.," *Vaccine*, vol. 26, no. 39, pp. 5030–9, Sep. 2008.

[7] M. Tiwari, M. Parida, S. R. Santhosh, M. Khan, P. K. Dash, and P. V. L. Rao, "Assessment of immunogenic potential of Vero adapted formalin inactivated vaccine derived from novel ECSA genotype of Chikungunya virus.," *Vaccine*, vol. 27, no. 18, pp. 2513–22, Apr. 2009.

[8] K. Plante, E. Wang, C. D. Partidos, J. Weger, R. Gorchakov, K. Tsetsarkin, E. M. Borland, A. M. Powers, R. Seymour, D. T. Stinchcomb, J. E. Osorio, I. Frolov, and S. C. Weaver, "Novel chikungunya vaccine candidate with an IRES-based attenuation and host range alteration mechanism.," *PLoS Pathog.*, vol. 7, no. 7, p. e1002142, Jul. 2011.

[9] S. Saul, M. Ferguson, C. Cordonin, R. Fragkoudis, M. Ool, N. Tamberg, K. Sherwood, J. K. Fazakerley, and A. Merits, "Differences in Processing Determinants of Nonstructural Polyprotein and in the Sequence of Nonstructural Protein 3 Affect Neurovirulence of Semliki Forest Virus.," *J. Virol.*, vol. 89, no. 21, pp. 11030–45, 2015.

[10] C. Schilte, T. Couderc, F. Chretien, M. Sourisseau, N. Gangneux, F. Guivel-Benhassine, A. Kraxner, J. Tschopp, S. Higgs, A. Michault, F. Arenzana-Seisdedos, M. Colonna, L. Peduto, O. Schwartz, M. Lecuit, and M. L. Albert, "Type I IFN controls chikungunya virus via its action on nonhematopoietic cells.," *J. Exp. Med.*, vol. 207, no. 2, pp. 429–442, 2010.

[11] T.-S. Teng, S.-S. Foo, D. Simamarta, F.-M. Lum, T.-H. Teo, A. Lulla, N. K. W. Yeo, E. G. L. Koh, A. Chow, Y.-S. Leo, A. Merits, K.-C. Chin, and L. F. P. Ng, "Viperin restricts chikungunya virus replication and pathology.," *J. Clin. Invest.*, vol. 122, no. 12, pp. 4447–60, Dec. 2012

The regularity of cycles in permutation groups

Liana Khazaliya
Supervisor Boris Doubrov
Gymnasium № 41 named after V. Serebriany, Minsk/Belarus, liana.xazaliya@mail.ru

1 Content

Since the end of previous centurythere has been a growing interest in applicationof probability in finite groups. Probability can be applied to the theory of finite groups in a number of cases like probabilistic statements about groups, construction of randomized algorithms in computational group theory or application of probabilistic methods to prove deterministic theorems in group theory. When we talk about probabilistic statements about groups, we talk about thestatistical group theory.
We are interested in the number of regular cycles in a given permutation group of degree n. In more detail, let$G$be a subgroup of S_n. Thenwe have a conjecture, that

$$\frac{|C(G)|}{|G|} \leq \frac{\varphi(n)}{n},$$

where$|C(G)|$ is a cardinality of the set of all cycles of length n, $\varphi(n)$ is*Euler's totient function.*

This problem also can be interpreted asthe probability, that a randomly selected element from permutation group will be a cycle of length n(generates a transitive group).Another interpretation of this problem is related to the notion ofthe cycle index. See thebook *Graphical enumeration* Frank Harary, Edgar M. Palmerfor further details.

Moreover it should be mentioned thatGareth A. Jones referred in his article*Primitive permutation groups containing a cycle*on similarly questions, which have been raised by Zvonkin.

The statistics of random permutation,such as the cycle structure are of fundamental importance in the analysis of algorithms, especially of sorting algorithms, which operate on random permutations.

2 The purpose of the investigation

There are three goals of the investigation:

a. Prove the conjecture set, specificallythatfor all subgroups Gin S_n an inequality

$$\frac{|C(G)|}{|G|} \leq \frac{\varphi(n)}{n},$$

holds.

b. Find all subgroups for which equality is achieved.

c. Improve the estimate for some specific classes.

3 Methods of the investigation (in comparison with known methods)

The methods used are combinatorial andprobabilistic methods in the theoryfinite groups.

We also used the computer algebra system GAP. We developed an algorithm to successfullyverify the conjecture for groups of degree 16 – 30. GAP was chosen, because it has a classification of all transitive subgroups of the symmetrical group up to conjugacy of order less than 31.

4 Results

In this work the hypothesis was proved for primitive and imprimitive groups separately.

A partition of theset$\{1, \dots, n\}$is

$$\{1, \dots, n\} = \bigcup_{i=1}^{m} B_i,$$

where$\{B_i\}_{i=1}^{m}$ are mutually disjoint sets. Primitive groups are groups, which do not preserveany nontrivial partition; otherwise groups arethe group is called imprimitive.

The case of primitive groups is based on the Jones'sclassification, which was published in 2004. He listed all primitive groups that contain at least one cycle of length n. But nothing about the number of such cycles was known.

We prove theconjecture for solvable primitive groups. For unsolvable primitive groups we improve an upper bound.

Theorem 1. Let G be an unsolvable primitive permitation group of degree n. Then

$$\frac{|C(G)|}{|G|} \leq \frac{2}{n}.$$

Moreover, the equality holds if and only if G is A_n for odd $n \geq 3$, $P\Gamma L_2(8) \subset S_9$, $PSL_2(11) \subset S_{11}$, $M_{11} \subset S_{11}$, $M_{23} \subset S_{23}$.

The case of imprimitive groupswas reduced to studyingsuch interesting structuresasthe wreath products of groups.

Wreath product of groups G and H ($GwrH$)can be constructed in the next way. Take m copies of group G

and let group Hacts on these$m$ copies. Other words, wreath productof groups G and H is a semidirect product of a direct product of m groups G with group H.

Theorem 2. Suppose the conjecture holds for subgroups $G \subset S_n$and $H \subset S_m$. Then it also holds for the wreath product $G\ wr\ H \subset S_{nm}$.

Theorem 3. The conjecture holds for arbitrary subgroups of the wreath product of two cyclic groups $C_n\ wr\ C_m \subset S_{nm}$.

In addition, we explicitly describe all cases from *Theorem 3*, when the equality holds. This involves various techniques from number theory.

5 Conclusion

Summing upwe obtained the following new results.The frequency of the cycles of the length $\boldsymbol{n}$ in permutations groups of degree $\boldsymbol{n}$was estimated. Forunsolvable primitive groups we obtained an exact upper bound of $\frac{\mathbf{2}}{\boldsymbol{n}}$ and described all cases when this bound is achieved. For imprimitive the estimate wasknown only trivial cases likewrest product of two cyclic groups. This paper presents the results for wreath product of arbitrary groups and for all subgroups of wreath product of cyclic groups.

In the latter case we found call such subgroups,when equality holds.

Triangle-free graphs

Hanna Zadarazhniuk

Supervisor: SimanenkaDzimitry

Secondary General School №8

*Gomel/Belarus*a_zadorozhnyuk@mail.ru

Graph theory today is a quickly developing section of discrete mathematics. Graphs are used in communicational schemes, electronic and electric circuits and other spheres.

Triangle-free graphs are mentioned in the article *Size in maximal triangle-free graphs and minimal graphs of diameter 2* by C. Barefoot, K. Casey, D. Fisher, K. Fraughnaugh and F. Harary. A triangle-free graph is called maximal if the addition of any edge creates a triangle. For $n \geq 5$ was shown that there is an n-node m-edge maximal triangle-free graph if and only if $m = k(n-k)$ or $2n-5 \leq m \leq \left[\frac{(n-1)^2}{4}\right]+1$. The number of such graphs, their structure also were being explored (*The number of maximal triangle free graphs* by J. Balogh and S. Petrickova, *The typical structure of maximal triangle-free graphs* by J. Balogh, H. Liu, M. Sharifzadeh and S. Petrickova)

By analogy, let the graph which doesn't contain complete p-node subgraphs be called maximal p-free, if the addition of any edge creates complete p-node subgraphs. We show that,for $n \geq p+2$, n-node m-edge maximal p-free graphs exists if it is a complete $(p-1)$-partite graph or $(p-1)n-\frac{p(p-1)}{2}-2 \leq m \leq \left[\frac{(n+2-p)^2}{4}\right]+1+\frac{(p-3)(2n-2-p)}{2}$. Also noted that every complete $(p-1)$-partite graph with at least one part more than 1 is a maximal p-free graph.Though, we don't know, are there any maximal p-free which neither satisfy the inequality, nor $(p-1)$-partite.

The girth of graph is the length of a shortest cycle contained in the graph. We show that the girth of maximal triangle-free graphs can be 4, 5 or ∞ (no cycle) and the girth of maximal p-free graph for $p>3$ is 3 for $n \geq p$.Also noted that if the independent domination number of a maximal triangle-free graph less than its minimum degree, then the girth of the graph can't be 5.

Was shown, that the minimum degree δ of n-node maximal p-free graph is at most $\left[\frac{n(p-2)}{p-1}\right]$.

Pythagorean Triple Siblings, with Conjugate Legs

Giorgi Bugechashvili, Natia Cheishvili

Supervisor: Mamuka Meskhishvili

Georgian-American High School, Tbilisi, Georgia, info@gahs.edu.ge

6 Main Goal

Main purpose of our research is investigation of the following Diophantine system:

$$\begin{cases} c^2 - (p^2 + q^2)^2 = \square \\ c^2 - (p^2 - q^2)^2 = \square \end{cases} \quad (1)$$

Firstly, we try to find solutions by using computer and we check

$$c \leq 650.$$

Unfortunately, computer search not give us non-trivial solutions so, we thought the following hypotheses is true: this system has no non-trivial solutions.

But, from the history of number theory we know a distinguished example about Euler quartic conjecture, which was thought to be true for more than two centuries.

In 1772, Euler proposed that the equation

$$A^4 + B^4 + C^4 = D^4$$

had no solutions in integers [1] .

This assertion is known as the Euler quartic conjecture. Ward [2] in 1948 showed there were no solutions for

$$D \leq 10\,000.$$

This was subsequently improved [1] to:

$$D \leq 220\,000.$$

However, the Euler quartic conjecture was disproved in 1987 by N. Elkies, who, using a geometric construction, found:

$$2682440^4 + 15365639^4 + 18796760^4 = 20615673^4$$

In 1988, Roger Frye found

$$95\,800^4 + 217\,519^4 + 414\,560^4 = 422\,481^4$$

and proved that there are no solutions in smaller integers and showed that infinitely many solutions existed.

What about our system? Of course it's possible for the system to have non-trivial solutions. But similarly to Elkies case, solutions, if they exist, must be in large numbers.

Our research is dedicated to proving the following theorems.

Theorem 1:

Diophantine system (1) has non-trivial solutions.

Theorem 2:

There are infinitely many non-trivial solutions of (1).

We obtain general parametric formulas for solutions of our Diophantine system.

7 Research

We use a theorem about rational solutions of Kummer's surface of special type [4]:

All nontrivial rational solutions of the following equation:

$$\mu^2 = \alpha\beta(1 - \alpha^2)(1 - \beta^2)$$

are given:

$$(\alpha, \beta, \mu) = \left(\frac{X}{N}, \frac{Z}{N}, \frac{YW}{N^3}\right)$$

where (X,Y) and (Z,W) are different rational nontrivial solutions of C_N congruent curve equation. i.e.

$$Y^2 = X(X^2 - N^2),\ W^2 = Z(Z^2 - N^2).$$

Nontrivial integer solutions of system

$$\begin{cases} c^2 - (p^2 + q^2)^2 = \square \\ c^2 - (p^2 - q^2)^2 = \square \end{cases}$$

are given by formulas:

$$c = k\sqrt{xz}(x + z)(xz + N^2)$$
$$p^2 = kxz(x + N)(z + N)$$
$$q^2 = kxz(x - N)(z - N)$$

Where, *N* is a congruent number, *x* and *z* are different non-trivial solutions with squared product to a congruent equation.

$$Y^2 = X^3 - N^2X$$

Therefore, by substituting *k, x, z* and *N* with numbers, we get the following numerical examples. Solutions of the corresponding congruent equation are taken from [4].

8 Numerical examples:

1) *N*=6; *x*=18; $z = \frac{19602}{47^2}$

$$15358381995^2 - (114774^2 + 35673^2)^2 = 5215702800^2$$

$$15358381995^2 - (114774^2 - 35673^2)^2 = 9708645804^2.$$

2) *N*=34; *x*=162; $z = \frac{2178}{7^2}$

$$3322469535^2 - (50127^2 + 14784^2)^2 = 1891797600^2$$

$$3322469535^2 - (50127^2 - 14784^2)^2 = 2403264864^2.$$

9 References:

1. *Lander, L. J.; Parkin, T. R.; and Selfridge, J. L. "A Survey of Equal Sums of Like Powers." Math. Comput. 21, 446-459, 1967.*
2. *Ward, M. "Euler's Problem on Sums of Three Fourth Powers." Duke Math. J. 15, 827-837, 1948.*
3. *Guy, R. K. "Sums of Like Powers. Euler's Conjecture" and "Some Quartic Equations." §D1 and D23 in Unsolved Problems in Number Theory, 2nd ed. New York: Springer-Verlag, pp. 139-144 and 192-193, 1994.*
4. *Mamuka Meskhishvili//Three-Century Problem; 2013.*

Infinite flow of random numbers and its possible uses

Nia Baramadze,, Ekaterine Akoubardia

Supervisor: Ia Mebonia, PhD

Georgian-American School, Tbilisi, Georgia

INTRODUCTION

Have you ever decoded any kind of an anagram or a puzzle, where bychanging the order of the lettersin a word, you get the different one (word)? Have you ever bought anything or checked your bank account via internet? If Yes, then you may have entered the world of codes, passwords, encrypted and decoded information. People change information by a message, for what they use different modes starting with direct contact and ending with complex equipment. The part of information is confidential and needs to be protected. Protecting the information means the costs, which a person gives for coding or decoding. Once there was a time, when only government, ambassadors, mysterious or military secret services used the encoder machines. But today, everything has changed. With the invention of computer and internet, protecting information can be done via different means, including passwords, which a consumer has to submit/log in every time before getting the needed information. But the password is information itself, which also needs to be protected. According to these, keeping the information safe has not been as vital/urgent as it is now.

Correspondingly, we are interested in how safe our private information is and how we canreinforce the security measures with minimum amount of charges.

THE PURPOSE AND METHOD OF THE INVESTIGATION

The aim/goal of the paper is to come up with an easily usable and inexpensive method of defending short electric messages. Our offered idea of covering

a message is an original usage of flow of random numbers. It grants an algorithm a specifics of ‘’unitary notebook’’. A source of random numbers flow is the machine itself which sends the message (this could be a mobile phone), thus we don’t need to make the special generator. In the process of encryption, we use text tabulation, classical movable crypt (Symbols move in a text) and Interchangeable one (One symbol or a group of symbols change with others in a text).Introduced terms and transformations are fully described in verbal way as well as analytical way. A usage of the specific sample is also represented.

CONTENT

Let's say, one customer is sending short electric message (SMS) to another person. Which numbers can this procedure be described with? This kind of numbers are, for example, the phone number of both - sender and receiver; mobile operator settings (Maximum quantity of symbols); quantity of symbols; date of sending (day, month, year); time/date of sending (hours, minutes, seconds). It's interesting that all these features never repeat and we may face them only once at the sorting. Also, It's impossible to consider the calculation for every sorting - To calculate it, we have to check every possible outcome. Let's call this described unity of numbers a "Initial Random Settings" (IRS). The method we offer for the privacy of messages is based exactly on IRS.

Every message so text is a strictly organized sequence of alphabets and punctuation marks. The first step of encryption is the replacement of alphabets and punctuation marks to double-digit codes, which is implemented according to the special table (this table is according to IRS) - We get a sorted sequence of two-digit codes. The next step is thetabulationso the division of a square matrix type subgroups, the size of it is also depending on IRS. The third step is a reversible conversion of tables, which is done/implemented by a randomly selected (Based on IRS) special operators of a set of pre-defined "instruments".

Let's say, Phone operator setting is K, also - the first step of SMS encryption is done and The text containing N symbol is already encrypted to a sorted sequence of two-digit codes, then

$$z = \left[\sqrt{\frac{min\{N;K\}}{2}}\right]$$

We called z a reasonable minimum of text-table (The minimum size of text-table is z x z). We chose n x n for a size of text-table, where n is possible smallest natural number, for which

$$n - z \equiv ((a_1 + 1)a_2 + (a_3 + 1))mod(z + 1)$$

Here and after herea_1 is/will be the selected settings from IRS. It's clear that text-table size varies from z to 2z. n defines a rule according to which, there is excreted four movable zone (quarter) in a table, and unmovable elements in private case.

Set of "Instruments" is described in the method - this is a unity of reversible transformations of table quarters, including axial symmetry, horizontal or vertical dislocation. In every specific case, it's defined from IRS which instruments we use for objects. Every instrument is described in a analytical way, for example, one of the instruments is a dislocation of first quarter line elements ("Horizontal conveyer"). If n is even, we establish designation$t = \frac{n}{2}$and find the smallest possible k natural number, for which$\equiv a_4(modt)$, then dislocationf_k^l of*i*-line elements(A_{ij}, $j = \overline{1,t}$) is defined by the formula :$f_k^l: A_{i\ t+j} \to A_{i\ t+p}$, where p is the smallest possible natural number, for which $p \equiv j + k\ (modt)$, and i=1,t. The same operator for odd n is defined so:

$$f_k^l: A_{i\ t+1+j} \to A_{i\ t+1+p}, \qquad \text{where } t = \left[\frac{n}{2}\right]$$

There is an illustration of method in the work: The sample text got encrypted at first and then opened by the reversible operator.

CONCLUSION

Presented method in the paper is structured based on the level of an algorithm, so is practically implementable and in the case of phone operator ability, it can provide people confidentiality of the private conversation. The method is easy and inexpensive, which doesn't need serious technical items. At the same time, breaking the crypt requires a lot of time and resources. Even if the crypt is broken result are disposable, since they can't be reused because of random numbers taking part in algorithm.

REFERENCES

1. Karabeinikov A. G, Gatchin Y. A. Mathematical foundations of cryptology. Saint Peter's Burge: ITMO Publishing 2004.
2. Karasev. I. "Fundamentals of cryptology." Rbardalzo. Accessed: January, 2016. http://www.rbardalzo.narod.ru/kripto1.html
3. Akubardia, E; Baramadze, N; and Mebonia, I. *Republic of Georgia Patent: 6449.* - Axis symmetry of text matrices, January 1st, 2016.

Diophantine Equation Involving Four Biquadrates and a Square

Nikita Tripathi, Nikoloz Kalatozishvili
Supervisor: Mamuka Meskhishvili
Georgian-American High School, Tbilisi, Georgia, info@gahs.edu.ge

10 Main Goal

The main goal of our research is investigation of a Diophantine biquadrate equation:

$$p^4 + q^4 - a^2 = r^4 + s^4 \quad (1)$$

under an additional condition:

$$pq = rs$$

All of humanity's knowledge regarding Diophantine equations is gathered in the books: "History of the Theory of Numbers, Volume II: Diophantine Analysis" by Leonard Eugene Dickson [1] and "An Introduction to Diophantine Equations" by Titu Andrescu, Dorin Andrica, Ion Cucurezeanu [2]. Unfortunately though, these books do not contain any information concerning our type of 4th degree equation. Therefore, our research is original and innovative.

11 Method

To research our equation, we have to use rational solutions of the congruent curve equation

$$C_N : y^2 = x(x^2 - N^2)$$

By using solutions of the congruent number equation C_N, it is possible to construct a three-term arithmetic progression of squares with *N* difference [3]. In our research, these solutions are used to find parametric solutions of the above-mentioned Diophantine system.

12 Research

Actually, our equation is equivalent to a Diophantine system:

$$\begin{cases}(p^2 + q^2)^2 - a^2 = (r^2 + s^2)^2 \\ (p^2 - q^2)^2 - a^2 = (r^2 - s^2)^2\end{cases} \quad (2)$$

because by adding up the equations in (2), we get equation (1) and by subtracting them we get the additional condition.

So, it's clear, that once we find a solution to (2) it will be a solution to (1) as well.

We begin to research the Diophantine system (2). It is possible to divide the system into two subsystems:

$$\begin{cases}(p^2 + q^2)^2 - a^2 = \square_1 \\ (p^2 - q^2)^2 - a^2 = \square_2\end{cases} \quad (3)$$

$$\begin{cases}a^2 + (r^2 + s^2)^2 = \square_3 \\ a^2 + (r^2 - s^2)^2 = \square_4\end{cases} \quad (4)$$

We use a theorem about rational solutions of Kummer's surface of special type [4]:

All nontrivial rational solutions of the following equation:

$$\mu^2 = \alpha\beta(1 - \alpha^2)(1 - \beta^2)$$

are given:

$$(\alpha, \beta, \mu) = \left(\frac{X}{N}, \frac{Z}{N}, \frac{YW}{N^3}\right)$$

where (X,Y) and (Z,W) are different rational nontrivial solutions of C_N congruent curve equation. i.e.

$$Y^2 = X(X^2 - N^2),\ W^2 = Z(Z^2 - N^2).$$

13 Solutions of (3)

We get, that all integer solutions of (3) can be given using these parametric formulas:

$$a = k_1 * 4N_1\sqrt{x_1 z_1}$$
$$p^2 = k_1 * (x_1 + N_1)(z_1 + N_1)$$
$$q^2 = k_1 * (x_1 - N_1)(z_1 - N_1)$$

14 Solutions of (4)

Similarly to (3), we get that all integer solutions of (4) are given using the following formulas:

$$a = k_2 * 4N_2\sqrt{x_2 z_2}$$
$$r^2 = k_2 * (x_2 + N_2)(z_2 - N_2)$$
$$s^2 = k_2 * (x_2 - N_2)(z_2 + N_2)$$

By uniting the solutions of (3) and (4) we get the parametric formulas for solutions of the original system.

15 Results of the research

Theorem:

Nontrivial integer solutions to (1) are given by formulas:

$$a = k * 4N\sqrt{xz}$$
$$p^2 = k * (x + N)(z + N)$$
$$q^2 = k * (x - N)(z - N)$$
$$r^2 = k * (x + N)(z - N)$$
$$s^2 = k * (x - N)(z + N)$$

Where k is an integer, while x and z are nontrivial different rational solutions of an arbitrary congruent curve. It must be noted, that, k, x and z must be chosen so that p, q, a, r and s are integers.

Therefore, by substituting k, x, z and N with numbers, we get the following numerical examples. Solutions of the corresponding congruent equation are taken from [3].

16 Numerical cases:

1) $N = 5,\ x = \left(\frac{5}{2}\right)^2,\ z = \left(\frac{41}{12}\right)^2$

$$735^4 + 155^4 - 492000^2 = 465^4 + 245^4;$$
$$735 * 155 = 465 * 245.$$

2) $N = 6,\ x = \left(\frac{5}{2}\right)^2,\ z = \left(\frac{1201}{140}\right)^2$

$$8743^4 + 1151^4 - 40353600^2 =$$
$$= 8057^4 + 1249^4;$$
$$8743 * 1151 = 8057 * 1249.$$

17 References:

1. *Leonard Eugene Dickson// History of the Theory of Numbers, Volume II: Diophantine Analysis; 2013*
2. *Titu Andrescu, Dorin Andrica, Ion Cucurezeanu// An Introduction to Diophantine Equations; 2010*
3. *Mamuka Meskhishvili//Three-Century Problem; 2013*
4. *Top.J. Yui. N.// Congruent number problems and their variants; Cambridge Uni. Press 2008/*

ICYS_2016 abstract India (Mathematics - Monumental Geometry)

Supreet Kaur and Gaganpreet

Mrs. Sudha Chand

St. Mark's Sr. Sec. Public School, New Delhi, India

stmarksmb@saintmarksschool.com

The Purpose of the Investigation

India has a rich history and the historical monuments of India have always been admired by everyone. From Mughal to modern period, monuments have attracted people because of their aesthetically pleasing designs. Geometry has played a very important role. Architecture, Mathematics and geometry all together have resulted in creations of buildings that are both inspiring and beautiful. Hence our research on monumental geometry.

Method of the investigation

After observing various monuments, we tried to understand the geometry and mathematical concepts involved in the designs of these structures. We built models using geometrical concepts which helped in investigating the designs of the following monuments.

LOTUS TEMPLE

The Lotus Temple, was designed by the architect Fariborz sahba as a worship place for the Baha'i community.

A few months ago, we visited Lotus Temple,Its geometry amazed us.The temple is like a lotus that looks afloat on water. The lotus has nine components in all. Ponds, arches and all the petals are nine in number. The structure is open from the top and covered with a glass which illuminates the whole dome. It has got an eco- friendly environment which complements the architecture of the superstructure.

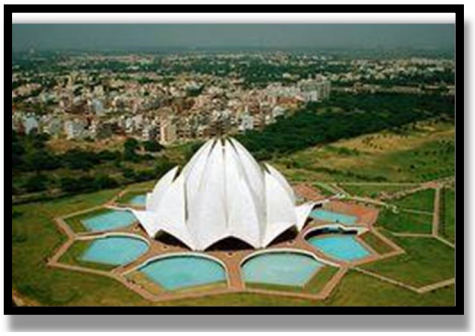

TAJ MAHAL

The Taj Mahal was built by the great ruler Shah Jahan, in the memory of his wife Mumtaz Mahal. One of the Seven Wonders of the World, whose symmetry and harmonious architecture compliment its beauty, the Taj Mahal was built in the 17 century. The concept of its architecture involves symmetrical designs. The minarets, rooms, walls, and even gardens follow perfect symmetry. The architecture is a tribute to mirror symmetry. Even the reflecting pool in front of the structure, which reflects the beautiful image of the entire monument ,has a lot of symmetry. This structure is a perfect example of blissful architecture.

EIFFEL TOWER

This great structure was built under the supervision of the architect Gustave Eiffel.

One of the most perfect examples of amazing European architecture is the Eiffel tower. The basic structure of the tower is lattice-work columns at each of the four corners of the Tower, in which diagonals connect four elements that help in making stiff, lightweight columns.

The tower reveals an exponential shape, where the lower section is specially designed to ensure resistance to wind forces.

Results of the Experiment

The investigation revealed the various mathematical and geometrical concepts that are involved in the making of buildings.

All the monuments have their own unique designs and harmonious patterns, be it European or Indian architecture.

Conclusion

Geometry plays a very important role in architecture.

We are able to recognize mathematics, architecture and geometry with an abundant essence of history all together in the monuments found in the world. Hence, geometry can result in creation of beautiful and pleasing designs, that too with a sense of uniqueness and harmony.

Reference

http://www.ce.jhu.edu/perspective/studies/Eiffel %20Fil es/ET_Geometry.htm

SOLUTION TO TRAVELLING SALESMAN PROBLEM (TSP) FOR LOGISTICS DISTRIBUTION IN PT JALUR NUGRAHA EKAKURIR (JNE) REGIONAL DEPOK USING THE APPLICATION OF LINEAR PROGRAMMING AND *SOLVER* PROGRAM

Mas Daffa Muhamad Pratamadirdja

Supervisor: Deni Irawan, STP, S.Pd.
Lazuardi GIS High School, Depok, Indonesia
pratamadirdja@gmail.com

1. Research purpose

One of the problems happening in logistic companies, especially PT JNE, is that the vehicles that deliver packages to several addresses and return back to the starting depot take such a long distance and time because they do not know and choose the shortest path. This can waste such amount of money, customer satisfaction, and competitiveness of the company.

The problem above can be formulated as a Travelling Salesman Problem, which can be solved quite easily because it is can be just simply formulated in linear programming and can be solved using executor engines which use algorithms or heuristics. One example is Premium Solver Platform in MS Excel, which is simple and easy to use, so it can be applicable in R&D office environment, without requiring one to learn difficult programming concepts.

With my background knowledge in mathematics and MS Excel, I want to solve this problem so JNE can perform better in the future and become able to compete with its other rivals.

2. Research method

In this research, I used linear programming which is formulated in MS Excel and then executed it using Gurobi Solver Engine in Premium Solver Platform.

Firstly, data of the 55 addresses were obtained. Then, the coordinates of those addresses were searched in Google Maps and a distance matrix between those 55 coordinates were created using Google Maps API. Next, the linear programming formulation was made in MS Excel. Finally, it was executed in Premium Solver Platform using LP Gurobi Solver Engine.

This engine, which uses branch-and-bound heuristic, is reliable and optimal for medium-sized TSP problem (50 to 100 nodes), solves it in short time and finds a good optimum solution. In addition, it is simple easy to use by R&D office workers, and they don't have to learn complex programming concepts.

3. Theoretical model

To solve this problem, I try to break down into 2 different shipments (vehicles) so it will save the time as well and thus increases customer satisfaction and profit. This model is known as multiple TSP. Here, two salesmen must leave the main depot to other different addresses and must return from another different addresses. Otherwise, there should be only one path—in total—taken between cities. The objective function can be formulated as:

$$Minimize\ Z = \sum_{i=1}^{55}\sum_{j=1}^{55} x_{ij} d_{ij}$$

with x_{ij} as the decision variable and d_{ij} as the distance between node i and j.

4. Experiment result and discussion

Table for Vehicle 1

Order no.	Node no.	Distance from prev address (km)
1	1	4.4
2	8	8
3	21	3
4	15	0.4
5	46	4.2
6	25	2.8
7	23	0.9
8	24	6.6
9	45	1.9
10	3	3.3
11	48	1.1
12	39	1.7
13	7	2.1
14	14	3.3
15	50	2
16	18	1.4
17	9	4.3
18	54	3.6
19	52	0
TOTAL		**55.0 km**

Table for Vehicle 2

Order no.	Node no.	Distance from prev address (km)
1	1	6.6
2	20	10.5
3	42	1.3
4	29	1.3
5	22	2.9
6	6	0.3
7	5	2.9
8	19	10.6
9	47	6.8
10	26	6.1
11	36	0.4
12	27	1
13	44	2.1
14	43	0.7
15	37	0.8
16	41	0.7
17	40	1.4
18	31	4.1
19	55	2.7
20	16	3.1
21	51	1.8
22	30	1.6
23	4	1.6
24	13	2.9
25	11	4
26	34	3.9
27	32	4.3
28	17	2.3
29	38	4.5
30	35	0.5
31	33	0.3
32	2	0.6
33	28	0.9
34	53	0.9
35	12	1.4
36	49	2.8
37	10	3.1
TOTAL		**103.7 km**

The solving time using Gurobi Solver Engine, which uses branch-and-bound, is 6.01 seconds—a short time to solve a medium-sized multiple TSP—and can find a good optimum value.

The first vehicle traverses 18 other nodes for 55.0 km before going back to the starting depot, while vehicle 2 traverses 36 other nodes for 103.7 km. The total distance covered by those two vehicles are 158.7 km. It is a very huge distance saving compared to the previous 613.8 km before experiment.

Time-wise, the first vehicle only takes 2.57 hours and the seconds takes 4.85 hours to circulate through Depok, compared to the previous 28.68 hours (which means this task couldn't be completed within one day). This is under the average speed of motor vehicles in Depok of 21.4 km/h.

Fuel-wise, the first vehicle only consumes Rp18,590 and the second consumes Rp35,050.60, with the total consumption of Rp53,640.60. It save a huge Rp153,823.80 compared to the previous Rp207,464,40. The motorcycles that JNE uses consumes one liter each 25 kilometers, with one liter of fuel is equivalent to Rp8,450.

5. Conclusion

In this research, it can be concluded that the Travelling Salesman Problem, especially for the case study of logistics distribution in PT JNE regional Depok, can be solved using the application of linear programming and Solver program efficiently and produce very optimal result and savings in such a short time.

References

[1]Pratiwi, Irmadani Intan. 2010. *Efektivitas Pemetaan Markas Pemadam Kebakaran di Kota Depok dengan Penerapan Program Linear dan Program* Solver. Depok: SMA Lazuardi Global Islamic School.

[2]Sukarmawati, Yuliana. 2012. *Optimisasi Rute Pengumpulan Sampah di Kawasan Perumahan Pesona Khayangan dengan Model Penyelesaian* Travelling Salesman Problem. Depok: Fakultas Teknik Universitas Indonesia.

[3]*http://ardhana12.wordpress.com/2008/02/08/metode-penelitian-studi-kasus/*, accessed December 12, 2014, 1420hrs

[4]*http://ojs.academypublisher.com/index.php/jsw/article/viewFile/0507761768/1956.*

SL_2-factorisation of twisted Lee-type groups

Davladov Dmitrii
Supervisor: Smolensky Andrey
Laboratory of Continuous Mathematical Education, Saint-Petersburg, Russia,
dima.davladov@student.su

The purpose of the investigation

SL_2-factorisation is used in constructing of graphs-expanders, which are necessary to create different networks such as telephone network, computer network, etc.

We are researching Lee-type groups' factorizations as group's decomposition into the product of subgroups which are isomorphic to SL_2 group. These decompositions are well known for Shevalle-type regular groups, but for the twisted Lee-type groups the existing proofs are implicit in nature and give a far from precision upper bound of the factorization's length.

We need to investigate SL_2-factorization of SU_3 group, because of existence of Lee-type groups' decomposition into the product of subgroups, which are isomorphic to SL_2 and SU_3 groups.

For example, the last attempt to assess the length of the factorization was in the article Martin W. Liebeck, Nikolay Nikolov, Aner Shalev *"Groups of Lie type as products of SL_2 subgroups"*, where it is 55, but it is far from precision upper bound of the factorization's length.

Thus, the purpose of our work is giving more precision upper bound of SL_2-factorization's length of SU_3 group.

18 Method of the investigation

19 The research was conducted over a finite field with the dimension equal to a Prime number in even powers of. In order to understand what in fact is happen with the factorization's length of the SU_3 group, we have used a computer program "GAP" (computational mathematics), where we conducted research cases of factorization with different dimensions of the field.

Results of the experiment

In the end we have received and proved more precision upper bound of the factorization's length of SU_3 group in the general case.

Conclusion

As a result, we have a much more accurate upper bound of the factorization's length of SU_3 group in the case when the dimension field is an even power of a Prime. In the future we plan to consider the work in case of arbitrary finite fields.

[1]

The Construction of the Derived Functor of the Functor Using the Category of Sheaves

Student: Gleb Novikov
Supervisor: Vladimir Sosnilo
Laboratory of Continuous Mathematical Education, Saint-Petersburg, Russia
glebnovikov98@gmail.com

1. Introduction

The category theory and homological algebra are the language of modern mathematics and algebra in particular. Last century gave rise not only to these theories, but also to the notion of the derived functor of the functor. Apparently, this notion as well as other ones from the category theory and homological algebra are of considerable importance for modern algebra, physics and theoretical informatics.

The classical definition of the derived functor of the functor suggests that the category-domain has enough projectives, but there are some categories which do not have enough projectives (or there are no projectives at all). The main purpose of this work is to develop a construction which allows us to define the derived functor of the functor without the category-domain having enough projectives.

2. Method of the investigations

Alexander Grothedieck is one of the major contributors to higher algebra. In the middle of the last century he introduced a topology on categories – Groethendieck topology. He also developed the sheaf theory and applied it to his new topology. So we can construct presheaves and sheaves on categories. The category of sheaves ("Sh" in the picture) depends on the properties of the category-codomain ("D" in the picture, it is always "good" and has all needed properties, like *Set* or *Ab*) and it does not depend on properties of the original category ("C" in the picture).

Instead of building the derived functor of the original functor (dotted) we introduce a construction which allows us to move all actions to the category of sheaves (using functor "S" in the picture). Then we can use the global sections functor to go to the category-codomain ("D" in the picture).

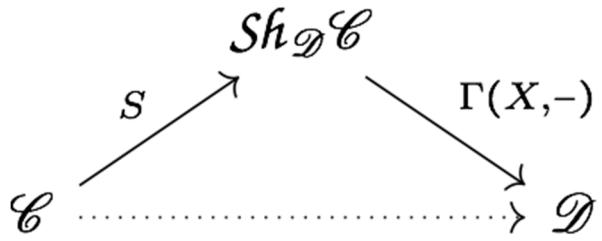

3. Results of the investigation

As a result of our research we have developed a method of constructing the derived functor, which "factors" the original functor through the category of sheaves. Such a construction does not use the property of a category which suggests "having enough projectives/injectives", as long as the classical definition did so.

Two theorems were proven. The first one states that the sheaves on Grothedieck topology are left exact contravariant functors (and inverse). This theorem allows us to regard such functors as sheaves and construct the category of them etc.

The second theorem shows that our construction of the derived functor is equivalent to the classic one, i.e. if we can define the derived functor of the functor, then all the values match and if we cannot, we can do that using our construction.

4. Conclusion

The notions that homological algebra and the category theory use are so abstract that all of them can be applied in modern physics and informatics. The notion of the derived functor is one of those and considered to be of paramount importance in homological algebra.

This research generalizes the notion of the derived functor and allows scientists to use it with structures which they could not use before. It means that there is a huge range of unsolved problems in mathematics, physics and other sciences, where the new notion could be applied.

5. References and literature

[GelMan] Sergei Gelfand and Yuri Manin, Methods of homological algebra, 2nd ed., Springer Monographs in Mathematics, Springer-Verlag, Berlin, 2003.

[Weib] Charles A. Weibel, An introduction to homological algebra, Cambridge studies in advanced mathematics 38, Cambridge University Press, 1994

[ExCat] Theo Buhler, Exact Categories, arXiv:0811.1480v2 [math.HO] 22 Apr 2009

The Group Commutator Length in Terms of Group Ring

Student: Pavel Solikov
Supervisor: Anatoliy Zaykovskiy
Laboratory of Continuous Mathematical Education, Saint-Petersburg, Russia, psolikov15@gmail.com

25 Introduction

26 Let G be a group and [G, G] be its commutator subgroup which is generated by special elements named commutators. Therefore, every element from the commutator subgroup can be represented as a product of commutators. Such representation of an element g from [G, G] that contains the least possible number of commutators is called a minimal commutator representation of g. The number of commutators in a minimal representation of g is called the commutator length of g.

26.1 Method of the investigation

26.2 The purpose of our work is creation of the instrument for transfer the work with commutator length from the group G to its group ring ZG. We give an equivalent definition of commutator length for element g from [G, G], which does not use concept of group commutator, but uses concept of ring commutator in the group ring.

26.3 Results of the experiment

26.4 Now we introduce the following concept. Suppose x, y is from ZG; then the element xy - yx is called the ring commutator of x, y.

26.5 Suppose g is from [G, G]; then there exist a representation of element g - 1 as sum of ring commutators, multiplied on elements from G. The least number of summands in the representation is called ring commutator length of element g - 1. The aim of this paper is to prove the equality commutator length of g and ring commutator length of g - 1.

26.6 Therefore, ring commutator length is equal to the group commutator length. Consequently, it is another definition of the well-known object.

26.7 Conclusion

We believe that the general commutator length theory will greatly benefit from using this definition.

[2]

CONTINUED FRACTIONS AND THE OPTIMIZATION OF HUYGENS' PLANETARIUM MODEL

Nikolina Marković

Supervisors: Nataša Ćirović, PhD, Branko Malešević, PhD, Faculty of Electrical Engineering, University of Belgrade

Regional Centre for Talented Youth Belgrade II, Belgrade, nikolinam98@gmail.com

1. Introduction

Continued fractions are expressions of the form

$$\alpha = a_0 + \cfrac{1}{a_1 + \cfrac{1}{a_2 + \cfrac{1}{a_3 + \cfrac{1}{\ddots}}}} \qquad (1)$$

where $a_0 \in Z \wedge a_i \in N (i \geq 1)$

Continued fraction is written in the short form $[a_0; a_1, a_2, \dots, a_{n\dots}]$, citing a sequence of continued fraction digits. For finite continued fraction

$$\alpha = \frac{p_n}{q_n} = [a_0; a_1, a_2, \dots, a_{n-1}, a_n] \qquad (2)$$

we introduce intermediate fractions

$$\alpha' = \frac{p'_n}{q'_n} = [a_0; a_1, a_2, \dots, a_{n-1}, a'_n] \qquad (3)$$

where $a'_n \in N \wedge 0 < a'_n < a_n$

All continued fractions are in the sequence of approximations of the first kind. We call them continued fraction approximations and mark them with (c). Besides them, in the sequence of approximations of the first kind, there can exist intermediate fractions and we call them intermediate fraction approximations, and mark them with (μ).

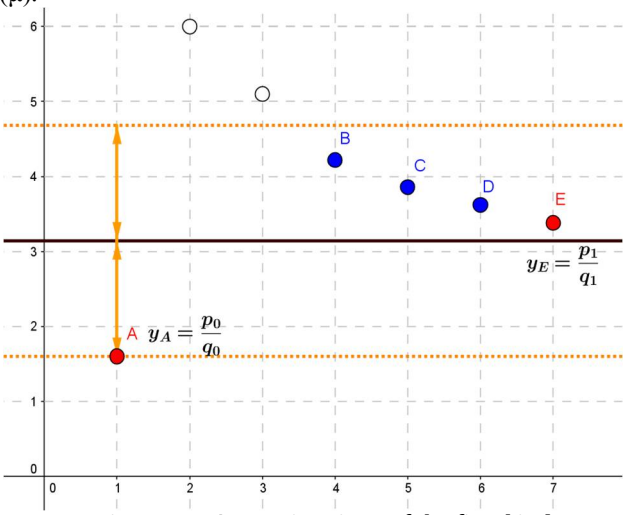

Picture 1. Approximations of the first kind

The Huygens' planetarium is a model of orbiting planets based on a system of gears. This provides that the speed at which planets are moving in relation to each other is determined by the ratio of gear teeth of the planets. This connection is found by Huygens through continued fraction approximations, where the 17th century data for orbital period of planets compared to the Earth's were used. Since intermediate fraction approximations provide more precise results than continued fraction approximations, they can be used in the planetarium for finding more accurate gear teeth relations.

The purpose of the project is to introduce Huygens' planetarium model optimization by using continued and intermediate fraction approximations along with NASA's modern day official data of planets' orbital period.

2. Method of the investigation

In order to successfully optimize Huygens' planetarium model an algorithm which finds continued fraction approximations and intermediate fraction approximations was developed and executed in *Python*. This algorithm consists of several parts of process of finding approximations. In the first part it finds continued fraction approximations, then it converts sequences of continued fraction digits to fraction form, so it could be used in the next part for finding intermediate fracitions. In the last section of the algorithm unnecessary checks of approximation quality conditions were avoided [2].

3. Results and discussion

The results obtained with the aforementioned method were compared with Huygens' results and shown in the Table 1. In this table of first smaller and larger approximations of first kind with (c) are marked continued fraction alternatives and with (μ) intermediate fraction alternatives in regard to Huygens' results. By choosing larger alternatives we could get models of planetarium which more correspond to reality.

Table 1 – Huygens' approximations for model of planetarium and found alterantives

	Huygens' approximations	**First smaller and larger approximation of the first kind**
Mercury	$\frac{p_5}{q_5} = \frac{33}{137}$	$\frac{13}{54}(c) < \frac{p_5}{q_5} < \frac{46}{191}(c)$
Venus	$\frac{p_5}{q_5} = \frac{8}{13}$	$\frac{5}{8}(\mu) < \frac{p_5}{q_5} < (\mu)\frac{131}{213}$
Earth	1	1
Mars	$\frac{p_5}{q_5} = \frac{79}{42}$	$\frac{47}{25}(c) < \frac{p_5}{q_5} < \frac{284}{151}(\mu)$
Jupiter	$\frac{p_3}{q_3} = \frac{83}{7}$	$\frac{71}{6}(c) < \frac{p_3}{q_3} < \frac{2395}{202}(\mu)$
Saturn	$\frac{p_1}{q_1} = \frac{59}{2}$	$\frac{29}{1}(c) < \frac{p_1}{q_1} < \frac{147}{5}(c)$

4. Conclusion

In this paper algorithm which finds continued fraction approximations and intermediate approximations was created. It was successfully executed to find the best possible optimizations for Huygens' planetarium model. Obtained results show that by choosing larger alternatives it is able to make calculations for the model of planetarium which more corresponds to reality. Use of continued fractions and intermediate continued fractions is still to be the subject of the future research.

5. References

[1] Khinchin, A. Ya. "Continued fractions, Translated from the 3rd Russian edition of 1961." (1964).

[2] Malesevic, Branko. Rational approximations of real numbers and some of applications, XLIII, 3, Belgrade, 1998.

[3] J. Widž: From the History of Continued Fractions, WDS'09 Proceedings of Contributed Papers, Part I, 176–181, 2009.

INVESTIGATION OF REGULAR, SEMI REGULAR AND ISOVALENT TILINGS USING GEOMETRICAL, COMBINATORICAL AND NUMBER THEORY METHODS

Eralp Akçay
Ümit Karademir
İzmir Private Fatih Science High School /Izmir/Turkey /umit.karademir@doganata.com

1. INTRODUCTION

Tiling used for making windows, floor covering and wallpapers of parks, palaces and mosque is one of the common areas of interest of science, art and construction. Different tilings shapes are used in work of artist and architect and modelling of capsid virus's geometric forms. In the research papers concerning tilings, there are rather art investigations. In the papers with mathematical approach the polygons which can be used are investigated and some different kinds of tilings were found. In last years these research are concantrated especially to monohedral pentagonal tilings. 15th type of monohedral pentagonal tiling found in 2015, created reaction in science.

Geometrical study of tilings is founded on the research of values of polygon's angles and edges and possible combinations of these angles and edges. The combinatorical approach that is used last 15-20 years is based on Euler's formula on planar graphs. Application of this formula provided some important progress especially on pentagonal tiling's studying.

2. PURPOSE

We developed our hypothesis considering possibilities that some solutions of Diofant Equations that will be obtained in our project will be realised as a tiling and some will be not.

Following this aim in this project we are going to:

- Classify of all regular and semi regular tilings.
- Prove impossibility of tiling by n-gons with $n \geq 7$ which can be found in the literature.
- Classify of tilings by polygons with a same set of valences that is not studied before
- Find cases of realization of this tilings.

Draw the realizable tilings using computer program of GeoGebra.

3. METHOD

To study tilings from mathematical view of point geometrical and combinatorical methods are used. Geometrical study finds all possible angles of polygons and their possible combinations.

Combinatorical approach use Euler's formula for planar graphs. In this project for classification of regular and semi regular tilings, we use geometrical method. To prove that for $n \geq 7$, the plane can not be tiled by convex n-gons we use Euler's formula for planar graphs and lemma of Delone et. al. To classify edge to edge tilings and tilings by polygons, we use the same set of valences, we use also Euler's formula for planar graphs, lemma of Delone et. al. and number theory methods for solving Diofant Equations. To draw realizable tilings and to show no realizability of some solutions of equations as a tiling. We use computer programs GeoGebra and Tessellation Creator.

Combinatorical approach is defined as:

Lemma 1: (Bagina, 2004) Let T be a tiling of the plane by polygons that are uniformly bounded. Then there exists an infinite sequence U_i ($i = 1, 2, 3, \dots$) of finite unions of polygons from T such that

(1) $\tau(U_i) \to \infty$, as $i \to \infty$

(2) $\frac{\gamma(U_i)}{\tau(U_i)} \to 0$, as $i \to \infty$

(3) $\chi(U_i) = 1$ for all i

We prove theorems using this lemma.

Theorem 2: For $n \geq 7$, there is no edge to edge tilings by convex n-gons.

We proved this theorem with classification as edge to edge and non-edge to edge. Then we find this corollary.

Corollary 3: There are no tilings by convex n -gons for $n \geq 7$

Denote the set of valences odd some n-gon A in tiling is denoted by $D_A = \{d_1, d_2, \dots, d_n\}$ (some numbers d_i in the set D_A may coinside)

Definition: If in a edge to edge tiling K consisting of n-gons the sets D_A of all n-gons D_A are the same then we will say that K an ***isovalent tiling***.

Theorem 4: For the edge to edge tiling consisting of triangles A with $D_A = \{a, b, c\}$, we have

$$\frac{1}{a} + \frac{1}{b} + \frac{1}{c} = \frac{1}{2}$$

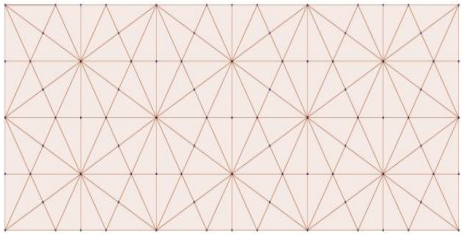

One of the solution comes from the equation

Theorem 5: For the edge to edge tiling consisting of quadrilaterals A with $D_A = \{a,b,c,d\}$, we have

$$\frac{1}{a}+\frac{1}{b}+\frac{1}{c}+\frac{1}{d}=1$$

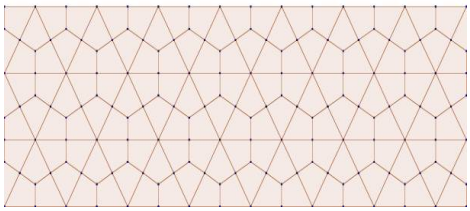

One of the solution comes from the equation

Theorem 6: For the edge to edge tiling consisting of pentagons A with $D_A = \{a,b,c,d,e\}$, we have

$$\frac{1}{a}+\frac{1}{b}+\frac{1}{c}+\frac{1}{d}+\frac{1}{e}=\frac{3}{2}$$

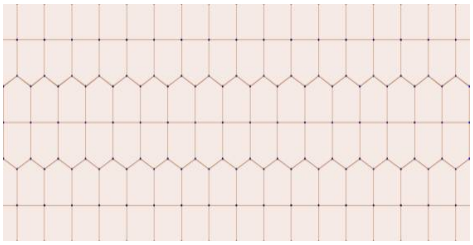

One of the solution comes from the equation

Theorem 7: For the edge to edge tiling consisting of hexagons A with $D_A = \{a,b,c,d,e,f\}$, we have

$$\frac{1}{a}+\frac{1}{b}+\frac{1}{c}+\frac{1}{d}+\frac{1}{e}+\frac{1}{f}=2$$

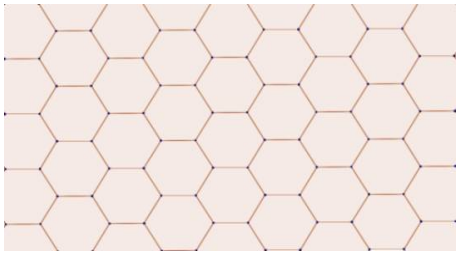

One of the solution comes from the equation

Geometrical approach is defined as:

To classify all regular and semi regular tilings, we study the polygons which can be combined in a vertex. After the combination of polygons in some vertex the sum of angles in this vertex must be 360°. Since the interior angles of a regular polygon is at least 60°, the number of polygons combined in one vertex is at most 6, this is tiling with equilateral triangles. Since we use convex polygons, the number of polygons combined in vertex at least 3. There are some examples of this case. The simplest of them is tiling with regular hexagons.

If we denote angles combined in one vertex by $x_1, x_2, x_3, x_4, x_5, x_6$ then we have the following equation, which we will call ***main equation***:

$$x_1 + x_2 + x_3 + x_4 + x_5 + x_6 = 360^\circ$$

If the number of angles is less than 6, we will assume that the rest valuables x_i are 0.

4. RESULTS AND CONCLUSION

In this Project, we consider tiling of the plane by polygons, investigate important developments including the last ones. We obtained the following results concerning the classification of tilings.

1- We give the classification of tilings by regular polygons with proof. Note that such a classification without proof is given in some research papers.

2- Using Euler's formula for planar graphs, we prove that the plane can not be tiled by n-gons with $n \geq 7$. This result is also given in some papers without proof.

3- Applying Euler's formula to the tilings by polygons with a same set of vertex's valences, we obtained some Diofant Equations.

4- Using number theory methods, we found all positive integer solutions of these Diofant Equations.

5- Using computer programs GeoGebra and Tessellation Creator, we drew tilings obtained from some solutions and proved that other solutions can not be realised as tiling.

By literature search shows that classification of tilings with a same set of vertex's valences is not made before. Giving of definition of isovalent tilings, their classification and the proof of the fact that the plane can not be tiled by n-gons with $n \geq 7$ are the *new (different) sides of the project*.

5. REFERENCES

1. Grünbaum B.; Shephard G. C. (1986). *Tilings and Patterns*, W.H. Freemanand Company, New York
2. Sugimoto T. (2012). Convex Pentagons for Edge-to-Edge Tiling,1, *Society for Science*, 27, 93-103
3. Bagina O. (2004). Tiling the plane with congruentequilateral convex pentagons, *Journal of Combinatorial Theory*, Series A 105, 221–232

A new view on differential games theory, or how to catch the fleeing person

Cherednichenko Alexander

Supervisor: Bilous Svitlana Yurivna, the head of the department scientific-research experimental laboratory of The National Centre "Minor Academy of Science of Ukraine", Ph.D.

Zaporizkii technical lyceum, Zaporizhya, Ukraine, chered-sasha@yandex.ru

1 Introduction

1.1 Main idea and aim of the research

Main aim and idea of the research appeared by solving known tasks about chasing and they are exists to find more effective methods of solving tasks about chasing due to transition to reference frame of fleeing person.

Problem of the research is in selecting and math justification of chasing strategy by the help of approaches different from traditional in differential games theory.

1.2 Theoretical part

The tasks about chasing which are met in the collection, where on the first sight the evident strategy of chasing is being realized (S-strategy) when the chaser is moving towards of the fleeing person in any moment of time has been analyzed in this work. When analyzing the comparison of S-strategy was made with the strategy of parallel rapprochement (P-strategy) that was worked out in the differential games theory.

For the simplification of differential games theory in solving tasks about chasing the transition to another reference frame was made. Basing on this L-strategy was worked out, where for any moment of time, in reference frame of fleeing person B the chaser P is moving towards B.

$t^* = \frac{x}{v} = \frac{L}{\sqrt{u^2 - v^2}}$ - time of the persecution in L-strategy

$t_k = \frac{uL}{u^2 - v^2}$ - time of the persecution in S-strategy

$t^* < t_k$ - time of the persecution in L-strategy is less than in S-strategy.

Thus, it means that L-strategy is more profitable for the chaser.

1.3 Experimental part

The experiment was made like computer modeling. The computer modeling of L-strategy clearly proves it's advantages. In the reference frame of fleeing person exactly it becomes clear that L-strategy in the most profitable for chaser.

Computer modeling gives possibilities to compare the players trajectory of movement for different speed ratios of the chaser and the fleeing person and it also allows to get the family of curves that determine the dependence of the distance between the participants of race from time, that makes it possible to watch the features of the relative movement of the chaser and the fleeing person.

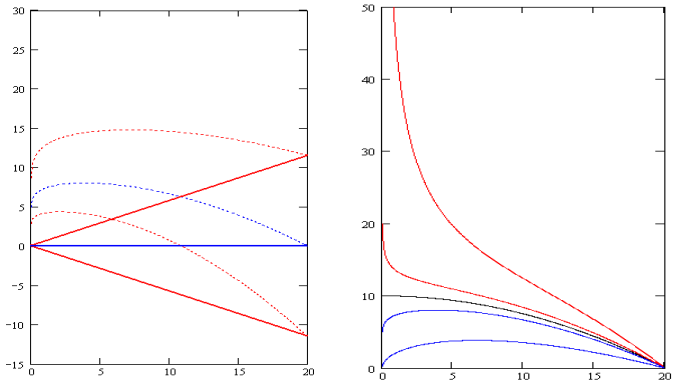

A B

Fig. 1 Computer modeling for analyzing of results:

A – the comparison of movement trajectories of the chaser in B-system for different values of angle between players (dotted lines – movement in S-strategy, solid curves – movement in L-strategy);

B - trajectories of movement of the chaser in B-system depending the ratio of speeds.

2 Results of the experiment

The results of the experimental prove that the suggested L-strategy coincides with the developed in the theory of differential games P-strategy during the transition into the reference frame connected with Earth. The suggested approaches simplify mathematical way of solving and allow easily transfer on 3d or n-d space.

The Computer program that modeling the movement of the chaser and the fleeing person in the reference frame, connected with Earth and allows to imagine the real movement and can be used for the demonstrating the subject of Kinematics.

3 Literary sources

1.Petrosjan L.A., Rihsiev B.B. Peresliduvannja na ploshhini. – Moskva, Nauka, 1991,-95 s.

2. Belous S.U. Novye podhody k resheniju zadach o presledovanii v teorii differencial'nyh igr na ploskosti // Trudy instituta mehaniki i matematiki URO RAN — Ekaterinburg, — 2000. — S. 182–193

4. Internet-resurs:http://spbu.ru/files/upload/ku4.pdf

5.Internetresurs: http://www.dissercat.com/content/chislennye-metody-resheniya-zadach-gruppovogo-presledovaniya#ixzz3yGa18I9F

6.Internet-resurs:http://fizmathim.com/nekotorye-zadachi-teorii-differentsialnyh-igr-gruppovogo-presledovaniya

The Aquarium Problem: Combinatorical Processes Research

Oleksi Oleksyshyn
Aleksandr Tolesnikov
Lyceum №1, Chernivtsi/Ukraine, o_oleksyshyn@ukr.net

Introduction

This paper is dedicated to one specific problem in the combinatorial processes filed: complex system develops according to its own laws and at some point meets resource depletion. Our aim is to study the characteristics of this process, first of all, the possible final positions.

Problem definition

We have n aquariums. Each aquarium starts having 1, 2, .., n fish inside respectively. Then we rearrange fish in aquariums according the following rules: we can take two aquariums having both even or both odd (but still different) number of fish and relocate fish to make its number in the aquariums equal. The process continues while we have possible moves. Describe the set of all possible final positions for the process.

Restrictions

We have found two important invariants in the process and the invariants helped us to prove that the process is finite and its maximal length is of cubic dependence on n.

We found two important restrictions for the possible final positions. The first stems from the fact that the number of fish is an integer value, therefore the final positions should be consistent with the number theory.

The second one has unexpected connections in algebra. It is a notion of majorization which is well-known both in matrix theory and inequality studies.

We say sequence x majorizes sequence y if:

a) x and y have the same element number and the same average.

b) for any possible k sum of k largest elements of x is greater than sum of k largest elements of y.

It turned out that in our problem the initial position should majorize all possible final positions.

The main conjecture

We hypothesize that the two restrictions that the final positions have are the only restrictions for the final positions in the problem, i. e. for every position which meet the restrictions there is a chain of steps ending in that position.

Number experiment

We composed a number of assistant computer programs to better understand the process under study. One of them output the full list of possible final positions for given n. Unfortunately, the computational complexity is quickly increasing with increase of n. So we supposed that every possible final position has large enough probability in random process and composed the Monte-Carlo-style program. For the comparison purpose we also composed the program whist enlists possible according to the main conjecture final positions.

Constructions

We have noticed that to get the specific final position it is sufficient to split the numbers 1 to n into two symmetrical (in some sense) sets. In the rest of the article we discuss if it is possible to construct these symmetric halves.

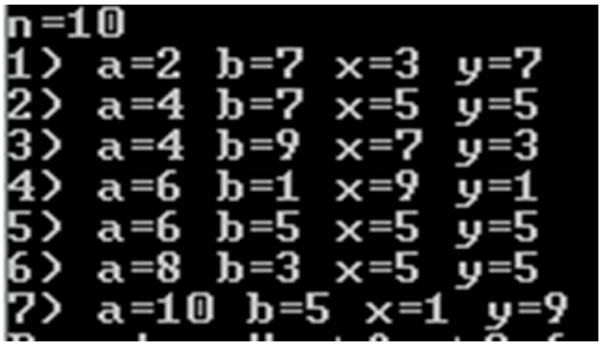

Fig.1. All possible final positions for $n = 10$ (x,y - amount of aquariums, a, b −amount of fish.

References

1) Номіровський Д. А. Нерівності Мюрхеда та Карамати // У світі математики. — 2001. — №4. — С. 30-44.

2) Толпыго А. Инварианты // Квант. — 1976. — №12. — С. 19-25.

3) Райгородский А. М. Вероятность и алгебра в комбинаторике. — Дубна: МЦНМО, 2008. — 47 с.

4) Гантмахер Ф.Р. Теория матриц. – Москва: Наука, 1968. — 576 с.